MGG

Molecular & General Genetics

An International Journal

Continuation of Zeitschrift für Vererbungslehre The First Journal on Genetics Founded in 1908

Volume 236 Number 2–3 January 1993

Continuation see back cover page

Springer International

Molecular & General Genetics

MGG provides publication in all areas of general and molecular genetics – developmental genetics, somatic cell genetics, and genetic engineering – irrespective of the organism. Articles on animal or plant breeding or human genetics will be accepted only if the results described have significance for fundamental genetics. Reports that are exclusively dealing with nucleic acid sequences are published only if they are judged to be of wide interest and biological significance. The findings reported should be novel and not under consideration for publication elsewhere. The presentation should be intelligible to as wide an audience as possible.

Springer International

Subscription information

ISSN 0026-8925
Volumes 235–240 (3 issues each) will appear in 1993.

The journal MGG appears monthly. It is published by Springer Pro.-Ges., Berlin, Heidelberger Platz 3, W-1000 Berlin 33, FRG.

Application to mail at second-class postage rates is pending at New York, New York and additional mailing offices.

Postmaster send all address changes to:

MGG, Springer Verlag New York, Inc., Inc. Journal Fulfilment Services Dept., 44 Hartz Way, Secaucus, NJ 07096, USA.

North America. Recommended annual subscription rate: approx. US $ 2194.00 (single issue price: approx. US $ 145.00) including carriage charges. Subscriptions are entered with prepayment only. Orders should be addressed to:

Springer-Verlag New York Inc.
Service Center Secaucus

44 Hartz Way
Secaucus, NJ 07094, USA
Tel. (201) 348-4033, Telex 0023-125 994,
Fax (201) 348-4505

All other countries. Recommended annual subscription rate: DM 3198.00 plus carriage charges; (Federal Republic of Germany: DM 58.74 incl. VAT; other countries: DM 78.30. SAL or airmail charges are available upon request. SAL delivery is mandatory to Japan, India, and Australia/New Zealand). Volume price: DM 533.00, single issue price: DM 213.00 plus carriage charges. Orders can either be placed via a bookdealer or sent directly to: Springer-Verlag, Heidelberger Platz 3, W-1000 Berlin 33, FRG, Tel. (0)30/82 07-1, Telex 1-83 319, Fax (0)30/8 21 40 91.

Personal subscriptions: Molecular & General Genetics is available at a personal subscription rate. Orders should be mailed to Springer-Verlag.

Changes of address: Allow six weeks for all changes to become effective. All communications should include both old and new addresses (with Postal Codes) and should be accompanied by a mailing label from a recent issue. According to § 4 section 3 of the German Postal Services Data Protection Regulations, the German Federal Post Office can inform the publisher of a subscriber's new address even if the subscriber has not submitted a formal application for mail to be forwarded. Subscribers not in agreement with this procedure may send a written complaint to Springer-Verlag's Berlin office within 14 days of publication this issue.

Back volumes: Prices are available on request.

Microform editions are available from:
University Microfilms International,
300 N. Zeeb Road,
Ann Arbor, MI 48106, USA

Production

Springer Produktions-Gesellschaft
3050 – Journal Production Department
Claudia Birkler
Heidelberger Platz 3
W-1000 Berlin 33, FRG
Tel. (0) 30/82 07 435, Telex 1-85 411,
Fax (0) 30/8 20 74 49

Responsible for advertisements

Springer-Verlag
E. Lückermann
Heidelberger Platz 3
W-1000 Berlin 33, FRG
Telephone (0) 30/82 07-0, Telex 01-85 411,
Fax (0) 30/8 20 73 00

Typesetting

Universitätsdruckerei H. Stürtz AG
W-8700 Würzburg, FRG

Printers

H. Heenemann, W-1000 Berlin 42, FRG

Bookbinding

Lüderitz & Bauer, W-1000 Berlin 11, FRG

Springer-Verlag GmbH & Co KG
W-1000 Berlin 33, FRG
Printed in Germany

Mol Gen Genet (1993) 236:315–325

MGG

Modulation of glutamine synthetase gene expression in tobacco by the introduction of an alfalfa glutamine synthetase gene in sense and antisense orientation: molecular and biochemical analysis

Stephen J. Temple[1], Thomas J. Knight[2], Pat J. Unkefer[3], and Champa Sengupta-Gopalan[1]

[1] Plant Genetic Engineering Labs/Department of Agronomy and Horticulture, New Mexico State University, Las Cruces, NM 88003, USA
[2] Biology Department, University of Southern Maine, Portland, ME 04103, USA
[3] Isotope and Nuclear Chemistry Division, INC-4 Los Alamos National Laboratory, Los Alamos, NM 87545, USA

Received March 5, 1992 / Accepted August 11, 1992

Summary. A glutamine synthetase (GS) cDNA isolated from an alfalfa cell culture cDNA library was found to represent a cytoplasmic GS. The full-length alfalfa GS_1 coding sequence, in both sense and antisense orientation and under the transcriptional control of the cauliflower mosaic virus 35S promoter, was introduced into tobacco. Leaves of tobacco plants transformed with the sense construct contained greatly elevated levels of GS transcript and GS polypeptide which assembled into active enzyme. Leaves of the plants transformed with the antisense GS_1 construct showed a significant decrease in the level of both GS_1 and GS_2 polypeptides and GS activity, but did not show any significant decrease in the level of endogenous GS mRNA. We have proposed that antisense inhibition using a heterologous antisense *GS RNA occurs at the level of translation. Our results* also suggest that the post-translational assembly of GS subunits into a holoenzyme requires an additional factor(s) and is under regulatory control.

Key words: Glutamine synthetase – Heterologous antisense RNA – Transgenic plants – Tobacco

Introduction

Glutamine synthetase (GS; EC 6.3.1.2) catalyzes the ATP-dependent formation of glutamine from glutamate and ammonia. GS catalyzes the reassimilation of ammonia released from a variety of metabolic pathways such as photorespiration, catabolism of amino acids and metabolism of phenylpropanoids. GS is also involved in nitrate (or nitrite) assimilation in leaves and roots and in dinitrogen fixation in root nodules of legumes (Miflin and Lea 1980). In plants, GS is an octamer and has a native molecular weight of approximately 320–380 kDa (Stewart et al. 1980).

In plants, GS is encoded by a small multigene family that show organ-specific patterns of expression, with separate genes encoding leaf cytoplasmic and chloroplastic GS isoforms (GS_1 and GS_2, respectively), root GS and nodule GS isoforms in legumes (Tingey et al. 1987; 1988; Gebhardt et al. 1986; Lightfoot et al. 1988; Forde and Cullimore 1989; Peterman and Goodman 1991). Based on the site of localization, the different GS isoforms assimilate ammonia derived from different sources. Analysis of photorespiratory mutants of barley has established that reassimilation of photorespiratory ammonia is the function of the chloroplast-localized GS_2 protein (Blackwell et al. 1987). Furthermore, analysis of transgenic plants containing GS_2 or GS_1 promoters, has shown that GS_1 genes are only expressed in the cells around the phloem, suggesting that the GS_1 isoform functions in generating glutamine for nitrogen transport (Brears et al. 1991).

The regulation of GS gene expression is not yet fully understood. The genes for GS_1 and GS_2 are differentially expressed during plant growth and development (Forde and Cullimore 1989; Edwards et al. 1990; Brears et al. 1991; Kamachi et al. 1991), reflecting the different roles and cellular compartmentalization of the two isoenzymes (Mann et al. 1980; Tingey et al. 1988; Edwards and Coruzzi 1989). In addition, it has been shown that the pea GS_2 promoter is light-induced (Tingey et al. 1988; Edwards et al. 1990) and that the accumulation of GS mRNA may in part be due to a phytochrome-mediated response (Sakamoto et al. 1990). Photorespiratory ammonia production also regulates pea GS_2 expression (Edwards and Coruzzi 1989). In root nodules, a nodule-specific GS isoform that appears to be primarily under developmental control has been reported for several species, including bean (Lara et al. 1983; Forde et al. 1989), alfalfa (Dunn et al. 1988), lupin (Konieczny et al. 1988) and soybean (Sengupta-Gopalan and Pitas 1986;

Correspondence to: C. Sengupta-Gopalan

Sengupta-Gopalan et al. 1991). However, soybean nodules also seem to have a cytoplasmic GS gene that is not nodule specific and appears to be regulated by ammonia or a related metabolite (Hirel et al. 1987). The promoter of the gene when used in β-glucuronidase (GUS) fusions, is ammonia-inducible in transgenic *Lotus corniculatus* but not in transgenic tobacco (Miao et al. 1991).

To increase our level of understanding of GS function and regulation in plants, we have attempted to alter the levels of GS expression, using both overexpression and downregulation, by genetic engineering (van der Krol et al. 1988b). Successful downregulation of plant genes using homologous antisense genes has been reported for a growing number of different systems: chalcone synthase (van der Krol et al. 1988a; 1990a, b), polygalacturonase (Smith et al. 1990), ribulose-1,5-bisphosphate carboxylase (Rubisco) small subunit (Quick et al. 1991) and the 10 kDa photosystem II polypeptide (Stockhaus et al. 1990). However, few examples of successful down-regulation in a heterologous system have been reported (van der Krol et al. 1988b; Visser et al. 1990; Schuch et al. 1990).

In this study, we have used an alfalfa GS_1 antisense RNA to test if it can down-regulate both GS_1 and GS_2 gene expression in the heterologous system, tobacco. Our experiments, while clearly demonstrating the effectiveness of this approach, suggest that the mechanism of downregulation using a heterologous antisense RNA does not fit the established model of RNA:RNA (or RNA:DNA) duplex formation resulting in rapid degradation or impaired transcript processing (van der Krol et al. 1988b). We have also overexpressed the alfalfa GS_1 gene in tobacco and established that the encoded polypeptide can assemble into a functional enzyme. The results of preliminary biochemical and molecular analysis of some of these plants are presented.

Materials and methods

Recombinant DNA techniques. Standard procedures were used for recombinant DNA manipulations (Maniatis et al. 1982). Plasmid pGS100 containing an alfalfa GS cDNA isolated from a *Medicago sativa* cell culture line (DasSarma et al. 1986) was a gift from Dr. H.M. Goodman (Dept of Molecular Biology and Genetics, Harvard Medical School, Mass., USA). A 1.35 kb *Ssp*I fragment encoding the entire GS coding region and extensive 5′ and 3′ untranslated regions was subcloned in both orientations into the *Sma*I site of pSP73. The gene was recovered as a *Cla*I-*Sal*I fragment that was inserted into the *Cla*I-*Xho*I polylinker sites of pMON316 (Rogers et al. 1987) in both sense and antisense orientations relative to the 35S cauliflower mosaic virus (CaMV) promoter and nopaline synthase (NOS) 3′ transcription terminator. The resulting plasmids, pGS111 and pGS121, contained the alfalfa GS gene in sense and antisense orientations with respect to the 35S promoter (Figs. 2 and 3).

Plant transformation. Plasmids pGS111 and pGS121 were mobilized from *Escherichia coli* DH5α into the *Agrobacterium tumefaciens* receptor strain pTiT37ASE by triparental mating as described by Rogers et al. (1987). *Nicotiana tabacum* cv. Xanthi plants were transformed using the leaf disc transformation procedure (Horsch et al. 1985). Transformants were selected and regenerated on MS medium containing 100 μg of kanamycin per ml. Shoots appeared 4–6 weeks after inoculation. These shoots were rooted on the same medium containing kanamycin, but minus the hormones, and transfered to potting soil:perlite:vermiculite (3:1:1) for maintenance in a greenhouse.

Isolation of poly(A)$^+$ RNA and Northern blot analysis. Total RNA was isolated using the LiCl precipitation procedure described by De Vries et al. (1982). Poly(A)$^+$ RNA was isolated by subjecting total RNA to poly(U) Sepharose chromatography (Murray et al. 1981). Poly(A)$^+$ RNA was fractionated in 1% agarose/formaldehyde gels and blotted onto nitrocellulose. Hybridization was carried out in 50% formamide at 42° C using standard conditions (Maniatis et al. 1982). Probes were prepared by either labeling purified DNA fragments by random priming (Feinberg and Vogelstein 1983) or using strand-specific RNA probes. The 1.0 kb *Bgl*II-*Bam*HI fragment from pGS100 that included most of the alfalfa GS coding region was subcloned into the *Bam*HI site of pSP73 in the sense orientation relative to the SP6 RNA polymerase transcription initiation site to give pGS301. A ^{32}P-labeled single-stranded GS antisense RNA probe was synthesized in vitro using *Sma*I-linearized pGS301, T7 RNA polymerase and [^{32}P]CTP (Riboprobe System, Promega, Wis.). Following hybridization using a riboprobe, the filter was washed at low stringency, 3 × 15 min at 42° C in 2 × SSC, 0.1% SDS. The extensive nonspecific background binding was removed by rinsing the filter in 2 × SSC followed by incubation in 1 μg/ml RNAase A in 2 × SSC at room temperature for 30 min. Finally the filter was washed at higher stringency in 0.1 × SSC, 0.1% SDS (2 × 15 min at 42° C).

Hybrid select translation. This was carried out essentially as previously described (Sengupta-Gopalan and Pitas 1986). The insert DNA (*Ssp*I fragment of pGS100) was immobilized on nitrocellulose filter disks and hybridized with 10 μg poly(A)$^+$ RNA isolated from alfalfa leaf and root. The selected RNA was recovered using 10 μg of calf liver tRNA as a carrier. The RNA was translated in vitro using the wheat germ system (Promega, Wis.) using [^{35}S]methionine (NEN) as the tracer amino acid. The translation products were separated by SDS-PAGE and made visible by fluorography and autoradiography (Laskey and Mills 1975).

Polyacrylamide gel electrophoresis. Two different PAGE systems were employed, both using the BioRad Protean II system:

A. SDS-PAGE system according to Laemmli (1970) using 14% slab gels. Proteins were then blotted onto nitrocellulose electrophoretically in 25 mM TRIS, 192 mM glycine, 5% methanol, pH 8.2. The nitrocellulose was blocked overnight with 1% BSA in TRIS-buffered saline

containing 0.05% Tween 20 and probed with a suitable antibody. The antisera used was raised against: (1) pea seed GS (Langston-Unkefer et al. 1987), diluted 1:1000; (2) *Mesembryanthemum crystallinum* phosphoenolpyruvate carboxylase (PEPC), diluted 1:1000 (a gift from Dr. H.J. Bohnert); and (3) NADH-dependent hydroxypyruvate reductase (HPR), diluted 1:16000 (Titus et al. 1983). Cross-reacting bands were made visible using an alkaline phosphatase-linked second antibody employing the substrates nitro blue tetrazolium and 5-bromo-4-chloro-3-indolyl-phosphate, used according to the supplier's instructions (Promega, Wis.).

B. A native PAGE system using 7.0% slab gels run in 25 mM TRIS, 192 mM glycine overnight at 4° C and 25 mA constant current. The GS activity on native polyacrylamide gels was detected using the transferase assay (Shapiro and Stadtman 1970). Following staining, the activity gels were photographed with Tech Pan film (2415) using a blue filter.

Determination of glutamine synthetase activity. Tobacco leaf tissue was ground in a mortar with ice-cold 100 mM TRIS-HCl (pH 7.8) containing 100 mM 2-mercaptoethanol, 10 mM $MgCl_2$, 5 mM glutamate and 1% (w/v) isoluble polyvinylpyrrolidone. An extraction buffer to tissue ratio of 4:1 was found to maximize the stabilization of GS activity even in older tobacco leaf tissue. The homogenate was clarified by centrifugation (40000 *g* for 15 min at 4° C). The GS activity of the supernatant was measured using the ADP-dependent transferase assay of Shapiro and Stadtman (1970). One unit of GS activity is defined as 1 µmol of γ-glutamyl hydroxamate formed per min. Protein concentration was determined by the dye-binding method of Bradford (1976) with bovine serum albumin as a standard.

Results

The GS cDNA clone from alfalfa cell culture represents the GS_1 gene and does not hybridize to GS_2 mRNA

The full-length alfalfa GS cDNA clone obtained from Dr. Goodman was isolated from a cDNA library made from RNA from alfalfa suspension culture (DasSarma et al. 1986). To determine which form of GS the cDNA clone represents and establish its relative level of expression in different alfalfa tissues, we analyzed the RNA from alfalfa root, nodule and leaf by Northern blot hybridization. As seen in Fig. 1A and B, all three probes (the 5′ and 3′ untranslated regions of the cDNA and the coding region) hybridized strongly to the root and nodule mRNA and very weakly to leaf RNA. Of the three probes, the coding sequence exhibits the highest relative level of hybridization to the leaf RNA (probe 2, Fig. 1A). Alfalfa leaves contain higher levels of GS protein and activity than roots and the major fraction of GS protein in leaves can be attributed to the chloroplast form. The absence of any significant hybridization between the alfalfa GS cDNA and leaf RNA would suggest that the cDNA represents a cytoplasmic GS and

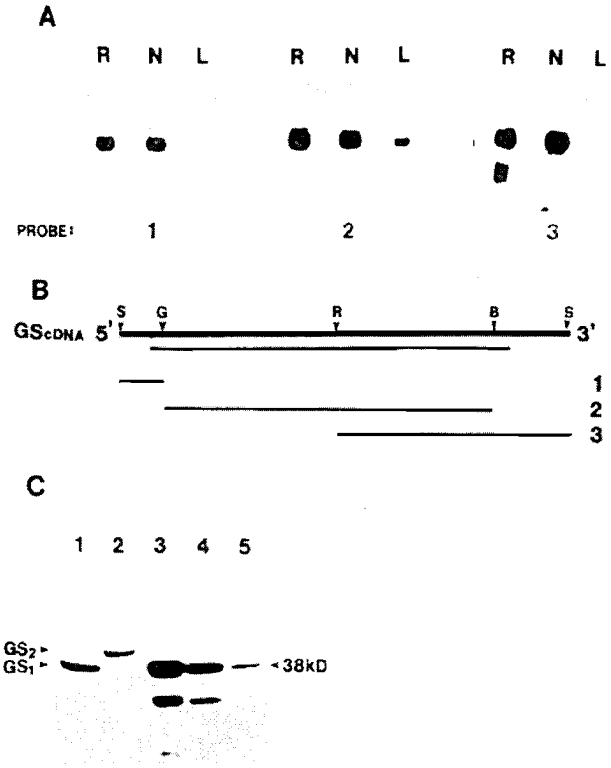

Fig. 1A–C. Characterization of the glutamine synthetase alfalfa (GS) cDNA clone (DasSarma et al. 1986). **A** Northern blot analysis of 3 µg poly(A)$^+$ RNA isolated from alfalfa root (R), nodule (N) and leaf (L). The blots were hybridized with ^{32}P-labeled DNA fragments 1, 2 and 3 isolated from the alfalfa GS cDNA (**B**). **B** Positions of the restriction sites used in the preparation of the probes: S, *Ssp*I; G, *Bgl*II; R, *Eco*RI; B, *Bam*HI. **C** Comparison of Western blot analysis of alfalfa root (lane 1) and leaf (lane 2) total soluble protein extracts (100 µg/lane) separated by SDS-PAGE and probed with pea seed GS antibody compared with the in vitro translation products obtained following hybrid select translation of alfalfa nodule (lane 3), root (lane 4) and leaf (lane 5) poly(A) RNA using the plasmid pGS100

that the cloned cDNA does not hybridize significantly to GS_2 mRNA.

The GS_2 and GS_1 polypeptides can be distinguished by their molecular weights. Thus, the primary translation products of mRNA hybrid-selected with the GS cDNA from the total mRNA population of leaf and root, should reflect the extent of sequence homology between the GS cDNA and GS_1/GS_2 mRNAs. While the root contains only GS_1 mRNA, the leaf tissue contains predominantly GS_2 mRNA and only a small fraction of GS_1 mRNA (Tingey et al. 1987; Cock et al. 1990; Peterman and Goodman 1991). The GS cDNA was used to hybrid select GS mRNA from root, leaf and nodule poly(A)$^+$ RNA populations. The RNA was translated in vitro in the wheat germ system and the translation products subjected to SDS-PAGE in parallel with total soluble proteins from root and leaf. Following electroblotting onto nitrocellulose, the strip containing the translation products was subjected to autoradiography while the strip with the total soluble protein was sub-

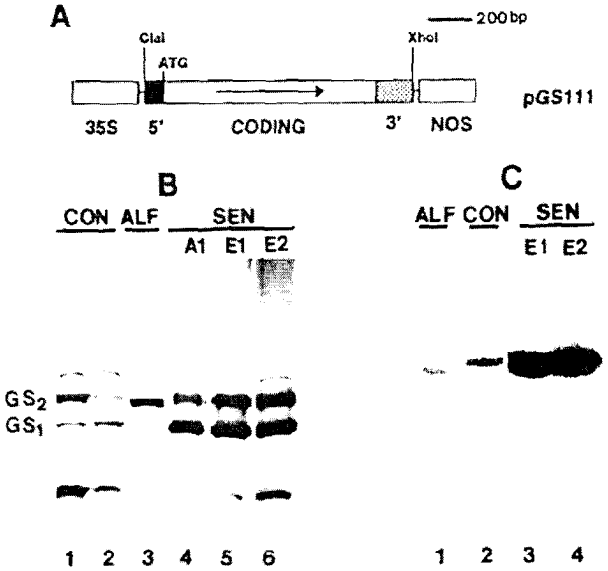

Fig. 2A–C. Analysis of tobacco plants transformed with a sense alfalfa GS_1 gene. A The sense construct pGS111. The full-length GS cDNA (DasSarma et al. 1986) was inserted in the sense orientation between the CaMV 35S promoter and the nopaline synthase (NOS) terminator into the polylinker of pMON316. The positions of the 5' and 3' untranslated regions and translation start codon (ATG) are indicated. B Western blot analysis of total soluble leaf protein extracts (200 μg/lane) from control tobacco (CON), alfalfa (ALF) and three independent tobacco sense transformants (SEN). The samples were separated by SDS-PAGE, transferred to nitrocellulose and the filter probed with pea seed GS antibody. The positions of GS_1 and GS_2 polypeptides are indicated. The plants used in this analysis were approximately 2–3 weeks post-planting in the soil. C Total soluble leaf protein (1 mg/lane) from alfalfa (ALF) control tobacco (CON) and sense tobacco transformants (SEN) were separated by native PAGE. The gel was then stained for GS activity using the transferase assay. The plants used in this analysis were approximately 6–8 weeks post-planting in the soil

jected to Western analysis. As seen in Fig. 1C, in all cases the higher molecular weight hybrid-selected translation (HST) product (38–39 kDa) comigrated with the major root GS isoform and the minor GS isoform from leaf (GS_1). No HST product migrating like the GS_2 precursor in the leaf was detected. While we do not know what the major lower molecular weight (34–35 kDa) HST product represents, we cannot rule out the possibility that it is the result of incomplete synthesis of the GS_1 polypeptide.

Taken together, our results suggest that the GS cDNA used for the antisense GS constructs encodes a GS_1 polypeptide that is expressed predominantly in the roots and nodules and forms a minor component in leaves.

Constitutive expression of the GS_1 gene in the sense orientation results in an increase in GS_1 protein in transgenic tobacco

The entire alfalfa GS_1 cDNA containing the coding region and the 5' and 3' flanking regions was placed behind the 35S promoter in the sense orientation (Fig. 2A) and introduced into tobacco. Western blot analysis of crude leaf extracts from young transformed (R_0) and control plants showed that plants with the GS_1 sense construct contained elevated levels of GS_1 and GS_2 polypeptides (Fig. 2B, lanes 4–6). The GS_1 polypeptide, however, showed a relatively greater increase. Of course, one cannot rule out the possibility of protein saturation on the blot in the case of the GS_2 protein. However, the GS_2 in transformed tobacco did not show any forms with an electrophoretic mobility similar to that of alfalfa GS_2 polypeptides, confirming that the introduced gene indeed codes for GS_1. While transformants E1 and E2 showed comparable levels of the GS proteins, transformant A1 showed a slightly lower level of GS proteins. An immunoreactive protein band with higher electrophoretic mobility than authentic GS was detected in all tobacco lanes, but at variable levels. The crude leaf extracts were also subjected to native gel electrophoresis and stained for GS activity. As seen in Fig. 2C, in the transformants a novel band of GS activity, in addition to the endogenous band of activity, was localized in a region comigrating with alfalfa leaf GS activity. An increase in activity was also observed in the region of endogenous tobacco leaf GS activity. Since the major GS activity in leaves is due to GS_2, an increase in the level of the endogenous GS activity band in the GS_1 sense transformants can be attributed to an increase in GS_2 protein.

Constitutive expression of the GS_1 gene in the antisense orientation results in a decrease in GS_1 and GS_2 proteins

The alfalfa GS_1 cDNA was placed in the antisense orientation distal to the 35S promoter (Fig. 3A) and introduced into tobacco. Crude total soluble protein extracts from leaves of alfalfa, young transformants (R_0) (with antisense GS_1 constructs) and control tobacco plants were subjected to SDS-PAGE followed by immunoanalysis with GS antibody (Fig. 3B). Transformants C2, D1 and D3 all showed a reduction in the level of GS_1 protein when compared to the control (Fig. 3B, lanes 4–6). A decrease in the level of GS_2 polypeptide was also observed in transformant D1 and to a very small extent in C2. The transformant D3, however, showed a slightly elevated level of GS_2 polypeptide. The results indicate that antisense alfalfa GS_1 constructs are effective in lowering the level of endogenous GS_1 protein levels and, to some extent, GS_2 protein in the heterologous plant, tobacco. Immunoreactive protein bands, one migrating faster and one migrating more slowly than the authentic GS proteins were present in most lanes containing tobacco proteins. The levels of these proteins appeared to be independent of the GS_1, GS_2 levels in the plant. The nature of these protein bands is not known at this stage. It is likely, however, that the small molecular weight immunoreactive products represent specific proteolytic products of GS.

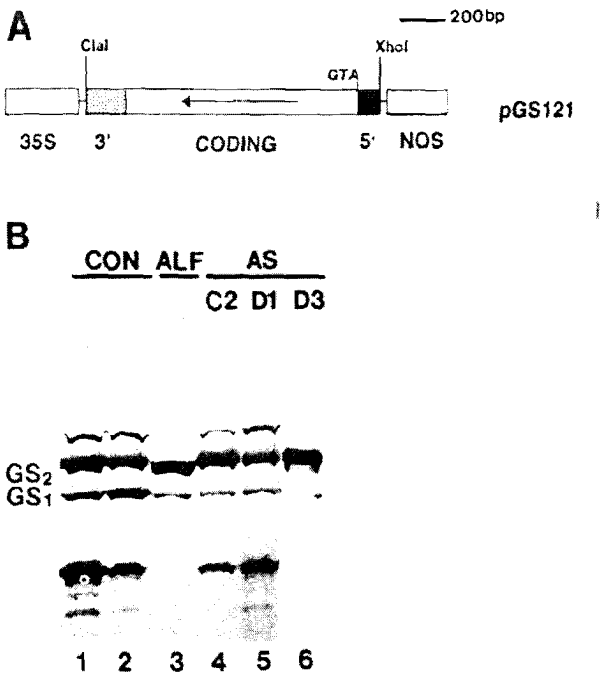

Fig. 3A and B. Analysis of tobacco plants transformed with an antisense alfalfa GS_1 gene. **A** The antisense construct pGS121. The full-length GS cDNA (Das Sarma et al. 1986) was inserted in the antisense orientation between the cauliflower mosaic virus (CaMV) 35S promoter and the nopaline synthase (NOS) terminator into the polylinker of pMON316. The positions of the 5' and 3' untranslated regions and GTA codon are indicated. **B** Western blot analysis of total soluble leaf protein extracts (200 μg/lane) from control tobacco (CON), alfalfa (ALF) and three independent tobacco antisense transformants (AS). The samples were separated by SDS-PAGE, transferred to nitrocellulose and the filter probed with pea seed GS antibody. The positions of GS_1 and GS_2 polypeptides are indicated. The plants used in this analysis were approximately 2–3 weeks post-planting in the soil

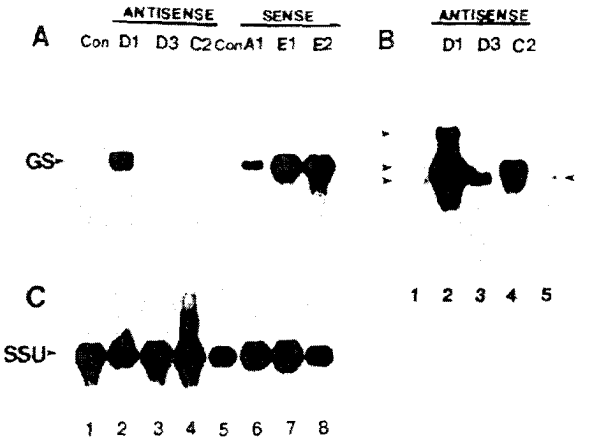

Fig. 4A–C. Analysis of the GS transcripts in the leaves of the transformed tobacco plants. A Poly(A)$^+$ RNA (2 μg/lane) from controls (lanes 1 and 5), three independent transformants containing antisense GS (lanes 2–4) and three containing the sense GS construct (lanes 6–8) were subjected to Northern analysis using probe 3 of the GS cDNA (Fig. 1B). **B** Longer exposure of lanes 1–5. **C** The same blot probed with the ribulose-1,5-bisphosphate carboxylase/oxygenase small subunit

GS sense and antisense transcripts accumulate to levels several-fold higher than the endogenous tobacco GS mRNA

Poly(A)$^+$ RNA from the leaves of plants transformed with the sense and antisense constructs and control plants was subjected to Northern blot analysis using a double-stranded GS gene fragment from pGS100 (Fig. 4). The accuracy of RNA loading was verified by probing the RNA blots with a rRNA gene probe (data not shown) and a Rubisco small subunit probe (De Rocher et al. 1991). As seen in Fig. 4A (lanes 2, 3, 4, 6, 7 and 8), both sets of transformants (containing either the sense or antisense GS constructs) exhibited higher levels of hybridization with the GS gene probe compared to the control (lanes 1, 5). The results suggest that both the sense and antisense transformants were accumulating high levels of the corresponding GS transcript. While the transformants with the sense GS constructs appeared to contain more GS transcripts than the transformants with the antisense GS constructs, a high degree of plant to plant variation in the level of GS transcripts was observed in both sets of transformants. Thus, sense GS transformant A1 appeared to have about a 10-fold lower level of GS transcripts than transformants E1 and E2 (based on the hybridization signal, Fig. 4A) and the antisense GS transformant D1 similarly appeared to have a 10- to 20-fold higher level of antisense GS transcript than the transformant D3. The antisense GS transcripts appeared to migrate as three different molecular weight species (Fig. 4B). This can probably be accounted for by the choice of polyadenylation sites and/or length of poly(A) tails.

There appears to be a correlation between the level of the sense GS transcripts and the increase in GS_1 polypeptide, and between the steady-state level of antisense GS transcript and the reduction in GS polypeptides in the transformants. However, the correlation is not entirely quantitative. The sense transformants E1 and E2, in spite of an approximately 10-fold higher level of GS transcripts compared to transformant A1, showed only a slight increase in the GS_1 polypeptide (Fig. 2B).

No decrease in endogenous GS mRNA in plants with antisense GS constructs

To check specifically for changes in the levels of the endogenous GS mRNA in the antisense plants, poly(A)$^+$ RNA from antisense GS and control plants was subjected to Northern analysis using the strand-specific riboprobe targeted against the endogenous sense GS transcripts. The RNA loadings were the same as in Fig. 4. As seen in Fig. 5A, no difference in hybridization to the riboprobe was observed between antisense GS plants and control plants. Our results suggest that the antisense alfalfa GS transcript does not lower the steady-state level of the endogenous GS transcripts in the heterologous plant, tobacco. Since a significant decrease in

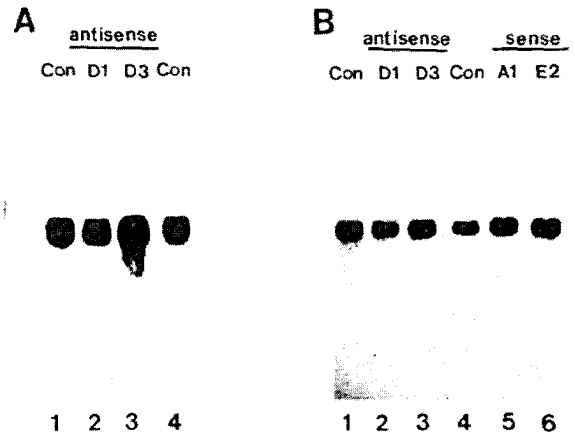

Fig. 5A and B. Analysis of the endogenous tobacco GS transcript levels in the leaves of transformants containing the antisense construct. **A** Analysis of the GS_1 transcript levels in the transformed tobacco plants. Poly(A)$^+$ RNA (2 μg/lane) from the leaves of controls (lanes 1 and 4) and two plants transformed with the antisense GS constructs (lanes 2 and 3) were subjected to Northern analysis using an antisense strand-specific riboprobe to the coding region of the alfalfa GS cDNA. **B** Analysis of the GS_2 transcript levels in the transformed tobacco plants. Poly(A)$^+$ RNA (2 μg/lane) from controls (lanes 1 and 4), two independent transformants containing antisense GS (D1 and D3, lanes 2–3) and two containing the sense GS construct (E1 and A1, lanes 5–6) were subjected to Northern analysis using a 1.5 kb *Eco*R1 fragment from pGS185 that encodes a pea GS_2 cDNA (Tingey and Coruzzi 1987)

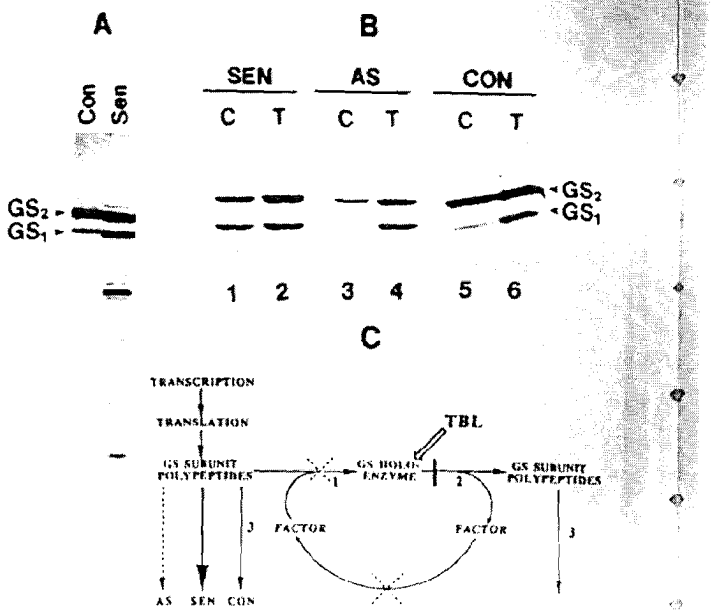

Fig. 6A–C. Analysis of possible regulatory control of GS holoenzyme assembly. **A** Western blot analysis of total soluble leaf protein extracts (200 μg/lane) from mature control tobacco (CON) and a mature sense transformant (SEN). The samples were separated by SDS-PAGE, transferred to nitrocellulose and the filter probed with pea seed GS antibody. The positions of GS_1 and GS_2 polypeptides are indicated. **B** Excised leaves from control tobacco (CON), sense transformant E2 (SEN) and antisense transformant D1 (AS) were incubated overnight in infusion buffer (10 mM D,L-malic acid, 10 mM K_2HPO_4, pH 4.1; Grabau et al. 1986) in the presence and absence of the GS inhibitor tabtoxinine-β-lactam (TβL; 25 μM). Total soluble protein extracts (100 μg/lane) were separated by SDS-PAGE, transferred to nitrocellulose and the filter probed with pea seed GS antibody. The positions of GS_1 and GS_2 polypeptides are indicated. **C** Proposed model for the post translational regulation of the assembly of the GS holoenzyme. Processes labeled 1, 2 and 3 denote assembly, turnover and proteolysis, respectively. *Thin arrows* represent normal rates of turnover, *dashed arrows* represent reduced rates, while *thick arrows* represent highly enhanced rates. The site of action of TβL is denoted as a *thick cross bar*, while the inhibitory effects of the blockage on GS assembly are represented by *broken crosses*. AS, SEN and CON represent antisense, sense and control plants, respectively

GS proteins is observed in the GS_1 antisense plants, it is likely that inhibition occurs at the level of translation.

No change in the steady state levels of GS_2 mRNA in the transformants

To check if overexpression or downregulation of GS_1 affects the level of GS_2 transcripts, leaf poly(A) RNA from the transformants and control plants was subjected to Northern blot analysis using a double-stranded GS_2 gene probe from pea (Tingey et al. 1988). The blot was probed with a rRNA gene probe to standardize loads (data not shown). As seen in Fig. 5B, while the antisense transformant D1 (lane 2) showed a slightly lower level of hybridization, the sense GS_1 transformants (lanes 5 and 6) showed no difference compared to the control (lanes 1 and 4). The results suggest that the pea GS_2 probe does not hybridize to the alfalfa or tobacco GS_1 transcript. Furthermore, the results also suggest that overexpression of GS_1 sense or GS_1 antisense transcripts does not significantly affect the level of GS_2 transcripts.

Assembly of GS subunits into a holoenzyme is under regulatory control

The steady-state level of GS_1 protein in the GS_1 overexpressing transformants did not show a direct correlation with the steady-state level of the corresponding transcript. Furthermore, analysis of the GS protein profile in crude leaf extracts from older GS_1 overexpressing plants has consistently shown the presence of higher levels of small molecular weight immunoreactive products compared to controls (Fig. 6A). These small molecular weight immunoreactive proteins most probably represent GS breakdown products. Taken together, these results suggest that GS_1 subunits synthesized in excess of a certain threshold level are degraded.

Hence we propose that the measured level of GS subunits, particularly in older plants, is not a true measure of synthesis, since this does not take GS turnover into account. To obtain a true measure of GS synthesis, we analyzed the effect of in vivo stabilization of GS by tabtoxine-β-lactam in control plants and transformants with either the sense or antisense GS constructs. Tabtoxinine-β-lactam (TβL), an irreversible inhibitor of GS en-

zyme, binds to the GS holoenzyme and prevents its dissociation into subunits, thus preventing its turnover (Temple et al. 1990). As seen in Fig. 6B, uptake of TβL by the leaves resulted in higher levels of accumulation of GS proteins compared to untreated tissue in all three cases. However, while the leaf from the plant with the antisense GS_1 construct showed about a fivefold increase in the level of GS_1 and GS_2 proteins as a result of TβL treatment, the TβL-treated leaf from the GS_1 overexpressing plants showed only a slight increase in GS_1 and GS_2 levels over the untreated control. The increase in GS levels in TβL treated control leaf over untreated leaf was intermediate between that obtained for the GS_1 antisense and the GS_1 overexpressing plants. Irrespective of the levels of GS proteins in the untreated samples, after TβL treatment the levels of GS subunits in the GS_1 antisense and GS_1 overexpressing plants were identical. This would imply that the amount of GS holoenzyme that is stabilized by TβL is about the same in both the GS_1 antisense and the GS_1 overexpressing plants. Taken together, the results suggest that the assembly of GS subunits into a holoenzyme is a rate-limiting step.

Manipulation of the level of GS protein in tobacco affects total GS activity and total protein content

While the antisense GS_1 transformant showing the highest level of GS_1 antisense RNA (D1) exhibited visible symptoms of nitrogen deficiency, the GS_1 overexpressing plants (E1 and E2) were visibly greener than control plants. This would imply that manipulation of the GS protein level affects overall plant performance. As seen in Fig. 7B, the GS_1 overexpressing plants exhibit about a 45% increase in total soluble protein over control, the GS_1 antisense plants (D1 and E3) exhibit a 40% decrease in total soluble protein. Furthermore, while the GS_1 depressed plants (D1 and E3) exhibit a 40% decrease in GS activity, the GS_1 overexpressing plants exhibit a 25% increase in GS activity (Fig. 7A). The weak antisense plants (C2 and D3) did not show any significant difference in GS activity and total soluble protein compared to the control. In these measurements, GS activity was calculated based on fresh weight, since the sense and antisense plants showed substantial changes in total soluble protein. This is despite the fact that, in older tissues, the transformants did not show such a large difference in GS protein levels compared to the control.

Modulation of GS protein levels affects phosphoenolpyruvate carboxylase (PEPC) and hydroxypyruvate reductase (HPR) levels in tobacco leaves

To check specifically if modulation of GS levels affects other related plant processes, we analyzed relative levels of PEPC and HPR in the most strongly affected antisense (D1) and sense (E2) plants. PEPC catalyzes the

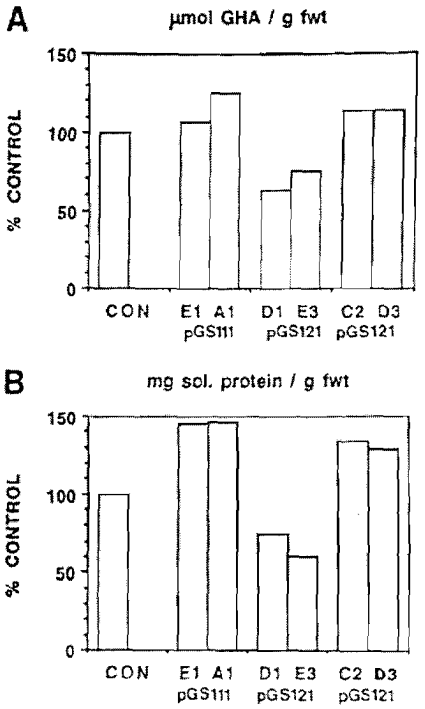

Fig. 7A and B. Analysis of leaf GS activity and total protein levels in the leaves of sense and antisense transformants. The fifth leaf from similarly aged mature control tobacco plants (CON), transformants containing both the sense (pGS111 E1 and A1) and transformants containing the antisense construct (pGS121 D1, E3, C2 and D3) were assayed as crude extracts for total leaf GS activity and total soluble protein. **A** GS activity based on fresh weight (µmol GHA/g fwt). **B** Total soluble protein (mg soluble protein/g fwt) is represented as the percentage difference over control values

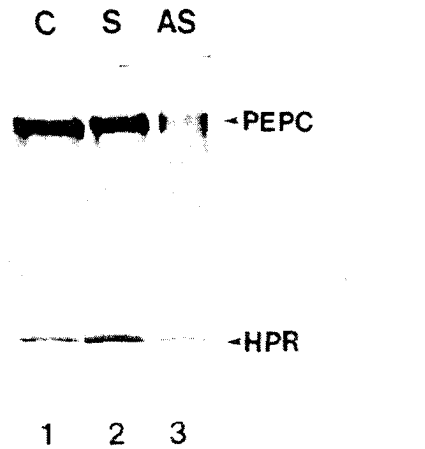

Fig. 8. Analysis of phosphoenolpyruvate carboxylase (PEPC) and hydroxypyruvate reductase (HPR) levels in the leaves of the sense and antisense transformants. Total soluble leaf protein (200 µg/lane) from mature control tobacco (C), sense transformant E2 (S) and antisense transformant D1 (AS) was fractionated by SDS-PAGE followed by Western blot analysis using antibodies to PEPC and HPR

anaplerotic fixation of CO_2 to form the precursor for the GS/GOGAT cycle and HPR catalyzes the conversion of hydroxypyruvate to glycerate in the photorespiratory cycle. Western blot analysis was performed on total soluble proteins from the control, a GS_1 antisense (D1) and a GS_1 overexpressing plant (E2) using a PEPC antibody and an HPR antibody (Fig. 8). While the GS_1 antisense plants exhibit decreased levels of both proteins, the GS_1 overexpressing plants exhibit only a very minor or no increase in the level of these proteins over the control.

Discussion

The results presented in this paper demonstrate that the full-length alfalfa GS_1 gene, when transcribed in an antisense orientation from the 35S promoter, is capable of downregulating both GS_1 and GS_2 in tobacco leaves. Besides demonstrating that the antisense RNA approach is effective in silencing GS gene expression, our results also show that a heterologous antisense GS_1 transcript is effective in inhibiting both GS_1 and GS_2 gene expression. Most of the reports on successful inhibition of target gene expression using the antisense RNA approach have utilized a homologous gene (van der Krol et al. 1988a; 1990a; Smith et al. 1990; Quick et al. 1991; Stockhaus et al. 1990). There are only a few reports on partial inhibition using heterologous antisense RNA (van der Krol et al. 1988b; Visser et al. 1990; Schuch et al. 1990). The antisense approach has also been shown not to be effective for certain genes (van der Krol et al. 1990b; Delauney et al. 1988). It is well established that a higher degree of sequence homology is maintained among the same GS isoform from different sources than among the different GS isoforms (Pesole et al. 1991; Tingey and Coruzzi 1987). We would thus predict that alfalfa GS_1 antisense RNA is more homologous to tobacco GS_1 than to the GS_2 genes. The alfalfa GS_1 coding sequence shares 81% homology at the nucleotide level to the GS_1 coding sequence of *Nicotiana plumbaginifolia* (Tingey and Coruzzi 1987). Five different regions that are highly conserved among the different GS isoforms were identified, based on multiple alignment (Pesole et al. 1991). It is interesting to note that while the alfalfa GS_1 gene did not hybridize to immobilized GS_2 mRNA of either tobacco or alfalfa, as determined by Northern analysis or analysis of hybrid selected translation products, the antisense alfalfa GS_1 transcript was capable of downregulating GS_2 in tobacco. While the mechanism of inhibition of gene expression by antisense RNA is not known, one of the proposed models assumes the mediation of hybrid formation between the mRNA and antisense RNA molecules (van der Krol et al. 1988b). If the mechanism is as proposed, our results would suggest that formation of short duplexes along the length of the GS transcript with the antisense alfalfa GS_1 RNA is sufficient for effective inhibition of expression of the GS genes in tobacco.

The steady-state level of antisense alfalfa GS_1 transcript in the leaves of transgenic tobacco was substantially higher than the endogenous GS mRNA level in the leaves of the control tobacco. We also observed that the level of antisense GS_1 transcript was indicative of the extent of inhibition. However, in spite of the accumulation of high levels of alfalfa GS_1 antisense transcripts and a decrease in the level of GS_1 and GS_2 polypeptides, no change in the level of endogenous steady-state GS mRNA was observed in these plants. This is somewhat in contrast to the more thoroughly investigated systems involving the chalcone synthase genes of petunia (van der Krol et al. 1988b; 1990a, b) and the polygalacturonase gene of tomato (Smith et al. 1990). In these cases involving homologous antisense RNA, the antisense gene transcript did not accumulate to high levels and no correlation between the antisense transcript level and the extent of inhibition was observed. Furthermore, in these and other well investigated systems (Delauney et al. 1988; Cannon et al. 1990; Oeller et al. 1991), inhibition of expression by antisense RNA has always been accompanied by a decrease in the level of the target gene message. In some of these systems (van der Krol et al. 1988a, b; Mol et al. 1990), it has been proposed that the antisense RNA forms a duplex with the corresponding endogenous sense RNA and the duplex is susceptible to degradation by RNases, resulting in the loss of the target mRNA. RNA (antisense or sense) in excess of the duplex then accounts for the remaining intact antisense or sense RNA, as the case may be. The relatively high steady-state level of antisense alfalfa GS_1 RNA, together with the absence of any effect on the endogenous GS transcript in our system, would imply that the heteroduplex is stable. The heteroduplex consisting of duplexed regions intermingled with single-stranded loops, could very well behave like RNA molecules with extensive secondary structure. This heteroduplex would differ in its physical properties from a duplex formed between homologous strands. It is likely that short duplexes, flanked by nonaligned sequences along the length of the heteroduplex, stabilize the hybrid. Eguchi (1991) has shown that an RNA double helix is stabilized by the presence of terminal unpaired bases.

A substantial lowering in the level of GS polypeptides without an accompanying decrease in the level of endogenous GS transcript in the GS_1 antisense plants, suggests that the inhibition of expression occurs at the translational level. It is likely that the stable heteroduplex formed between tobacco GS transcripts and the antisense alfalfa GS_1 transcripts is not accessible to the translational machinery. The heteroduplex is either not able to exit the nucleus or the duplex does not allow for ribosome binding and interaction with the required translation factors.

Our results suggest that the alfalfa GS_1 antisense RNA, when produced in a constructive manner downregulates both GS_1 and GS_2, in spite of the fact that the level of GS_2 transcripts far exceeds that of GS_1 (Edwards et al. 1990). This is contradictory to the general belief that antisense inhibition requires a large excess

of antisense RNA (van der Krol et al. 1988 b). However, the molecular analysis of the mechanism by which the alfalfa GS_1 antisense RNA inactivates GS_1 and GS_2 is complicated by the fact that the two genes are expressed in different cell types (Edwards et al. 1990; Brears et al. 1991) and the local concentration of each transcript type is not known. This implies that steady-state levels of antisense GS_1 RNA measured by Northern blot analysis cannot reflect the ratio of antisense to sense RNA in each cell type. Of course, it remains unresolved whether the decreased expression of GS_2 in the GS_1 antisense plants is a direct effect of antisense inhibition or an indirect effect resulting from the poor overall performance of the plants.

It is not surprising that in the GS_1 sense tobacco plants, the alfalfa GS_1 subunits are not only synthesized but also assembled into an active enzyme. Eckes et al. (1989) had previously demonstrated the successful expression of this particular alfalfa gene in tobacco at the enzymatic level. What is, however, interesting is that an increase in GS_1 protein is also accompanied by an increase in GS_2 protein subunits and active GS_2 enzyme (Fig. 2). Since no increase in GS_2 transcript was observed in the GS_1 overexpressing transformants, the increase in GS_2 protein in these transformants can be attributed either to improved translation efficiency or to increased GS enzyme stability. Changes in the level of protein synthesis and turnover, in turn, can be attributed to the overall performance of the plants.

GS_1 genes are specifically expressed around the vascular tissue (Edwards et al. 1990; Brears et al. 1991). Based on that, it has been proposed that GS_1 protein functions in the synthesis of glutamine for nitrogen transport (Brears et al. 1991). Furthermore, based on the fact that GS_1 gene expression is enhanced in senescing rice leaves and is accompanied by a marked decrease in glutamate content, Kamachi et al. (1991) have also suggested that GS_1 functions in the synthesis of glutamine for transport from senescing leaves to growing tissue. How does modulation of GS_1 levels contribute to plant performance? Can improved performance by the GS_1 overexpressing plants be simply due to increased GS activity in the transport cells or does the GS_1 protein, now synthesized in the photosynthetic cells, assist in the assimilation of photorespiratory ammonia that diffuses out of the chloroplast? Similarly, is the poor performance of the GS_1 antisense transformants attributable to downregulation of GS_1 or GS_2 protein? These questions can only be addressed if the expression of these genes is modulated individually and in specific cell types. Such experiments are in progress.

A decrease in the steady-state level of HPR and PEPC in the GS_1 antisense plants and a minor increase in these proteins in the GS_1 overexpressing plants is probably reflective of the overall status of the plant. However, we cannot rule out the possibility that changes in these proteins are a direct outcome of GS levels. HPR catalyzes a step in the photorespiratory cycle and thus changes in the level of this protein probably are a result of changes in GS_2 levels. Similarly, changes in PEPC levels accompanying changes in GS levels might indicate that synthesis of an empty C-skeleton is somehow influenced by the plant's potential to load these C-skeletons with nitrogen. This interesting observation indeed merits further investigation.

Based on the analysis of GS protein levels in leaves of GS_1 overexpressing sense, and GS_1 antisense, plants incubated with the toxin TβL, it appears that the assembly of the GS holoenzyme is under some type of regulatory control (Fig. 6C). The toxin binds irreversibly to the GS holoenzyme (Langston-Unkefer et al. 1987), thus preventing its turnover (Temple et al. 1990). In its presence, the GS subunits that assemble into a holoenzyme are locked in and the subunits are not proteolytically degraded (Temple et al. 1990). If all the GS subunits that are synthesized in a plant are assembled into a holoenzyme, the GS_1 overexpressing plants should show relatively higher accumulation of GS_1 polypeptide in the presence of TβL, when compared to control or antisense plants. In our studies, however, irrespective of the plant background (transformed with sense or antisense GS constructs), the steady-state level of GS subunits in the presence of TβL was more or less similar (Fig. 6B). Based on these results, we propose that assembly of GS subunits into a holoenzyme requires a factor which is released when the enzyme is turned over and recycled (Fig. 6C). In the presence of TβL, the holoenzyme, along with the factor, is locked into the assembled form and the factor is no longer available for assembling more GS subunits. Blocking the GS holoenzyme turnover in the GS overexpressing plants will very rapidly inhibit the assembly process. Thus, over an extended period of time, blockage in turnover will result in the same amount of GS subunits being locked into a holoenzyme, irrespective of the concentration of available GS subunits (sense versus antisense plants). In this context, it is interesting to note that Hemon et al. (1990) showed that tobacco plants transformed with the *Phaseolus vulgaris* γGS coding sequence driven by the 35S promoter contained high levels of γGS; and the corresponding enzymatic activity in young plants, but very insignificant levels of γGS in mature plants. The γGS transcript level was, however, comparable in both young and mature plants. Our results also point to a similar phenomenon. While the younger transformants (sense and antisense) showed a dramatic difference in the level of GS protein when compared to the control (Figs. 2 and 3), the older plants did not show such substantial differences (Fig. 6B). Our interpretation of our data and those of Hemon et al. (1990) is that the post-translational assembly of GS polypeptides is probably under some form of developmental control. It is crucial that we understand this regulatory step if we wish to successfully modulate GS levels in plants.

Acknowledgements. We thank Dr. Jeff Velton and Dr. Mel Oliver for the critical reading of the manuscript. This material is based upon work supported by the Southwestern Consortium for Plant Genetics and Water Resources and the Agriculture Experiment Station at New Mexico State University.

References

Blackwell RD, Murray AJS, Lea PJ (1987) Inhibition of photosynthesis in barley with decreased levels of chloroplastic glutamine synthetase activity. J Exp Bot 38:1799–1809

Bradford MM (1976) A rapid and sensitive method for the quantitation of microgram quantities of protein utilizing the principle of protein dye-binding. Anal Biochem 72:248–252

Brears T, Walker EL, Coruzzi GM (1991) A promoter sequence involved in cell-specific expression of the pea glutamine synthetase GS3A gene in organs of transgenic tobacco and alfalfa. Plant J 1:235–244

Cannon M, Platz J, O'Leary M, Sookdeo C, Cannon F (1990) Organ-specific modulation of gene expression in transgenic plants using antisense RNA. Plant Mol Biol 15:39–47

Cock JM, Mould RM, Bennett MJ, Cullimore JV (1990) Expression of glutamine synthetase genes in roots and nodules of *Phaseolus vulgaris* following changes in the ammonium supply and infection with various *Rhizobium* mutants. Plant Mol Biol 14:549–560

DasSarma S, Tischer E, Goodman HM (1986) Plant glutamine synthetase complements a *ghlA* mutation in *Escherichia coli*. Science 232:1242–1244

Delauney AJ, Tabaeizadeh Z, Verma DPS (1988) A stable bifunctional antisense transcript inhibiting gene expression in transgenic plants. Proc Natl Acad Sci USA 85:4300–4304

De Rocher EJ, Michalowski CB, Bohnert HJ (1991) cDNA sequences for transcripts of the ribulose-1,5-bisphosphate carboxylase/oxygenase small subunit gene family of *Mesembryanthemum crystallinum*. Plant Physiol 95:976–978

De Vries SC, Springer J, Wessels JGH (1982) Diversity of abundant mRNA sequences and patterns of protein synthesis in etiolated and greened pea seedlings. Planta 156:129–135

Dunn K, Dickstein R, Feinbaum R, Burnett BK, Peterman TK, Thoidis G, Goodman HM, Ausubel FM (1988) Developmental regulation of nodule-specific genes in alfalfa root nodules. Mol Plant-Microbe Interact 1:66–74

Eckes P, Schmitt P, Daub W, Wengenmayer F (1989) Overproduction of alfalfa glutamine synthetase in transgenic tobacco plants. Mol Gen Genet 217:263–268

Edwards JW, Coruzzi GM (1989) Photorespiration and light act in concert to regulate the expression of the nuclear gene for chloroplast glutamine synthetase. Plant Cell 1:241–248

Edwards JW, Walker EL, Coruzzi GM (1990) Cell-specific expression in transgenic plants reveals nonoverlapping roles for chloroplast and cytosolic glutamine synthetase. Proc Natl Acad Sci USA 87:3459–3463

Eguchi Y (1991) Antisense RNA. Annu Rev Biochem 60:631–652

Feinberg AP, Vogelstein B (1983) A technique for radiolabeling DNA restriction endonuclease fragments to high specific activity. Anal Biochem 132:6–13

Forde BG, Cullimore JV (1989) The molecular biology of glutamine synthetase in higher plants. Oxf Surv Plant Mol Cell Biol 6:247–296

Forde BG, Day HM, Turton JF, Shen W-J, Cullimore JV, Oliver JE (1989) Two glutamine synthetase genes from *Phaseolus vulgaris* L. display contrasting developmental and spatial patterns of expression in transgenic *Lotus corniculatus* plants. Plant Cell 1:391–401

Gebhardt C, Oliver JE, Forde BG, Saarelainen R, Miflin BJ (1986) Primary structure and differential expression of glutamine synthetase genes in nodules, roots and leaves of *Phaseolus vulgaris*. EMBO J 5:1429–1435

Grabau LJ, Blevins DG, Minor HC (1986) Stem infusions enhanced methionine content of soybean storage protein. Plant Physiol 82:1013–1018

Hemon P, Robbins MP, Cullimore JV (1990) Targeting of glutamine synthetase to the mitochondria of transgenic tobacco. Plant Mol Biol 15:895–904

Hirel B, Bouet C, King B, Layzell D, Jacobs F, Verma DPS (1987) Glutamine synthetase genes are regulated by ammonia provided externally or by symbiotic nitrogen fixation. EMBO J 6:1167–1171

Horsch RB, Fry FE, Hoffmann NL, Eichholtz D, Rogers SG, Fraley RT (1985) A simple and general method for transferring genes into plants. Science 227:1229–1231

Kamachi K, Yamaya T, Mae T, Ojima K (1991) A role for glutamine synthetase in the remobilization of leaf nitrogen during natural senescence in rice leaves. Plant Physiol 96:411–417

Konieczny A, Szczyglowski K, Boron L, Przybylska M, Legocki AB (1988) Expression of lupin nodulin genes during root nodule development. Plant Sci 55:145–149

van der Krol AR, Lenting PE, Veenstra J, van der Meer IM, Koes RE, Gerats AGM, Mol JNM, Stuitje AR (1988a) An anti-sense chalcone synthase gene in transgenic plants inhibits flower pigmentation. Nature 333:866–869

van der Krol AR, Mol JNM, Stuitje AR (1988b) Modulation of eukaryotic gene expression by complementary RNA or DNA sequences. Bio Techniques 6:958–976

van der Krol AR, Mur LA, de Lange P, Mol JNM, Stuitje AR (1990a) Inhibition of flower pigmentation by antisense CHS genes: Promoter and minimal sequence requirements for the antisense effect. Plant Mol Biol 14:457–466

van der Krol AR, Stuitje AR, Mol JNM (1990b) Modulation of floral pigmentation by antisense technology. In: Mol JNM, van der Krol AR (eds) Antisense nucleic acids and proteins: fundamentals and applications. Marcel Dekker, New York, pp 125–139

Laemmli UK (1970) Cleavage of structural proteins during the assembly of the head of bacteriophage T4. Nature 227:680–685

Langston-Unkefer PJ, Robinson AC, Knight TJ, Durbin RD (1987) Inactivation of pea seed glutamine synthetase by the toxin, Tabtoxinine-β-lactam. J Biol Chem 262:1608–1613

Lara M, Cullimore JV, Lea PJ, Miflin BJ, Johnston AWB, Lamb JW (1983) Appearance of a novel form of plant glutamine synthetase during nodule development *in Phaseolus vulgaris* L. Planta 157:254–258

Laskey RA, Mills AD (1975) Quantitative film detection of ^{3}H and ^{14}C in polyacrylamide gels by fluorography. Eur J Biochem 56:335–341

Lightfoot DA, Green NK, Cullimore JV (1988) The chloroplast-located glutamine synthetase of *Phaseolus vulgaris* L.: Nucleotide sequence, expression in different organs and uptake into isolated chloroplasts. Plant Mol Biol 11:191–202

Maniatis T, Fritsch EF, Sambrook J (1982) Molecular cloning: A laboratory manual. Cold Spring Harbor Laboratory Press, Cold Spring Harbor, New York

Mann AF, Fentem PA, Stewart GR (1980) Tissue localization of barley (*Hordeum vulgare*) glutamine synthetase isoenzymes. FEBS Lett 110:265–267

Miao G-H, Hirel B, Marsolier MC, Ridge RW, Verma DPS (1991) Ammonia-regulated expression of a soybean gene encoding cytosolic glutamine synthetase in transgenic *Lotus corniculatus*. Plant Cell 3:11–22

Miflin BJ, Lea PJ (1980) Ammonia assimilation. In: Miflin BJ (ed) The Biochemistry of Plants, vol 5. Academic Press, New York, pp 169–202

Mol JNM, van der Krol AR, van Tunen R, van Blokland R, de Lange P, Stuitje AR (1990) Regulation of plant gene expression by antisense RNA. FEBS Lett 268:427–430

Murray MG, Peters DL, Thompson WF (1981) Ancient repeated sequences in the pea and mung bean genomes and implications for genome evolution. J Mol Evol 17:31–42

Oeller PW, Min-Wong L, Taylor LP, Pike DA, Theologis A (1991) Reversible inhibition of tomato fruit senescence by antisense RNA. Science 254:437–439

Pesole G, Bozzetti MP, Lanave C, Preparata G, Saccone C (1991) Glutamine synthetase gene evolution: A good molecular clock. Proc Natl Acad Sci USA 88:522–526

Peterman TK, Goodman HM (1991) The glutamine synthetase gene family of *Arabidopsis thaliana*: light-regulation and differential expression in leaves, roots and seeds. Mol Gen Genet 230:145–154

Quick WP, Schurr U, Fichtner K, Schulze E-D, Rodermel SR, Bogorad L, Stitt M (1991) The impact of decreased Rubisco on photosynthesis, growth, allocation and storage in tobacco plants which have been transformed with antisense rbcS. Plant J 1:51–58

Rogers SG, Klee HJ, Horsch RB, Fraley RT (1987) Improved vectors for plant transformation: Expression cassette vectors and new selectable markers. Methods Enzymol 153:253–277

Sakamoto A, Takeba G, Shibata D, Tanaka K (1990) Phytochrome-mediated activation of the gene for cytosolic glutamine-synthetase (GS_1) during imbibition of photosensitive lettuce seeds. Plant Mol Biol 15:317–323

Schuch W, Knight M, Bird A, Grima-Pettenati J, Boudet A (1990) Modulation of plant gene expression. In: Lycett GW, Grierson D (eds) Genetic engineering of crop plants. Butterworth, England, pp 221–230

Sengupta-Gopalan C, Pitas JW (1986) Expression of nodule-specific glutamine synthetase genes during nodule development in soybeans. Plant Mol Biol 7:189–199

Sengupta-Gopalan C, Gambliel H, Feder I, Richter H, Temple SJ (1991) Different modes of regulation involved in nodulin gene expression in soybean. In: Hennecke H, Verma DPS (eds) Advances in molecular genetics of plant-microbe interactions, vol 1. Kluwer Academic Publishers, Netherlands, pp 304–309

Shapiro BM, Stadtman ER (1970) Glutamine synthetase (*E. coli*). Methods Enzymol 17A:910–922

Smith CJS, Watson CF, Morris PC, Bird CR, Seymour GB, Gray JE, Arnold C, Tucker GA, Schuch W, Harding S, Grierson D (1990) Inheritance and effect on ripening of antisense polygalacturonase genes in transgenic tomatoes. Plant Mol Biol 14:369–379

Stewart GR, Mann AF, Fentem PA (1980) Enzymes of glutamate formation: glutamate dehydrogenase, glutamine synthetase and glutamate synthase. In: Miflin BJ (ed) The biochemistry of plants, vol 5. Academic Press, New York, pp 271–327

Stockhaus J, Höfer M, Renger G, Westhoff P, Wydrzynski T, Willmitzer L (1990) Antisense RNA efficiently inhibits formation of the 10 kd polypeptide of photosystem II in transgenic potato plants: analysis of the role of the 10 kd protein. EMBO J 9:3013–3021

Temple SJ, Knight TJ, Unkefer PJ, Sengupta-Gopalan C (1990) Stabilization of glutamine synthetase protein by the toxin, tabtoxinine-β-lactam. In: Gresshoff PM, Roth LE, Stacey G, Newton WE (eds) Nitrogen fixation: Achievements and objectives. Chapman and Hall, New York London

Tingey SV, Coruzzi GM (1987) Glutamine synthetase of *Nicotiana plumbaginifolia*. Plant Physiol 84:366–373

Tingey SV, Walker EL, Coruzzi GM (1987) Glutamine synthetase genes of pea encode distinct polypeptides which are differentially expressed in leaves, roots and nodules. EMBO J 6:1–9

Tingey SV, Tsai F-Y, Edwards JW, Walker EL, Coruzzi GM (1988) Chloroplast and cytosolic glutamine synthetase are encoded by homologous nuclear genes which are differentially expressed *in vivo*. J Biol Chem 263:9651–9657

Titus DE, Hondred D, Becker WM (1983) Purification and characterization of hydroxypyruvate reductase from cucumber cotyledons. Plant Physiol 72:402–408

Visser RGF, Feenstra WJ, Jacobsen E (1990) Manipulation of granule-bound starch synthase activity and amylose content in potato by antisense genes. In: Mol JNM, van der Krol AR (eds) Antisense nucleic acids and proteins: fundamentals and applications. Marcel Dekker, New York, pp 141–155

Communicated by J. Schell

MGG

Molecular & General Genetics

An International Journal

Continuation of Zeitschrift für Vererbungslehre. The First Journal on Genetics Founded in 1908

Volume 239 Number 3 June 1993

Continuation see back cover page

Springer International

Molecular & General Genetics

MGG provides publication in all areas of general and molecular genetics – developmental genetics, somatic cell genetics, and genetic engineering – irrespective of the organism. Articles on animal or plant breeding or human genetics will be accepted only if the results described have significance for fundamental genetics. Reports that are exclusively dealing with nucleic acid sequences are published only if they are judged to be of wide interest and biological significance. The findings reported should be novel and not under consideration for publication elsewhere. The presentation should be intelligible to as wide an audience as possible.

Subscription information

ISSN 0026-8925

Volumes 235–240 (3 issues each) will appear in 1993.

The journal MGG appears monthly. It is published by Springer Produktions-Gesellschaft, Berlin, Heidelberger Platz 3, W-1000 Berlin 33, Germany. Application to mail at Second-Class Postage rates is pending at New York, New York and additional mailing offices.

Postmaster send all address changes to:

MGG, Springer-Verlag New York, Inc., Journal Fulfillment Services Dept., 44 Hartz Way, Secaucus, NY 07096, USA.

North America. Recommended annual subscription rate: approx. US $ 2194.00 (single issue price: approx. US $ 145.00) including carriage charges. Subscriptions are entered with prepayment only. Orders should be addressed to:

Springer-Verlag New York Inc.
Service Center Secaucus

44 Hartz Way
Secaucus, NJ 07094, USA
Tel. (201) 348-4033, Telex 0023-125 994,
Fax (201) 348-4505

All other countries. Recommended annual subscription rate: DM 3198.00 plus carriage charges; (Germany: DM 58.74 incl. VAT; other countries: DM 78.30. SAL or airmail charges are available upon request. SAL delivery is mandatory to Japan, India, and Australia/New Zealand). Volume price: DM 533.00, single issue price: DM 213.00 plus carriage charges. Orders can either be placed via a bookdealer or sent directly to: Springer-Verlag, Heidelberger Platz 3, W-1000 Berlin 33, Germany, Tel. (0)30/82 07-1, Telex 1-83 319, Fax (0)30/8 21 40 91.

Personal subscriptions: Molecular & General Genetics is available at a personal subscription rate. Orders should be mailed to Springer-Verlag.

Changes of address: Allow six weeks for all changes to become effective. All communications should include both old and new addresses (with Postal Codes) and should be accompanied by a mailing label from a recent issue. According to § 4 section 3 of the German Postal Services Data Protection Regulations, the German Federal Post Office can inform the publisher of a subscriber's new address even if the subscriber has not submitted a formal application for mail to be forwarded. Subscribers not in agreement with this procedure may send a written complaint to Springer-Verlag's Berlin office within 14 days of publication this issue.

Back volumes: Prices are available on request.

Microform editions are available from:
University Microfilms International,
300 N. Zeeb Road,
Ann Arbor, MI 48106, USA

Production

Springer Produktions-Gesellschaft
3050 – Journal Production Department
Claudia Perkhoff
Heidelberger Platz 3
W-1000 Berlin 33, Germany
Tel.: (0) 30/82 07 435, Telex: 1-85 411,
Fax: (0) 30/8 20 74 40, e-mail: c=DeGeo-Mail; RZB1:sv-pg/sv-pgs@ dcfrz1.das.net

Responsible for advertisements

Springer-Verlag
E. Lückermann
Heidelberger Platz 3
W-1000 Berlin 33, Germany
Telephone (0) 30/82 07-0, Telex 01-85 411,
Fax (0) 30/8 20 73 00

Typesetting

Universitätsdruckerei H. Stürtz AG
W-8700 Würzburg, Germany

Printers

H. Heenemann, W-1000 Berlin 42, Germany

Bookbinding

Lüderitz & Bauer, W-1000 Berlin 11, Germany

Springer-Verlag GmbH & Co KG
W-1000 Berlin 33, Germany
Printed in Germany

Springer International

Mol Gen Genet (1993) 239:425–434

MGG

Inhibition of tobacco NADH-hydroxypyruvate reductase by expression of a heterologous antisense RNA derived from a cucumber cDNA: Implications for the mechanism of action of antisense RNAs

Melvin J. Oliver[1], **David L. Ferguson**[1], **John J. Burke**[1], **Jeff Velten**[2]

[1] United States Department of Agriculture, Agricultural Research Service, Cropping Systems Research Laboratory, Plant Stress and Water Conservation Unit, Lubbock, Texas 79401, USA

[2] New Mexico State University, Plant Genetic Engineering Laboratory, Las Cruces, New Mexico 88003, USA

Received: 31 August 1992 / Accepted: 27 January 1993

Abstract. Tobacco plants were genetically transformed to generate antisense RNA from a gene construct comprised of a full-length cucumber NADH-dependent hydroxypyruvate reductase (HPR) cDNA placed in reverse orientation between the cauliflower mosaic virus 35S promoter and a nopaline synthase termination/polyadenylation signal sequence. In vivo accumulation of antisense HPR RNA within eight independent transgenic tobacco plants resulted in reductions of up to 50% in both native HPR activity and protein accumulation relative to untransformed tobacco plants (mean transgenote HPR activity = 67% wild type, mean transgenote HPR protein = 63% wild type). However, in contrast to previous reports describing antisense RNA effects in plants, production of the heterologous HPR antisense RNA did not systematically reduce levels of native tobacco HPR mRNA (mean transgenote HPR mRNA level = 135% wild type). Simple regression comparison of the steady-state levels of tobacco HPR mRNA to those of HPR antisense RNA showed a weak positive correlation (r value of 0.548, $n = 9$; n is wild type control plus eight independent transformants; significant at 85% confidence level), supporting the conclusion that native mRNA levels were not reduced within antisense plants. Although all transgenic antisense plants examined displayed an apparent reduction in both tobacco HPR protein and enzyme activity, there is no clear correlation between HPR activity and the amount of either sense ($r = 0.267$, $n = 9$) or antisense RNA ($r = 0.175$, $n = 9$). This compares to a weak positive correlation between HPR mRNA levels and the amount of HPR activity observed in wild-type SR1 tobacco plants ($r = 0.603$, $n = 5$). The results suggest that in vivo production of this heterologous HPR antisense RNA is inhibitory at the level of HPR-specific translation and produces its effect in a manner not dependent upon, nor resulting in, a reduction in steady-state native HPR mRNA levels. In this context, the observed antisense effect appears to differ mechanistically from most antisense systems described to date.

Key words: NADH-hydroxypyruvate reductase (HPR) – Heterologous antisense RNA – Antisense RNA inhibition – Transgenic tobacco

Communicated by J. Schell

Correspondence to: M.J. Oliver

Introduction

Photorespiration is a pathway in C3 plants that counterproductively generates CO_2 in the light as a consequence of an oxygenase activity associated with the carbon fixation enzyme, ribulose bisphosphate carboxylase. Although this activity results in a decline in plant productivity, and so is anthropocentrically non-beneficial, it is thought to be advantageous to the plant because of its role in limiting the amount of toxic oxygen species present within photosynthesizing plant cells (Ogren, 1984). Under drought conditions, where stomata are closed during daylight hours, atmospheric CO_2 cannot enter the leaves. Photorespiration provides a sink for the electron transport pathway through both ribulose bisphosphate oxygenase activity and refixation of CO_2 (Ogren 1984). This, in turn, limits the production of toxic oxygen species and thus suggests a role for photorespiration in stress protection. Our interests center on determination of which enzymes in this pathway control the flux of carbon through it and are major contributors to its proposed stress protection properties. One of the strategies available to us is the use of antisense technology to create mutants deficient in specific enzyme activities to determine their overall importance in these processes. This strategy, for pragmatic reasons, would become more powerful if heterologous antisense constructs could be used effectively to inhibit target enzymes. Several reports have suggested that heterologous antisense RNAs can be effective in inhibiting the expression of target genes in plants (Visser 1989; Visser et al. 1991; Temple et al. 1992), in one case apparently as effectively

as homologous antisense RNA (van der Krol et al. 1988a).

In order to test the use of heterologous antisense RNAs and evaluate their effectiveness in our system, we elected to introduce into tobacco chimeric genes that would generate antisense RNA molecules from a cucumber peroxisomal NADH-dependent hydroxypyruvate reductase (HPR, EC 1.1.1.29) cDNA. This enzyme is an integral part of the glycolate pathway involved in photorespiration in plants (Tolbert 1981), catalyzing the reduction of hydroxypyruvate to glycerate with the simultaneous oxidation of the cofactor NADH (Zelitch 1953; Stafford et al. 1954).

We chose HPR as the target enzyme for several reasons. The full-length cDNA for the cucumber HPR was available (as a kind gift from W. Becker, University of Wisconsin) and its sequence and properties are well characterized (Greenler et al. 1989). In addition, in order to have an effective evaluation of the heterologous antisense behavior it was critical that inhibition of the target enzyme should not have a lethal effect. HPR appeared to fit this criterion in that barley mutants having only 5% of wild-type HPR activity in leaf tissues are fully viable (Murray et al. 1989). These plants are deficient in a NADH-preferring HPR (Kleczkowski et al. 1990) but are still capable of photorespiration and allow for levels of carbon fixation that are 75% of those seen in wild-type barley under identical conditions. The same is also true (75% of wild-type levels) for plants tested under photorespiratory conditions in an atmosphere containing 50% oxygen. The capability of the barley mutant to contend with stresses other than 50% oxygen (e.g. drought or water stress) was not evaluated.

This report documents our successful use of the cucumber HPR antisense RNA to inhibit expression of the native tobacco gene and our examination of potential mechanisms by which inhibition occurs. Our findings demonstrate a reduction of HPR production associated with in vivo production of HPR antisense RNA (mean transgenote protein level and activity are 63% and 67% wild type). However, contrary to most reports of antisense effect, accumulation of steady-state tobacco HPR mRNA in leaf tissues, relative to wild type SR1 tobacco controls, is not systematically inhibited, and is instead often enhanced in the presence of the cucumber HPR antisense RNA. Possible molecular mechanisms contributing to the observed heterologous antisense RNA effect are presented and discussed.

Materials and methods

Construction of the cucumber HPR antisense gene. The full-length cucumber HPR cDNA sequence contained in the plasmid pBSH18 (Greenler et al. 1989) was excised with *Eco*RI and purified by electroelution from a 0.7% agarose gel. This fragment was inserted into the plant expression vector pMON316 (described by Rogers et al. 1987) at the *Eco*RI site situated between the cauliflower mosaic virus (CaMV) 35S promoter and the nopaline synthase (NOS) 3′ untranslated region. A plasmid containing the *Eco*RI fragment in reverse orientation, relative to the 35S promoter, was identified by restriction enzyme digestion and was designated pMONHPR$^-$ (see Fig. 1).

Conjugation into Agrobacterium tumefaciens *and transformation of tobacco.* The pMONHPR$^-$ constructs were conjugated into *A. tumefaciens* by the triple mating procedure described by Fraley et al. (1983). In these conjugations the *A. tumefaciens* strain GV3111SE was used as a recipient. This strain contains a disarmed Ti-plasmid, pTiB6S3-SE, in which the T-DNA phytohormone biosynthetic genes, the T_L DNA right border and all of T_R DNA have been deleted and replaced with a bacterial kanamycin resistance marker (Fraley et al. 1985). Transformation of sterile leaf segments of *Nicotiana tabacum* cv. SR1 and regeneration of transformed plants (R_0 plants) was achieved using the procedure described by Horsch et al. (1985). Putative transformants, plantlets surviving on kanamycin sulfate (Km) at 100 μg/ml, were further screened for the production of nopaline as described by Otten and Schilperoort (1978). After curing of *A. tumefaciens*, plants were grown in the laboratory at room temperature in 4 in pots containing a peat/soil/vermiculite mix under a 16 h day/8 h night light regime emitting approximately 50 $\mu E/m^2/s^1$. R_0 plants expressing high levels of the cucumber HPR antisense RNA were identified by isolation and analysis of leaf tissue RNA (as described below). Eight independently transformed HPR antisense plants were selfed and the resulting seed collected and germinated on MS medium containing 200 μg/ml Km. Five Km-resistant plants (R_1 plants) from each of the eight original transformants ($n = 8$) were grown for further analysis as described below.

Determination of HPR activity and protein levels in transgenic leaf tissue. The R_1 plants analyzed were simultaneously germinated and maintained within the same chamber in order to minimize developmental, physiological and environmental differences between plants. However, in a further attempt to average any remaining intra- and inter-plant variation in HPR expression, leaf tissue was randomly sampled from populations of five R_1 plants derived from each of the eight original transformants. Therefore, the single assay results reported for each of the eight independent transformants represent the average value from several leaves harvested from five separate R_1 plants. The pooled samples were ground to a fine powder in liquid nitrogen, the powder transferred to pre-cooled microcentrifuge tubes, and the extraction medium (50 mM TRIS-HCl pH 6.8), 1 mM PMSF, 1 mM EDTA, 10 μM leupeptin, 5.6 μM N-[N-(L-3-trans-carboxyoxiran-2-carbonyl)-L-leucyl]-agmatine) added (50 μl/50 mg tissue). The resulting slurry was vigorously mixed for 3 min at room temperature before centrifuging at 14 000 rpm in an Eppendorf microcentrifuge for 5 min. The supernatant was collected, given a second brief centrifugation at 14 000 rpm, and divided into aliquots. One aliquot was used immediately to determine HPR activity and protein concentration, whereas the

remainder were stored at −90° C for later use in Western blot analyses.

The HPR activity was determined by the method of Titus et al. (1983) with a Gilford* Response spectrophotometer (Gilford Instrument Labs, Oberlin, Ohio). Protein concentration was measured using the procedure of Bradford (1976) with bovine gamma-globulin as the protein standard.

The relative amount of HPR in the extracts of the different transformants was measured on Western blots by the following procedure. The samples from the previously frozen aliquots were separated using SDS-PAGE (Laemmli 1970), and transferred to a nitrocellulose filter. Anti-serum to HPR (provided by Dr. Wayne Becker, University of Wisconsin) was used as the primary antibody, and anti-rabbit IgG antibodies conjugated to alkaline phosphatase as the secondary antibody. Immunochemical staining was achieved by the method of Billingsley et al. (1987). A standard curve was determined for each blot by the use of different amounts of protein from the SR1 extract and the amount of HPR protein in each transformant was calculated relative to untransformed SR1.

Isolation and analysis of RNA from transgenic leaf tissue. RNA from leaf tissue, randomly sampled from five R_1 plants as described above, was isolated through a series of phenol extractions (Lane and Tumaitis-Kennedy 1981). Total and poly(A)$^+$ RNA, selected by oligo-dT cellulose chromatography, was resolved by electrophoresis through a 1.2% agarose gel containing formaldehyde as described in Ausubel et al. (1989). The RNA was transferred onto Duralon-UV nylon membranes using the Posiblot Pressure Blotter system (Stratagene, La Jolla, Calif.) as detailed by the manufacturer. RNA was crosslinked to the nylon membranes by exposure to 120 000 μJ cm^2 of UV radiation in a model 1800 Stratalinker (Stratagene, La Jolla, Calif).

Probes and hybridization conditions

Cucumber HPR antisense RNA. The probe for cucumber antisense RNA was the full-length cDNA fragment isolated by *Eco*RI digestion of the plasmid pBSH18 (Greenler et al. 1989). The cDNA was radiolabeled with α[^{32}P]dCTP by nick-translation using a kit and protocol supplied by Bethesda Research Laboratories (Gaithersberg, Md. Hybridization was achieved in a solution containing 25 mM potassium phosphate (pH 7.4), 5 × SSC, 5 × Denhardt's solution, 50% formamide and 50 μg/ml of sonicated salmon sperm DNA at 42° C.

Tobacco HPR mRNA. The probe for the native tobacco HPR mRNA was a 3′ non-translated fragment isolated from a partial tobacco HPR cDNA by *Eco*RI digestion. The partial cDNA used was isolated from a tobacco leaf cDNA library purchased from Stratagene (La Jolla, Calif.) utilizing the cucumber HPR cDNA as a probe. The conditions for use of this probe to identify the tobacco counterpart were at a stringency that allowed hybridization to the tobacco HPR mRNA on Northern blots (room temperature annealing and washed in 0.5 × SSC at 42° C). The tobacco HPR cDNA is 750 bp in length displaying 79% nucleic acid sequence similarity with the cucumber HPR coding region (86.3% at the amino acid level). The tobacco HPR cDNA non-translated 3′ sequence has no significant similarity to the cucumber cDNA. The probe, isolated by *Eco*RI digestion, is 305 bp in length and contains the complete 3′ end of the cDNA and 76 bp of the tobacco coding sequence (the small portion of coding region is also approximately 80% similar to the cucumber HPR cDNA but under the conditions of hybridization used, see conditions for the antisense RNA described above, this probe is specific for the tobacco HPR; see Fig. 4, SR1 lane).

Small subunit (SSU) of ribulose bisphosphate carboxylase. The probe for the SSU of ribulose bisphosphate carboxylase was a partial fragment of the cDNA clone rbcS-1 from *Mesembryanthemum crystallinum* (de Rocher et al. 1991) received as a kind gift from H. Bohnert (University of Arizona). The fragment was isolated by *Eco*RI digestion and contains coding sequences as well as the 3′ non-translated sequence. The probe was used under the hybridization conditions described above for the cucumber HPR cDNA.

Image analysis for quantification of RNA and protein. In order to quantify relative levels of RNA and protein, autoradiograms derived from the Northern analyses and the Western blots were digitized using a Bio Image Visage 2000 (Bio Image Products, MilliGen/Biosearch Division of Millipore, Ann Arbor, Mich.) image analysis system. Briefly, the images of Northerns or Westerns were scanned, captured and quantified using a comparative log software program (Whole Band Analysis) and the results reported as total integrated intensity in each band.

Statistical analysis of data. In order to minimize observer bias during comparison of the various measured values for protein and RNA levels within the eight independent transformants examined, simple linear regression (Siegel 1988) was applied pairwise to selected data sets (e.g. enzyme activity, protein levels and both sense and antisense RNA levels). Using plants showing a range of values, such an analysis can suggest the existence of positive or negative relationships between the steady-state levels of the gene products measured.

Results

A full-length cDNA clone, containing the entire coding sequence for a cucumber hydroxypyruvate reductase, a 40 base 5′ non-coding leader sequence and a 210 base 3′

* Mention of trademark or proprietary product does not constitute a guarantee or warranty of the product by the US Department of Agriculture and does not imply its approval to the exclusion of other products that may also be suitable

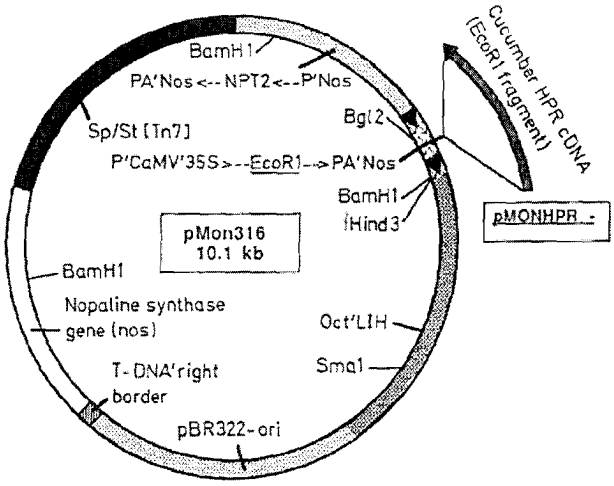

Fig. 1. Plasmid map for pMONHPR[-]. The cucumber NADH-dependent hydroxypyruvate reductase (HPR) cDNA (flanked by *Eco*RI linkers) was inserted into the plant expression vector pMON316 (Rogers et al. 1987) at the unique *Eco*RI site within a multiple cloning site between the CaMV 35S promoter and the nopaline synthase polyadenylation signal (P'CaMV'35S → MCS → PA'NOS). Other pertinent features of the plasmid include: P'NOS → NPT2 → PA'NOS (a plant functional kanamycin resistance marker consisting of the nopaline synthase promoter, neomycin phosphotransferase II gene of Tn*5* and the nopaline synthase signal); St/Sp [Tn7] (a streptomycin/spectinomycin resistance marker from Tn*7*) and Oct'LIH (the "left internal homology" from the octopine TL region)

non-coding sequence, was cloned into the *Eco*RI site of the intermediate vector pMON316, placing the 3′ non-coding sequence proximal to the 35S promoter element (Fig. 1). This construct was used to insert the antisense 35S-HPR chimeric gene, via an *Agrobacterium*-based leaf disc system, into the genome of tobacco (SR1). Independently transformed plants were selected by their ability to survive in media containing kanamycin and screened for nopaline synthesis. Transgenic plants meeting these criteria were further tested for expression of the introduced HPR antisense gene by Northern analysis using the cucumber HPR cDNA as a probe (under hybridization conditions that did not detect the native tobacco HPR RNA, data not shown). Eight independent plant transformants (R_0 plants), each containing easily detectable levels of HPR antisense RNA, were self-crossed and seedling progeny (R_1 plants) selected on media containing 200 μg/ml Km and propagated for further analysis. Transgenic plants normally display a range of transgene expression levels, usually attributed to the so-called position effect (Peach and Velten 1991) and, less often, to differences in transgene copy number. Consistent with the findings of others, the anti-HPR transformants chosen for analysis show a range of antisense RNA levels (ca 16-fold difference between the highest and lowest measured values). Such a range in antisense RNA levels is desired in that it allows examination of the relationship(s), if any, between measured antisense RNA concentrations and target gene expression, both at mRNA and protein levels.

In order to average inter-plant HPR expression variability between R_1 plants derived from the same R_0 transformant, analysis was performed on samples consisting of several leaves from five separate R_1 plants. Independent determinations of HPR protein levels and enzymatic activity (from three pooled samples), as well as native HPR mRNA levels (from five samplings, data not shown) indicated a standard error in sampling ranging from 5% to 25% for protein measurements and ap-

Table 1. Quantification of NADH-dependent hydroxypyruvate reductase (HPR) expression

Plant identity[a]	IOD[b] Tob[c] HPR mRNA	IOD Cuc[d] antisense HPR mRNA	IOD SSU Rubisco[e] mRNA	Corrected[f] IOD Tob HPR mRNA	Corrected IOD Cuc HPR mRNA	HPR protein level[g]	HPR activity[h]
SR1 control	2.6 (0.3)[i]	0.0	20.9	12.2 (1.9)[i]	0.0	100	1301 (132)[i]
R6-2	1.4	5.4	7.1	19.1	76.5	79	1247 (210)
R6-3	2.7	2.7	24.3	10.9	11.1	69	979 (166)
R6-5	1.8	1.0	12.9	13.6	7.9	36	756 (33)
R6-6	3.5	3.4	16.0	22.1	21.4	58	736 (137)
R6-7	1.3	10.9	13.8	9.5	78.6	96	1136 (186)
R6-8	3.3	17.0	32.7	10.1	52.1	45	731 (111)
R6-10	4.6	21.0	16.5	27.7	127.4	54	653 (94)
R6-14	3.3	12.2	38.4	8.5	31.9	60	745 (210)

[a] Each R6 identifier refers to the R_1 (selfed) progeny of an independently transformed tobacco plant

[b] IOD denotes the integrated optical density of the total hybridization signal contained in the single band on the autoradiogram of the Northern blot

[c] Tob, tobacco

[d] Cuc, cucumber

[e] SSU, small subunit of ribulose bisphosphate carboxylase (Rubisco)

[f] Corrected indicates the initial value divided by the SSU value and multiplied by 100

[g] HPR protein levels are relative to those determined for untransformed SR1 tobacco plants

[h] One unit equals 10 nmol NADH per min per mg total soluble protein

[i] The value given is derived from a single analysis (five pooled plant samples) of SR1 HPR mRNA from the same blot used to determine the mRNA levels within the antisense tranformants. The value in brackets represents the standard error predicted from a separate determination of HPR mRNA within five individual SR1 plants

[j] The value given for HPR enzyme activity is the mean of three independent assays (using separate pools of tissue from five plants). The number in brackets represents the standard error of the three determinations

proximately 10% for RNA quantification (see Fig. 1 and Table 1).

Enzyme and protein level analysis in antisense plants

Leaf samples, randomly collected as described above, were analyzed for HPR enzyme activity, total protein and tobacco HPR protein (via cross-reaction with a cucumber HPR antibody). The results, presented in Fig. 2, indicate a consistent reduction in the level of the native tobacco HPR within trangenotes expressing the cucumber HPR antisense construct.

Figure 2a exhibits a Western blot of leaf protein extracts separated by SDS-polyacrylamide gel electrophoresis and immunoreacted with a polyclonal antibody synthesized against the pure cucumber HPR enzyme. The antibody cross-reacts with the tobacco HPR enzyme and thus serves as a convenient tool for an estimation of native HPR protein levels. The Western analysis visually demonstrates that expression of the cucumber HPR antisense RNA inhibits accumulation of the native tobacco HPR protein. To assess more accurately the effect of the cucumber HPR antisense RNA, the immunoreactive bands were quantified by image analysis (as described in Materials and methods) and the native HPR protein levels calculated relative to a standard curve obtained from a graduated series of SR1 extracts of known total soluble protein concentrations (lanes 1–5). Samples used to construct standard curves were actually electrophoresed on both sides of the transgenote protein samples on the Western blots (not shown) to compensate for possible blotting variations. The resulting quantification of native HPR protein in the transgenic plants (reported in Table 1) is expressed relative to the amount of the same protein in untransformed SR1 and not as absolute HPR protein levels. The average of two such determinations from two separate Western analyses were used to generate the values, presented as a percentage of the native HPR level in SR1 untransformed tobacco, given in Fig. 2b and Table 1.

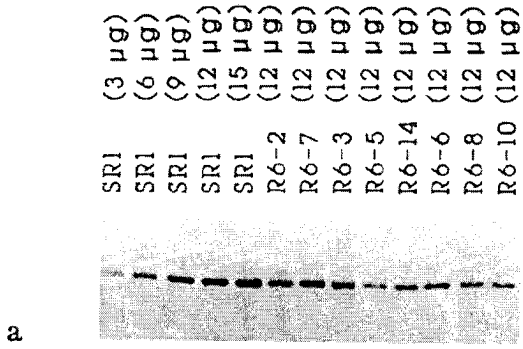

a

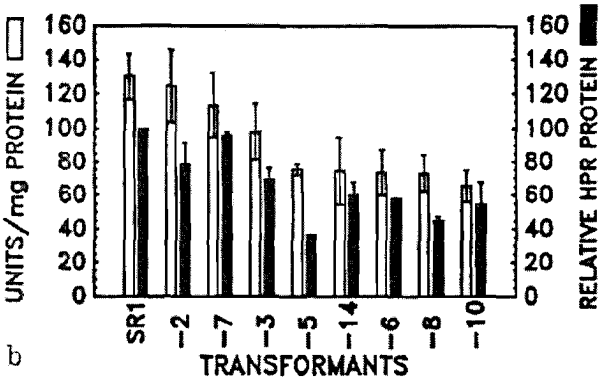

b

Fig. 2a, b. Tobacco HPR protein and activity analyses. **a** Western blot of partially purified leaf protein extracts. Microgram quantities refer to the amount of total leaf protein electrophoresed in individual lanes. **b** Comparison of enzyme activity and relative protein in leaf extracts. Units of enzyme are defined as the quantity of enzyme that oxidizes 10 nmol of NADH per min per mg total soluble protein in the extract. HPR protein levels are estimated from a standard curve of integrated optical densities of SR1 HPR leaf protein extracts. The error bars shown for enzyme activity are for three separate experiments. The error bars on the protein determinations (the mean of two determinations) represent the variance between the two separate HPR protein measurements.

As was anticipated, the reduction in level of tobacco HPR protein accumulation is also manifested as a drop in the levels of leaf HPR enzyme activity compared to the level seen in SR1. Most of the transgenic plants (R6-5, R6-6, R6-8, R6-10, R6-14) exhibit HPR activities reduced to at least 3 times standard error below the wild type SR1 level, with a maximal inhibition to approximately 50% wild type (R6-10). For the same plants, levels of the tobacco HPR protein range from 45-60% (with the exception of R6-5 which exhibits approximately 35% of the SR1 level). Transgenics R6-2, R6-3 and R6-7 show a less significant (10–20%, within one standard error) reduction in HPR activity, however, none of the antisense transformants tested exceeded either the wild-type protein amount or activity level. As expected, statistical analysis of the data ($n = 9$, eight transformants and wild-type SR1) demonstrates a positive correlation (simple linear regression r value of 0.880; Siegel 1988) between the measured level of enzyme activity and the amount of HPR protein in the leaf tissue extracts.

Total and poly(A)$^+$ RNA analysis

In order to determine if the decrease in both enzyme activity and tobacco HPR protein in the transgenic plants results from a reduction in the accumulation of tobacco HPR, mRNA Northern analysis of leaf RNA was undertaken. Total RNA extracts from leaf samples, again consisting of several leaves from five separate R_1 transgenotes, were analyzed by Northern blot and successive hybridizations with probes specific to either cucumber HPR mRNA (from the cucumber HPR cDNA), or the tobacco HPR mRNA (consisting of the 3′ nontranslated region of a tobacco HPR cDNA clone), as well as a probe for the SSU of ribulose bisphosphate carboxylase (from *M. crystallinum*). As an example of the analysis the results from one of the blots using leaf RNA from primary transformants (R_0 plants) are shown in Fig. 3. The results demonstrate that within each sample both the cucumber HPR antisense RNA and the tobacco

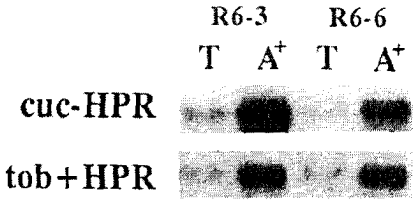

Fig. 3. Total and poly(A)$^+$ RNA comparisons. T, total RNA; A$^+$, poly(A)$^+$ RNA (oligo-dT cellulose selected). RNA samples are from the original R_0 (possibly chimeric) transformants and were not used for expression level comparison

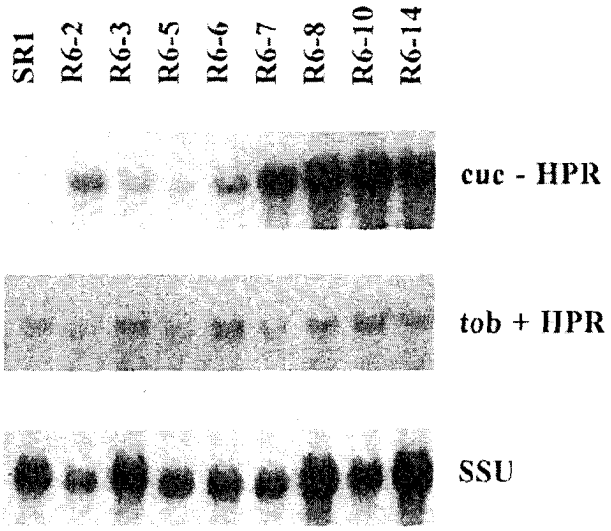

Fig. 4. Comparative northern hybridizations. Total RNA analysis. All hybridizations were performed on the same Northern blot. Each lane contains 20 µg of total leaf RNA isolated from R_1 plants. Individual probes are: cuc – (minus) HPR, cucumber HPR cDNA probe for the cucumber HPR antisense RNA (Northern wash: 0.1 × SSC, 0.1% SDS at 50° C); tob + (plus) RNA, 3′ non-translated region of a tobacco HPR cDNA for the tobacco HPR mRNA (Northern wash: 0.1 × SSC, 0.1% SDS at 56° C); SSU, fragment of a cDNA clone for the small subunit of ribulose bisphosphate carboxylase mRNA (Northern wash: 0.1 × SSC, 0.1% SDS at 50° C)

HPR mRNA are detectable, even without enrichment by poly(A) selection. The cucumber HPR antisense RNA is enriched by passage over oligo-dT cellulose, suggesting correct processing and polyadenylation of the antisense RNA (see Fig. 3). The size of both the HPR antisense RNA (ca 1800 bases) and the tobacco HPR mRNA (ca 1640 bases) were estimated using florescently stained RNA molecular weight markers and are consistent with predicted sizes.

To facilitate analysis of the molecular effect(s) of expression of the cucumber HPR antisense RNA, total unselected RNA samples extracted from populations of the R_1 generation from each independent transformant (selected as described in the Materials and methods) were subjected to Northern analysis (see Fig. 4). From these data it appears that accumulation of the cucumber HPR antisense RNA does not consistently inhibit the steady-state levels of the native tobacco HPR mRNA. In order to define further the relationship between the antisense and native HPR mRNA populations, autoradiograms from the hybridizations were subjected to digital image analysis (as described in Materials and methods). To allow eventual comparison between separate experiments (e.g. between the RNA and protein quantifications), the same blot was also hybridized to a probe directed against the SSU of ribulose bisphosphate carboxylase and the resulting value used to normalize for sample preparation, loading variability, transfer effectiveness and hybridization efficiency between lanes. The SSU probe was chosen because accumulation of SSU mRNA is light-regulated in a manner similar to the HPR mRNA (Greenler et al. 1989), thus minor differences resulting from variation in the physiological and environmental state of the plants are minimized. In addition, measured SSU levels closely followed the values obtained through quantification of ethidium bromide UV fluorescence from ribosomal RNA bands in the Northern gel (obtained by image analysis of photographic reproductions, data not shown). The results of the RNA quantification are summarized in Table 1.

Despite minor differences in probe specific activities and autoradiogram exposure times (designed to give maximum signal without burnout of photographic emulsion), the hybridization results from the individual probes used in this analysis qualitatively reflect the expected relative abundances of each RNA within the leaf tissue, with SSU > cucumber HPR antisense RNA > tobacco HPR mRNA. The minor differences in probe specific activity and exposure times do not affect comparisons within samples as all hybridizations and comparison were carried out using the same Northern blot and thus the relationship between signals from each lane should accurately reflect the ratio of in vivo RNA levels. Plant-to-plant variation in RNA levels is also minimized by the use of a random sampling procedure in which tissue from a population of five separate transgenic progeny plants was pooled.

Contrary to expectation – an antisense-induced reduction in native tobacco HPR (sense) mRNA – the measured levels of tobacco mRNA within the antisense expressing transgenotes were often found to exceed the steady-state HPR mRNA levels within wild-type plants (see Table 1, Corrected Tob HPR mRNA). These data clearly do not indicate any net reduction in native HPR mRNA levels resulting from the presence of antisense RNA. In fact, comparison of the two RNAs (tobacco +RNA vs cucumber −RNA) by simple linear regression suggests a possible positive correlation between the levels of cucumber HPR antisense RNA and tobacco HPR mRNA (n = 8, simple linear regression r = 0.548, significant at approximately 85% confidence level; Siegel 1988).

Comparison of HPR protein, RNA and cucumber HPR antisense RNA

In order to gain better insight into the means by which a heterologous antisense RNA may inhibit native gene

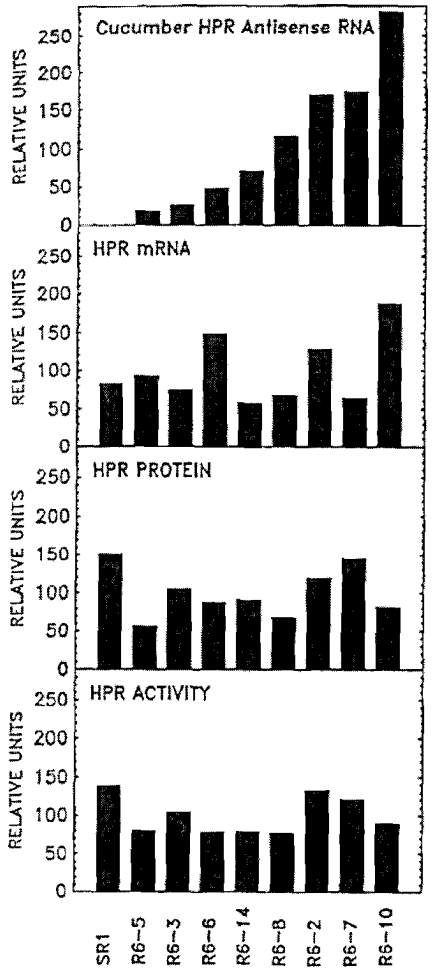

Fig. 5. Overall comparison of tobacco HPR activity, protein and mRNA levels with the level of cucumber HPR antisense RNA within individual transgenic lines

expression, it is pertinent to compare the results from the protein and enzyme analyses with those for the two different HPR RNA species (cucumber HPR antisense and tobacco sense HPR mRNA). In order to compare such diverse data sets, it was necessary to present the various component levels as the ratio of each measured value to the mean for that data group (we multiplied by 100 for convenience in plotting the data). The results of this overview are exhibited in Fig. 5.

In all cases where there is accumulation of cucumber HPR antisense RNA there is also an apparent decrease in both tobacco HPR activity and protein level. However, the exact relationships between the four measured parameters vary from one set of R_1 progeny to another. There is no obvious correlation between HPR levels and the amount of antisense RNA. This is most clearly seen when one compares R6-5 and R6-10. In R6-10 the relative level of the cucumber HPR antisense RNA is at the highest level seen in all the R_1 progeny sets whilst the decrease in HPR activity and protein levels are similar to that seen for R6-5 where the level of antisense is the lowest of all the samples. Simple linear regression analysis gives values of $r = 0.175$ and 0.183 for an antisense-to-HPR activity and an antisense-to-HPR protein comparison, respectively. Interestingly, there is also little obvious relationship between the accumulation of tobacco HPR mRNA and either HPR activity or protein level in the transgenic plants. Simple linear regression analysis gives values (of $r = 0.267$ and $r = 0.212$ for a tobacco HPR mRNA-to-HPR activity and a tobacco HPR mRNA-to-HPR protein comparison, respectively. Comparisons of HPR activity to tobacco HPR mRNA levels, without the conflicting presence of the cucumber HPR antisense RNA, were monitored in a separate experiment utilizing five separate SR1 samples (data not presented). In these plants the comparison of HPR activity levels and HPR mRNA levels by linear regression analysis gives an r value of 0.601 ($n = 5$).

Discussion

The results we have presented demonstrate the successful use of a heterologous antisense HPR RNA to modulate the activity of the corresponding enzyme in a plant. Expression of the cucumber HPR antisense RNA inhibited both the enzyme activity and protein levels of the tobacco NADH-hydroxypyruvate reductase, although the reduction in this enzyme never exceeded 50%. Wether the relatively mild reduction in HPR activity observed results from the use a heterologous antisense RNA and could be enhanced with a fully homologous antisense RNA remains to be tested. There is some evidence that heterologous antisense RNAs are not as effective as homologous antisense RNAs. Visser et al. (1991) reported that the use of antisense RNAs for maize granule-bound starch synthase (GBSS) in potato resulted in an approximately 20–90% inhibition of potato GBSS activity in transgenic tubers. The use of a homologous GBSS antisense RNA resulted in an approximately 80–100% inhibition in the same system. In both cases the amount of GBSS protein closely followed the enzyme activity data (the accumulation levels of the potato GBSS mRNA were not reported and so a direct comparison with our data is not possible). Using a heterologous glutamine synthetase (GS) antisense RNA, Temple et al. (1992) also failed to attain high levels of inhibition of enzyme activity (maximal 40% reduction), possibly due to a direct selection against extensive inhibition of GS. Although the mature HPR antisense tobacco plants produced in this study did not display any obvious phenotype associated with HPR reduction, it is possible that at some stage during the process of regeneration from *A. tumefaciens* transformed tissue, cells heavily depleted in HPR activity may have been counter-selected, producing regenerated transgenotes showing only moderate HPR inhibition. There are many additional explanations for the failure to obtain complete, or nearly complete, elimination of HPR gene expression within the antisense plants, including the possibility that tissue-specific patterns of expression of the native HPR gene(s) and introduced antisense construct may not consistently overlap within the transgenic plants.

The attainment of a 100% inhibition of enzyme activity is not an absolute necessity in our quest to explore the importance of photorespiratory enzymes in plant stress protection as partial inhibition is likely to result in a measurable impairment in the ability of the plant to withstand drought and oxidative stresses. This is also the case in many other systems that lend themselves to this use of antisense technology, in particular where null mutations may lead to a lethal phenotype. Our data confirm that the use of heterologous antisense RNAs is a viable option when attempting to engineer plant photorespiratory systems metabolically.

In our system the inhibition of tobacco HPR gene expression by heterologous cucumber HPR antisense RNA may operate in a very different way from that seen for gene expression reduction through homologous antisense RNAs in plants. In most reported cases in which antisense RNAs have been successfully used to inhibit expression of specific target genes in plants, accumulation of the target mRNA (when measured) has been significantly reduced. Such reports include both artificially introduced target genes: glucuronidase (Robert et al. 1989; Cannon et al. 1990), chloramphenicol acetyltransferase (Ecker and Davis 1986; Delauney et al. 1988) and nopaline synthetase (Rothstein et al. 1987; Sandler et al. 1988; Goring et al. 1991); phosphinotricin acetyltransferase (Cornelissen and Vandewiele 1989); and authentic resident plant genes: chalcone synthase (van der Krol et al. 1988a; 1990a,b), granule-bound starch synthase (Visser et al. 1990, 1991), polygalacturonase (Smith et al. 1988, 1990; Sheehy et al. 1988), ribulose bisphosphate carboxylase (Rodermel et al. 1988), cDNA pTOM5 encoding a 46.7 kDa protein (Bird et al. 1991), a photosystem II 10 kDa protein (Stockhaus et al. 1990), a ripening- and wound-related gene family (Hamilton et al. 1990), pectin methyltransferase (Tieman et al. 1992) and a β-1,3-glucanase (Neuhaus et al. 1992). Reduction in the steady-state level of a target RNA upon expression of antisense RNA is not restricted to introduced constructs and has also been shown to occur within at least one eukaryotic system where the homologous antisense RNA is a natural part of the gene control strategy (Hildebrandt and Nellen 1992). Our use of a heterologous antisense RNA clearly exhibits no measurable negative effect upon the level of the target mRNA and indeed the data suggest that the antisense RNA may actually enhance accumulation of the target mRNA. Although the weak positive correlation between the levels of antisense and target mRNA reported here is based upon a relatively small data set, it does argue convincingly against any net decrease in the level of target mRNA. Thus, the mechanisms(s) by which the cucumber HPR antisense RNA inhibits expression of the native HPR protein and enzyme activity appears to differ, at least qualitatively, from those systems that evoke a reduction in the target mRNA.

We are aware of only two additional reported cases where an antisense RNA did not produce a net reduction of target mRNA steady state level. One study employed a Cd^{2+}-inducible antisense *c-src* gene to inhibit production of its target (homologous) $pp60^{c\text{-}src}$ within polyomavirus-transformed rat cells (Amini et al. 1986). More closely related to our results, expression of a heterologous antisense glutamine synthase RNA in tobacco also failed to affect the steady-state levels of the native target mRNA (Temple et al. 1992). Based upon our data, and those of Temple et al. (1992), it is tempting to speculate that a relatively stable target RNA may be more common with heterologous antisense systems, although in at least one system the use of heterologous antisense RNA significantly reduced accumulation of the target mRNA (van der Krol et al. 1988a). It seems likely that the degree of homology, as well as the specific regions of homology, between an antisense RNA and its target nucleic acid are critical factors affecting how the antisense RNA interacts with its target and thus dictate the mechanism(s) by which gene expression is affected. The ways in which heterologous RNAs work may be expected to vary somewhat between different systems, cell types and possibly even between different antisense RNAs directed against the same target.

Our results suggest that the cucumber antisense RNA does not exert its effect by inhibition of either the transcriptional rate or the processing of the tobacco HPR gene, as has been proposed for other eukaryotic systems (Yokoyama and Imamoto 1987). We propose that, as has been suggested for most antisense effects (see reviews by van der Krol et al. 1988b; Mol et al. 1990; Eguchi et al. 1991), the cucumber HPR antisense RNA and the native tobacco HPR mRNA form a duplex molecule that interferes with translation, thereby decreasing HPR protein production and consequently HPR activity in the transformants. If an antisense-target RNA duplex is formed in our system, the observed molecular weight of the native HPR mRNA from transgenic tobacco plants, and its enrichment after passage over oligo-dT cellulose, indicate that neither splicing (if it occurs in the HPR premessenger) nor polyadenylation are significantly affected. If RNA heteroduplex formation reduces translation efficiency, one expected consequence would be reduced association of the target RNA with ribosomes and a net destabilization of the target RNA. In our case, the heteroduplex may compensate for decreased ribosomal protection by an increase in the stability of the native HPR mRNA within the duplex. In the context of our results, it is perhaps pertinent that an RNA double helix is thermodynamically stabilized by the presence of terminal unpaired bases (see Eguchi et al. 1991 for review), hence it may be possible that the cucumber HPR antisense and the tobacco HPR mRNA form more stable duplexes, reducing the rate of mRNA breakdown relative to homologous duplexes. It should be noted that in at least three cases where antisense-target RNA duplexes (homologous) were detected (Kim and Wold 1985; Knecht and Loomis 1987; Yokoyama and Imamoto 1987), the presence of reduced steady-state target mRNA levels suggests that, at least in the case of homologous duplex formation, mRNA stability and/or production rate are reduced.

It is possible to envision several mechanisms by which antisense-mRNA duplex formation might inhibit subsequent translation of the target mRNA. If RNA-RNA

interaction occurs within the nucleus or nuclear pore complexes, transport of the tobacco HPR mRNA into the cytoplasm may be inhibited, diminishing the translatable pool of this message without necessarily reducing the overall concentration of the target mRNA. This model has been suggested for several cases of antisense inhibition of translation (see van der Krol et al. 1988b for review), specifically for the case of thymidine kinase inhibition by antisense RNA induced by methotrexate in a human cell line (Kim and Wold 1985) and for discoidin inhibition by antisense RNA in *Dictyostelium* (Crowley et al. 1985). It is also possible that duplex formation occurs in the cytoplasm, directly inhibiting translation. In this scenario it is likely that the duplex structure would reduce the rate of translation initiation and/or slow the rate of elongation (in either case resulting in less protein produced), possibly in a manner qualitatively different from that of homologous duplexes. Any model invoking changes in RNA stability, duplex formation and translation efficiency, must also consider the potential effects of enzymes such as RNA helicases and cytoplasmic RNAses. Unfortunately, at present very little published data specifically address the nature and control of these classes of enzymes in plants and their in vivo effects remain largely uncontrolled. All the possibilities suggested above offer testable hypotheses for future studies.

Acknowledgements. The authors wish to thank Mrs. Janet Hack and Mrs. Patti Havstead for their excellent technical assistance and Dr. Doug Stocco of the Texas Tech Health Science Center for the unselfish donation of his time and the use of the Bio Image Visage 2000. We would also like to thank Dr. Wayne Becker, University of Wisconsin, for the gift of the full-length cucumber HPR cDNA and Dr. Hans Bohnert, University of Arizona, for the gift of a SSU clone. This work was supported in part by NIH grant GM0766712 (J.V.).

References

Amini S, DeSeau V, Reddy S, Shalloway D, Bolen JB (1986) Regulation of $pp60^{c\text{-}src}$ synthesis by inducible RNA complementary to *c-src* mRNA in polyomavirus-transformed rat cells. Mol Cell Biol 6:2305–2316

Ausubel FM, Brent R, Kingston RE, Moore DD, Seidman JG, Smith JA, Struhl K (1989) Current Protocols in Molecular Biology. Greene Publishing Associates and Wiley-Interscience, New York

Billingsley ML, Pennypacker KR, Hoover CG, Kinkaid RL (1987) Biotinylated proteins as probes of protein structure and protein-protein interactions. Biotechniques 5:22–31

Bird CR, Ray JR, Fletcher JD, Boniwell JM, Bird AS, Teulieres C, Blain I, Bramley PM, Schuch W (1991) Using antisense RNA to study gene function: Inhibition of carotenoid biosynthesis in transgenic tomatoes. Biotechnology 9:635–639

Bradford MM (1976) A rapid and sensitive method for the quantification of microgram quantities of protein utilizing the principle of protein-dye binding. Anal Biochem 72:248–254

Cannon M, Platz J, O'Leary M, Sookdeo C, Cannon F (1990) Organ-specific modulation of gene expression in transgenic plants using antisense RNA. Plant Mol Biol 15:39–47

Cornelissen M, Vandewiele M (1989) Both RNA level and translational efficiency are reduced by antisense RNA in transgenic tobacco. Nucleic Acids Res 17:833–843

Crowley TE, Nellen W, Gomer RH, Firtel RA (1985) Phenocopy of discoidin I-minus mutants by antisense transformation in *Dictyostelium*. Cell 43:633–641

Delauney AJ, Tabaeizadeh Z, Verma DPS (1988) A stable bifunctional antisense transcript inhibiting gene expression in transgenic plants. Proc Natl Acad Sci USa 85:4300–4304

Ecker JR, Davis RW (1986) Inhibition of gene expression in plant cells by expression of antisense RNA. Proc Natl Acad Sci USA 83:5372–5376

Eguchi Y, Itoh T, Tomizawa J-I (1991) Antisense RNA. Annu Rev Biochem 60:631–652

Fraley RT, Rogers SG, Horsch RB, Sanders PR, Flick JS, Adams SP, Bittner ML, Brand LA, Fink CL, Fry JS, Galuppi GR, Golgberg SB, Hoffman NL, Woo SC (1983) Expression of bacterial genes in plant cells. Proc Natl Acad Sci USA 80:4803–4807

Fraley RT, Rogers SG, Horsch RB, Eicholtz DA, Flick JS, Fink CL, Hoffman NL, Sanders PR (1985) The SEV system: A new disarmed Ti plasmid vector system for plant transformation. Biotechnology 3:629–635

Goring DR, Thomson L, Rothstein SJ (1991) Transformation of a partial nopaline synthase gene into tobacco suppresses the expression of a resident wild-type gene. Proc Natl Acad Sci USA 88:1770–1774

Greenler JMcC, Sloan JS, Swartz BW, Becker WM (1989) Isolation, characterization and sequence analysis of a full length cDNA clone encoding NADH-dependent hydroxypyruvate reductase from cucumber. Plant Mol Biol 13:139–150

Hamilton AJ, Lycett GW, Grierson D (1990) Antisense gene that inhibits synthesis of the hormone ethylene in transgenic plants. Nature 346:284–287

Hildebrandt M, Nellen W (1992) Differential antisense transcription from the *Dictyostelium* Eb4 gene locus: Implication on antisense mediated regulation of messenger RNA stability. Cell 69:197–204

Horsch RB, Fry JE, Hoffman NL, Eicholtz D, Rogers SG, Fraley RT (1985) A simple and general method for transferring genes into plants. Science 227:1229–1231

Kim SK, Wold BJ (1985) Stable reduction of thymidine kinase activity in cells expressing high levels of antisense RNA. Cell 42:129–138

Kleczkowski LA, Edwards GE, Blackwell RD, Lea PJ, Givan CV (1990) Enzymology of the reduction of hydroxypyruvate and glyoxylate in a mutant of barley lacking peroxisomal hydroxypyruvate reductase. Plant Physiol 94:819–825

Knecht D, Loomis WF (1987) Antisense RNA inactivation of myosin heavy chain gene expression in *Dictyostelium discoidium*. Science 236:1081–1086

van der Krol AR, Lenting PE, Veenstra J, van der Meer IM, Koes RE, Gerats AGM, Mol JNM, Stuitje AR (1988a) An antisense chalcone synthase gene in transgenic plants inhibits flower pigmentation. Nature 333:866–869

van der Krol AR, Mol JNM, Stuitje AR (1988b) Modulation of eukaryotic gene expression by complementary RNA or DNA sequences. Biotechniques 6:958–976

van der Krol AR, Mur LA, de Lange P, Gerats AGM, Mol JNM, Stuitje AR (1990a) Antisense chalcone synthase genes in petunia: Visualization of variable transgene expression. Mol Gen Genet 220:204–212

van der Krol AR, Mur LA, de Lange P, Mol JNM, Stuitje AR (1990b) Inhibition of flower pigmentation by antisense CHS genes: Promoter and minimal sequence requirements for the antisense effect. Plant Mol Biol 14:457–466

Laemmli UK (1970) Cleavage of structural proteins during the assembly of the head of bacteriophage T4. Nature 227:680–685

Lane BG, Tumaitis-Kennedy TD (1981) Comparative study of levels of secondary processing in bulk mRNA from dry and germinating wheat embryos. Eur J Biochem 114:457–463

Mol JNM, van der Krol AR, van Tunen AJ, van Blokland R, de Lange P, Stuitje AR (1990) Regulation of plant gene expression by antisense RNA. Febs Lett 268:427–430

Murray AJS, Blackwell RD, Lea PJ (1989) Metabolism of hydroxypyruvate in a mutant of barley lacking NADH-dependent hy-

droxypyruvate reductase, an important photorespiratory enzyme activity. Plant Physiol 91:395–400

Neuhaus J-M, Flores S, Keefe D, Ahl-Goy P, Meins F Jr (1992) The function of vacuolar β-glucanase investigated by antisense transformation. Susceptibility of transgenic *Nicotiana sylvestris* plants to *Cercospora nicotianae* infection. Plant Mol Biol 19:803–813

Ogren WL (1984) Photorespiration: pathways, regulation and modification. Annu Rev Plant Physiol 35:415–442

Otten L, Schilperoort R (1978) A rapid microscale method for the detection of lysopine and nopaline dehydrogenase activities. Biochim Biophys Acta 527:497–500

Peach C, Velten J (1991) Transgene expression variability (position effect) of CAT and GUS reporter genes driven by linked divergent T-DNA promoters. Plant Mol Biol 17:49–60

Robert LS, Donaldson PA, Ladaique C, Altosaar I, Arnison PG, Fabijanski SF (1989) Antisense RNA inhibition of β-glucuronidase gene expression in transgenic tobacco plants. Plant Mol Biol 13:399–409

de Rocher EJ, Michalowski CB, Bohnert HJ (1991) cDNA sequences for transcripts of the ribulose-1,5-bisphosphate carboxylase/oxygenase small subunit gene family of *Mesembryanthemum crystallinum*. Plant Physiol 95:967–978

Rodermel SR, Abbott MS, Bogorad L (1988) Nuclear-organelle interactions: Nuclear antisense gene inhibits ribulose bisphosphate carboxylase enzyme levels in transformed tobacco plants. Cell 55:673–681

Rogers SG, Klee HJ, Horsch RB, Fraley RT (1987) Improved vectors for plant transformation: Expression cassette vectors and new selectable markers. Methods Enzymol 153:253–277

Rothstein SJ, DiMajo J, Strand M, Rice D (1987) Stable and heritable inhibition of nopaline synthase in tobacco expressing antisense RNA. Proc Natl Acad Sci USA 84:8439–8443

Sandler SJ, Stayton M, Townsend JA, Ralston ML, Bedbrook JR, Dunsmuir P (1988) Inhibition of gene expression in transformed plants by antisense RNA. Plant Mol Biol 11:301–310

Sheehy RE, Kramer H, Hiatt WR (1988) Reduction of polygalacturonidase activity in tomato fruit by antisense RNA. Proc Natl Acad Sci USA 85:8805–8809

Siegel AF (1988) Statistics and Data Analysis; an Introduction. John Wiley and Sons Publishers, New York

Smith CJS, Watson CF, Ray J, Bird CR, Morris PC, Schuch W, Grierson D (1988) Antisense RNA inhibition of polygalacturonase gene expression in transgenic tomatoes. Nature 334:724–726

Smith CJS, Watson C, Morris PC, Bird CR, Seymour GB, Gray JE, Arnold C, Tucker GA, Schuch W, Harding S, Grierson D (1990) Inheritance and effect on ripening of antisense polygalacturonase genes in transgenic tomatoes. Plant Mol Biol 14:369–379

Stafford HA, Magaldi A, Vennesland B (1954) The enzymatic reduction of hydroxypyruvic acid to D-glyceric acid in higher plants. J Biol Chem 207:621–629

Stockhaus J, Hofer M, Renger G, Westhoff P, Wydrzynski T, Willmitzer L (1990) Antisense RNA efficiently inhibits formation of the 10 kD polypeptide of photosystem II in transgenic potato plants: Analysis of the role of the 10 kD protein. EMBO J 9:3013–3021

Temple SJ, Knight TK, Unkefer PJ, Sengupta-Gopolan C (1992) Modulation of glutamine synthetase gene expression by the introduction of an alfalfa glutamine synthetase gene in sense and antisense orientation: Molecular and biochemical analysis. Mol Gen Genet (in press)

Tieman DM, Harriman RW, Ramamohan G, Fischer RL (1992) An antisense pectin methyltransferase gene alters pectin chemistry and soluble solids in tomato fruit. Plant Cell 4:667–679

Titus DE, Hondred D, Becker WM (1983) Purification and characterization of hydroxypyruvate reductase from cucumber cotyledons. Plant Physiol 72:402–408

Tolbert NE (1981) Metabolic pathways in peroxisomes and glyoxisomes. Annu Rev Biochem 50:133–157

Visser RGF (1989) Manipulation of the starch composition of *Solanum tuberosum* L. using *Agrobacterium rhizogenes*-mediated transformation. PhD thesis, University of Groningen, The Netherlands

Visser RGF, Feenstra WJ, Jajobsen E (1990) Manipulation of granule-bound starch synthase activity and amylose content in potato by antisense genes. In: Mol JNM, van der Krol AR (eds) Antisense nucleic acids and proteins (fundamentals and applications). Marcel Dekker, New York pp 141–155

Visser RGF, Somhorst I, Kuipers GJ, Ruys NJ, Feenstra WJ, Jacobsen E (1991) Inhibition of the expression of the gene for granule-bound starch synthase in potato by antisense constructs. Mol Gen Genet 225:289–296

Yokoyama K, Imamoto F (1987) Transcriptional control of the endogenous MYC protooncogene by antisense RNA. Proc Natl Acad Sci USA 84:7363–7367

Zelitch I (1953) Oxidation and reduction of glycolic and gloxylic acids in plants II. Glyoxylic acid reductase. J Biol Chem 201:719–726

deleteriously affected by dystrophin deficiency. This correlation might explain the muscle group dependence[19], age dependence[12,19], and species dependence[1] of dystrophin deficiency on muscle fibre necrosis.

We acknowledge the generous support of the Muscular Dystrophy Association (USA) (LMK), and the National Institutes of Health (HSS and LMK). EPH is the Harry Zimmerman Post-doctoral Fellow of the Muscular Dystrophy Association. LMK is an Associate Investigator of the Howard Hughes Medical Institute.

Received 9 May; accepted 19 May 1988

1. Hoffman, E. P., Brown, R. H. & Kunkel, L. M. *Cell* **51**, 919-928 (1987).
2. Hoffman, E. P. *et al. New Engl. J. Med.* **318**, 1363-1368 (1988).
3. Hoffman, E. P., Knudson, C. M., Campbell, K. P. & Kunkel, L. M. *Nature* **330**, 754-758 (1987).
4. Knudson, C. M., Hoffman, E. P., Kahl, S. D., Kunkel, L. M. & Campbell, K. P. *J. biol. Chem.* (in the press).
5. Sugita, H. *et al. Proc. Japan Acad.* **64**, 37-39.
6. Bonilla, E. *et al. Cell* (in the press).
7. Zubrzycka-Gaarn, E. E. *et al. Nature* **333**, 466-469 (1988).
8. Koenig, M., Monaco, A. P. & Kunkel, L. M. *Cell* **53**, 219-228 (1988).
9. Hammond, R. G. *Cell* **51**, 1 (1987).
10. Davison, M. D. & Critchley, D. R. *Cell* **52**, 159-160 (1988).
11. Bulfield, G., Siller, W. G., Wight, P. A. & Moore, K. J. *Proc. Natn. Acad. Sci. U.S.A.* **81**, 1189-92 (1984).
12. Hoffman, E. H., Hudecki, M. S., Rosenberg, P. A., Pollina, C. M. & Kunkel, L. M. *Neuron* (in the press).
13. Eisenberg, B. R. in *Handbook of Physiology, Section 10: Skeletal Muscle* (ed. Peachy, L. D.) 73-112 (American Physiological Society, Bethesda, 1983).
14. Lazarides, E. *Cell* **51**, 345-356 (1987).
15. Lazarides, E. & Capetanaki, Y. G. in *Molecular Biology of Muscle Development* (eds Emerson, C., Fischman, D., Nadal-Ginard, B. & Siddiqui, M. A. Q.) 749-772 (Alan R. Liss, New York, 1986).
16. Rowland, L. P. *Muscle Nerve* **3**, 3-20 (1980).
17. Lotz, B. P. & Engel, A. G. *Neurology* **37**, 1466-75 (1987).
18. Cullen, M. J. & Mastaglia, F. L. *Br. Med. Bull.* **36**, 145-152 (1980).
19. Engel, A. G. in *Myology: Basic and Clinical* (ed. Engle, A. G. & Banker, B. Q.) 1185-1240 (McGraw-Hill, New York, 1986).
20. Watkins, S. C., Samuel, J. L., Marotte, F., Bertier-Savalle, B. & Rappaport, L. *Circ. Res.* **60**, 327-336 (1987).

An anti-sense chalcone synthase gene in transgenic plants inhibits flower pigmentation

Alexander R. van der Krol, Peter E. Lenting, Jetty Veenstra, Ingrid M. van der Meer, Ronald E. Koes, Anton G. M. Gerats, Joseph N. M. Mol & Antoine R. Stuitje

Department of Applied Genetics, Vrije Universiteit, de Boelelaan 1087, 1081 HV Amsterdam, The Netherlands

In most plants flower pigments derive from the flavonoid biosynthesis pathway. Consistent with this pathway in *Petunia hybrida* the key enzyme in flavonoid synthesis, chalcone synthase, is synthesized in the flower corolla, tube and anthers[1]. Here we show that constitutive expression of an 'anti-sense' chalcone synthase gene in transgenic petunia and tobacco plants results, with high frequency, in an altered flower pigmentation due to a reduction in levels of both the messenger RNA for the enzyme and the enzyme itself. The pattern of pigmentation varies among flowers of different transgenic plants, indicating that the activity of the anti-sense gene is influenced by DNA sequences that border its site of insertion in both a quantitative and a qualitative way. Backcrossing experiments show that the different pigmentation phenotypes resulting from the expression of anti-sense chalcone synthese gene(s) are stably inherited. These data establish that secondary metabolism in plants can be manipulated using transgenic plants that constitutively synthesize anti-sense RNA.

Recently strategies have been developed to mimic mutations by reducing gene expression using RNA that contains the complementary sequence to a given RNA, and hence is termed anti-sense RNA.[2-7] This approach has shown that the activity of introduced genes encoding nopaline synthase[6] and chloramphenicol acetyltransferase[7] can be effectively inhibited in plant and plant-cell model systems respectively. Here we describe the use of transgenic plants to study the effects of anti-sense RNA on the expression of endogenous genes, in this case those encoding chalcone synthase (CHS). Inactivation of expression of these genes can be scored phenotypically as a change in flower pigmentation, as CHS is the key enzyme in flavonoid biosynthesis. This system also enables us to monitor expression of the anti-sense gene in plant tissues that do not express the target gene(s).

In *Petunia hybrida* CHS is encoded by a multi-gene family of which one member (gene A) is predominantly expressed in floral tissue[1]. There are nucleotide sequence differences between different petunia genotypes even within this particular gene[1,8] and we chose the entire CHS gene A coding sequence from cultivar V30 as the template for construction of an anti-sense gene.

Previous experiments using anti-sense RNA suggest that a high ratio of anti-sense to sense mRNA is required for effective reduction of the expression of the target gene[2,3,6,7,9] and therefore we used the strong Cauliflower Mosaic Virus (CaMV) 35S-promoter[10] to direct the transcription of the anti-sense CHS gene in transgenic plants. Constitutive transcription from this promoter could thus create a pool of anti-sense RNA before the onset of endogenous CHS gene expression, providing an

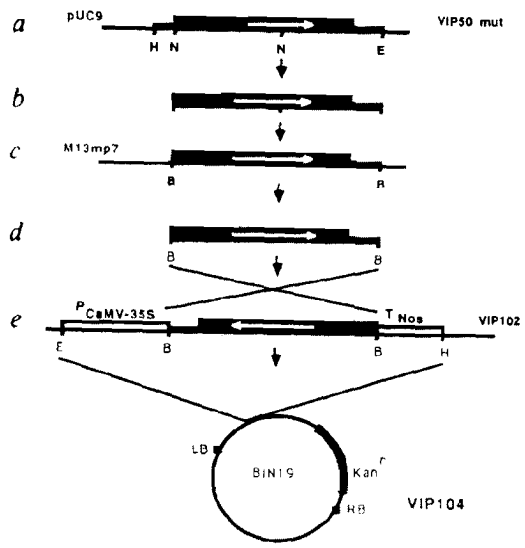

Fig. 1 Construction of the anti-sense CHS gene (VIP104). A complementary DNA clone (VIP50 mut) of the petunia cultivar V30 CHS gene *A* with an introduced *Nco*I site at the initiation codon was used as the donor CHS coding sequence. *a*, VIP50 mut was partially digested with *Nco*I and completely with *Eco*RI; the sticky ends were made blunt using the Klenow fragment of DNA polymerase I and dNTPs. *b*, The resulting blunt-ended fragment was cloned into the *Hin*cII site of phage M13 mp7. *c*, The CHS coding sequence could now be isolated as *Bam*HI fragment. *d*, This fragment was cloned into the *Bam*HI site separating the CaMV 35S promoter and a nopaline synthase 3' flanking region that contains a poly(A) addition signal. *e*, A clone with the CHS coding sequence in reverse orientation behind the CaMV 35S-promoter (VIP102) was used to isolate the entire *Eco*RI–*Hin*dIII fragment and this was cloned into the polylinker site of the binary vector BIN19 (ref. 15) resulting in VIP104. E, *Eco*RI; B, *Bam*HI; N, *Nco*I; H, *Hin*dIII.

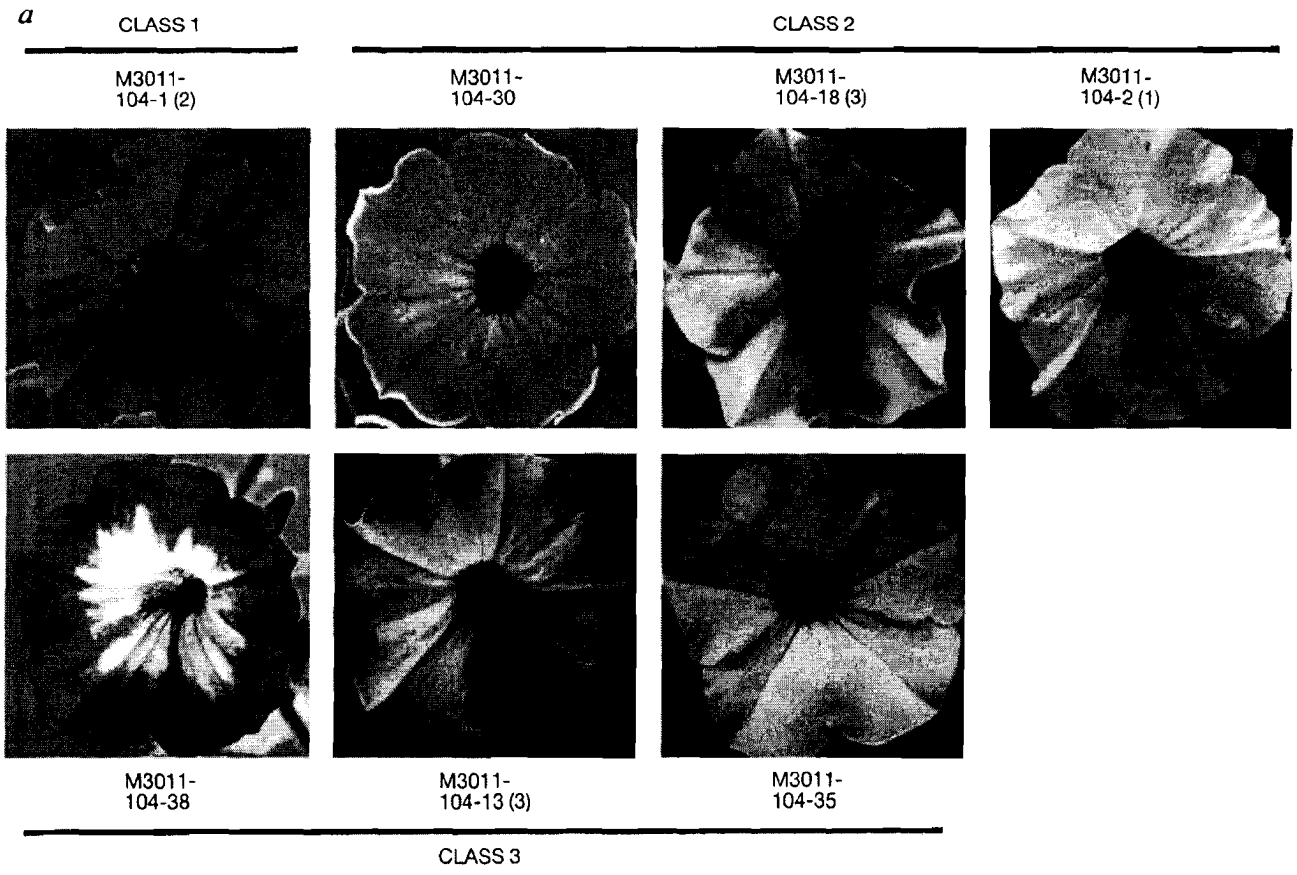

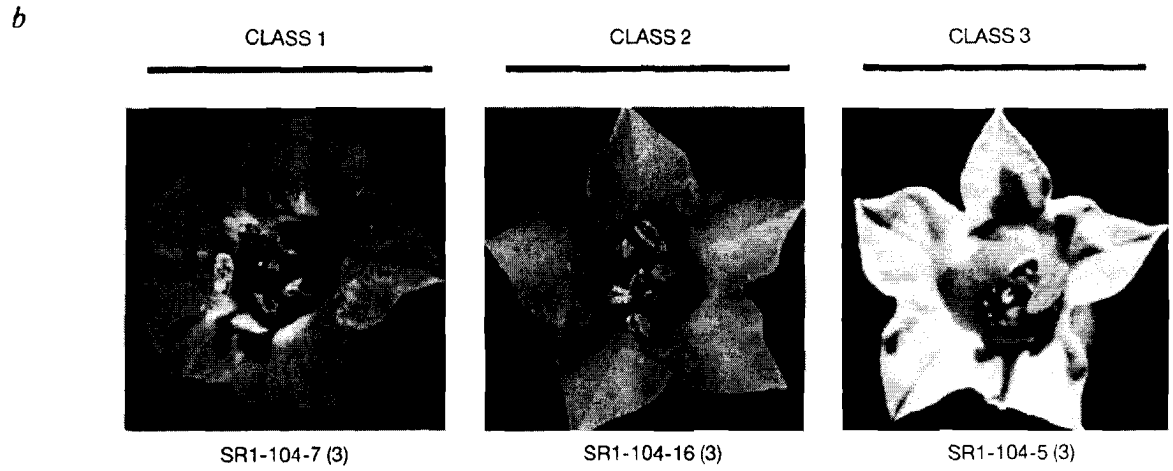

Fig. 2 Flower pigmentation patterns of transformants of Petunia VR hybrid (*a*) and *Nicotiana tabacum* SR_1 plants (*b*). The flowers of transgenic petunia plants are divided into three classes. Those of tobacco transgenic plants also exhibit three phenotypes: 36 out of 40 had flowers indistinguishable from wild-type tobacco flowers (class 1); 3 plants gave flowers with sectored pigmentation (class 2); and 1 plant gave entirely white flowers (class 3).

Methods. Plasmid VIP104 was mobilized into *Agrobacterium tumefaciens* strain 4404 using standard triparental mating techniques[16]. Plants were transformed using the leaf disc transformation method[17] and were regenerated on shoot-induction medium containing 250 $\mu g\ ml^{-1}$ kanamycin to select for cells expressing the neomycin phosphotransferase (NPT) gene contained in the T-DNA region of vector BIN19. Transformation of each plant was confirmed by Southern blot analysis of genomic DNA as follows. Total DNA was isolated from each transformant[18], 5 μg DNA was digested with *Hin*dIII, electrophoretically separated on a 1% agarose gel and transferred to Genescreen Plus membrane (NEN Research Prod.). The blot was then probed with ^{32}P-labelled NPT DNA or ^{32}P-labelled CHS cDNA as described[18]. As digestion with *Hin*dIII should produce a unique fragment for each NPT copy integrated into the genome, the number of bands that hybridized with NPT was used as a measure of the copy number, given between brackets for some transformants.

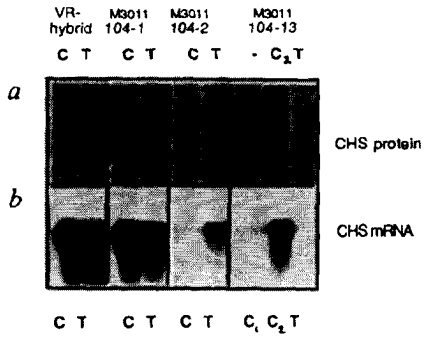

Fig. 3 Western blot (*a*) and Northern blot (*b*) analysis of class, 1, 2 and 3 petunia transformants.
Methods. Between five and seven full-length but still closed flower-buds were harvested from each transformant. Tube and corolla tissue were separated and frozen in liquid nitrogen. Corolla tissue from transformant M3011/104/13 was separated into colourless (C_1) and coloured (C_2) parts. *a*, Western blots were made as described[19]. Equal amounts of protein extracted from either tube (T) or corolla (C) tissue, were used for each sample. CHS protein was immunologically detected using rabbit CHS anti-serum[19] and alkaline phosphatase conjugated to goat anti-rabbit IgG[20]. *b*, Northern blots on Genescreen Plus membrane from equal amounts (2 μg) total RNA extracted from tube (T) or corolla (C) tissue were made as described (manuscript in preparation). CHS mRNA was detected using ^{32}P-labelled anti-sense CHS RNA transcribed by T7-polymerase from the pTZ18U vector (US Biochem. Corp.) containing the *Eco*RI-*Hin*dIII fragment of VIP50. Hybridization and washing of the blot occurred according to suppliers instructions, but at 75 °C instead of 60 °C.

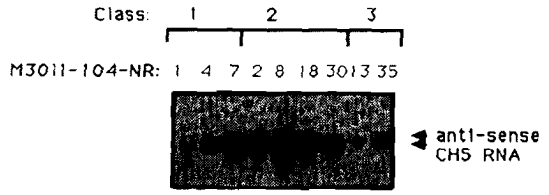

Fig. 4 Northern analysis of anti-sense CHS-A gene expression in leaves of class 1, 2 and 3 petunia VIP104 transformants. The anti-sense CHS gene expresses two RNAs of about 1,300 and 1,100 base pairs (bp) in both petunia and tobacco transgenic plants. As a putative extra poly(A) addition signal (AATAAT) was found in the anti-sense orientation of the CHS sequence 220 bp upstream of the nopaline synthase poly(A) addition site, we assume the two RNAs result from polyadenylation at different sites.
Methods. Northern analysis was performed as described in the legend of Fig. 3. Anti-sense CHS RNA was detected using ^{32}P-labelled sense CHS RNA transcribed by T7 polymerase from the pTZ19U vector (US Biochem. Corp.) containing the *Eco*RI-*Hin*dIII fragment of VIP50.

instantaneous high ratio of anti-sense to sense CHS mRNA. Figure 1 shows the construction of the anti-sense CHS gene (VIP104) which we used to transform petunia VR hybrids[11] and *Nicotiana tabacum* SR_1 plants.

Normal petunia VR hybrid flowers have uniformly coloured corollas, tubes and anthers, but flowers of the petunia transgenic plants exhibited three different types of pigmentation patterns (Fig. 2*a*). Class 1 (12 out of 25 transformants) have flowers indistinguishable from wild-type VR hybrid flowers. Eight independent transformants in class 2 show a reduction of flower pigmentation in the corolla, often resulting in alternating coloured and colourless (white) sectors, although the tube remains coloured in these transformants. A similar pattern of expression has been reported in transgenic *Petunia hybrida* flowers that carry the A1 maize gene (which encodes another enzyme of the flavonoid biosynthesis pathway) also driven by the CaMV 35S-promoter[12]. In the five transformants in class 3 the colouration pattern seems to be fundamentally different from that of class 2 in that inhibition of flower pigmentation starts in the tube and extends outward into the corolla tissue, leading either to white flowers with a coloured ring or to entirely white flowers. Pigmentation of the anthers did not seem to be affected in any of the transgenic plants.

TLC analysis of extracts from white flower tissue showed an absence of flavonoids. The block in pigment biosynthesis could be bypassed, however, by feeding naringenin-chalcone, the product of CHS activity, to white corolla tissue. Thus the enzymes that operate after CHS in the pathway are present and active in these transgenic plants (results not shown).

Western (protein) and Northern (RNA) blot analyses using flowers of different classes showed that CHS protein levels and CHS mRNA steady-state levels in the tube and corolla correlate well with the observed phenotypes (Fig. 3*a* and *b*). Restriction analysis of the genomic DNA of some transformants did not reveal any changes in the endogenous CHS gene copies (data not shown). The altered pigmentation patterns described above were not observed in plants transformed with 'sense' CHS gene-constructs (20 transgenic petunia plants analysed). This makes it unlikely that these phenotypes are the result of somaclonal variation, homologous recombination or gene conversion events. The effectiveness of the anti-sense CHS gene-construct is demonstrated by the fact that CHS gene expression can be inhibited even in a heterologous plant system, that is, when tobacco plants are transformed with the petunia anti-sense CHS gene construct (Fig. 2*b*, analysis not shown).

A number of petunia transformants were backcrossed to both VR parents (V23 and R51). The progeny of the backcrossed transformant containing one insert showed 53/43 (anti-sense/wild-type) segregation ($\chi^2 = 1.04$, $p = 0.31$). Moreover, Southern blot analysis shows the complete co-segregation of the anti-sense phentoype (pigmentation in sectors) with the insert (10 anti-sense and 10 wild-type plants analysed, data not shown). Chromosomal localization studies are in progress and will be published elsewhere.

It is generally believed that, as in prokaryotes, anti-sense gene effects in eukaryotes are caused by the formation of duplex RNA structures. Preliminary experiments do indicate the presence of such RNA duplexes in the flower tissue of some transformants. Unlike in prokaryotes, the presence of an anti-sense 5′ leader sequence is not a prerequisite[13] in our system (see Fig. 1), suggesting that inactivation of gene expression is not at the level of initiation of translation. The actual mechanism of inactivation of gene expression by the anti-sense gene seems to be rather complex. First, there is no correlation between the number of anti-sense CHS gene copies introduced and the steady-state level of anti-sense CHS RNA in leaf tissue (Fig. 4, for example, transformant 18 versus 13). This confirms and extends the general observation that bordering sequences influence gene expression in a quantitative way—the so-called position effect[14]. Second, several independent transgenic plants exhibiting the same steady-state level of anti-sense CHS RNA in leaf tissue, show a difference in flower pigmentation (Fig. 4, for example transformant 7 versus 18). Third, some independent transgenic plants with a very low steady-state level of anti-sense CHS RNA in leaf tissue, show a pronounced effect on flower pigmentation (Fig. 4, transformant 13).

The different classes of flower pigmentation found are very striking. Assuming stable integration of the anti-sense CHS gene and a normal transcription of endogenous CHS genes in each transformant, the difference between flowers of class 2 and 3 indicates that the integrated anti-sense CHS gene(s) are expressed in fundamentally different ways. This must also be due to the position effect and it shows that bordering sequences may also influence gene expression in a qualitative way, perhaps

affecting the timing or spatial distribution of gene expression. Extensive analysis of anti-sense and sense CHS gene expression during flower development is in progress to elucidate the actual mechanism of the anti-sense gene effect. The results presented here demonstrate the potency of anti-sense RNA in manipulating secondary metabolite pathways in both a quantitative and a qualitative manner.

We thank J. J. A. Büsse for his excellent care of the plants. J. Meijer and W. Bergenhenegouwen for photography, H. Bartelson for typing the manuscript and G. Mahler for inspiration. This research is supported in part by a grant from the Netherlands Organisation for the Advancement of Pure Research (NWO).

Received 25 January; accepted 4 May 1988.

1. Koes, R. E. *et al. Nucl. Acids Res.* **4**, 5229–5239 (1986).
2. Rosenberg, U. B., Preiss, A., Seifert, E., Jäckle, H. & Knipple, D. C. *Nature* **313**, 703–706 (1985).
3. Cabrera, C. V., Alonso, M. C., Johnston, P., Phillips, R. G. & Lawrence, P. A. *Cell* **50**, 659–663 (1987).
4. Boulay, J. L., Dennefeld, C. & Alberga, A. *Nature* **330**, 395–398 (1987).
5. Knecht, D. A. & Loomis, W. F. *Science* **236**, 1081–1086 (1987).
6. Rothstein, S. J., DiMaio, J., Strand, M. & Rice, D. *Proc. natn. Acad. Sci. U.S.A.* **84**, 8439–8443 (1987).
7. Ecker, J. R. & Davis, R. W. *Proc. natn. Acad. Sci. U.S.A.* **83**, 5372–5376 (1986).
8. Reif, H. J., Niesbach, U., Deumling, B. & Saedler, H. *Molec. gen. Genet.* **199**, 208–215 (1985).
9. Izant, J. G. & Weintraub, H. *Science* **229**, 345–352 (1985).
10. Bevan, M. W., Mason, S. E. & Goelet, P. *EMBO J.* **4**, 1921–1926 (1985).
11. Wallroth, M., Gerats, A. G. M., Rogers, S. G., Fraley, R. T. & Horsch, R. B. *Molec. gen. Genet.* **202**, 6–15 (1986).
12. Meyer, P., Heidmann, I., Forkmann, G. & Saedler, H. *Nature* **330**, 677–678 (1987).
13. Green, J. P., Pines, O. & Innouge, M. *A. Rev. Biochem.* **55**, 569–597 (1986).
14. Jones, J. D. G., Dunsmuir, P. & Bedbrook, J. *EMBO J.* **4**, 2411–2418 (1985).
15. Bevan, M. *Nucl. Acids Res.* **12**, 8711–8721 (1984).
16. Ditta, G., Stanfield, S., Corbin, D. & Helinski, D. R. *Proc. natn. Acad. Sci. U.S.A.* **77**, 7347–7351 (1980)
17. Horsch, R. B. *et al. Science* **227**, 1229–1231 (1985).
18. Koes, R. E., Spelt, C. E., Mol, J. N. M. & Gerats, A. G. M. *Plant molec. Biol.* **10**, 159–169 (1987).
19. Mol, J. N. M. *et al. Molec. gen. Genet.* **192**, 424–429 (1983).
20. Tunen, A. J. van & Mol, J. N. M. *Archs Biochem. Biophys.* **257**, 85–91 (1987).

The structure of *trp* pseudorepressor at 1.65Å shows why indole propionate acts as a *trp* 'inducer'

Catherine L. Lawson* & Paul B. Sigler†

Department of Biochemistry and Molecular Biology, The University of Chicago, Chicago, Illinois 60637, USA

The *trp* repressor is a small dimeric regulatory protein which controls the expression of three operons in *Escherichia coli*[1–3]. The inactive aporepressor protein must bind two molecules of L-tryptophan to form the active repressor[4]. If desamino analogues of L-tryptophan such as indole propionate (IPA) are substituted for L-tryptophan, an inactive pseudorepressor is formed[1,5,6]. Because the desamino analogues thus cause derepression of operons under control of the *trp* repressor, they appear to be 'inducers'. We have determined the crystal structure of the pseudorepressor and refined it to 1.65 Å. The molecular structure was compared to that of the nearly isomorphous orthorhombic form of the repressor. Surprisingly, the indole ring of IPA is in the same position as the indole ring of L-tryptophan in the repressor, but is 'flipped over'. As a result, the carboxyl group of IPA is oriented toward the DNA-binding surface of the protein and is in a position where it sterically and electrostatically repels the phosphate backbone of both operator and non-operator DNA. This explains why IPA acts as an apparent *trp* inducer.

The *trp* pseudorepressor is an inactive complex formed when the *trp* aporepressor binds indole analogues of L-tryptophan which, unlike L-tryptophan, confer no affinity for the *trp* operator. These indole analogues compete with L-tryptophan for binding *in vitro*[7], and produce adducts that are similar in structure[8,9] but have lost their ability to bind operator. The effect of these analogues *in vivo* is presumably the same as they induce, or more precisely derepress, expression of the operons that are repressed by the *trp* repressor. The common features of these analogues are (1) an indole ring and a carboxyl group spaced with a variable length hydrocarbon chain and (2) lack of an α-amino group. Interestingly, several desamino analogues bind with higher affinity to the aporepressor than does L-tryptophan[7]. These include indole 3-propionate (IPA), which is isostructural with L-tryptophan except for the replacement of the α-amino group with a hydrogen atom.

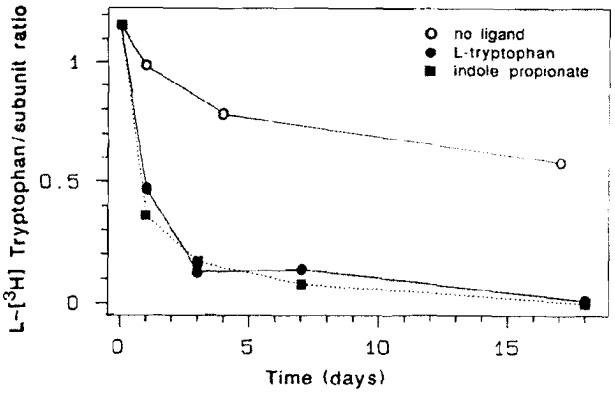

Fig. 1 Ligand exchange in orthorhombic *trp* repressor crystals. Orthorhombic crystals of *trp* repressor were grown and stabilized as described[12], but in the presence of L-[^{3}H]tryptophan (Amersham). Selected well-formed crystals were transferred into 200 µl droplets of stabilizer containing either 1.75 mM L-tryptophan, 1.75 mM IPA or no ligand. The stabilizer was immediately removed and replaced twice to wash away excess radioactive ligand. Single crystals were removed at the time points indicated for analysis. The crystal was placed on a filter set on a sintered glass funnel and was quickly washed three times with 100 µl of stabilizer, with complete removal of each stabilizer wash by vacuum filtration. The filter was turned upside down into a 100 µl stabilizer droplet on a siliconized depression slide. The stabilizer was removed with a micropipette, and the crystal was dissolved in 100 µl of 100 mM sodium phosphate, *p*H 7.0. The protein content[15] and radioactivity of the dissolved crystal solution were measured.

Because desamino analogues of L-tryptophan do not act as corepressors, it has been postulated that the α-amino group is critical for activation of the aporepressor protein[1,5,6,10]. From comparison of repressor and aporepressor structures[11–12], it is clear that the binding of L-tryptophan is associated with a conformational change in the protein which allows two symmetry-related reading-head domains (D and E helices) to penetrate two successive major grooves of DNA. Because nearly isomorphous crystals of pseudorepressor (aporepressor plus IPA) can be obtained in at least two repressor crystal forms (ref. 8, and see below), the overall conformation of the active and inactive adducts must be quite similar. Also, nuclear magnetic resonance studies[9] suggest that there are no large conformational differences between repressor with L-tryptophan bound and pseudorepressor with IPA bound. As IPA produces the same global conformational change in the protein as L-tryptophan, the inability of IPA to confer operator affinity must be due to more subtle structural differences between the repressor and pseudorepressor.

The orthorhombic crystal form of *trp* repressor will readily exchange the L-tryptophan ligand for IPA and other desamino analogues (Fig. 1). The ligand exchange is associated with modest intensity differences in the crystal diffraction pattern

* Present address: Laboratory of Chemical Physics, Department of Chemistry, University of Groningen, Groningen, The Netherlands.
† To whom correspondence should be addressed.

THEORETICAL AND APPLIED GENETICS

International Journal of Breeding Research and Cell Genetics

Volume 87 Number 8 March 1994

Indexed in *Current Contents*

THAGA 6 (1994) [illegible]

87 (8) 893–1028 March 1994

Printed on acid-free paper

Springer International

THEORETICAL AND APPLIED GENETICS

International Journal of Breeding Research and Cell Genetics

Founded in 1929 as "Der Züchter", a German journal for theoretical and applied plant breeding. In 1965 its structure changed from national to international and from plant breeding to genetics and breeding research. The title changed in 1966 to "Theoretical and Applied Genetics". Edited by H. Stubbe from 1946 to 1976 and by H. F. Linskens 1977 to 1987 (Vol. 73).

TAG will publish original articles in the following areas:

- **Genetic fundamentals of plant and animal breeding;**
- **Physiological fundamentals of plant and animal breeding;**
- **Application of cell genetics to breeding;**

Each paper is limited to six printed pages (approx. 18 manuscript pages including figures and tables); thereafter there will be charge of DM 700.00 for every additional printed page. When the page proof is sent, the author will also be informed as to the amount to be paid for any excess pages.

Instructions to authors

1. **Manuscripts** must be written in standard grammatical English; this is the responsibility of the author. They should be submitted in duplicate with one set of the **original illustrations** to one of the Editors according to his field of competence (see back cover) or to the Managing Editor.

2. The **title page** should contain: title of paper; name(s) of first author(s) and co-author(s); author(s)' complete address(es) (author's institute and business); referring to the title (indicated by asterisks). Please state also to whom the proofs should be sent.

3. The **manuscript** must be typed double-spaced on one side of the paper only (format: DIN A4 or equivalent), and the right margin **ready for press**. Wrong corrections should be blacked out on both sides to keep subsequent situations of a transition. Be sparing to reduce printing costs. Abbreviations and unit symbols are standard.

The manuscript must be preceded by an abstract (about 200 words) which briefly and precisely states the problem, the principal results and conclusions reached. A few (3–5) index terms or phrases should be provided in addition.

Please indicate underneath the **summary** up to **five key words** should be supplied, indicating the scope of the paper.

4. Passages to be printed in **small print** should be marked with a vertical line in the left margin.

5. **Footnotes**, other than those referring to the title (see 2nd), should be numbered consecutively.

6. **Genus** and **species names** are printed in italics and should be underlined in blue. Do not mark anything else (e.g. authors names in the text).

7. Check that **symbols** are used consistently in figures, tables and text (lower case or capital letters, arabic or roman numerals).

8. **Tables** must be numbered with arabic numerals, separately from the figures. Each table should have a heading. Tables should not be included in the text but submitted together at the end of the paper. Footnotes in tables should be given in small letters consecutively.

9. **References:** The list of references should be placed after the text. Please arrange the list as follows:

Hutchinson (1977 a)
Hutchinson (1977 b)
Hutchinson (1978)
Hutchinson and Hamilton (1959)
Hutchinson and Smith (1968)
Hutchinson, Smith, and Hamilton (1953)
Hutchinson, Hamilton, and Smith (1963)

For the abbreviation of journal titles please use *Bibliographic Guide for Editors and Authors* (published by The American Chemical Society).

Examples:

Falk DE, Kasha KJ (1983) Genetic studies of the crossability of hexaploid wheat with rye and *Hordeum bulbosum*. Theor Appl Genet 64:303–307

Michelsen A (1984) Hearing in invertebrates. In: Kessel NU, Neff WD (eds) Auditory neurons. Springer, Berlin Heidelberg New York, pp [illegible]

[illegible] (1966) [illegible]

Nelson in the text: Solari and Pasteur (1987) or Michelsen 1974. If there are more than two authors, only the first should be named, followed by "et al."

10. **Illustrations.** Each paper should not have more than 18 illustrations. The originals must be reproduction-proof. When the desired size has not been specifically stated, the publisher reserves the right to reduce or enlarge the illustration. They will, if possible, be prepared for reduction to column width (8.1 cm) or smaller and up to full page size (16.8 cm). The originals should have a maximum width of 16.2 or 33.6 cm for 50% reduction.

For both halftone illustrations and line drawings, clear glossy photos of excellent quality in the sizes mentioned above should be attached to the manuscript.

Inscriptions and symbols must be clear and large enough to be legible e.g. 2 to 3 mm high after reduction.

If an illustration is made up of [illegible] result (e.g. 12 cm high) [illegible] and to be labeled [illegible]. All illustrations should have the author's name and figure number (arabic numerals) on the reverse.

If plates are submitted, the figures must be mounted on regular bond paper, not on cardboard.

Color illustrations will be accepted; however the authors will be expected to make a contribution towards the extra costs (approx. DM 1200.– for the first and DM 600.– for each additional page).

Legends should be as brief as possible and attached to the manuscript on a separate sheet. Check that figures are referred to in the main text and that **desired position of illustrations** and tables are [illegible].

Proof reading.

[illegible] within 3 days of receipt. Further [illegible] proofs will be read in the editorial office. Proofreading should be limited to the correction of typographical errors. Should extensive corrections or "notes added in proof" prove unavoidable, the additional correction costs must be borne by the author.

12. **Offprints.** Offprints may be ordered at cost price when the page proofs are returned. Springer will supply the corresponding author with one free copy of the relevant issue.

This journal is included in the Springer Journals Preview Service, i.e. the tables of contents and BiblioAbstracts are available via Internet several weeks before the new issue reaches the subscribers. Tables of contents are free of charge; BiblioAbstracts are available for a small annual fee. Details can be obtained by sending an e-mail message containing the line help to svjps@vax.ntp.springer.de

Subscription information

ISSN 0340-5761

Volumes 87 and 88 (8 issues each) will appear in 1994.

North America: Recommended annual subscription rate: US $ 1818.00, single issue price: US $ 142.00, including carriage charges. Subscriptions are entered with prepayment only. Orders should be addressed to: Springer-Verlag New York Inc., Service Center Secaucus, 44 Hartz Way, Secaucus, NJ 07094, USA. Tel. (201) 348-4033, Telex 023-125994, Fax [illegible]

[illegible] Rates: DM 2448.00, plus DM 244.80 [illegible] DM 58.40, including VAT [illegible] DM 19.00. Sea delivery charges are available upon request. SAL delivery is mandatory to Japan, India and Australia/New Zealand; volume price: DM 1480.00; single issue price: DM 222.00, plus carriage charges. Orders can either be placed via a bookdealer or sent directly to: Springer-Verlag, Heidelberger Platz 3, D-14191 Berlin, Germany, Tel. (0) 30/8207-0, Telex 1-83319, Fax (0) 30/8214091.

Changes of address: Allow six weeks for all changes to become effective. All communications should include both old [illegible]

Back volumes: Prices are available on request.

Microform: Microfilm editions are available from: University Microfilms International, 300 N. Zeeb Road, Ann Arbor, MI 48106, USA.

Production

Springer Produktions-Gesellschaft, 3050 Journal Production Department, Annett Pietri, Heidelberger Platz 3, D-14197 Berlin, Germany, Tel. (0) 30/82 07 [illegible], Fax (0) 30/821 [illegible], e-mail: svjps@vax.ntp.springer.de (Internet), 0721319 90 (GeoMail)

Responsible for advertisements

[illegible]

Typesetting

Thomson [illegible]

Printers

Graphischer Betrieb K. Triltsch, Würzburg, Germany

Theor Appl Genet (1994) 87:1006–1015

THEORETICAL AND APPLIED GENETICS

Genetic modification of condensed tannin biosynthesis in *Lotus corniculatus*. 1. Heterologous antisense dihydroflavonol reductase down-regulates tannin accumulation in "hairy root" cultures

T. R. Carron, M. P. Robbins, P. Morris

AFRC Institute of Grassland and Environmental Research, Plas Gogerddan, Aberystwyth, Dyfed, SY23 3EB, Wales, UK

Received: 28 January 1993 / Accepted: 23 July 1993

Abstract. An antisense dihydroflavonol reductase (DFR) gene-construct made using the cDNA for DFR from *Antirrhinum majus* was introduced into the genome of a series of clonal genotypes of *Lotus corniculatus* via *Agrobacterium rhizogenes*. After initial screening, 17 antisense and 11 control transformation events were analysed and tannin levels found to be reduced in antisense root cultures. The effect of this antisense construct, (pMAJ2), which consisted of the 5′ half of the DFR cDNA sequence, was compared in three different recipient *Lotus* genotypes. This construct effectively down-regulated tannin biosynthesis in two of the recepient genotypes (s33 and s50); however, this construct was relatively ineffective in a third genotype (s41) which accumulated high levels of condensed tannins in derived transgenic root cultures. Four pMAJ2 antisense and three control lines derived from clonal genotypes s33 and s50 were selected and studied in greater detail. The antisense DFR construct was found to be integrated into the genome of the antisense "hairy root" cultures, and the antisense RNA was shown to be expressed. Tannin levels were much lower in antisense roots compared to the controls and this reduction in tannin levels was accompanied by a change in condensed tannin subunit composition.

Key words: *Lotus corniculatus* – Condensed tannins – Antisense RNA – *Agrobacterium rhizogenes*

Communicated by M. Koornneef

Correspondence to: M. P. Robbins

Introduction

Condensed tannins (proanthocyanidins) are polyphenylpropanoid compounds which accumulate in various tissues of many plant species. They are polymers of flavan-3,4-diols (catechin-4-ols), typically joined by 4→8 interflavan bonds, with flavan-3-ols (catechins) attached to the 4′ terminal end of the chains. Both the tannin monomers are C15 flavonoid based and are derived from naringenin chalcone via the phenylpropanoid pathway (Fig. 1). Flavan-3,4-diols are common intermediates in the biosynthesis of condensed tannins and anthocyanins, and their synthesis is well documented (Doone et al. 1991; Tanner and Mol 1991). The enzymatic conversion of flavan-3,4-diols to flavon-3-ols was described by Stafford and Lester (1985). A number of models for the condensation of the tannin subunits have been proposed (Haslam 1989; Stafford 1990) but the exact nature of the condensation process has not been determined.

Tannins are of agronomic significance because many plant species that are used as animal feeds contain tannins in their vegetative tissue, and the ability of these tannins to bind dietary protein can have profound effects on animal nutrition. In ruminants, tannins have been shown to be effective anti-bloat agents (Reid et al. 1974). This property is thought to be due to reduced foaming of the rumen as a result of binding of the tannins to protein causing an effective decrease in rumen protein concentration. Tannins have also been shown to act as protein protectants, reducing bacterial deamination in the rumen (Reid et al. 1974). In ruminant animals, dietary tannin can lead to poor nitrogen uptake and weight loss (Griffiths 1986). Condensed tannins have also been implicated in fungal pathogen resistance (Brownlee et al. 1992) and as insect

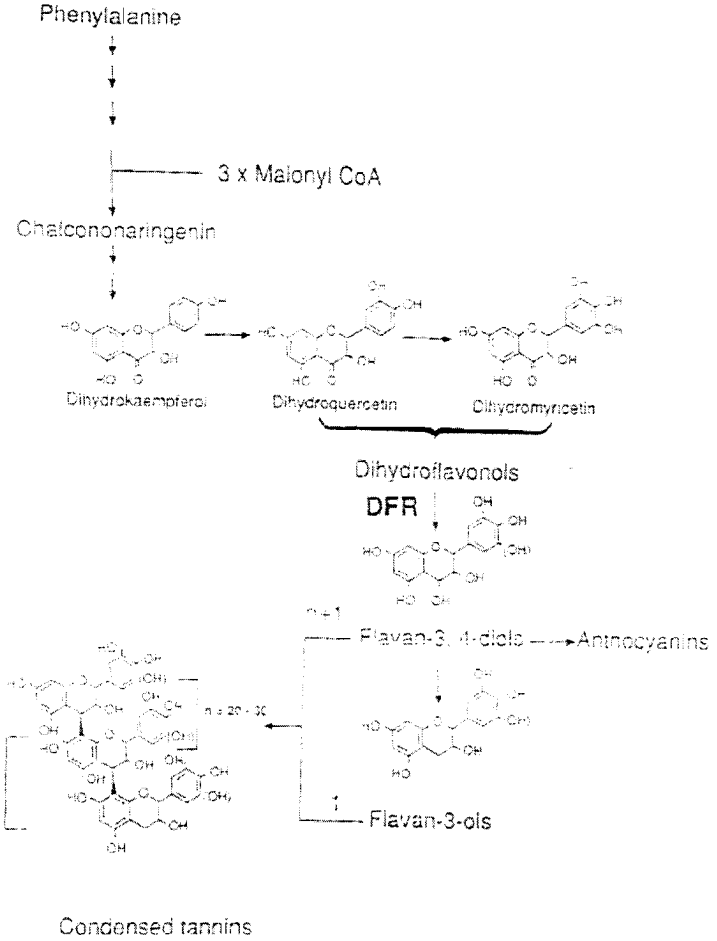

Fig. 1. Pathway for the biosynthesis of condensed tannins in *Lotus corniculatus*. The enzyme dihydroflavonol reductase (*DFR*) is marked

antifeedants (Seadbert and Haslam 1987). The major forage legumes of European and U.S. agriculture, *Trifolium repens* (white clover) and *Medicago sativa* (alfalfa), do not contain tannins in their vegetative tissue whereas some of the lesser grown forage legumes, *Lotus corniculatus* (birds foot trefoil) and *Onobrychis viciifolia* (sainfoin), do accumulate tannins in these tissues.

L. corniculatus has a number of features that make it suitable as a model organism in the molecular study of condensed tannin accumulation. It produces polymeric, mostly insoluble, tannins in its stems, roots, leaves, flowers and seeds (Morris and Robbins 1992), at levels as high as 10% dry weight. *L. corniculatus* is also very amenable to genetic transformation and tissue culture. *Agrobacterium rhizogenes* will readily infect wounded *L. corniculatus* tissue and produce "hairy roots". These roots can be cultured on solid or liquid growth media, and can be propagated with regular subculture for many years. The root cultures will spontaneously produce shoots when illuminated, and these can be propagated as shoot cultures (Morris and Robbins 1992), or regenerated into plants which are phenotypically similar, to non-transformed plants (Webb et al. 1990).

A. rhizogenes-transformed root cultures of *L. corniculatus* have already proven to be useful tools in the study of condensed tannin biosynthesis. Morris and Robbins (1992) showed that root cultures produce tannins in a similar manner to non-transformed roots and that the tannins are accumulated in specific "tannin cells". Additionally, they have shown that tannin accumulation could be modified by certain plant growth regulators. *A. rhizogenes*-transformed *L. corniculatus* has also been used in studies of phenylpropanoid metabolism related to plant defence (Robbins et al. 1991) as well as nitrogen fixation (Petit et al. 1987) and nitrogen metabolism (Forde et al. 1989).

Antisense RNA, used as a method of blocking the transcription/translation pathway of a particular gene,

and so producing an organism with an absent or a much reduced gene product, has proved to be a useful tool in the genetic manipulation of metabolic pathways. The exact nature of the mechanism of this inhibition is a subject of debate (Grierson et al. 1991; Krol et al. 1991; Mol et al. 1991). In some systems it has been shown that the formation of sense: antisense RNA duplexes is involved (Melton 1985), though in other systems no such duplexes have been found. Antisense transcripts of as little as ±1 bp have been shown to be effective (Cannon et al. 1990), and it has also been shown that an excess of antisense transcript is not necessary for the effective inhibition of gene expression (Krol et al. 1991). Antisense RNA has already proven to be a powerful tool in the manipulation of plant metabolism. Tomatoes with modified fruit ripening characteristics have been produced using this technique (Smith et al. 1988), and in two cases this has lead to the identification of function in genes whose function was previously unknown.

Phenylpropanoid metabolism has also been a target for manipulation using antisense RNA. *Petunia hybrida* plants with altered levels of anthocyanin in their flowers have been produced by introducing the gene for chalcone synthase into the plants in antisense orientation (Krol et al. 1988). The gene for chalcone isomerase has also been used in antisense experiments, but these did not produce plants with altered flavonoid levels (Tunen and Mol 1991). The gene for dihydroflavonol reductase (DFR) has not, to our knowledge, been used in antisense experiments, though it has been shown to co-suppress (Tunen and Mol 1991), a phenomenon thought to be due to antisense RNA expression (Grierson et al. 1991; Mol et al. 1991).

Heterologous antisense has also been shown to be effective in a number of systems. Krol et al. (1988) demonstrated that the antisense CHS A gene effectively down-regulated the expression of the CHS B gene in *P. hybrida*, despite having only 87% homology to it, whereas Visser et al. (1991) found that the *Zea mays* granule-bound starch synthase (GBSS) down-regulated potato GBSS activity, though not as effectively as an homologous GBSS.

In the present study we have brought together the techniques of *A. rhizogenes* transformation and antisense RNA technology to modify condensed tannin biosynthesis in *L. corniculatus* root cultures.

Materials and methods

Plasmid DNA manipulations

Restriction enzymes, bovine alkaline phosphatase, and T4 ligase were supplied by Boehringer Mannheim UK, and standard procedures performed using the manufacturer's recommended conditions. *E. coli* transformations were carried out using the CaCl$_2$ method described by Maniatis et al. (1982) and all plasmids were propagated and maintained in *E. coli* host JM83. Plasmid DNA was prepared using the alkaline-lysis method [Maniatis et al. (1982), for small scale; Lev (1987), for large scale].

Antisense gene cassette construction

Three different antisense constructs were produced by ligating fragments of the *Antirrhinum majus* cDNA for DFR, [pJAM 212 (Beld et al. 1989)], in the antisense orientation, between the CaMV35S promoter and the nos terminator of the binary vector pROK2 (Hemon et al. 1990). The first construct, pMAJ1, was produced by first cloning the 330-bp *Bam*HI fragment from pJAM212 into the *Bam*HI site of pROK2 and selecting for the correct orientation. The second construct, pMAJ2, was produced by first cloning the 858-bp *Kpn*I *Eco*RV fragment of pJAM212 into *Kpn*I *Sma*I-cut pIC19H (Lawrence-Marsh et al. 1984) to give the plasmid pICMAJA, followed by the cloning of the *Kpn*I *Bgl*II fragment of pICMAJA into the *Kpn*I, *Bam*HI sites of pROK2. The third construct, pMAJ3 was produced by first cloning the 771-bp *Eco*RV (complete digest) *Eco*R1 (partial digest) fragment into the *Eco*R1/*Sma*I sites of pIC19H to give the plasmid pICMAJB, and then cloning the *Bam*HI/*Bgl*II fragment of pICMAJB into the *Bam*HI site of pROK2 and selecting for the correct orientation. Hence, three constructs were produced spanning the first quarter, first half, and second half of the cDNA for DFR (Fig. 2). In this paper we present results relating to pMAJ2, a gene construct that includes the first half of the *A. majus* cDNA sequence.

Transformation of plants with A. rhizogenes

Binary vectors were introduced into *A. rhizogenes* strain LBA9402 by triparental mating using a modification of the method of Herrera-Estrella and Simpson (1988). One hundred microliters of a culture of *A. rhizogenes* LBA9402 (grown 2 days in YEB plus 50 μg/ml rifampicin at 28 °C with shaking

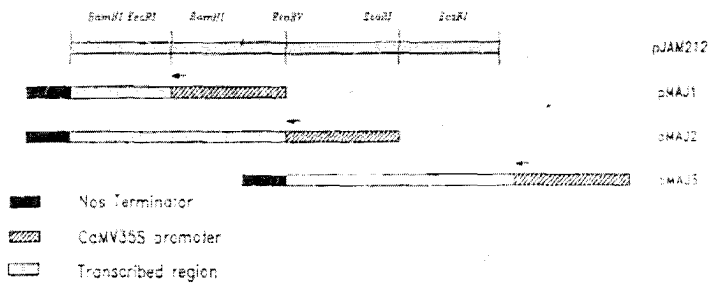

Fig. 2. Diagram representing the three DFR antisense gene constructs.

100 µl of *E. coli* JM83 containing the binary vector (grown overnight in LB plus 50 µg/ml kanamycin at 37 °C with shaking), and 100 µl of *E. coli* containing the mobilisation plasmid pRK2013 (grown overnight in LB plus 50 µg/ml kanamycin at 37 °C) were combined in an Eppendorf tube, vortexed gently to mix, and pelleted in a microcentrifuge. The supernatant was discarded and the cells resuspended in 200 µl of 10 mM TRIS (pH7.2), 10 mM $MgSO_4$. Ten microliters of this was spotted onto YEB agar plates and grown overnight at 28 °C. The cells were then resuspended in 1 ml of λ buffer and 100 µl of this spread on a YEB agar plate containing 50 µg/ml rifampicin and 50 µg/ml kanamycin and grown for 2 days. The resulting bacterial growth was streaked to single colonies on YEB plates containing 50 µg/ml rifampicin and 50 µg/ml kanamycin.

Selection and micropropagation of plants for transformation with A. rhizogenes

To select a series of clonal genotypes that were sensitive to *A. rhizogenes*, *L. corniculatus* cv Leo seeds were surface sterilized as described by Webb et al. (1987) and germinated on 1.5% water agar (20 °C, 125 µEm^{-2} sec^{-1} for 14 days). The shoots were excised and transferred to 30-ml universal tubes containing 10 ml of MS medium with 3% sucrose, without hormones, and grown as above. The cut surface of the residual hypocotyl was then immediately inoculated with *A. rhizogenes* LBA 9402. The infected hypocotyls were incubated in the light at 20 °C (under the above conditions), and "hairy root" production scored after 26 days. Eight of the genotypes producing roots were selected, and the uninfected cut shoots grown and propagated on MS medium, 3% sucrose, without hormones in universal tubes, under the temperature and light conditions as described above. Three of these selected clonal genotypes were used as recipients for antisense constructs in the experiments described in this paper.

Plant transformations and maintenance of root cultures

The stems of the micropropagated clonal genotypes were stripped of leaves and side branches and cut into pieces approximately 3 mm long with a scalpel that had been infected with *A. rhizogenes*. The stem pieces were then placed on sterile Whatman filter paper on the surface of a 60-mm Petri dish (Sterilin) containing 0.5 × Gamborgs B5 media (Flow Laboratories) 3% sucrose and 1% agar without hormones. These were incubated at 20 °C in the light (70 µE m^{-2} s^{-1}). After 7 days the stem pieces (some of which had begun to develop roots) were transferred to 90-mm Petri dishes containing solid 0.5 × B5 media with 500 µg/ml ampicillin. As "hairy roots" developed individual root tips were excised from the explant and maintained according to Webb et al. (1990), except that ampicillin was the only antibiotic used in the media unless bacterial growth persisted, in which case roots were grown on ampicillin/cefotaxime/carbenicillin (concentrations as in Webb et al. [1990]). Roots were transferred into liquid culture (Gamborgs B5 media, 3% sucrose, no hormones) once free of bacterial contamination, and maintained as described by Morris and Robbins (1992).

Kanamycin selection

Individual 0.5-cm root tips from cultures grown on solid media were transferred to a compartment of a 5 × 5 repli dish (Sterilin) containing 1 ml of solidified B5 media. Four replicates of each culture were prepared. These were then incubated for 14 days at 25 °C in the dark. Two replicates growing at approximately equivalent rates were selected and the cube of agar containing the growing root was removed from the dish and placed on solid Gamborgs B5 media in a 60-mm Petri dish, one replicate of each on media containing 25 µg/ml kanamycin, and one on media without antibiotic. The cultures were grown at 25 °C in the dark and growth scored after 21 days.

DNA and RNA extraction and hybridisation

Genomic DNA was isolated according to the method of Dellaporta et al. (1983) with the following modifications: after the first isopropanol precipitation the pellet was resuspended in 10 × concentration TE buffer and extracted with phenol:chloroform:isoamyl alcohol (50:49:1), the DNA was then precipitated with isopropanol and the final pellet was resuspended in 1 × concentration TE buffer plus 50 µg/ml RNase A. The DNA concentration was determined fluorometrically (Cesarone et al. 1979). RNA was extracted from root cultures by the method of Ougham and Davies (1990). Blotting of nucleic acids was performed using Zetaprobe (for Southern- and DNA slot-blots) (Biorad Ltd.) or Hybond-N (for Northern blots) (Amersham International). Slot-blots were performed using a Biorad slot-blot apparatus and Southern-, Northern- and slot-blots carried out according to the relevant manufacturer's instructions. Hybridisations were performed using a Hybaid blot processing system, under conditions as described by Webb et al. (1990) (Southern- and slot-blots) or Bettany (1988) (Northern-blots). Double-stranded DNA probes were prepared using a random primed DNA labelling kit (Boehringer Mannheim UK), and single-stranded RNA probes using a SP6/T7 transcription kit (Boehringer Mannheim UK). Antisense T-DNA was detected using the insert from pJAM212 as a probe. T_L using the *Bam*HI fragment 8a (derived from pRi15834) as a probe, and T_R using the *Sma*I fragment 5 (derived from pRiHRI) as a probe. Antisense RNA was detected using labelled complementary RNA transcribed from pTC101 (the insert of pJAM212, cloned into the SP6/T7 transcription vector, pSP218 (Boehringer Mannheim UK)).

Estimation of tannin content

Tannins were estimated based on their conversion to anthocyanidins upon acid hydrolysis. Between 100 mg and 400 mg fresh weight of root tissue was placed in a screw-capped 15 ml glass tube, and 2 ml of butanol:HCl (95:5) was added. The tubes were heated to 100 °C for 1 h and then allowed to cool. The spectrum of the hydrolysate was determined between 400 nm and 700 nm and the absorption at 550 nm measured. The absorption at 550 nm not due to anthocyanidins was estimated by interpolation of the underlying curve, not part of the 550 nm peak, and subtracted from the total absorption at 550 nm. The resulting value was used to calculate the tannin content of the sample using the $E^{1\%}_{1cm}$ of 150 determined by Stafford and Cheng (1980). This butanol:HCl hydrolysis method for the determination of condensed tannins gives an accurate and linear determination of total (i.e. soluble and insoluble) condensed tannins and has recently been validated in a range of forage species by Terrill et al. (1992). Estimation of percentage procyanidin (% PC) of condensed tannins was performed as described by Morris and Robbins (1992).

Results

Selection of sensitive seedlings and plant transformation

To produce a series of clonal genotypes sensitive to *A. rhizogenes* 50 seedlings were selected, 25 of which were

inoculated with *A. rhizogenes*, and 25 of which were untreated. Of the inoculated group 15 (60%) produced "hairy roots" after 26 days, while none of the untreated group produced "hairy roots". Of the 15 genotypes that produced "hairy roots", eight were micropropagated and used as recipients for the antisense constructs. These were designated s26, s28, s33, s35, s41, s46, s47, and s50; this paper discusses results using three of these genotypes, s33, s41 and s50.

Transformations were performed on these three genotypes, using *A. rhizogenes* LBA 9402 harbouring the antisense construct, pMAJ2. Control transformations were carried out using either wild-type LBA9402 or LBA9402 housing the binary plant transformation vector, pROK2. Initially 60 antisense transformants were tested for kanamycin sensitivity and 45 showed the ability to grow on media containing 25 mg ml^{-1} of kanamycin, indicating a co-transformation rate of 75%.

Analysis of condensed tannin levels in transgenic root cultures

Condensed tannin levels were determined in transgenic root cultures derived from three different recipient *Lotus* genotypes. Comparisons were made between independent control lines transformed with wild-type *A. rhizogenes* LBA9402 and kanamycin-resistant lines transformed with LBA9402 harbouring the antisense vector construct, pMAJ2. After initiation in liquid culture, control (C) and antisense (RFD) root cultures were subcultured at 14-day periods and harvested for analysis after the third subculture. Analysis of control transformed lines indicated that independent control lines derived from individual genotypes showed consistent patterns of tannin accumulation (Fig. 3). Five control lines derived from genotype s33 had a mean tannin level of 0.39 ± 0.06 mg g fresh weight (FW); three control lines derived from s50 accumulated 0.51 ± 0.15 mg/g FW of condensed tannin, while for five lines derived from s41 mean tannin levels were 3.29 ± 0.66 mg/g FW. Tannin levels of lines transformed with *A. rhizogenes* LBA9402 harbouring the unmodified plant transformation vector pROK2 were similar to values for wild-type LBA9402 (data not shown).

In subsequent analyses, tannin levels were analysed in kanamycin-resistant *Lotus* root cultures transformed with the antisense DFR construct, pMAJ2. In genotype s33 two antisense lines, RFD 7 and RFD 4, had tannin levels statistically indistinguishable from control lines; however, all the remaining six antisense lines showed a marked reduction in tannin accumulation in comparison to controls (Fig. 3). The most extreme example of low tannin levels was line RFD 21, which accumulated condensed tannin levels of 0.03 ± 0.03 mg/g FW in comparison to mean s33 control values of 0.39 mg/g FW. In genotype s50 a different distribution of tannin levels was found in individual antisense lines. One line, RFD 3, had significantly-higher levels of condensed tannins in root culture material than controls; two lines, RFD37 and RFD31, had similar levels to controls; while two further lines, RFD40 and RFD28, had significantly-lower

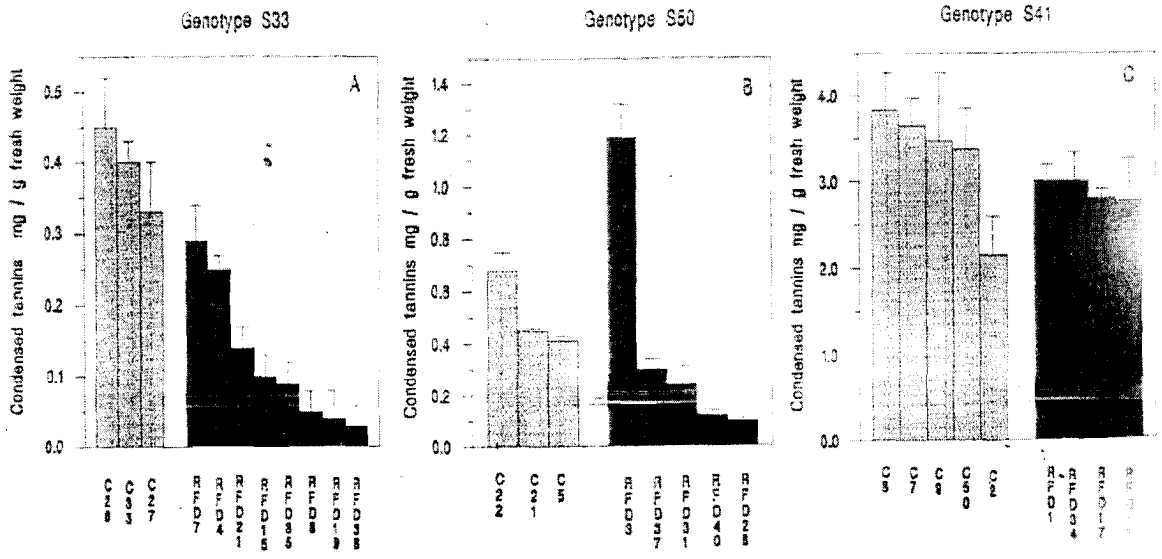

Fig. 3. Condensed tannin levels in control and antisense (pMAJ2) transformed root cultures of three different clonal genotypes of *L. corniculatus*. Tannin levels were determined from triplicate flasks harvested after the third liquid subculture

than s50 control lines. In genotype s41 antisense lines accumulated condensed tannins with similar levels to s41 control lines (Fig. 3).

In order to analyse whether the reductions in tannin levels noted in genotypes s33 and s50 resulted in alterations in tannin polymer structure, the degree of hydroxylation of tannin polymers was determined in tissue from control and antisense root cultures at the third subculture. The results of the PC:PD analysis are shown in Fig. 4. In genotype s33, control PC:PD values lay in the region of 70–80% procyanidin, while four antisense lines with reduced tannin levels had PC:PD values of 80–100%, with one line which yielded 100% procyanidin on hydrolysis. In s50, control lines had PC:PD ratios of 70–80%, while three low-tannin antisense lines had PC:PD values of greater than 80%. In s41, PC:PD values were indistiguishable between control and antisense lines and ranged between 50 and 80%.

Molecular analysis of control and antisense lines

In view of the condensed-tannin results for control and antisense lines in genotypes s33 and s50, detailed molecular analysis was carried out on three typical control lines and four selected antisense lines. The s33 lines selected for study were: C26, C27, C33, RFD8, RFD19, RFD21 and RFD38; and for s50 the selected lines were: C5, C21, C22, RFD28, RFD31, RFD37 and RFD40. Genomic DNA was extracted from each of these lines and analysed for the presence of three classes of T-DNA sequences (the binary antisense T-DNA and two T-DNAs from the *A. rhizogenes* Ri plasmid, T_L and T_R). DNA slot-blots were used to determine the presence or absence of three T-DNAs, and to estimate their copy number and the results are shown in Fig. 5. All of the control and antisense transformed lines were shown to contain the T_L T-DNA, indicating that all the lines were *A. rhizogenes*-transformed, and all but one (RFD28) of the antisense transformants, but none of the controls, were shown to contain the antisense T-DNA, indicating that these lines were co-transformed. Though no antisense DCR sequences were detected in the genome of RFD28, it was strongly kanamycin-resistant, indicating the transfer of some of the binary T-DNA, and so was treated as an antisense line. Four of the six controls, and six of the eight antisense lines were shown to contain the T_R T-DNA. A greater proportion of the s50 transformants than the s33 transformants contained the T_R T-DNA (Fig. 5e), and this may reflect a greater susceptibility to T_R transfer in s50 than in s33. A correlation, significant at the 5% level (coefficient 0.613), was found between the number of T_R copies transferred and the number of T_L copies transferred, though no significant correlation was found between either the number of T_R or T_L copies transferred and the number of antisense T-DNA copies transferred. The slot-blot was also hybridised to total *L. corniculatus* genomic DNA to ensure even-loading of the samples. No large differences between amounts of genomic DNA loaded for each sample were found (Fig. 5d). The presence and integration into the genome of the antisense T-DNA was further confirmed by Southern hybridisation (Fig. 6d).

The antisense lines were also analysed for expression of the antisense gene by Northern hybridisation. Single-stranded RNA probes specific to the antisense RNA were used to detect antisense RNA transcript in

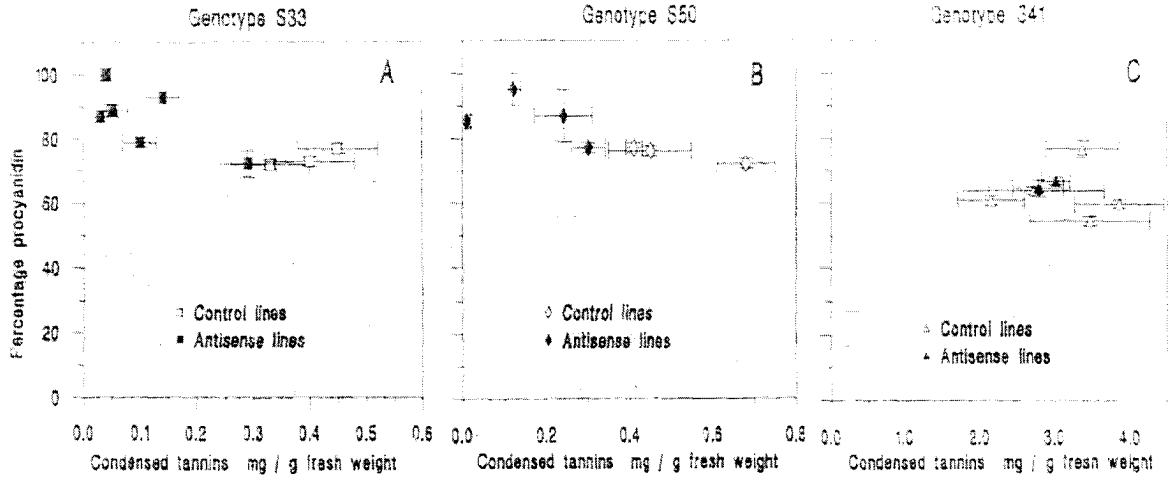

Fig. 4. Relationship between condensed tannin levels in root cultures of *L. corniculatus*, and the percent procyanidin content of the tannin, in antisense and control root cultures produced from three different clonal genotypes. Standard errors of the means (three determinations) are shown for both tannin level and percent procyanidin.

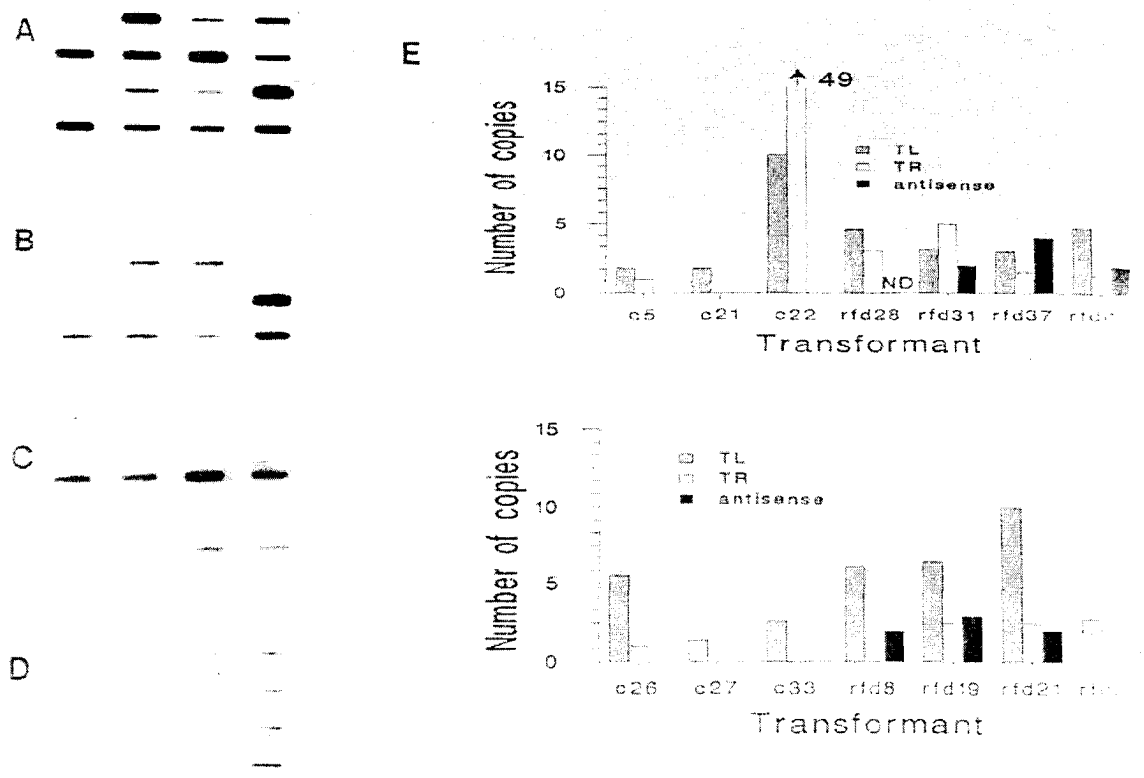

Fig. 5a–e. Analysis of the copy number for T_L, T_R, and the antisense T-DNA in selected antisense and control root cultures. **a**–**d** show a *L. corniculatus* genomic DNA slot-blot hybridised to probes for: T_L (a), T_R (b), the antisense T-DNA (c), and total *L. corniculatus* DNA (d). The slots are, from left to right, top row: s33 (non-transformed), c26, c27, c33; second row: RFD8, RFD19, RFD21, RFD38; third row: s50 (non-transformed), c5, c21, c22; bottom row: RFD28, RFD31, RFD37, RFD40. **e** is a bar chart showing the copy number of the three T-DNAs, as determined by comparison to copy number reconstructions. ND, not detected

total RNA isolated from the root cultures. Antisense transcript was found in six of the eight antisense transformants, but not in the control transformants (Fig. 6a, c).

Discussion

As an outbreeding crop, *L. corniculatus* shows much heterogeneity in phenotype, including its chemical composition (Roberts et al. 1989), and for this reason it was considered necessary to produce a series of clonal genotypes which were sensitive to *A. rhizogenes* infection and which gave good "hairy root" formation and regeneration. This allowed antisense transformants to be compared directly with control transformants of the same genotype. Subsequent data showed this to be an essential prerequisite for the detailed analysis of the experiment as tannin levels varied greatly between genotypes (Fig. 3).

The exact nature of the mechanism of antisense RNA suppression of gene expression is not fully understood (Grierson et al. 1991; Krol et al. 1991; [illegible] 1991) and the features of the antisense transgene confer optimum suppression of gene expression [illegible] well defined. Comparison of effects of different parts of transcripts used in antisense experiments give different results in different biological systems. Krol et al. (1990) demonstrated that the 3′ end of the CHS coding region was enough to confer antisense suppression, whereas the 5′ sequence alone did not. In contrast Melton (1985) showed that the 5′ sequence of frog oocyte globin was essential for antisense-mediated down-regulation of the protein. Short oligonucleotides have also proven to be effective in down-regulating gene expression in some systems. Cannon et al. showed effective inhibition of *gus* expression using a 41-bp antisense gene homologous to the 5′ end of the *gus* cDNA, whereas Smith et al. (1986) showed that

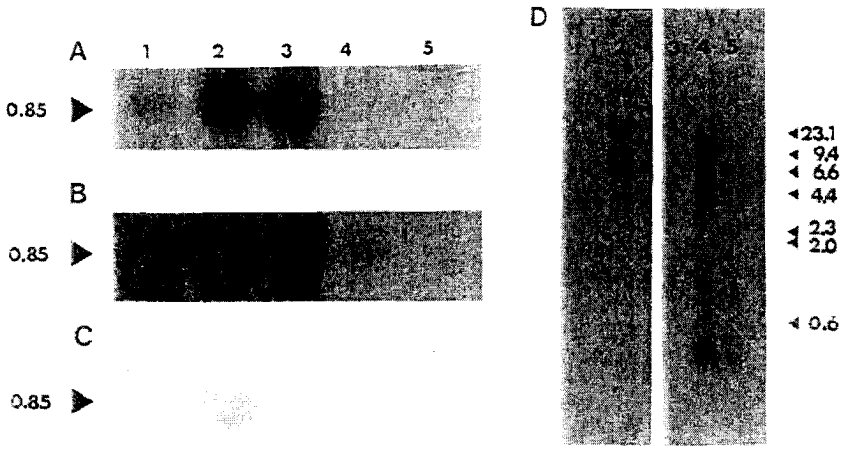

Fig. 6. Southern and Northern analysis of selected transformed root cultures. a shows a Northern-blot of RNA from *lane 1*, RFD28; 2, RFD19; 3, RFD21; 4, RFD25; 5, e26, probed with an RNA probe specific for the antisense RNA, and exposed for 16 h. b is as a except that it is a 5 day exposure. c shows a Northern of RNA from root cultures of, *lane 1*, RFD28; 2; RFD31; 3, RFD37; 4, RFD40; 5, e5, probed with an RNA probe specific for the antisense RNA, and exposed for 16 hours. d is a Southern-blot of DNA from root cultures of lane *1*, e26; 2, RFD19; 3, e5; 4, RFD37; 5, RFD40, probed with the construct pMAJ2. Sizes of antisense transcript and DNA molecular weight markers are in kbp

antisense treatment directed to the intron-exon splice sites of herpes simplex I reduced virus production by 90% in mammalian cell culture.

These contrasting observations make it difficult to predict whether or not a given antisense construct will be effective. In these experiments we have used a construct consisting of the 5′ half of a dihydroflavonol reductase cDNA from *A. majus*. Two other constructs consisting of the first quarter and the second half of the *A. majus* DFR cDNA have also been produced and results comparing the effectiveness of these three different constructs will be published elsewhere. With regard to homologies required for effective antisense phenotypes there are a number of pieces of evidence that have suggested that the *A. majus* DFR gene would be a suitable heterologous sequence. Firstly, stringency washes have indicated an homology of approximately 80% between the *A. majus* cDNA sequence and sequences present in the genome of *L. corniculatus* (Robbins, unpublished data). In fact we have detected a small family of 2–4 genes in a range of *Lotus* genotypes. Other evidence supporting heterologous DFR experiments comes from the outstanding homologies noted between DFR gene sequences in different plant species. Sequence comparisons of the *A. majus* DFR cDNA with other cloned DFRs has shown significant homologies to cDNA sequences from a range of other species including *P. hybrida* (Beld et al. 1989), *Z. mays* (Schwartz-Sommer et al. 1988) and *Arabidopsis thaliana* (Shirley et al. 1992). Comparisons of these sequences indicate between-species homologies of up to 85%, with these homologies being most marked in the 5′ half of cDNA sequences.

Initial analysis of antisense and control root cultures showed that the presence of the antisense construct, pMAJ2, was correlated with reduced tannin levels strongly suggesting that the construct was effectively down-regulating tannin accumulation. Comparison of tannin levels between antisense and control transformants in genotypes s33 and s50 indicated a number of antisense transformants which exhibited reductions in relative tannin levels. In addition there were examples of transformants in which there was no detectable antisense phenotype, e.g., RFD7 and RFD4 in genotype s33 and RFD37 and RFD31 in genotype s50, and these may be regarded as ineffective antisense transformation events. In s41, there were no examples of antisense transformants with reduced tannin levels relative to the controls. This observation, that the pMAJ2 T-DNA has a more significant effect on tannin accumulation in low-tannin genotypes than in the high-tannin genotypes, is novel. To the authors' knowledge this is the first published report of differential effects of antisense inhibition of secondary metabolic pathways noted with genotypes of different biosynthetic capacities.

The analysis of antisense transformants of the two selected genotypes, s33 and s50, showed the binary DNA to be integrated into the genome of the antisense-transformed plants (Figs. 5c, 6d), that the antisense RNA was expressed (Fig. 6a–c), and that the presence of the antisense T-DNA was strongly associated with a reduction in tannin levels. Southern analysis of *Hin*dIII digests of genomic DNA from three of the antisense lines, (RFD19, RFD37, and RFD40), indicated the presence of a diagnostic 1.3-kbp fragment (Fig. 6d).

comprising the CaMV35S promotor and 530 bp of the *A. majus* DFR gene, demonstrating that the antisense construct was intact in these lines. This band was clearly visible in the DNA from RFD37, a line containing five antisense copies as determined by slot-blot analysis (Fig. 5), but less visible in the DNA from RFD19 and RFD40 (containing four and two antisense copies respectively). Other hybridising bands were found in all three antisense lines examined. These were of varying molecular weight, suggesting, that they were border fragments, comprising DNA from the pMAJ2 plasmid with *Lotus* genomic DNA surrounding the integration sites (Fig. 6d). The presence of these border fragments is strong evidence for the integration of the binary vector into the genome of *Lotus*. In one antisense line, RFD28, we were unable to detect any antisense sequence in genomic DNA using slot-blots (Fig. 5); however, this line has shown consistantly low tannin levels both in root cultures and in regenerated plants (unpublished data). We suspect that pMAJ2 may have undergone some sort of structural rearrangement and we are currently continuing with a genetic analysis of RFD28 in order to clarify the details of this transformation event.

The observation that antisense RNA is easily detectable in the transformed root cultures may seem to contradict the findings of other workers (Krol et al. 1988; Smith et al. 1988) that antisense RNA is not detectable in tissue where the sense message is also expressed. However, in this case the RNA was isolated from whole-root cultures, whereas there is strong evidence that tannin biosynthesis (and presumably DFR expression) occurs only in certain cell lineages, and only in a region of the root directly behind the meristem (Morris and Robbins 1992). Therefore, the RNA extracted from antisense transformants may represent the RNA from cells in which both the antisense and the sense gene are active (those cells actively synthesising the DFR protein), and cells in which only the antisense gene is active (those cells not actively synthesising the DFR protein). Observations from other systems (Krol et al. 1988; Smith et al. 1988) would suggest that antisense RNA would be easily detected in RNA extracted from cells in which the sense gene is inactive.

Despite the strong correlation between the presence of the antisense T-DNA and the reduction in tannin levels no correlations could be found between the degree of reduction in tannin levels and either the number of copies of the antisense T-DNA integrated into the genome or the steady-state levels of antisense RNA. This is in accordance with the findings of other workers who showed that an excess of antisense RNA is not necessary for the antisense phenotype (Krol et al. 1991). Also the presence and copy number of the *A. rhizogenes* T-DNAs did not appear to affect the tannin levels in the transformed root cultures. The correlation between the number of T_L copies and the number of T_R copies was significant, but not great, and may reflect differences in the level and duration of *A. rhizogenes* plasmid vir activity during different transformation events.

The changes in tannin composition associated with the antisense-mediated reduction in tannin accumulation probably reflect alterations in the regulation of tannin biosynthesis. These alterations are not specific to cultures with genetically-modified tannin levels but also hold true for cultures that have naturally low, genotype-dependant, tannin levels. However, the use of some chemical inhibitors of tannin biosynthesis has also been shown to reduce tannin levels by similar amounts to the antisense constructs but do not cause any change in the percent of procyanidin (unpublished data). These observations may have implications for the mechanisms of developmental control of condensed tannin biosynthesis and these phenomena are currently under investigation.

Acknowledgements. The authors thank Dr. Judith Webb for the selection and preparation of the eight clonal genotypes used in this study and for her valuable advice throughout this work. We also thank Teri Evans for excellent technical support, Dr. Potter for assistance with statistical analysis, and Ian Sanders for photography. The authors are grateful to Dr. Cathy Martin for her generous gift of the plasmid pJAM212. TRC was supported by the AFRC Plant Molecular Biology Initiative, research grant PG203/504. This work was carried out under MAFF licences Nos. PHF 162A 48 (109), 52 (70), 71 (81) and PHF 162B 13 (62).

References

Beld M, Martin C, Huits H, Stuitje AR, Gerats AGM (1989) Flavonoid synthesis and partial characterisation of dihydroflavonol-4-reductase genes. Plant Mol Biol 13:491–502

Bettany AJE (1988) Messenger RNA translation in *Saccharomyces cerevisiae*. PhD thesis, University of Glasgow, UK

Brownlee HE, Hedger J, Scott IM (1992) Effects of a range of procyanidins on the cocoa pathogen *Crinipellis perniciosa*. Physiol Mol Plant Path 40:227–232

Cannon M, Platz J, O'Leary M, Sookdeo C, Cannon F (1989) Organ-specific modulation of gene expression in transgenic plants using antisense RNA. Plant Mol Biol 15:39–47

Cesarone CF, Bolognesi C, Santi L (1979) Improved fluorometric DNA determination in microtiter plates using 33258 Hoechst. Anal Biochem 100:188–197

Dellaporta SL, Wood J, Hicks JB (1983) A plant DNA minipreparation: version II. Plant Mol Biol Rep 1:19–21

Doone HK, Robbins TP, Jorgensen RA (1992) Genetic and developmental control of anthocyanin biosynthesis. Annu Rev Genet 25:173–199

Forde BG, Day HM, Turton JF, Wen-Jun S, Cullimore JV, Oliver JE (1989) Two glutamine synthetase genes from *Phaseolus vulgaris* L. display contrasting developmental and spatial patterns of expression in transgenic *Lotus corniculatus* plants. Plant Cell 1:391–401

Grierson D, Fray RG, Hamilton AJ, Smith CJS, Watson CF (1991) Does co-suppression of sense genes in transgenic plants involve antisense RNA? Trends Biotechnol 9:122–123

Griffiths DW (1989) Polyphenolics and their possible effects on nutritive value. Aspects Appl Biol 19:93–103

Haslam E (1989) Plant polyphenols: vegetable tannins revisited. Cambridge University Press, Cambridge, UK

Hemon P, Robbins MP, Cullimore JV (1990) Targeting of glutamine synthetase to the mitochondria of transgenic tobacco. Plant Mol Biol 15:895–904

Herrera-Estrella L, Simpson J (1988) Foreign gene expression in plants. In: Shaw CH (ed) Plant molecular biology, a practical approach. IRL Press, Oxford, pp 131–158

Krol AR van der, Lenting PE, Veenstra J, Meer IM van der, Koes RE, Gerats AGM, Mol JNM, Stuitje AR (1988) An anti-sense chalcone synthase gene in transgenic plants inhibits flower pigmentation. Nature 833:866–869

Krol AR van der, Mur LA, Lange P de, Mol JNM (1990) Inhibition of flower pigmentation by antisense CHS genes: promoter and minimal sequence requirements for the antisense effect. Plant Mol Biol 14:457–466

Krol AR van der, Stuitje AR, Mol JNM (1991) Modulation of floral pigmentation by antisense technology. In: Mol JNM, Krol AR van der (eds) Antisense nucleic acids and proteins. Marcel Decker, New York, pp 125–140

Lawrence-Marsh J, Erfle M, Wykes EJ (1984) The pIC plasmid and phage vectors with versatile cloning sites for recombinant selection by insertional inactivation. Gene 32: 481–485

Lev Z (1987) A procedure for the large-scale isolation of RNA-free plasmid and phage DNA without the use of RNase. Anal Biochem 166:332–336

Maniatis T, Fritsch EF, Sambrook J (1982) Molecular cloning. Cold Spring Harbor Laboratory, Cold Spring Harbor, New York

Melton DA (1985) Injected anti-sense RNAs specifically block messenger RNA translation in vivo. Proc Natl Acad Sci USA 82:144–148

Mol J, Blokland R van, Kooter J (1991) More about cosupression. Trends Biotechnol 9:182–183

Morris P, Robbins MP (1992) Condensed tannin formation by *Agrobacterium rhizogenes*-transformed root and shoot organ cultures of *Lotus corniculatus*. J Exp Bot 43:221–231

Ougham HJ, Davies TGE (1990) Leaf development in *Lolium temulentum* gradients of RNA complement and plastid and non-plastid transcripts. Physiol Plant 79:331–338

Petit A, Stougaard J, Kuhle A, Marcker KA, Tempe J (1987) Transformation and regeneration of the legume *Lotus corniculatus*: a system for molecular studies of symbiotic nitrogen fixation. Mol Gen Genet 207:245–250

Reid CSW, Ulyatt MJ, Wilson JM (1974) Plant tannins, fibre and nutritive value (cattle). Proc NZ Soc Anim Prod 34: 82–93

Robbins MP, Hartnoll J, Morris P (1991) Phenylpropanoid defence responses in transgenic *Lotus corniculatus*. I. Glutathione elicitation of isoflavan phytoalexins in transformed root cultures. Plant Cell Rep 10:59–62

Roberts CA, Bueselink PR, Derks JA, Marek SM (1989) Tannins in *Lotus corniculatus* accessions. *Lotus* Newslett 20:38–41

Scalbert A, Haslam E (1987) Polyphenols and chemical defence of the leaves of *Quercus robur*. Phytochemistry 26: 3191–3195

Schwartz-Sommer Z, Shepherd N, Tacke E, Gierl A, Rohde W, Leclercq L, Mattes M, Berndtgen R, Peterson PA, Saedler H (1987) Influence of transposable elements on the structure and function of the A1 gene of *Zea mays*. EMBO J 6: 287–294

Shirley BW, Hanley S, Goodman HM (1992) Effects of ionizing radiation on a plant genome: analysis of two *Arabidopsis* transparent testa mutations. Plant Cell 4:333–347

Smith CC, Aurelain L, Reddy PM, Miller PS (1986) Antiviral effects of an oligo (nucleoside methylphosphonate) complementary to the splice junction of herpes simplex virus type 1 immediate early pre-mRNAs 4 and 5. Proc Natl Acad Sci USA 83:2787–2791

Smith CJS, Watson CF, Ray J, Bird CR, Morris PC, Schuch W, Grierson D (1988) Antisense RNA inhibition of polygalacturonase gene expression in transgenic tomatoes. Nature 334:724–726

Stafford HA (1989) The enzymology of proanthocyanidin biosynthesis. In: Hemingway RW, Karchesy JJ (eds) Chemistry and significance of condensed tannins. Plenum Press, New York, pp 47–70

Stafford HA, Cheng T-Y (1980) The procyanidins of douglas fir seedlings, callus and cell suspension cultures derived from cotyledons. Phytochemistry 19:131–135

Stafford HA, Lester HH (1985) Flavan 3-ol biosynthesis. The conversion of (+)-dihydroquercetin and flavan 3,4-cis-diol (leucocyanidin) to (+)-catechin by reductases extracted from cell-suspension cultures of Douglas fir. Plant Physiol 76: 184–186

Terrill TH, Rowan AM, Douglas GB, Barry TN (1992) Determination of extractable and bound condensed tannin concentrations in forage plants, protein concentrate meals and cereal grains. J Sci Food Agric 58:321–329

Tunen AJ van der, Mol JMN (1991) Control of flavonoid synthesis and manipulation of flower colour. In: Grierson D (ed) Plant biotechnology, vol 2. Developmental regulation of plant gene expression. Blackie, Glasgow, pp 94–131

Visser RGF, Feenstra WJ, Jacobsen E (1991) Manipulation of granule-bound starch synthase activity and amylose content in potato by antisense genes. In: Mol JNM, Krol AR van der (eds) Antisense nucleic acids and proteins. Marcel Decker, New York, pp 141–155

Wood KJ, Woodcock S, Chamberlain DA (1987) Plant regeneration from protoplasts of *Trifolium repens* and *Lotus corniculatus*. Plant Breed 98:111–118

Webb KJ, Jones S, Robbins MP, Minchin FR (1990) Characterization of transgenic root cultures of *Trifolium repens*, *Trifolium pratense* and *Lotus corniculatus*, and transgenic plants of *Lotus corniculatus*. Plant Sci 70:243–254

Plant Cell, Tissue and Organ Culture **46**: 137–141, 1996.

Differential expression of antisense in regenerated tobacco plants transformed with an antisense version of a tomato ACC oxidase gene

John W. Einset
Department of Biology and Nature Conservation, Agricultural University of Norway, 1432 Aas, Norway

Received 10 July 1995; accepted in revised form 15 July 1996

Key words: Nicotiana tabacum, transformed plants, 35S CaMV promoter

Abstract

Ethylene production was measured during vegetative and reproductive development in normal tobacco plants and in transgenic tobacco plants carrying antisense genes for tomato ACC oxidase driven by the 35S CaMV promoter (Hamilton et al., 1990). When expressed in three independently derived transgenic plants, the antisense ethylene gene failed to affect ethylene production in young/mature leaves or in stems but it did inhibit ethylene production in roots by 37-58%. Ethylene production in developing flowers (i.e. from small unopened flower buds up until open flowers at anthesis) was not affected in transgenic plants but ethylene production in fruits was inhibited by 35%. The most dramatic effect on ethylene production in transgenic plants was seen immediately after wounding leaf tissue, in which case the antisense gene inhibited wound ethylene production by 72%. Thus, the antisense gene composed of a 35S CaMV promoter driving a heterologous ACC oxidase sequence had differential effects on ethylene production in tobacco plants.

Introduction

Antisense technology has been used successfully to inhibit several different plant processes; e.g. photosynthesis, starch synthesis, floral organ development, flower pigmentation, flower senescence and fruit ripening (Watson and Grierson, 1993; Stitt and Schulze, 1994). By using antisense genes for ethylene biosynthesis, it has been possible to produce slower-ripening tomato varieties (Hamilton et al., 1990; Oeller et al., 1991) as well as carnation varieties with longer-lasting flowers (Michael et al., 1993). At the same time that antisense ethylene genes have been used for practical objectives, they have also provided insight into basic processes involving ethylene. Several reviews have summarized characteristics of antisense-ethylene transgenics, pointing out that major effects involve fruit ripening and flower senescence (Klee and Estelle, 1991; Romano and Klee, 1993; Gray et al., 1994; John et al., 1995).

Genes for the key enzymes of ethylene biosynthesis, ACC synthase and ACC oxidase, exist in plants as multigene families with, for example, nine and three copies, respectively, occurring in the tomato genome (Zarembinski and Theologis, 1994). Different members of these multigene families are expressed at different times during development and considerable sequence variability exists among members of both multigene families (Kende, 1993).

We have produced tobacco transgenics carrying an antisense version of a gene for tomato ACC oxidase (Hamilton et al., 1990). This report summarizes studies dealing with the effects of this antisense gene on ethylene production in different organs during the life cycle of plants. Of particular interest is the finding that ethylene production is differentially affected, showing that heterologous genes can inhibit ethylene production in an organ-specific fashion.

Materials and methods

Plant transformation

The antisense gene for tomato ACC oxidase was obtained as binary plasmid pBASC (Hamilton et al.,

1990) from D. Grierson, University of Nottingham. This plasmid was introduced into *Agrobacterium tumefaciens* LBA4404 by triparental mating (Van Haute et al., 1983). Tobacco (*Nicotiana tabacum* cv Petit Havana SR1) was transformed by the leaf disc method (Horsch et al., 1985). The numbers of independently segregating loci were determined by selfing followed by analysis of progeny for kanamycin resistance (Reynaerts et al., 1988). Kanamycin resistance in progeny from transgenics BASC-1, BASC-2 and BASC-3 segregated as 3, 4 and 4 loci, respectively.

Ethylene determinations

Ethylene production was measured as described by Rodrigues-Pousada et al., (1993). Tissues were placed in 20 ml test tubes with moist filter paper. After a 6-h preincubation period to avoid measuring wound-induced ethylene production, the flasks were sealed for 24 h, after which time accumulating ethylene was measured by gas chromatography.

PCR and other nucleic acid methods

To verify the presence of T-DNA sequences in transgenic plant material, genomic DNA was analyzed by PCR (Mullis and Faloona, 1987) using primers based on tomato ACC oxidase (sense 5'-GAATTCGCTTGTGAGAACTGGGGTTTC-3' and antisense 5'-GGATCCTTCAAATCTTGGCTCCTTGGC-3'). DNA was isolated using a conventional high-salt extraction procedure (Gelvin et al., 1991) followed by DNA purification with a Qiagen 100 column (Qiagen Inc.). RNA was isolated using a Qiagen Kit. For nucleic acid hybridization experiments, Gene Screen (Dupont) membranes were used along with probe labeled with the Prime-a-Gene system (Promega). Protocols for probe preparation, hybridization of membranes, etc. followed the recommendations of the manufacturers.

Results

Ethylene production during vegetative growth and in developing fruits is differentially affected by antisense ethylene genes

Transgenic tobacco plants carrying antisense ethylene genes, selected using kanamycin resistance and verified by PCR, were grown alongside nontransformed SR1. Patterns of ethylene production among three transgenics expressing an antisense ACC oxidase gene were essentially the same. Table 1 compares ethylene production in different tissues from transformed and nontransformed plants. No consistent inhibition of ethylene production in leaves or stems could be detected in antisense plants, although root ethylene production was inhibited by 37-58% and fruit ethylene production was inhibited by 35%. Consistent with results for *Arabidopsis* (Rodrigues-Pousada et al., 1993), we observed significantly higher ethylene production in young (immature) leaves compared to mature leaves.

Ethylene production by developing flowers is not inhibited in antisense plants

Figure 1 shows the fluctuation of ethylene production rates during flower development, using flower stages as defined by Drews et al. (1992). As indicated, small unopened flowers (Stage 1) produced nearly 30 nl g^{-1} h^{-1} ethylene but subsequently ethylene production declined (Stages 2-3). A burst of ethylene production then occurred, coinciding with the expansion growth of the corolla (Stages 4-6), followed by a sharp drop (Stages 7-11) and then a rise in ethylene production leading up to anthesis (Stage 12). Ethylene production by antisense ACC oxidase plants was not significantly different from controls.

Wound ethylene production is dramatically reduced in antisense transgenics

Figure 2 presents the fluctuation in ethylene production that occurred after wounding leaf tissues by making leaf discs using a hand-held paper punch (Horsch et al., 1985). Ethylene production in nontransformed tissue increased rapidly, reaching an average of nearly 20 nl g^{-1} h^{-1} during the first hour. Subsequently, wound ethylene production declined with average rates corresponding to 11.2, 5 and 4 nl g^{-1} h^{-1} during the second, third and fourth hours after wounding, respectively. By the sixth hour after wounding, the rate of ethylene production had returned to control levels.

Wound ethylene production was inhibited by 72% in antisense plants during the first hour after wounding. Significant suppression of wound ethylene production in transgenic plants was also clearly evident during the second and third hours after wounding.

Table 1. Comparison of ethylene production rates (nl g^{-1} h^{-1}) in different organs of normal (SR1) and transgenic plants.

	Mature Leaf	Young Leaf	Stem	Root	Fruit
SR1	0.6(0.2)	1.1(0.1)	2.4(0.4)	19(3)	2.2(0.4)
BASC-1	0.5(0.1)	0.9(0.3)	1.4(0.1)	8(0.3)	
BASC-2	0.5(0.1)	1.4(0.2)	2.5(0.2)	12(3)	1.4(0.4)
BASC-3	0.5(0.2)	1.9(0.2)	2.4(0.2)	9(0.4)	

Each data point represents the mean of at least 4 independent determinations with SE in parenthesis. The experiment was repeated three times with similar results.

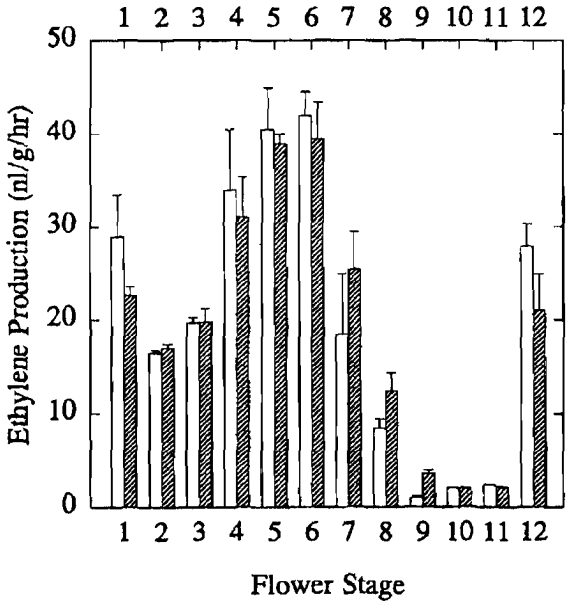

Figure 1. Ethylene production during flower development by normal and by transgenic tobacco. Flower stages are defined according to Drews et al., 1992); for each stage, the unshaded bar shows ethylene production for normal plants while the shaded bar shows production for transgenic plants. Each value for normal plants is the mean of three independent ethylene determinations with three different flowers with SE bars. In the case of transgenic plants, each value was obtained by pooling results from all three transgenics, using three independent ethylene determinations with three different flowers for each plant.

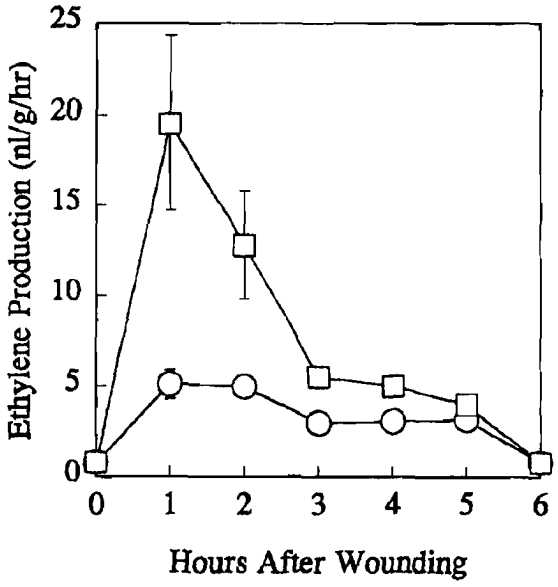

Figure 2. Wound ethylene production by leaf discs (0.5 cm diameter) from normal and transgenic (BASC-2) tobacco. Each point represents the mean ethylene production of three samples, each consisting of 20 leaf discs, with SE. This experiment was conducted on three different occasions with similar results.

Gene expression studies

Figure 3 shows a dot blot, probing RNA preparations from tobacco leaves and flowers with the tomato ACC oxidase gene. A strong signal became evident in leaves 10 min after wounding but this signal disappeared after 60 min. This result is similar to results obtained by Hamilton et al., (1990) who detected a rapid increase-and-decrease in ACC oxidase mRNA in wounded leaf pieces from tomato plants.

The relative expression of the 35S-antisense gene is shown by the signal for BASC-1 leaves, 60 min after wounding. By comparison, expression of the antisense gene was considerably lower in BASC-1 flowers. Based on this and similar blots, we estimate that the 35S-antisense gene is expressed only about 1/5 as strongly in flowers compared to leaves.

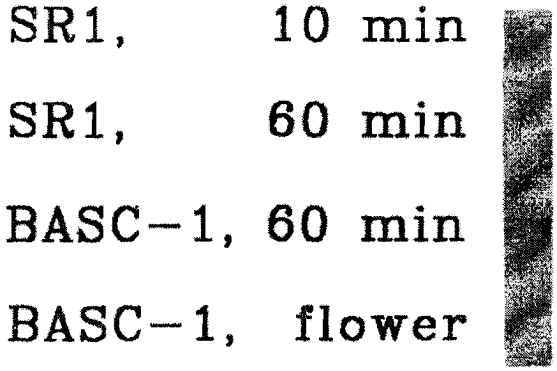

Figure 3. Dot blot analysis of gene expression in normal and transgenic tobacco. Fifty microgram samples of RNA, quantitated by UV spectroscopy, were spotted on a Gene Screen membrane which was then probed with labeled ACC oxidase from tomato.

Discussion

The antisense gene for tomato ACC oxidase exhibited tissue-specific effects, significantly inhibiting ethylene production in roots, fruits and wounded leaves but not affecting ethylene production in leaves, stems or flowers. Possible explanations for this differential effect include;

- varying degrees of homology of the tomato gene to the different tobacco genes expressed at different times during development,
- tissue-to-tissue fluctuations in the availability of other components required for antisense action (Nellen and Lichtenstein, 1993) and
- variable expression of the 35S promoter.

Strong suppression of wound ethylene production in plants having no inhibition of ethylene production during flower development was particularly striking. It is possible that this was caused by a lower level of expression of the antisense gene in flowers in as much as we found only about 1/5 as much transcript in flower tissues compared to leaves. On the other hand, antisense strategies have been used successfully before with tobacco flowers. Examples of effective antisensing using 35S-driven genes in tobacco flowers are transgenics expressing antisense constructions for homeotic genes controlling flower development (Kempin et al., 1993; Mandel et al., 1992). A second possibility for the differential effect of antisense on wound versus flower ethylene production is that a different ACC oxidase is induced by wounding in tobacco than the gene(s) that is induced during the course of flower development. At any rate, the results illustrate one example of what can happen when a heterologous antisense gene for an ACC oxidase is expressed in a transgenic plant. Ethylene is known to be produced in virtually all plant tissues, at rates varying from 0.05 to several thousand nl g^{-1} h^{-1} (Abeles, 1973). So far, ethylene antisense has been used successfully only in cases such as tomato fruit ripening (Oeller et al., 1991; Gray et al., 1994) or carnation flower senescence (Michael et al., 1993) where ethylene production rates are very high. Presumably, these processes are controlled by the so-called "system 2" ethylene receptor (Yang, 1987). Whether processes regulated by lower ethylene levels, such as several phenomena in plant tissue cultures (Biddington, 1992), can also be inhibited using ACC synthase or ACC oxidase antisense is unclear.

References

Abeles FB (1973) Ethylene in Plant Biology. Academic Press, New York

Biddington NL (1992) The influence of ethylene in plant tissue culture. Plant Growth Regul. 11: 173–187

Drews GN, Beals TP, Bui AQ & Goldberg RB (1992) Regional and cell-specific gene expression patterns during petal development. Plant Cell 4: 1383–1404

Gelvin B, Schilperoort RA & Verma DPS (1991) Plant molecular biology manual. Kluwer Academic Publ., Dordrecht

Gray JE, Picton S, Giovannoni JJ & Grierson D (1994) The use of transgenic and naturally occurring mutants to understand and manipulate tomato fruit ripening. Plant Cell Environ. 17: 557–571

Hamilton AJ, Lycett GW & Grierson D (1990) Antisense gene that inhibits synthesis of ethylene in transgenic plants. Nature 346: 284–287

Horsch RB, Fry JE, Hoffman NL, Eichholtz D, Rogers SG & Fraley RT (1985) A simple and general method for transferring genes into plants. Science 227: 1229–1231

John I, Drake R, Farrell A, Cooper W, Lee P, Horton P & Grierson D (1995) Delayed leaf senescence in ethylene-deficient ACC oxidase tomato plants: molecular and physiological analysis. Plant J. 7: 483–490

Kempin SA, Mandel MA & Yanofsky MF (1993) Conversion of perianth into reproductive organs by ectopic expression of the tobacco floral homeotic gene NAG1. Plant Physiol. 103: 1041–1046

Kende H (1993) Ethylene biosynthesis. Ann. Rev. Plant Physiol. Plant Mol. Biol. 44: 283–307

Klee H & Estelle M (1991) Molecular genetic approaches to plant hormone biology. Ann. Rev. Plant Physiol. Plant Mol. Biol. 42: 529–551

Mandel MA, Bowman JL, Kempin SA, Ma H, Meyerowitz EM & Yanofsky MF (1992) Manipulation of flower structure in transgenic tobacco. Cell 71: 133–143

Michael MZ, Savin KW, Baudinette SC, Graham MW, Chandler SF, Lu C-Y, Caesar C, Gautrais I, Young R, Nugent GD, Stevenson KR, O'Connor EL-J, Cobbett CS & Cornish EC (1993) Cloning of ethylene biosynthetic genes involved in petal senes-

cence of carnation and petunia, and their antisense expression in transgenic plants. In: Pech JC, Latche A & Balague C (eds) Cellular and Molecular Aspects of the Plant Hormone Ethylene (pp 298–303), Kluwer Academic Publ., Dordrecht

Mullis KB & Faloona FA (1987) Specific synthesis of DNA *in vitro* via polymerase-catalyzed chain reaction. Methods Enzymol. 155: 335–350

Nellen W & Lichtenstein C (1993) What makes an mRNA anti-sense-itive? TIBS 18: 419–423

Oeller PW, Wong L-M, Taylor LP, Pike DA & Theologis A (1991) Reversible inhibition of tomato fruit senescence by antisense RNA. Science 254: 437–439

Reynaerts A, DeBlock M, Hernalsteens J-P & Van Montagu M (1988) Selectable and screenable markers. In: Gelvin SB, Schilperoort RA & Verma DPS (eds) Plant Molecular Biology Manual, Vol 1 (A9: 1–16). Kluwer Academic Publ., Dordrecht

Rodrigues-Pousada RA, De Rycke R, Dedonder A, Van Caeneghem W, Engler G, Van Montagu M & Van Der Straeten D (1993) The Arabidopis 1-aminocyclopropane-1-carboxylate synthase gene 1 is expressed during early development. Plant Cell 5: 897–911

Romano CP & Klee H (1993) Hormone manipulation in transgenic plants. In: Hiatt A (ed) Transgenic Plants, Fundamentals and Applications (pp 23–36). Marcel Dekker Inc., New York

Stitt M & Schulze D (1994) Does Rubisco control the rate of photosynthesis and plant growth? An exercise in molecular ecophysiology. Plant Cell Environ. 17: 465–487

Van Haute E, Joos H, Maes M, Warren G, Van Montagu M & Schell J (1983) Intergeneric transfer and exchange recombination of restriction fragments cloned in pBR322: a novel strategy for the reversed genetics of the Ti plasmids of *Agrobacterium tumefaciens*. EMBO J. 2: 411–418

Watson CF & Grierson D (1993) Antisense RNA in plants. In: Hiatt A (ed) Transgenic Plants, Fundamentals and Applications (pp 255–281). Marcel Dekker Inc., New York

Yang SF (1987) The role of ethylene and ethylene synthesis in fruit ripening. In: Thomson WW, Nothnagel EA & Huffaker RC (eds) Plant Senescence: Its Biochemistry and Physiology (pp 156–166). American Society of Plant Physiologists, Rockville

Zarembinski TI & Theologis A (1994) Ethylene biosynthesis and action: case of conservation. Plant Mol. Biol. 26: 1579–1597

Plant Physiol. (1997) 113: 1153–1165

NADP-Malate Dehydrogenase in the C_4 Plant *Flaveria bidentis*

Cosense Suppression of Activity in Mesophyll and Bundle-Sheath Cells and Consequences for Photosynthesis

Stephen J. Trevanion[1], Robert T. Furbank, and Anthony R. Ashton*

Cooperative Research Centre for Plant Science, c/o Research School of Biological Sciences, Australian National University, P.O. Box 475, Canberra, ACT 2601, Australia (S.J.T., R.T.F., A.R.A.); and Commonwealth Scientific and Industrial Research Organization, Division of Plant Industry, P.O. Box 1600, Canberra, ACT 2601, Australia (R.T.F., A.R.A.)

***Flaveria bidentis*, a C_4 dicot, was transformed with sorghum (a monocot) cDNA clones encoding NADP-malate dehydrogenase (NADP-MDH; EC 1.1.1.82) driven by the cauliflower mosaic virus 35S promoter. Although these constructs were designed for over-expression, many transformants contained between 5 and 50% of normal NADP-MDH activity, presumably by cosense suppression of the native gene. The activities of a range of other photosynthetic enzymes were unaffected. Rates of photosynthesis in plants with less than about 10% of normal activity were reduced at high light and at high $[CO_2]$, but were unaffected at low light or at $[CO_2]$ below about 150 $\mu L\ L^{-1}$. The large decrease in maximum activity of NADP-MDH was accompanied by an increase in the activation state of the enzyme. However, the activation state was unaffected in plants with 50% of normal activity. Metabolic flux control analysis of plants with a range of activities demonstrates that this enzyme is not important in regulating the steady-state flux through C_4 photosynthesis in *F. bidentis*. Cosense suppression of gene expression was similarly effective in both the mesophyll and bundle-sheath cells. Photosynthesis of plants with very low activity of NADP-MDH in the bundle-sheath cells was only slightly inhibited, suggesting that the presence of the enzyme in this compartment is not essential for supporting maximum rates of photosynthesis.**

The photosynthetic efficiency of C_3 plants is often limited by the competition of O_2 with CO_2 at the active site of Rubisco, the primary carboxylating enzyme of photosynthesis (Andrews and Lorimer, 1987). C_4 plants have evolved a complex mechanism involving both structural and biochemical adaptations to overcome this (Hatch, 1987). The primary role of the C_4 mechanism is to increase the ratio of CO_2 to O_2 in the bundle-sheath cell chloroplast, the site of CO_2 fixation by Rubisco. This adaptation increases both the maximum rate of photosynthesis and the efficiency of the process at low light. Other advantages of the C_4 pathway are improved efficiency of water and nitrogen use (Hatch, 1987). However, the advantage conferred to a plant by these adaptations is temperature-dependent, declining as the temperature decreases (Hatch, 1987).

Although the properties of many enzymes of C_4 photosynthesis have been extensively studied in vitro, until recently we have had no way of examining the role of key enzymes in regulating photosynthetic flux in the intact plant. Gene-suppression technology, in particular, antisense, has proven invaluable in identifying the important regulatory enzymes in C_3 photosynthesis under a range of environmental conditions (Furbank and Taylor, 1995). The recent development of an efficient transformation system for the C_4 dicot *Flaveria bidentis* (Chitty et al., 1994) has allowed us to apply these techniques to the study of C_4 photosynthesis. This approach has demonstrated that, as in C_3 plants, Rubisco is an important determinant of the rate of C_4 photosynthesis at air concentrations of CO_2 and at high light intensities (Furbank et al., 1996). However, C_4 photosynthesis is compartmented between two cell types, and the regulatory properties of both the photosynthetic carbon reduction cycle and the C_4 cycle enzymes must be considered. Some of these enzymes have complex regulatory properties (Hatch, 1987), and it is quite likely that one or more of them is also involved in regulating photosynthetic carbon flux. One potential target for regulation is the reaction catalyzed by NADP-MDH (EC 1.1.1.82): oxaloacetate + NADPH + H^+ ⇌ malate + $NADP^+$.

In maize NADP-MDH is localized exclusively in the mesophyll cell chloroplasts. Activity of the enzyme is regulated by changes in the concentrations of substrates (Ashton and Hatch, 1983a), and also varies in response to changes in light intensity (Johnson and Hatch, 1970) due to changes in activation state. This is due to covalent modification of the enzyme involving the reduction and oxidation

[1] Present address: IACR-Rothamsted, Harpenden, Hertshire, AL5 2JQ, UK.

* Corresponding author; e-mail tony.ashton@pi.csiro.au; fax 61–6–246–5000.

Abbreviations: CaMV, cauliflower mosaic virus; MDH, malate dehydrogenase; *nos*, nopaline synthase; OAA, oxaloacetate; 2OG, 2-oxoglutarate; PEPCX, PEP carboxylase; PGA, phosphoglycerate; PPDK, pyruvate phosphate dikinase.

of Cys residues by thioredoxin *m* (Kagawa and Hatch, 1977; Jacquot et al., 1984). The oxidized form of the enzyme extracted from darkened leaves is almost completely inactive, with less than 0.001% of the activity of the reduced enzyme (Ashton and Hatch, 1983a). The activation state is regulated by the ratio of NADPH to NADP both in vitro (Ashton and Hatch, 1983b) and in vivo (Rebeille and Hatch, 1986). These properties of the enzyme provide it with a sensitive mechanism by which activity can respond to changes in the redox potential of the chloroplast (Edwards et al., 1985). Although this suggests a potential role for the enzyme in regulating photosynthetic flux, the degree to which this occurs in vivo is not known.

The individual amino acids involved in the covalent regulation of the sorghum enzyme have been identified (Issakidis et al., 1992, 1994), and mutagenesis has produced, among others, an always active, thiol-insensitive enzyme (Issakidis et al., 1994). We have used clones encoding both the wild-type and the mutated sorghum enzymes to manipulate the activity of NADP-MDH in transgenic *F. bidentis*. Analysis of these plants has allowed us to assess the role of this enzyme in regulating the rate of C_4 photosynthesis. *F. bidentis* differs from maize in that it has significant activities of NADP-MDH in the bundle-sheath cell chloroplast (Meister et al., 1996). Therefore, we have also considered the significance of this form of the enzyme in the regulation of C_4 photosynthesis in this plant.

MATERIALS AND METHODS

Biochemicals were obtained from either Boehringer Mannheim or Sigma. Thioredoxin was purified from *Escherichia coli* transformed with the multicopy plasmid pPMR18, provided by Marjorie Russel (The Rockefeller University, New York), which contains the *E. coli* thioredoxin (*TrxA*) gene (Russel and Model, 1986). The thioredoxin was purified to homogeneity by a procedure involving sequential $(NH_4)_2SO_4$ and PEG fractionation followed by DEAE-Sepharose chromatography (A.R. Ashton, unpublished data). Restriction enzymes were from New England Biolabs. Molecular biological techniques were performed as described by Sambrook et al. (1989).

Transformation and Growth of Plants

Wild-type and mutant sorghum NADP-MDH clones differing in kinetic and regulatory properties (Issakidis et al., 1992, 1994) in either pUC19 or M13 mp19 were a gift from Emmanuelle Issakidis and Myroslawa Miginiac-Maslow (Centre National de la Recherche Scientifique, Orsay, France). The clones were excised with *Eco*RI and subcloned in the sense orientation into the vector pJ35SN (Landsmann et al., 1988) between the CaMV 35S promoter and the *nos* terminator. The constructs were digested with *Hind*III, and the DNA fragments containing the 35S promoter-sorghum NADP-MDH gene-*nos* terminator were ligated into the binary vector pGA470 (An et al., 1985). This vector contains the neomycin phosphotransferase gene *nptII* driven by the *nos* promoter to confer kanamycin resistance. The NADP-MDH sense construct and the *nptII* gene are transcribed in the same direction from the transferred DNA. This will prevent the generation of antisense NADP-MDH message from the *nos* promoter of the *nptII* gene. The constructs produced in this way were (a) wtSorg (wild-type sorghum cDNA clone), (b) dmNSorg (double N-terminal mutant, C64S/C69S), (c) dmCSorg (double C-terminal mutant, C405A/C417A), and (d) QmSorg (quadruple mutant, C64S/C69S/C405A/C417A). Transformation of *Flaveria bidentis* using *Agrobacterium* strain *AglI* (Lazo et al., 1991) was exactly as described by Chitty et al. (1994). Transformants were selected on kanamycin and then transferred to the greenhouse in pots containing a mixture of 50% (v/v) compost, 50% (v/v) perlite. The plants were initially hardened off under a 50% shade cloth for 2 weeks, and then transferred to full sunlight. The temperature was maintained at 29°C during the day and 21°C at night. Fertilization was with both a slow-release fertilizer (Osmocote, Scotts Australia, Castle Hill, Australia) and daily with a liquid fertilizer, Hoagland no. 2 (Hewitt, 1966). Cuttings were propagated using rooting powder (Rootex-P, Bass Laboratories, Bayswater, Australia). Plants were grown for 2 to 4 months, and enzymatic and physiological analyses were performed on the youngest, fully expanded leaves taken from plants before the onset of flowering.

Confirmation of Transformation

Activity of neomycin phosphotransferase in leaf discs of *F. bidentis* was measured using the extraction method and dot blot assay described by McDonnell et al. (1987). The presence of the sorghum NADP-MDH gene insert was confirmed by PCR analysis of genomic DNA isolated from leaf material as described by Shure et al. (1983). The oligonucleotide primers used in PCR reactions were NOSSEQ4 (complementary to a region in the *nos* terminator) and TRANSCONF1 (identical to a sequence at the 3′ end of the coding region of the sorghum gene). The sequences of these primers were GGCAACCTTCCGGCGTTCGTG and TAGCGGATGCTATTAAATCC, respectively. These primers amplify a region of about 500 bp from DNA samples containing any of the four sorghum NADP-MDH gene constructs but not from untransformed *F. bidentis* DNA. PCR reactions used about 1 μg of genomic DNA per 20 μL of reaction volume, with an annealing temperature of 50°C. Thirty cycles in a capillary thermal cycler (model FTS1, Corbett Research, Sydney, Australia) were performed.

Enzyme Extraction and Assays

NADP-MDH was extracted from fresh leaf tissue by grinding with 4 to 10 volumes of ice-cold extraction buffer A (25 mM Hepes [K^+], pH 7.5, 10 mM $MgSO_4$, 1 mM Na_2EDTA, 5 mM DTT, 1 mM PMSF, 5% [w/v] insoluble PVP, and 0.05% [v/v] Triton X-100) with a small amount of quartz sand in a 1.5-mL microfuge tube. The enzyme was also extracted from leaf tissue that had been frozen in $N_{2(l)}$ and stored at −80°C by first precooling the microfuge tube containing the sample in $N_{2(l)}$ and then adding extraction buffer A. The tissue was then ground with sand as the extraction buffer thawed. In either case an aliquot was

removed for chlorophyll analysis and the extract then centrifuged for 5 min (14,000*g*, 4°C) to remove insoluble material. The supernatant was retained for measurements of NADP-MDH activity. The enzyme was routinely activated by incubating with approximately 1 μg of *E. coli* thioredoxin in 25 mM Hepes (K^+), pH 7.5, 1 mM Na_2EDTA, 500 mM KCl, 20 mM DTT, and 0.01% (v/v) Triton X-100 for 30 min at 30°C. Alternatively, the enzyme was activated by incubating with 40 mM Tricine (K^+), pH 9, 0.4 mM Na_2EDTA, 120 mM KCl, 100 mM DTT, and 0.0025% (v/v) Triton X-100 for 2 h at 25°C. NADP-MDH activity was measured spectrophotometrically essentially as described by Ashton et al. (1990), except that 150 mM KCl was included in the assay buffer.

Other photosynthetic enzymes were measured in leaf samples extracted in ice-cold buffer A plus 1 mg/mL BSA, 2 mM $MnCl_2$, and 20 μg/mL pyridoxal P. Protease inhibitors, benzamidine (0.5 mM), and ε-amino caproic acid (2.5 mM) were also included in the extraction buffer for the measurement of Rubisco. PPDK was measured in extracts made from illuminated leaves stored at room temperature. Enzymes were assayed as described by Ashton et al. (1990) and Leegood (1990), except for Rubisco, which was measured by following the incorporation of $H^{14}CO_3^-$ into acid-stable products, as described by Furbank et al. (1996). NAD-MDH was assayed in 25 mM Hepes (K^+), pH 7.5, 0.5 mM Na_2EDTA, 0.2 mM NADH, and 0.5 mM OAA.

Light Activation of NADP-MDH in Attached Leaves

We measured the maximum activation state of NADP-MDH by first darkening plants for 1 h to completely oxidize and inactivate the enzyme. While still attached to the plant, a leaf was then placed at 1200 μmol photons m^{-2} s^{-1} for 15 min. Illumination was from a 150-W incandescent lamp with a 2-cm water filter. A small (0.35 cm^2) leaf disc was then removed and ground, together with quartz sand, in 25 volumes of ice-cold extraction buffer B (25 mM Hepes [K^+], pH 6.5, 10 mM $MgSO_4$, 1 mM Na_2EGTA, 5 mM DTT, 1 mM PMSF, 5% [w/v] insoluble PVP, and 0.05% [v/v] Triton X-100). An aliquot was removed for chlorophyll measurement, the sample was centrifuged, and NADP-MDH was assayed as described above. The enzyme was then fully activated with *E. coli* thioredoxin and assayed again.

We also examined the response of activation state to a gradual increase in light intensity by first illuminating an attached leaf at low light (100 μmol photons m^{-2} s^{-1}) for 15 min, removing a small leaf disc, and assaying for NADP-MDH as described above. The incident light on the leaf was then increased to 200 μmol photons m^{-2} s^{-1} for 15 min, and NADP-MDH activity was measured in another leaf disc. The light was gradually increased up to 1600 μmol photons m^{-2} s^{-1} in this manner, with leaf discs being removed and NADP-MDH being assayed at each intensity.

Measurement of NADP-MDH in Bundle-Sheath Cell Strands

Plants were placed in the dark for up to 48 h to deplete starch, and then put in full sunlight for 1 h prior to harvesting. About 5 g of deribbed plant material was blended with 70 mL of ice-cold buffer C (0.3 M sorbitol, 20 mM Hepes [K^+], pH 7.7, 2 mM Na_2EDTA, 2 mM isoascorbate, 2 mM Na_2HPO_4, and 1 mM PMSF) in a mixer (Omnimixer, Sorvall), as described by Meister et al. (1996), to prepare bundle-sheath cell strands for O_2-exchange measurements. A filtrate enriched in mesophyll cell contents was obtained from a portion of the leaf extract after the first blend (10 s at 60% of line voltage) by filtration through an 80-μm nylon net. Samples of the whole leaf extract were taken after the final blending. Bundle-sheath cell strands were resuspended in 10 to 15 mL of buffer D (0.3 M sorbitol, 20 mM Hepes [K^+], pH 7.7, 10 mM KCl, 1 mM Na_2EDTA, and 0.5 mM Na_2HPO_4). DTT (10 mM) and Triton X-100 (0.1%, v/v) were added to all three fractions, which were then extracted in a ground-glass pestle and tube Duall tissue grinder (Kontes Glass Co., Vineland, NJ) and used for measurement of enzymes and chlorophyll. The extent of cross-contamination of cell contents was followed with the use of marker enzymes (NADP-malic enzyme and PEPCX) and by microscopic examination.

O_2-Exchange Measurements of Isolated Bundle-Sheath Cell Strands

Bundle-sheath cell strands prepared as described above were immediately added to an O_2 electrode (Rank Brothers, Cambridge, UK), and O_2-exchange properties were measured at 25°C as described by Meister et al. (1996). The concentrations of substrates used were as follows: $NaHCO_3$, 10 mM; PGA, 5 mM; Asp, 12.5 mM; 2OG, 12.5 mM; and malate, 12.5 mM.

Chlorophyll Determinations

Chlorophyll was measured in 80% (v/v) acetone, as described by Porra et al. (1989).

Photosynthesis Measurements

Photosynthesis rates of attached leaves were measured at 25°C using a portable IR gas analyzer with a clamp-on leaf chamber (model LCA-2, ADC, Hoddesdon, UK). Illumination was from a 150-W incandescent lamp with a 2-cm water filter.

RESULTS AND DISCUSSION

Reliability of NADP-MDH Extraction and Assay

We confirmed that our extraction and assay methods for NADP-MDH from leaves of *F. bidentis* are reliable as follows. First, in two experiments, the recovery of sorghum NADP-MDH from a mixture of *F. bidentis* and sorghum leaf tissue was 87 and 105%. Second, NADP-MDH activity was completely recovered from leaf samples frozen and stored at −80°C for at least 24 d. In addition, activity was completely recovered even if the samples were thawed and allowed to stand at 25°C for 5 min before extraction. Third, activation of the enzyme by *E. coli* thioredoxin was essentially complete after 5 min at 30°C, with negligible loss of

activity over the next 55 min. We included Triton X-100 in the activation buffer to stabilize the reduced form of the enzyme (Hatch and Agostino, 1992). Fourth, the concentration of each component of the spectrophotometric activity assay was optimized to measure maximum activity. Although the rate could be increased by about 20% by using 100 mM Pi rather than 150 mM KCl in the assay buffer, this concentration of Pi is much higher than what we expected to find in the chloroplast. Together, these results allow us to be confident that our measurements of maximum activity made in a crude extract accurately represent the maximum activity of the enzyme in vivo.

NADP-MDH Activity in Primary Transformants

F. bidentis was transformed with full-length sense constructs containing either the wild-type or mutant forms of the sorghum NADP-MDH cDNA clone (Issakidis et al., 1992, 1994) flanked by the CaMV 35S promoter and the *nos* terminator. The dmNSorg and dmCSorg enzymes are both largely inactive when oxidized. The dmNSorg form is more readily reduced by thioredoxin in vitro than the wild-type enzyme, whereas the reductive activation of the dmCSorg form, unlike that of the wild-type enzyme, is not inhibited by NADP. The QmSorg enzyme cannot form disulfide bonds and is therefore active even under oxidizing conditions. In total, 17 transformation experiments, each with about 150 explants, were performed. Forty-one neomycin phosphotransferase-positive plants from different calli were assayed for maximum catalytic activity of NADP-MDH (Fig. 1). We were unable to detect any sorghum NADP-MDH protein in six transformed plants with the highest NADP-MDH activity by immunoblotting using antibodies specific to the sorghum enzyme (not shown). In 21 of these primary transformants NADP-MDH activity was less than 50% of that in untransformed plants. There was apparently no difference between the four constructs in the frequency of transformants with reduced activity.

The reason we failed to identify transformants expressing sorghum NADP-MDH is uncertain. All four of the clones produce functional protein when expressed in *E. coli* (Issakidis et al., 1992; 1994), and tobacco plants transformed with the wild-type clone correctly target and process the sorghum enzyme (Gallardo et al., 1995). We have also transformed tobacco with wild-type and mutant clones and looked for expression by immunoblotting with antibodies specific for sorghum NADP-MDH. Although we could detect a low-level expression of sorghum NADP-MDH in tobacco transformed with wtSorg or dmCSorg, we could not identify any sorghum protein in plants transformed with dmNsorg or QmSorg (not shown). We have examined the possibility that the lack of expression could be due to cloning artifacts by determining the nucleotide sequence at the junction of the 3′ end of the CaMV 35S promoter and the 5′ end of the NADP-MDH coding sequence in each of these four constructs. In two of them, dmNSorg and QmSorg, there is an upstream, out-of-frame ATG translation initiation codon, whereas no upstream ATG codons were present in the other constructs (not shown). Although the presence of this extra ATG could presumably reduce the efficiency of translation of functional enzyme from dmNSorg and QmSorg (Rogers et al.,

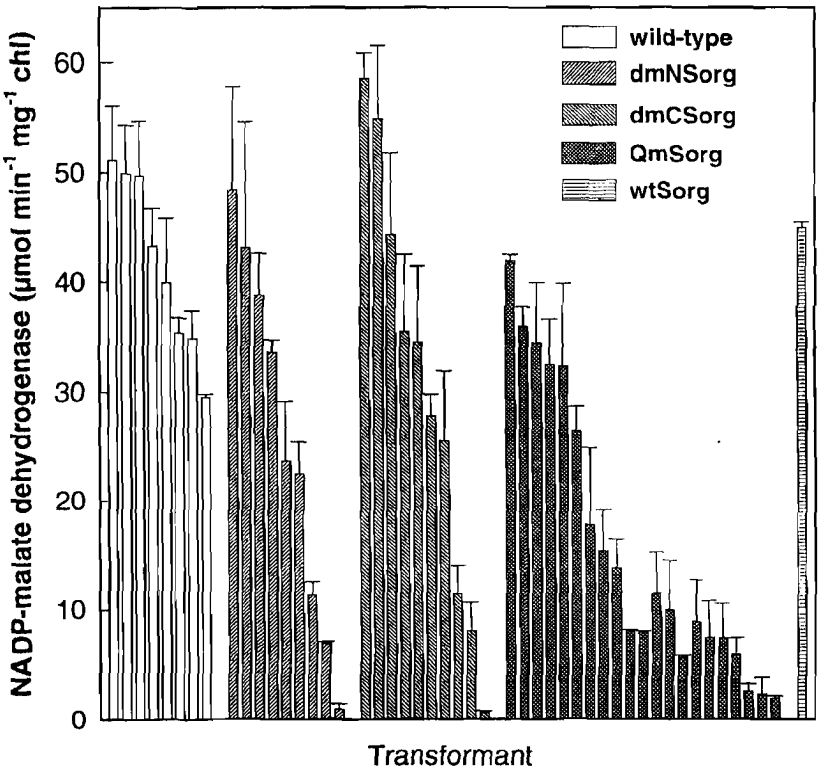

Figure 1. NADP-MDH activities in primary transformants. *F. bidentis* plants transformed with constructs designed to overexpress sorghum NADP-MDH were grown in soil in the greenhouse. The activity of NADP-MDH was measured in leaf discs taken from the youngest, fully expanded leaves of these plants. Activities are mean ± SE ($n \geq 2$) of measurements made on different leaves from an individual plant. chl, Chlorophyll.

1985), it does not explain the apparent lack of expression from all four constructs.

As shown in Figure 1, the majority of *F. bidentis* transformants actually have decreased activity of NADP-MDH, presumably due to cosense suppression of gene expression (Jorgensen, 1991; Flavell, 1994). This phenomenon was first reported for chalcone synthase in petunia (Napoli et al., 1990; van der Krol et al., 1990), and there have since been many other examples reported in the literature (e.g. Vanlerberghe et al., 1994; Brusslan and Tobin, 1995; Paul et al., 1995; Flipse et al., 1996). Three nonmutually exclusive mechanisms have been proposed to explain the occurrence of cosense suppression: (a) alterations in chromatin structure, (b) changes in methylation of promoter sequences, and (c) posttranscriptional mechanism(s) resulting in the degradation of both introduced and endogenous mRNA (Flavell, 1994). We do not have evidence for any one of these particular mechanisms being involved in the suppression of NADP-MDH activity in transformed *F. bidentis*. We suggest that cosense suppression of gene expression is responsible for our inability to detect expression of the sorghum NADP-MDH protein.

Initial Characterization of Reduced-Activity T_1 Plants

T_0 transgenic plants were allowed to self-fertilize and produce seed. The biochemical and physiological analyses described in the following sections were performed on T_1 plants germinated from this seed. We identified some transgenic plants in which the activity of NADP-MDH varied significantly between different portions of an individual leaf. This was seen in plants transformed either with the sorghum gene constructs or with homologous antisense constructs (S.J. Trevanion, R.T. Furbank, A.R. Ashton, unpublished data). Since uneven expression of NADP-MDH would significantly complicate analysis of these plants, we analyzed plants in which we were unable to detect this phenotype. A further important consideration when analyzing transgenic plants is to confirm that the reduced expression of the target gene has not affected expression of other photosynthetic enzymes. For example, undesirable alterations in gene expression could occur from the insertion of the transgene into either the regulatory or the coding sections of an endogenous gene. In addition, reducing the activity of the target enzyme could in itself alter the expression of other genes (e.g. Hudson et al., 1992) by as yet undefined mechanisms. We have addressed these possibilities by initially characterizing T_1 plants from three independent lines: 12–7–20, 22–1–6, and 22–8–1. PCR analysis of genomic DNA from each of these individuals confirmed that they are transformed with the sorghum NADP-MDH gene. No comparable DNA fragment was detected in untransformed plants. We measured the activities of a range of enzymes involved in both the C_4 cycle and photosynthetic carbon reduction cycle enzymes (Table I). In each of the transgenic lines the activity of NADP-MDH was less than 25% of that in untransformed plants. There were slight variations in the activities of some other enzymes between the different lines, but we did not observe any consistent trend in these differences. Although the measured activities of Rubisco were low in both untransformed and reduced-activity plants, this was presumably due to problems with extraction and/or activation of the enzyme. Of course, we cannot exclude the possibility that the activity of another, unassayed enzyme may also be affected, but we can be reasonably confident that we are working with plants that have a specific change in the amount of NADP-MDH.

The decrease in NADP-MDH activity was sometimes accompanied by a decrease in chlorophyll content. There was no change in the chlorophyll *a* to chlorophyll *b* ratio in any of the reduced activity plants. The plant with reduced chlorophyll (12–7–20) was characterized by a decrease in growth rate, whereas plants with normal levels of chlorophyll (22–1–6 and 22–8–1) had apparently normal growth rates (not shown). An association between reduced enzyme activity, chlorophyll content, and growth rate has previously been observed in tobacco (Hudson et al., 1992) and *F.*

Table I. *Enzyme activities in untransformed and transformed F. bidentis*

Activities of C_3 and C_4 enzymes were measured in the youngest, fully expanded leaves of both untransformed and individual T_1 plants transformed with the plasmid pBQmsorg (12–7–10) or pBdmNsorg (22–1–6 and 22–8–1). Activities are mean ± SE ($n \geq 3$).

Enzyme	Activity			
	Wild type	12-7-20	22-1-6	22-8-1
	μmol min^{-1} mg^{-1} chlorophyll			
PPDK	2.9 ± 0.3	2.9 ± 0.04	3.4 ± 0.2	2.6 ± 0.5
PEPCX	21 ± 3	21 ± 3	20 ± 2	36 ± 9
NAD-MDH	61 ± 3	63 ± 5	74 ± 6	97 ± 1
NADP-ME	7.5 ± 0.4	9.2 ± 0.3	8.6 ± 0.5	10 ± 1
Asp aminotransferase	10 ± 1	14 ± 1	7.5 ± 0.3	11 ± 0.2
Ala aminotransferase	20 ± 1	25 ± 2	16 ± 0.7	18 ± 0.6
NADP-MDH	25 ± 1	2.1 ± 0.5	4.2 ± 0.7	4.5 ± 0.8
Rubisco	1.8 ± 0.04	3.4 ± 0.4	2.3 ± 0.1	2.1 ± 0.1
Phosphoglycerate kinase	20 ± 2	24 ± 2	24 ± 2	28 ± 5
Phosphoribulokinase	27 ± 1	29 ± 4	24 ± 0.7	56 ± 3
Chlorophyll (mg m^{-2})	535 ± 29	323 ± 10	685 ± 39	460 ± 22
Chlorophyll *a*:Chlorophyll *b*	4.6 ± 0.2	4.6 ± 0.2	4.7 ± 0.1	4.7 ± 0.1

bidentis (Furbank et al., 1996) with decreased levels of Rubisco, in tobacco with reduced Rubisco activase (Mate et al., 1993), and in *F. bidentis* with decreased PPDK (R.T. Furbank, unpublished data).

Response of Photosynthesis to Changes in Light Intensity

We examined the response of photosynthesis to changes in light intensity at saturating concentrations of CO_2 (>400 μL L^{-1}) for untransformed *F. bidentis* and a reduced-activity plant from each of the lines (Fig. 2). At the maximum light intensity available using our system (1250 μmol photons m^{-2} s^{-1}), photosynthesis of the untransformed plant was about 5.5 μmol min^{-1} mg^{-1} chlorophyll. The maximum rate of photosynthesis of each of the reduced-activity plants was less than this, although the actual rate varied considerably between the different plants. This decrease in photosynthesis reflects a limitation imposed by the severe decrease in NADP-MDH activity in these plants (see below). There were also differences between the untransformed and the reduced-activity plants in the light intensity required to saturate photosynthesis. The untransformed plant showed a typical response for a C_4 plant, with a doubling of the rate of photosynthesis when the light was increased from 500 to 1250 μmol photons m^{-2} s^{-1}. However, photosynthesis of two of the reduced-activity plants (12–7–20 and 22–8–1) was saturated at about 500 μmol photons m^{-2} s^{-1}, and the other plant (22–1–6) showed only a slight increase in rate at higher light intensities. NADP-MDH activities in these lines were 12, 18, and 17% of normal, respectively. The similar behavior of three different transgenic lines further confirms that we are dealing with transgenic plants that have a specific change in the activity of NADP-MDH.

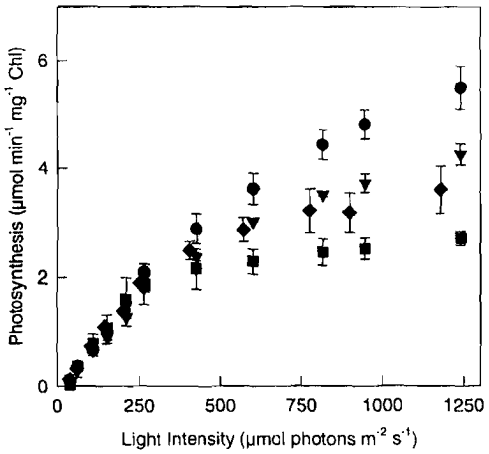

Figure 2. Light-response curve of untransformed and reduced-activity plants. Photosynthesis of attached leaves from untransformed and reduced-activity plants were measured at different light intensities using IR gas analysis. The $[CO_2]$ was between 400 and 500 μL L^{-1}. Results are mean ± SE of measurements made on different leaves from an individual plant. ●, Untransformed (n = 4), NADP-MDH = 30 ± 3 μmol min^{-1} mg^{-1} chlorophyll; ■, 12–7–20 (n = 3), NADP-MDH = 3.9 ± 0.5 μmol min^{-1} mg^{-1} chlorophyll; ▼, 22–1–6 (n = 2), NADP-MDH = 7.7 ± 3.4 μmol min^{-1} mg^{-1} chlorophyll; ◆, 22–8–1 (n = 2), NADP-MDH = 4.0 ± 1.1 μmol min^{-1} mg^{-1} chlorophyll (Chl).

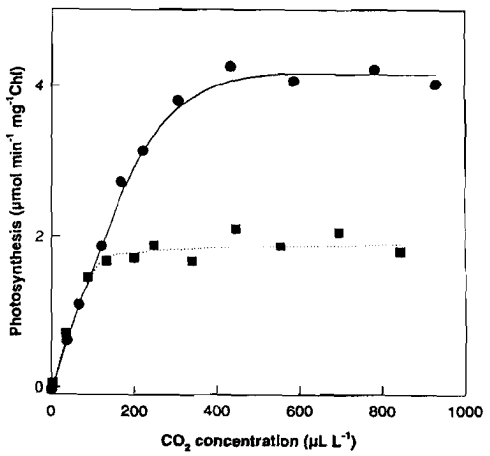

Figure 3. CO_2-response curve of untransformed and reduced-activity plants. Photosynthesis of attached leaves from an untransformed and a reduced-activity plant (12–7–20) were measured at different CO_2 concentrations using IR gas analysis. Results shown are from a single experiment. Light intensity was 1150 μmol photons m^{-2} s^{-1}. ●, Untransformed, NADP-MDH = 20 μmol min^{-1} mg^{-1} chlorophyll; ■, 12–7–20, NADP-MDH = 3.2 μmol min^{-1} mg^{-1} chlorophyll (Chl).

Unlike the situation at high light, the response of photosynthesis to changes in light intensity below 250 μmol photons m^{-2} s^{-1} was identical in the untransformed plant and in the three reduced-activity plants. This strongly implies that the quantum yield of photosynthesis was unaffected in these plants and supports the idea that photosynthesis in C_4 plants is limited by the regeneration of either PEP or ribulose bisphosphate (Collatz et al., 1992).

Response of Photosynthesis to Changes in $[CO_2]$

The typical response of photosynthesis to changes in $[CO_2]$ in an untransformed and a reduced-activity plant (12–7–20) are shown in Figure 3. These experiments were done at a light intensity of 1150 μmol photons m^{-2} s^{-1}. Compared with the untransformed plant, 12–7–20 had a much lower rate of photosynthesis at saturating $[CO_2]$. The $[CO_2]$ required to saturate photosynthesis was also decreased, from about 400 μL L^{-1} in the untransformed plant to about 150 μL L^{-1} in 12–7–20. There was no difference in the response of photosynthetic rate of the two plants to changes in $[CO_2]$ between 0 and 150 μL L^{-1}. This is not surprising given that the response of photosynthesis to $[CO_2]$ in C_4 plants is thought to be largely determined by the activity and kinetic properties of PEPCX (Edwards and Walker, 1983).

Activation State of NADP-MDH

The activation state of maize NADP-MDH is dependent on the redox state of thioredoxin *m*, and on the NADPH/NADP ratio (Ashton and Hatch, 1983b). Slight changes in either of these parameters may have large consequences for

Table II. *Activation state of NADP-MDH in untransformed and reduced-activity plants*

The activation state of NADP-MDH was measured in leaves of untransformed and reduced-activity plants illuminated at 1200 μmol photons m^{-2} s^{-1} for 15 min. Results are mean ± SE (n = 3).

Plant	Activity		Activation State
	μmol min⁻¹ mg⁻¹ chlorophyll	*% of untransformed*	*%*
Untransformed	32 ± 10	100	52 ± 7
12–7–7	16 ± 3	51	44 ± 7
12–7–20	3.3 ± 0.2	10	107 ± 6

the activation state of the enzyme. Assuming that the *F. bidentis* enzyme behaves similarly to the maize enzyme, two observations suggest that the activation state of NADP-MDH might differ between the untransformed and the reduced-activity plants. First, since the maximum rate of photosynthesis is reduced in transgenic plants, this will affect the rate of chloroplast electron transport and the consumption of reducing power by the reactions of the photosynthetic reduction carbon cycle. This could potentially lead to changes in both the NADPH/NADP ratio and the redox state of thioredoxin *m*. Second, since NADPH is a substrate and NADP is a product of the NADP-MDH reaction, changes in the activity of the enzyme could itself alter the NADPH/NADP ratio.

This possibility of changes in activation state is of particular significance for measurements of the metabolic flux control coefficient of NADP-MDH (see below). Therefore, we measured the activation state of NADP-MDH in different transgenic lines at a range of light intensities. The activation state is expressed as the activity of the unactivated enzyme as a percentage of that of the thioredoxin-activated enzyme. We first confirmed that the extraction method used did not alter the activation state of either the inactivated or activated enzyme by extracting NADP-MDH from leaves either predarkened for 1 h, or predarkened and then illuminated at 800 μmol photons m^{-2} s^{-1} for 15 min, respectively, and following the activity of the extracted enzyme over time (not shown). Next, we measured the maximum activation state of the enzyme by illuminating attached leaves at 1200 μmol photons m^{-2} s^{-1} for 15 min (Table II). This period was sufficient for the activation state to reach steady state (not shown). The enzymes from either an untransformed plant or a transgenic plant with 50% of normal activity (12–7–7) were only activated to about 50% by this treatment. However, the enzyme from 12–7–20 (10% of normal activity) was completely activated under these conditions.

We also examined the response of the activation state of the enzyme to step-wise changes in light intensity in an untransformed plant and in 12–7–20. This was done by first predarkening the plant and then illuminating an attached leaf at sequentially higher light intensities. The activity in darkened extracts was 0.19 ± 0.04 μmol min^{-1} mg^{-1} chlorophyll from untransformed leaves (n = 5), and 0.12 ± 0.05 μmol min^{-1} mg^{-1} chlorophyll from 12–7–20 (n = 3). These equate to activation states of 0.46 ± 0.04% and 5.0 ± 2.3%, respectively, demonstrating the effectiveness of the covalent modification in inactivating the *F. bidentis* enzyme. The results of changes in light intensity on activation state in one experiment are shown in Figure 4. For the enzyme extracted from the untransformed plant, the highest activation state of NADP-MDH achieved (only 50% of maximum) was reached at a light intensity of about 800 μmol photons m^{-2} s^{-1}. However, 100% activation of the enzyme from 12–7–20 was observed at a much lower light intensity, about 200 μmol photons m^{-2} s^{-1}. The slight decrease in the activation state of enzyme extracted from untransformed leaves illuminated at 1600 μmol photons m^{-2} s^{-1} was observed on each of the three occasions this experiment was performed. The significance of this is not clear. Although we did not measure photosynthesis at such high light intensities, Furbank et al. (1996) did not see any decline in the rate of CO_2 fixation in untransformed plants when the light intensity was increased from 1100 to 1800 μmol photons m^{-2} s^{-1}.

Compared with measurements of photosynthetic rates (Fig. 2), these results suggest that regulation of the activation state of NADP-MDH plays a role in maintaining rates of photosynthesis in the reduced activity plants. Figure 5, a and b, shows the relationship between actual activity of the enzyme (i.e. activation state × maximum activity) and photosynthesis in untransformed and reduced-activity plants, respectively. As expected, the activity of NADP-MDH in both plants is in excess of the rate of photosyn-

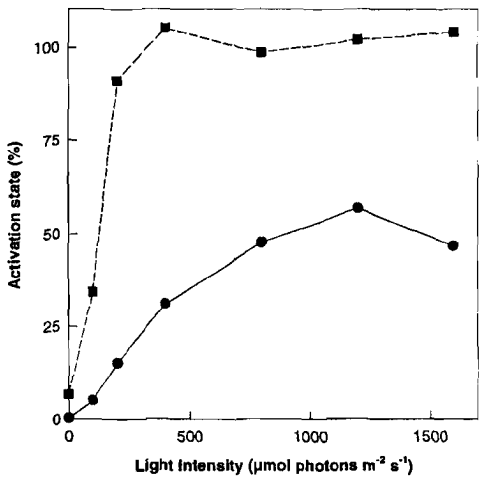

Figure 4. Activation state of NADP-MDH in untransformed and reduced-activity (12–7–20) plants. Plants were placed in the dark for 1 h to completely inactivate NADP-MDH. Individual leaves, still attached to the plant, were then illuminated at 100 μmol photons m^{-2} s^{-1} for 15 min, and the activation state of NADP-MDH was measured in a small disc. The light intensity was then sequentially increased to 1600 μmol photons m^{-2} s^{-1}, and the activation state of NADP-MDH was measured after 15 min of illumination of the leaf at each light intensity. All measurements were made on a single leaf from each plant. The results shown are from a single experiment. ●, Untransformed, NADP-MDH = 52 ± 2 μmol min^{-1} mg^{-1} chlorophyll; ■, 12–7–20, NADP-MDH = 2.9 ± 0.2 μmol min^{-1} mg^{-1} chlorophyll.

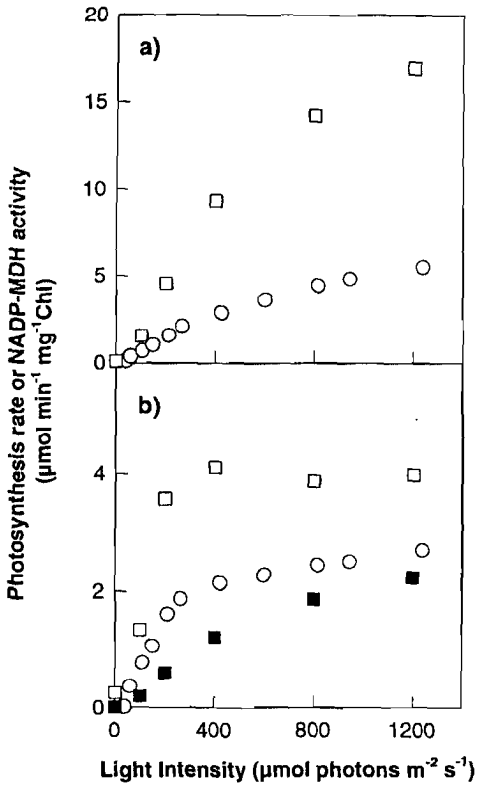

Figure 5. Relationship between activity of NADP-MDH and rate of photosynthesis in untransformed and reduced-activity (12–7–20) plants. Activity of NADP-MDH was calculated by multiplying the maximum catalytic activity of the enzyme in leaves used for measurements of photosynthesis rates (Fig. 2) by the activation state of the enzyme in leaves from identical plants (Fig. 4). O, Photosynthesis rates; □, NADP-MDH activities; ■, activity of NADP-MDH in the reduced-activity plant, assuming that the activation state is equal to that in the untransformed plant. a, Untransformed; b, 12–7–20. Chl, Chlorophyll.

thesis. However, Figure 5b also shows that in the absence of the increase in activation state of the enzyme in the reduced-activity plants, there would be insufficient activity of NADP-MDH to maintain the observed rates of photosynthesis.

Changes in the activation state of the enzyme are most readily explained by differences in the NADPH/NADP ratio and/or the redox state of thioredoxin *m* between the different lines. Indeed, it is hard to imagine the redox state of the thioredoxin pool not changing when the redox state of the NADPH/NADP pool changes and vice versa because of the multiple connections between the pools. Both are reversibly reduced by Fd, and NADPH can reduce some chloroplast thiols via glutathione reductase, thus to some extent influencing the rate of oxidation of the thioredoxin pool. Of the connections between the thioredoxin pool and the NADPH/NADP pool, NADP-MDH may itself be most important, since altering the redox state of thioredoxin will alter NADP-MDH activity and thus the rate of consumption of NADPH. Chlorophyll fluorescence measurements can be used to monitor the redox state of some chloroplast components. Furbank (1988) found in experiments with isolated maize mesophyll chloroplasts that the redox state of the primary electron-accepting plastoquinone of PSII was considerably more oxidized when the chloroplasts were reducing OAA than in the absence of an electron acceptor. However, measurements of chlorophyll fluorescence quenching of untransformed and reduced-activity plants did not reveal any significant difference in either the effective quantum yield of PSII (a measure of the redox state of the primary electron-accepting plastoquinone of PSII) (Genty et al., 1989) or nonphotochemical quenching of chlorophyll fluorescence (not shown). This suggests that untransformed and reduced-activity plants do not differ greatly in the redox state of the chloroplast electron transport chain, the photoprotective function of PSII, or thylakoid pH, or, alternatively, that any changes of redox state in the reduced-activity plants are not as extreme as the differences occurring in isolated chloroplasts in the presence and absence of an electron acceptor such as OAA.

Because the activation state of NADP-MDH depends on the redox states of both the thioredoxin pool and the NADP(H) pool (Ashton and Hatch, 1983b; Rebeille and Hatch, 1986), and the interaction between these two regulators seems to be synergistic, it may be that small changes in both are sufficient to achieve the changes in NADP-MDH activation state seen in the transformed plants. Although it would be interesting to measure the redox state of the NADP(H) pool in the transformed and untransformed plants, such an experiment would be technically demanding, since we would need to distinguish the chloroplastic from the cytoplasmic pools, the mesophyll from the bundle-sheath pools, and, most difficult of all, the bound from the free pool.

NADP-MDH Activities in Isolated Bundle-Sheath Cell Strands

Unlike C_4 monocot grasses, *F. bidentis* contains significant NADP-MDH activity in the bundle-sheath cell chloroplast (Meister et al., 1996). The effectiveness of cosense suppression of NADP-MDH in each of these compartments will depend on the sequence similarity between the transgene and the endogenous gene. Although we do not have any direct evidence for NADP-MDH gene copy number in *F. bidentis*, there is only one gene for NADP-MDH in the range of C_3, C_3-C_4, and C_4 species of the genus *Flaveria* (McGonigle and Nelson, 1995). There are two genes for NADP-MDH in sorghum (Luchetta et al., 1991), but only one of these is light-regulated and expressed to a high level. It is therefore highly probable that there is only one gene encoding NADP-MDH in *F. bidentis*, which is expressed in both the bundle-sheath cells and the mesophyll cells. In this situation cosense suppression should be equally effective in both compartments. However, if the mechanism of cosense suppression in these plants involves posttranscriptional degradation of mRNA, then its effectiveness will also depend on the abundance of the transgene and the endogenous gene transcripts (Lindbo et al., 1993). If these differ between the bundle sheath and the

mesophyll, then the degree to which gene expression is suppressed could vary between the two compartments. This would obviously have important consequences for our interpretation of the analysis of these plants. Although the relative levels of expression of the CaMV 35S promoter appear to be similar in both compartments (Chitty et al., 1994), they have not been accurately quantified. It is therefore possible that the levels of sorghum transcript could vary between the two cell types. In addition, since the amounts of NADP-MDH protein in the two compartments are very different, it is probable that the levels of endogenous mRNA also differ widely between the cell types (McGonigle and Nelson, 1995).

Therefore, we have examined the extent of cosense suppression in each cell type by measuring NADP-MDH activity in bundle-sheath cell strands and mesophyll cell-enriched fractions prepared from plants differing in total activity of NADP-MDH. We initially confirmed that we can routinely activate NADP-MDH from different compartments using *E. coli* thioredoxin by activating the enzyme from the whole leaf or from mesophyll-enriched and purified bundle-sheath cell strands prepared from untransformed and reduced activity (12–7–20) plants. In each case the maximum activity of NADP-MDH was the same whether activation of the enzyme was with *E. coli* thioredoxin or with high pH (not shown). The distribution of enzymes between mesophyll and bundle-sheath cells was then determined by measuring the maximum activities of NADP-MDH and marker enzymes in each of these fractions (Table III). Untransformed plants had about 2.4 μmol min^{-1} mg^{-1} chlorophyll NADP-MDH in the bundle-sheath cells. This is considerably less than the 11 μmol min^{-1} mg^{-1} chlorophyll reported by Meister et al. (1996), but is nonetheless a significant activity. In reduced-activity plants, the activity of the bundle-sheath cell NADP-MDH was much reduced, about 0.12 μmol min^{-1} mg^{-1} chlorophyll. When expressed as a percentage, 12-7-20 had 9% of normal activity in mesophyll cell-enriched fractions, and 5% in bundle-sheath cell strands, demonstrating that cosense suppression is similarly effective in reducing activity of NADP-MDH in both the bundle-sheath and the mesophyll compartments.

Table III. *Enzyme activities in bundle-sheath and mesophyll cell fractions from untransformed and transformed F. bidentis*

Activities of NADP-MDH and the marker enzymes PEPCX and NADP-malic enzyme were measured in whole-leaf extracts, and in mesophyll-enriched and purified bundle-sheath cell strands prepared from both untransformed and reduced-activity plants. Activities are *mean* ± SE (n = 3).

Fraction	Activity		
	PEPCX	NADP-malic enzyme	NADP-MDH
	μmol min^{-1} mg^{-1} chlorophyll		
Untransformed			
Whole leaf	9.0 ± 3.4	8.7 ± 2.3	21 ± 5
Mesophyll-enriched	24 ± 7	6.5 ± 0.7	49 ± 2
Bundle sheath	0.8 ± 0.1	23 ± 4	2.4 ± 1.1
Reduced			
Whole leaf	16 ± 5	11 ± 1	3.6 ± 1.9
Mesophyll-enriched	30 ± 6	7.3 ± 0.4	4.2 ± 1.5
Bundle sheath	0.9 ± 0.1	29 ± 9	0.12 ± 0.06

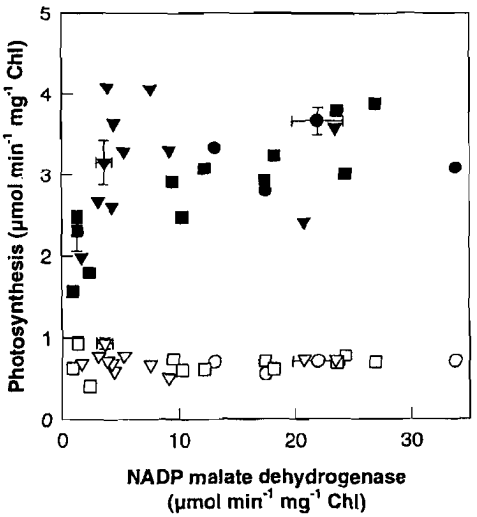

Figure 6. *Control analysis of NADP-MDH. The rate of photosynthesis and NADP-MDH activity were measured in leaves of untransformed plants and T_1 progeny from two reduced-activity lines. Closed symbols, Measured at high light (1200 μmol photons m^{-2} s^{-1}); open symbols, measured at low light (150 μmol photons m^{-2} s^{-1}). The symbols represent single measurements except where error bars are shown (mean ± SE, $n \geq 3$). ●, Untransformed; ■, line 12–7–20; ▼, line 22–1–6. Chl, Chlorophyll.*

Metabolic Flux Control Analysis of NADP-MDH

Although the maximum rate of photosynthesis is inhibited in reduced-activity plants, the decrease was difficult to quantitate due to the variability of the rate between different leaves that was seen for both the untransformed and the reduced-activity plants (Fig. 2). We therefore examined the relationship between maximum catalytic activity of NADP-MDH activity and photosynthesis rate by measuring these parameters in a large number of T_1 plants with a wide range of activities. We used untransformed and reduced-activity plants from two lines for this analysis (Fig. 6). These data show that at high light, the rate of photosynthesis was affected only in plants with a severe (less than about 10% of normal) decrease in activity; plants with greater than about 10% of normal activity had apparently normal rates of photosynthesis. When measurements were made at low light, even plants with the most severe reduction in activity had normal rates of photosynthesis.

The control over the rate of flux through a metabolic pathway that is exerted by a particular enzyme can be quantified by metabolic flux control analysis (Kacser and Burns, 1973). The metabolic flux control coefficient for an enzyme (C_j) can be calculated from a graph such as that shown in Figure 6, as the slope of the line where activity is reduced from 100%. We conclude from our data that even under high light, when there is the greatest flux of fixed carbon through NADP-MDH, C_j for NADP-MDH is low, i.e. the enzyme exerts little control over the steady-state

rate of photosynthesis. It is only in transformants with a large decrease in activity that NADP-MDH becomes limiting and the maximum rate of photosynthesis is reduced. Since the activation state of the enzyme does not change until there is a severe decrease in total activity (Table II), we can be confident that our measurements of activity in untransformed and T_1 plants with less than a 50% decrease in activity are comparable.

As shown in Table III, cosense suppression of expression appears to be equally effective at reducing activity of NADP-MDH in the bundle-sheath cell and in the mesophyll cell chloroplast of 12–7–20 (10% of normal activity). It is quite probable that T_1 plants with just a slight decrease in total activity of NADP-MDH are reduced in both bundle-sheath and mesophyll cell NADP-MDH. If this is indeed the case, we can conclude that C_j for both bundle-sheath and mesophyll enzyme will be low.

Metabolic Activities of Isolated Bundle-Sheath Cell Strands

In maize, fixed carbon is transported from the mesophyll cells to the bundle-sheath cells largely as malate (Hatch, 1971). However, from measurements of the metabolic properties of bundle-sheath cell strands isolated from *F. bidentis*, and from $^{14}CO_2$-labeling experiments, Meister et al. (1996) suggested that in this plant approximately 35 to 40% of fixed carbon is transported to the bundle-sheath cells as Asp rather than malate. The Asp is transaminated to OAA by Asp aminotransferase, which is then reduced to malate by bundle-sheath-localized NADP-MDH. As described above, the transgenic plants with low total activity of NADP-MDH have extremely low activities of this enzyme in the bundle-sheath cells, and might therefore be expected to differ from untransformed plants in the pathway of carbon transport between the mesophyll and bundle-sheath cells. We have examined the light-dependent metabolic activities of isolated bundle-sheath cell strands prepared from untransformed and reduced-activity plants to investigate this possibility. The results from a typical experiment are shown in Table IV. Strands isolated from both an untransformed plant and 12-7-20 showed substantial rates of light-dependent O_2 evolution when supplied with Asp, 2OG, PGA, and $NaHCO_3$. However, strands from the two plants differed in the extent to which they could metabolize Asp and 2OG alone; whereas those from untransformed plants were able to support significant rates of O_2 evolution (about 38% of maximum) under these conditions, strands from 12–7–20 could support rates of only about 13% of maximum (experiments 1 and 3). Similarly, whereas the addition of Asp and 2OG in the presence of PGA and $NaHCO_3$ stimulated the rate of O_2 evolution of untransformed strands, it had no effect on metabolism of strands from 12–7–20 (experiments 2 and 4). The rate of Asp plus 2OG-dependent O_2 evolution in the 12–7–20 strands (0.09–0.12 μmol min^{-1} mg^{-1} chlorophyll) is similar to the maximum activity of NADP-MDH in the bundle-sheath cell strands (0.12 μmol min^{-1} mg^{-1} chlorophyll). In untransformed plants the rate of Asp plus 2OG-

Table IV. *O_2 exchange of isolated bundle-sheath cell strands from untransformed and reduced-activity plants*

Bundle-sheath cell strands prepared from untransformed or reduced-activity (12–7–20) plants were incubated in an O_2 electrode at 25°C. The rate of O_2 release into the medium in the presence of the appropriate substrates was measured.

Substrate	Untransformed		12-7-20	
	μmol min^{-1} mg^{-1} chlorophyll	%[a]	μmol min^{-1} mg^{-1} chlorophyll	%[a]
Experiment 1				
+ Light	0.0	0	0.0	0
+ Asp + 2OG	0.28	36	0.09	11
+ PGA	0.71	89	0.63	80
+ $NaHCO_3$	0.79	100	0.79	100
Experiment 2				
+ Light	0.0	0	0.0	0
+ $NaHCO_3$	0.0	0	0.18	17
+ PGA	0.79	92	1.04	100
+ Asp + 2OG	0.86	100	1.04	100
Experiment 3				
+ Light	0.0	0	0.0	0
+ Asp + 2OG	0.30	39	0.12	15
+ $NaHCO_3$	0.36	48	0.16	20
+ PGA	0.75	100	0.79	100
+ Malate	0.62	82	0.64	81
Experiment 4				
+ Light	0.0	0	0.0	0
+ PGA	0.57	72	0.62	68
+ $NaHCO_3$	0.71	90	0.92	100
+ Asp + 2OG	0.79	100	0.92	100

[a] Percentage of maximum rate during each experiment.

dependent O_2 evolution (0.3 μmol min^{-1} mg^{-1} chlorophyll) was only 12.5% of the maximum NADP-MDH activity.

These measurements confirm that bundle-sheath cell strands isolated from untransformed *F. bidentis* can sustain significant rates of O_2 evolution with Asp and 2OG as substrates. In addition, activities of NADP-MDH measured in bundle-sheath cells are sufficient to account for about 50% of the maximum rate of photosynthesis of untransformed plants, supporting the scheme proposed by Meister et al. (1996). However, two lines of evidence suggest that the pathway of C_4 acid metabolism is altered in the reduced-activity plants. First, as described above, bundle-sheath cell strands isolated from reduced-activity plants can sustain only a low rate of O_2 evolution with Asp and 2OG as substrates. Second, the activity of NADP-MDH in bundle-sheath cell strands prepared from reduced-activity plants is extremely low (Table III). Typical activities in these strands of 0.12 μmol min^{-1} mg^{-1} chlorophyll would be sufficient to catalyze only 6% of the maximum rate of photosynthesis of the reduced-activity plants (2 μmol min^{-1} mg^{-1} chlorophyll). These results suggest that bundle-sheath cell-localized NADP-MDH cannot be essential for sustaining high rates of photosynthesis in *F. bidentis*. It is likely that *F. bidentis* is able to adapt to a decrease in the amount of bundle-sheath cell NADP-MDH by transferring more carbon to this compartment in the form of malate, although further experiments are required to confirm this.

The fact that *F. bidentis* can function reasonably efficiently with very little NADP-MDH in the bundle-sheath cells implies that the presence of the enzyme in this compartment may represent an intermediate step in the evolution of C_4 photosynthesis. There was no increase in the chlorophyll *a* to chlorophyll *b* ratio in the bundle-sheath cell strands of reduced-activity plants (not shown). This indicates that, despite the probable shift in the pathway of C_4 acid metabolism, the plant does not acclimate by reducing activity of PSII in the bundle-sheath cells.

CONCLUDING COMMENTS

NADP-MDH, either in the mesophyll or in bundle-sheath cells, has a low metabolic flux control coefficient for photosynthesis in the C_4 plant *F. bidentis*. Previous work in this laboratory has shown that Rubisco partially limits the steady-state rate of photosynthesis at moderate to high light intensities in *F. bidentis* (Furbank et al., 1996) with an estimated C_i of 0.4 at 2000 μmol photons m^{-2} s^{-1} (from figure 9 of Furbank et al., 1996). Another highly regulated enzyme, PPDK, contributes to the limitation on photosynthesis in *F. bidentis* at high light intensities (C_i approximately 0.3–0.4) but not at low light intensities (R.T. Furbank, J.A. Chitty, C.L.D. Jenkins, S.J. Trevanion, S. von Caemmerer, and A.R. Ashton, unpublished data). Mutants of *Amaranthus edulis*, a NAD-malic enzyme-type C_4 plant deficient in PEPCX, have been produced by Dever et al. (1995). F_1 heterozygotes with about 50% of normal activity appear to grow normally in air, but do have a slightly reduced rate of photosynthesis at very high light intensities (2000 μmol photons m^{-2} s^{-1}). However, this decrease is only slight, and the plants appear to behave normally at lower light. This demonstrates that PEPCX also has very little control over the steady-state rate of photosynthesis in C_4 plants. Together these observations suggest that significant control of the rate of photosynthesis in C_4 plants at high light intensities may be shared by Rubisco in the C_3 cycle and by PPDK in the C_4 cycle. It is also clear that all of the limitations on C_4 photosynthesis at high light intensity have yet to be identified.

Since NADP-MDH is a highly regulated enzyme but does not limit photosynthesis in *F. bidentis*, one could ask what is the purpose of the complex regulation of the enzyme. One role of the covalent regulation may be to switch the enzyme off in the dark to limit the potential for transferring reducing equivalents into and out of the chloroplast. Another, and perhaps more important, role of the covalent regulation may be to maintain the NADP pool largely reduced during steady-state photosynthesis. This would allow the other NADPH-requiring reactions of the chloroplast, such as amino acid, lipid, and secondary product biosynthesis, to compete for NADPH in the face of the vastly greater catalytic capacity of the enzymes of photosynthetic CO_2 assimilation (A.R. Ashton and S.J. Trevanion, unpublished data; R.T. Furbank, J.A. Chitty, C.L.D. Jenkins, S.J. Trevanion, S. von Caemmerer, and A.R. Ashton, unpublished data). Answers to specific questions regarding the role of the regulatory properties of NADP-MDH might have been provided by analysis of plants overexpressing the mutant forms of the enzyme. However, in light of the high frequency of cosense suppression between the sorghum and *F. bidentis* enzymes, this approach of genetic transformation of the nuclear genome is unlikely to be successful.

A review of the literature shows that the sequence identity between an introduced and endogenous gene that is required for cosense suppression is not generally documented, or even known. Although it has generally been assumed that sequences have to be nearly identical to observe this phenomenon, the coding region for NADP-MDH from *F. bidentis*, a dicot, has only 71% overall sequence identity with the coding sequence of the clone from sorghum, a monocot (S.J. Trevanion and A.R. Ashton, unpublished data). This observation extends the range of combinations of clones that should be considered in attempts to produce plants with reduced levels of enzymes. However, it also stresses the need for choosing widely divergent heterologous clones when attempting to overexpress enzymes in plant tissues.

ACKNOWLEDGMENTS

The authors thank Emmanuelle Issakidis and Myroslawa Miginiac-Maslow for the use of wild-type and mutated forms of the sorghum NADP-MDH cDNA clone, and for antibodies specific to the sorghum enzyme. We are grateful to Julie Chitty and Michelle Couzens for excellent technical assistance.

Received September 18, 1996; accepted November 6, 1996.

LITERATURE CITED

An G, Watson BD, Stachel S, Gordon MP, Nester EW (1985) New cloning vehicles for transformation of higher plants. EMBO J **4:** 277–284

Andrews TJ, Lorimer GH (1987) Rubisco: structure, mechanisms, and prospects for improvement. *In* M Hatch, N Boardman, eds, The Biochemistry of Plants, Vol 10. Academic Press, New York, pp 131–218

Ashton AR, Burnell JN, Furbank RT, Jenkins CLD, Hatch MD (1990) Enzymes of C_4 photosynthesis. *In* P Lea, ed, Methods in Plant Biochemistry, Vol 3. Academic Press, London, pp 39–72

Ashton AR, Hatch MD (1983a) Regulation of C_4 photosynthesis: physical and kinetic properties of active (dithiol) and inactive (disulphide) NADP-malate dehydrogenase from *Zea mays*. Arch Biochem Biophys **227:** 406–415

Ashton AR, Hatch MD (1983b) Regulation of C_4 photosynthesis: regulation of activation and inactivation of NADP-malate dehydrogenase by NADP and NADPH. Arch Biochem Biophys **227:** 416–424

Brusslan JA, Tobin EM (1995) Isolation of new promoter-mediated co-suppressed lines in *Arabidopsis thaliana*. Plant Mol Biol **27:** 809–813

Chitty JA, Furbank RT, Marshall JS, Chen Z, Taylor WC (1994) Genetic transformation of the C_4 plant *Flaveria bidentis*. Plant J **6:** 949–956

Collatz GJ, Ribas-Carbo M, Berry JA (1992) Coupled photosynthesis-stomatal conductance model for leaves of C_4 plants. Aust J Plant Physiol **19:** 519–538

Dever LV, Blackwell RD, Fullwood NJ, Lacuesta M, Leegood RC, Onek LA, Pearson M, Lea PJ (1995) The isolation and characterization of mutants of the C_4 photosynthetic pathway. J Exp Bot **46:** 1363–1376

Edwards GE, Nakamoto H, Burnell JN, Hatch MD (1985) Pyruvate, Pi dikinase and NADP-malate dehydrogenase in C_4 photosynthesis: properties and mechanism of light/dark regulation. Annu Rev Plant Physiol **36:** 255–286

Edwards GE, Walker DA (1983) C_3, C_4, Mechanisms, and Cellular and Environmental Regulation of Photosynthesis. Blackwell Scientific Publications, Oxford, UK, pp 410–444

Flavell RB (1994) Inactivation of gene expression in plants as a consequence of specific sequence duplication. Proc Natl Acad Sci USA **91:** 3490–3496

Flipse E, Suurs L, Keetels CJAM, Kossman J, Visser RGF (1996) Introduction of sense and antisense cDNA for branching enzyme in the amylose-free potato mutant leads to physicochemical changes in the starch. Planta **198:** 340–347

Furbank RT (1988) Regulation of electron transport in maize mesophyll chloroplasts: the relationship between chlorophyll *a* fluorescence quenching and O_2 evolution. Planta **176:** 433–440

Furbank RT, Chitty JA, von Caemmerer S, Jenkins CLD (1996) Antisense RNA inhibition of *Rbc*S gene expression reduces Rubisco level and photosynthesis in the C_4 plant *Flaveria bidentis*. Plant Physiol **111:** 725–734

Furbank RT, Taylor WC (1995) Regulation of photosynthesis in C_3 and C_4 plants: a molecular approach. Plant Cell **7:** 797–807

Gallardo F, Miginiac-Maslow M, Sangwan RS, Decottignies P, Keryer E, Dubois F, Bismuth E, Galvez S, Sangwannorreel B, Gadal P and others (1995) Monocotyledonous C-4 $NADP^+$-malate dehydrogenase is efficiently synthesized, targetted to chloroplasts and processed to an active form in transgenic plants of the C-3 dicotyledon tobacco. Planta **197:** 324–332

Genty B, Briantais J-M, Baker N (1989) The relationship between the quantum yield of photosynthetic electron transport and quenching of chlorophyll fluorescence. Biochim Biophys Acta **990:** 87–92

Hatch MD (1971) Mechanism and function of the C_4-pathway of photosynthesis. *In* MD Hatch, CB Osmond, RO Slayter, eds, Photosynthesis and Photorespiration. John Wiley & Sons, New York, pp 139–152

Hatch MD (1987) C_4 photosynthesis: a unique blend of modified biochemistry, anatomy and ultrastructure. Biochim Biophys Acta **895:** 81–106

Hatch MD, Agostino A (1992) Bilevel disulfide group reduction in the activation of C_4 leaf nicotinamide adenine dinucleotide phosphate-malate dehydrogenase. Plant Physiol **100:** 360–366

Hewitt EJ (1966) Sand and Water Culture Methods Used in the Study of Plant Nutrition, Ed 2. Commonwealth Agricultural Bureaux, Farnham Royal, UK, pp 187–193

Hudson GS, Evans JRE, von Caemmerer S, Arvidsson YBC, Andrews TJ (1992) Reduction of ribulose-1–5-bisphosphate carboxylase-oxygenase content by antisense RNA reduces photosynthesis in transgenic tobacco plants. Plant Physiol **98:** 294–302

Issakidis E, Miginiac-Maslow M, Decottignies P, Jacquot J-P, Crétin C, Gadal P (1992) Site-directed mutagenesis reveals the involvement of an additional thioredoxin-dependent regulatory site in the activation of recombinant sorghum leaf NADP-malate dehydrogenase. J Biol Chem **267:** 21577–21583

Issakidis E, Saarinen M, Decottignies P, Jacquot J-P, Crétin C, Gadal P, Miginiac-Maslow M (1994) Identification and characterization of the second regulatory disulphide bridge of recombinant sorghum leaf NADP-malate dehydrogenase. J Biol Chem **269:** 3511–3517

Jacquot J-P, Gadal P, Nishizawa AN, Yee BC, Crawford NA, Buchanan BB (1984) Enzyme regulation in C_4 photosynthesis: mechanism of activation of NADP malate dehydrogenase by reduced thioredoxin. Arch Biochem Biophys **228:** 170–178

Johnson HS, Hatch MD (1970) Properties and regulation of leaf nicotinamide-adenine dinucleotide phosphate-malate dehydrogenase and "malic" enzyme in plants with the C_4-dicarboxylic acid pathway of photosynthesis. Biochem J **119:** 273–280

Jorgensen R (1991) Silencing of plant genes by homologous transgenes. Agbiotech News and Information **4:** 265N–273N

Kacser H, Burns JA (1973) The control of flux. Symp Soc Exp Biol **27:** 65–104

Kagawa T, Hatch MD (1977) Regulation of C_4 photosynthesis: characterization of a protein factor mediating the activation and inactivation of NADP-malate dehydrogenase. Arch Biochem Biophys **184:** 290–297

Landsmann J, Llewellyn D, Dennis ES, Peacock WJ (1988) Organ regulated expression of the *Parasponia andersonii* haemoglobin gene in transgenic tobacco plants. Mol Gen Genet **214:** 68–73

Lazo GR, Stein PA, Ludwig RA (1991) A DNA transformation-competent *Arabidopsis* genomic library in *Agrobacterium*. Bio/Technology **9:** 963–967

Leegood RC (1990) Enzymes of the Calvin cycle. *In* P Lea, ed, Methods in Plant Biochemistry, Vol 3. Academic Press, London, pp 15–37

Lindbo JA, Silva-Rosales L, Proebsting WM, Dougherty WG (1993) Induction of a highly specific antiviral state in transgenic plants: implications for regulation of gene expression and virus resistance. Plant Cell **5:** 1749–1759

Luchetta P, Crétin C, Gadal P (1991) Organization and expression of the two homologous genes encoding the NADP-malate dehydrogenase in *Sorghum vulgare* leaves. Mol Gen Genet **228:** 473–481

Mate CJ, Hudson GS, von Caemmerer S, Evans JR, Andrews TJ (1993) Reduction of ribulose carboxylase activase in tobacco (*Nicotiana tabacum*) by antisense RNA reduces ribulose bisphosphate carboxylase carbamylation and impairs photosynthesis. Plant Physiol **102:** 1119–1128

McDonnell RE, Clark RD, Smith WA, Hinchee MA (1987) A simplified method for the detection of neomycin phosphotransferase II activity in transformed plant tissues. Plant Mol Biol Rep **5:** 380–386

McGonigle B, Nelson T (1995) C_4 isoform of NADP-malate dehydrogenase. cDNA cloning and expression in leaves of C_4, C_3, and C_3-C_4 intermediate species of *Flaveria*. Plant Physiol **108:** 1119–1126

Meister M, Agostino A, Hatch MD (1996) The roles of malate and aspartate in C_4 photosynthetic metabolism of *Flaveria bidentis*. Planta **199:** 262–269

Napoli C, Lemieux C, Jorgensen R (1990) Introduction of a chimeric chalcone synthase gene into petunia results in reversible co-

suppression of homologous genes *in trans*. Plant Cell **2:** 279–289

Paul M, Sonnewald U, Hajirezaei M, Dennis D, Stitt M (1995) Transgenic tobacco plants with strongly decreased expression of pyrophosphate-fructose-6-phosphate 1-phosphotransferase do not differ significantly from wild type in photosynthate partitioning, plant growth or their ability to cope with limiting phosphate, limiting nitrogen and suboptimal temperatures. Planta **196:** 277–283

Porra RJ, Thompson WA, Kriedemann PE (1989) Determination of accurate extinction coefficients and simultaneous equations for assaying chlorophyll *a* and *b* extracted in four different solvents. Biochim Biophys Acta **975:** 384–394

Rebeille F, Hatch MD (1986) Regulation of NADP-malate dehydrogenase in C_4 plants: relationship among enzyme activity, NADPH to NADP ratios, and thioredoxin redox states in intact maize mesophyll chloroplasts. Arch Biochem Biophys **249:** 171–179

Rogers SG, Fraley RT, Horsch RB, Levine AD, Flick JS, Brand LA, Fink CL, Mozer T, O'Connell K, Sanders PR (1985) Evidence for ribosome scanning during translation initiation of mRNAs in transformed plant cells. Plant Mol Biol Rep **3:** 111–116

Russel M, Model P (1986) The role of thioredoxin in filamentous phage assembly: construction, isolation, and characterization of mutant thioredoxins. J Biol Chem **261:** 14997–15005

Sambrook J, Fritch EF, Maniatis T (1989) Molecular Cloning: A Laboratory Manual, Ed 2. Cold Spring Harbor Laboratory Press, Cold Spring Harbor, NY

Shure M, Wessler S, Fedoroff N (1983) Molecular identification of the waxy locus in maize. Cell **35:** 225–233

van der Krol AR, Mur LA, Beld M, Mol JNM, Stuitje AR (1990) Flavonoid genes in petunia: addition of a limited number of gene copies may lead to suppression of gene expression. Plant Cell **2:** 291–299

Vanlerberghe GC, Vanlerberghe AE, McIntosh L (1994) Molecular genetic alteration of plant respiration. Silencing and overexpression of alternative oxidase in transgenic tobacco. Plant Physiol **106:** 1503–1510

Plant Physiol. (1997) 115: 705–715

Transgenic Tobacco Plants Expressing Pea Chloroplast *Nmdh* cDNA in Sense and Antisense Orientation[1]

Effects on NADP-Malate Dehydrogenase Level, Stability of Transformants, and Plant Growth

Maria Faske, Jan E. Backhausen, Martina Sendker, Marielle Singer-Bayrle, Renate Scheibe, and Antje von Schaewen*

Pflanzenphysiologie, FB 5, Biologie/Chemie, Universität Osnabrück, D-49069 Osnabrück, Germany

A full-length cDNA encoding light-activated chloroplast NADP-malate dehydrogenase (NADP-MDH) (EC 1.1.1.82) from pea (*Pisum sativum* L.) was introduced in the sense and antisense orientation into tobacco (*Nicotiana tabacum* L.). Transgenic plants with decreased or increased expression levels were obtained. Because of substantial age-dependent differences in individual leaves of a single plant, standardization of NADP-MDH levels was required first. Then, extent and stability of over- or under-expression of *Nmdh*, the gene encoding NADP-MDH, was characterized in the various transformants. Frequently, cosuppression effects were observed, indicating sufficient homology between the endogenous tobacco and the heterologous pea gene. Analysis of the T_1 and T_2 progeny of a series of independent transgenic lines revealed that NADP-MDH capacity ranged between 10% and ≥10-fold compared with the wild type. Under ambient conditions whole-plant development, growth period, and fertility were unaffected by NADP-MDH reduction to 20% of the wild-type level; below this threshold plant growth was retarded. A positive growth effect was registered in young plants with stably enhanced NADP-MDH levels within a defined developmental window.

In plants MDHs catalyze the reversible pyridine-dinucleotide-dependent interconversion between OAA and malate in various cellular compartments. NAD-dependent isoforms are present in mitochondria, microbodies, and the cytosol (Gietl, 1992), whereas chloroplasts possess an NADP-dependent enzyme (NADP-MDH, EC 1.1.1.82) that is subject to posttranslational light/dark modulation mediated by the Fd/thioredoxin system (Scheibe, 1987).

In contrast to C_4 photosynthesis, in which NADP-MDH plays a well-known role in CO_2 prefixation (Edwards et al., 1985), the function of the enzyme in C_3 plants is less clear, since no example of a similar role in carbon assimilation is known. Here NADP-MDH probably fulfills other tasks. There is evidence that the enzyme is involved in fine-tuning of the stromal redox state (Scheibe, 1987; Backhausen et al., 1994) via the so-called "malate valve": the controlled reduction of OAA is able to poise the ATP/NADPH ratio inside the chloroplast when alterations in electron use or ATP levels occur, which are caused by changes in light intensity or by stomatal opening. A large part of the malate formed in the light is due to NADP-MDH activity. Mediated by the malate-OAA shuttle, malate, and concomitantly reducing equivalents, can be transferred from the chloroplasts into the cytosol (Heber, 1974; Heineke et al., 1991).

In plant-cell metabolism malate claims a central role for various reactions (Lance and Rustin, 1984). The export of reducing power into the cytosol is assumed to be involved in nitrate assimilation (House and Anderson, 1980; Champigny, 1995), to drive mitochondrial respiration (Raghavendra et al., 1994), and to stabilize the cytosolic pH (Davies, 1986). Furthermore, malate can be stored in the vacuole (Winter et al., 1994). Together with the anaplerotic CO_2-fixation reaction catalyzed by PEP carboxylase (Melzer and O'Leary, 1987; Lepiniec et al., 1994), malate can account for up to 15% of the ^{14}C-labeled metabolites in spinach leaves at the end of the light period (Gerhardt and Heldt, 1984). Malate is also transported from the leaf into the root system, where it can provide electrons and serve as the carbon skeleton for N assimilation (Lee, 1980), or be involved in the uptake of nutrient salts (Smirnof and Stewart, 1985).

To gain insight into the role of light-activated NADP-MDH in C_3 plants, we obtained transgenic tobacco (*Nicotiana tabacum* L.) plants with either increased or decreased levels of this chloroplast enzyme. A cDNA encoding NADP-MDH from pea (*Pisum sativum* L.), driven by the constitutive cauliflower mosaic virus 35S promoter, was introduced into tobacco in sense or antisense orientation. Transformants with reduced or increased NADP-MDH levels were identified and expected to provide a useful tool with which to study the effects on regulatory processes and plant-growth behavior.

MATERIALS AND METHODS

Plant Material and Growth Conditions

Tobacco (*Nicotiana tabacum* L. var Xanthi) seeds were a kind gift from the laboratory of M.J. Chrispeels (Depart-

[1] This work was supported by the Deutsche Forschungsgemeinschaft (grant nos. SFB 171/C15 and Sche 217/5).

* Corresponding author; e-mail schaewen@sfbbio1.biologie.uni-osnabrueck.de; fax 49–541–969–2870.

Abbreviations: NADP-MDH, NADP-dependent malate dehydrogenase; OAA, oxaloacetate.

ment of Biology, University of California, San Diego). After tissue culture, wild-type plants and transformants (T_0) were grown in commercial soil mixture (10% sand, 10% pumice, 10% loam, 35% compost, and 35% peat) in growth chambers. Up to d 30 after germination the pot size was 5 cm in diameter (70 mL), and from then on it was 14 cm in diameter (1.3 L). After potting the plants were transferred to their final growth regimes. In the growth chamber light intensity was 250 to 350 μmol quanta m^{-2} s^{-1} at plant height for a daily period of 16 h of light (22°C), 8 h of darkness (18°C), and 75% RH. Greenhouse facilities were used during the summer months (June through September of 1995). The average daily temperature was 20.4°C and the average daily sunshine period was 9.6 h. Peak light intensities at plant height ranged between 200 and 1400 μmol quanta m^{-2} s^{-1}.

Seeds of the transgenic progeny and control plants were surface sterilized using a method communicated by A. Rodrigues-Franco (Facultad de Ciencias, Universidad de Cordoba, Spain). Up to 100 seeds were spread evenly inside a closed, sterile, 1.5-mL microfuge tube and placed inside of a microwave oven along with a 1-L Erlenmeyer flask filled with 800 mL of cold water, and set twice for 7 min at 650 to 700 W (in between, seeds were allowed to cool for 2 min and the water was replaced). Sterilized seeds were spread on solidified (0.8% agar) Murashige and Skoog medium (Sigma) containing 2% Suc and 250 mg L^{-1} Claforan (cefotaxime sodium, Duchefa, Haarlem, The Netherlands) supplemented with 100 mg L^{-1} kanamycin (medium A) or without kanamycin (medium B). After 3 d in the dark at 4°C for synchronizing germination, further cultivation was performed in growth chambers for about 7 d at 70 μmol quanta m^{-2} s^{-1} for a daily period of 16 h of light (24°C) and 8 h of darkness (20°C). Seedlings were then transferred to soil and grown as described above.

For assessing whole-plant growth, surface-sterilized seeds of selected transgenic lines (T_1 and T_2 progeny) were germinated on sterilized sand that was moistened with water. After 10 d seedlings were planted in commercial soil mixture and grown as described above. For interpolation of biomass development, the scored data were fitted by a fifth-order polynomial regression using the software package GRAFIT version 3.0 (Erithacus Software Ltd., Staines, UK).

Cloning Procedures

Plasmids containing the complete cDNA sequence coding for NADP-MDH from pea (*Pisum sativum* L.) were constructed as shown in Figure 1, starting from two cDNA clones termed *r-mdh* and *t-mdh* (W. Reng, Institut für Biophysik und Physikalische Biochemie, Universität Regensburg, Germany). The insert of clone *r-mdh* encodes the mature part of the enzyme and clone *t-mdh* encodes the missing 5′ end, comprising the plastidic transit peptide plus part of the mature N terminus (Reng et al., 1993). The complete cDNA sequence was assembled in vector pASK40 (Skerra, 1989) and termed *g-mdh*. From this construct, the 1,356-bp *Eco*RI fragment was purified, blunt-ended, and inserted into the *Sma*I site in plant-expression vector pA35S (Höfte et al., 1991), flanked by the cauliflower mosaic virus 35S promoter and octopine synthase termination sequences. Sense or antisense orientation of the cDNA fragments was verified by *Hin*dIII restriction digests (Fig. 1). Both plant-expression cassettes containing the complete *Nmdh* cDNA in either sense or antisense orientation were introduced as 2,161-bp *Eco*RI/*Hin*dIII fragments into the T-DNA region of binary vector pDE1001 (Denecke et al., 1990). Two different *Agrobacterium tumefaciens* C58C1 strains, LBA4404 and GV2260 (Deblaere et al., 1985), were transformed with the sense- and antisense-pDE1001 con-

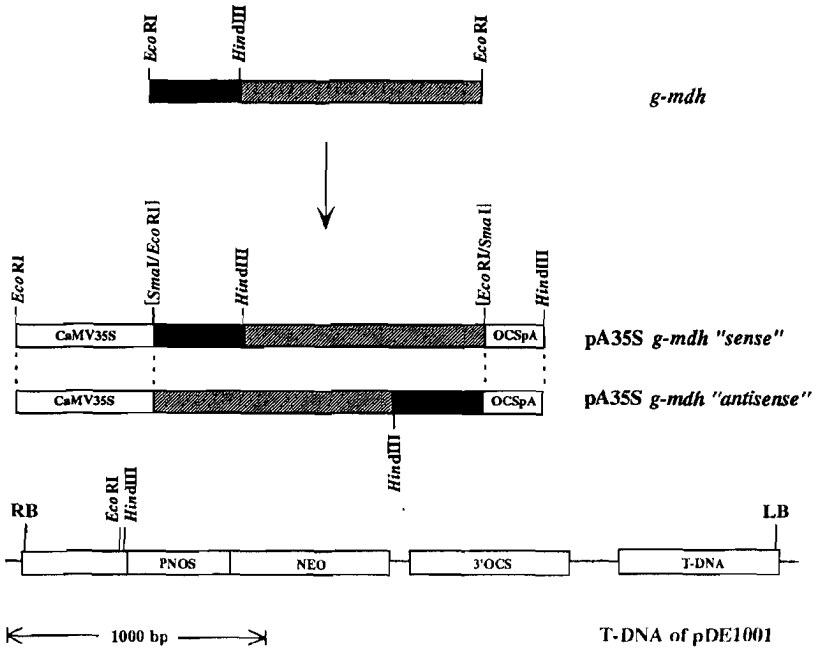

Figure 1. Construction scheme of plasmids with *Nmdh* in sense and antisense orientation. The complete cDNA fragment (1356 bp, coding for pea NADP-MDH and its transit peptide) was inserted between the cauliflower mosaic virus (CaMV35S) promoter and the octopine synthase (OCS) termination sequences of plant expression cassette pA35S (Höfte et al., 1991). The 2161-bp *Eco*RI/*Hin*dIII fragments of constructs pA35S *g-mdh* sense and pA35S *g-mdh* antisense were inserted into the respective *Eco*RI/*Hin*dIII sites of binary vector pDE1001 (Denecke et al., 1990). RB/LB, Right and left T-DNA borders, respectively; PNOS, nopaline synthase promoter driving the neomycin phosphotransferase gene (NEO); and hatched box, cDNA fragment used as a probe for hybridization experiments.

structs using the freeze-thaw method described by Höfgen and Willmitzer (1988) and used for cocultivation of tobacco leaf discs.

Leaf-Disc Transformation and Regeneration of Transgenic Plants

A. tumefaciens-mediated transformation of tobacco leaf discs followed the procedure described by Voelker et al. (1987). Combined callus and shoot induction was on solidified (0.8% agar) Murashige and Skoog medium containing 2% Suc, supplemented with 0.1 mg L^{-1} naphthalene acetic acid and 1 mg L^{-1} benzylaminopurine. For selection of transformed shoots Claforan (500 mg L^{-1}) and kanamycin (100 mg L^{-1}) were included. After 6 to 8 weeks regenerated shoots were transferred to kanamycin-supplemented agar (medium A). Shoot cuttings that formed roots were planted in soil and grown for at least 3 weeks before the determination of NADP-MDH capacity. As controls, kanamycin-sensitive (i.e. pseudo-wild-type) and wild-type tobacco plants were regenerated in parallel, the latter by omitting kanamycin selection (medium B).

Preparation of Leaf Extracts

To reduce stress effects resulting from tissue culture, plants were grown for at least 3 weeks in soil before experiments were started. The youngest leaf measuring about 1.5 cm in length was defined as the first leaf of an individual plant. The third leaf was about 30% of the size of a fully expanded source leaf. The complete third leaf of each plant was ground in liquid nitrogen and the frozen powder was subsequently homogenized in 500 μL of degassed extraction medium: 50 mM Tris-HCl, 1 mM EDTA, 14 mM 2-mercaptoethanol, 0.01% (w/v) BSA, 0.5% (v/v) Triton X-100, and 1% (w/v) polyvinylpolypyrrolidone, pH 8.0. Under these conditions degradation and/or inactivation of NADP-MDH was undetectable. Aliquots for measuring chlorophyll content were withdrawn, and the remaining samples were stored in liquid nitrogen for determination of NADP-MDH activity and protein concentration.

Determination of NADP-MDH Activities

For routine measurements of NADP-MDH activity in the third leaf (counted from the top) of individual plants, preparation of leaf extracts was simplified as follows: two leaf discs of 1 cm in diameter were cut with a cork borer from both sides of the midrib (central area) and ground under liquid nitrogen in a 1.5-mL microfuge tube. The frozen powder was suspended in 200 μL of extraction medium as described above, but without polyvinylpolypyrrolidone. To determine maximal NADP-MDH activity (i.e. NADP-MDH capacity), the enzyme was fully activated by incubation for 20 min in the presence of 100 mM DTT (reduced form, dissolved in 100 mM Tris-HCl, pH 8.0) and 0.1% (w/v) BSA. NADP-MDH activity was measured at 340 nm in a standard assay mixture, as described by Scheibe et al. (1986). Plants that were used for growth analyses were preselected according to samples taken 30 d after germination. Final categorization was based on measurements at the time of harvest.

For the estimation of in vivo NADP-MDH activities, samples were taken using the freeze-clamp method and extracted according to Scheibe and Stitt (1988). For freeze-clamping, an LCA4 gas-exchange system (ADC, Hoddesdon, UK) with a specially modified PLC2 leaf chamber was used (fine-mechanic shop of the Universität Osnabrück, Germany).

Chlorophyll concentration was determined according to Arnon (1949) before centrifugation of the samples. Total soluble protein was measured in cleared extracts using the method of Bradford (1976) with BSA as a reference protein.

Estimation of Molecular Masses and NADP-MDH Protein Contents

Discontinuous SDS-PAGE of protein extracts (Laemmli, 1970) was conducted in a vertical minigel system (Mini-Protean II, Bio-Rad), including a molecular weight standard mixture (Dalton Mark VII-L, Sigma).

Preparation of protein blots with subsequent immunodetection was essentially as described by Graeve et al. (1994). Extraction of total protein was in 50 mM Hepes-NaOH, pH 7.0, 0.1% (w/v) SDS, 2 mM sodium bisulfite, and 0.01% (w/v) BSA. A polyclonal rabbit antiserum, raised against purified pea NADP-MDH, was used for the detection of NADP-MDH from pea and tobacco. Relative amounts were estimated from a dilution series.

Nucleic Acid Analyses

Genomic DNA was prepared from frozen leaf tissue as described by Dellaporta et al. (1983). Total RNA was isolated from the fourth leaf (counted from the top) of individual plants according to the method of Logemann et al. (1987). Nucleic acids were blotted from agarose gels onto Nytran membranes (Schleicher & Schuell). DNA- and RNA-blot analyses were conducted using standard techniques (Sambrook et al., 1989). For an estimation of signal strength, dot-blot filters with serial dilutions of pea cDNA clone *r-mdh* were prepared essentially as described by von Schaewen et al. (1995). The blots were probed with radioactively labeled cDNA fragments (970 bp) of plasmid *r-mdh*, purified from agarose gels using the Geneclean-II kit (BIO 101, San Diego, CA). Labeling of DNA fragments with [α-^{32}P]dCTP and removal of nonincorporated nucleotides was as described previously (von Schaewen et al., 1995).

RESULTS

Assessment of NADP-MDH Capacity in Wild-Type and Pseudo-Wild-Type Tobacco Plants

To analyze the distribution of NADP-MDH in tobacco wild-type plants, maximal enzyme activity (i.e. capacity) was monitored in discs cut from every leaf of individual plants during a period of 3 to 9 weeks after germination. The results shown in Figure 2 demonstrate that in tobacco leaves NADP-MDH capacity depends strictly on plant age

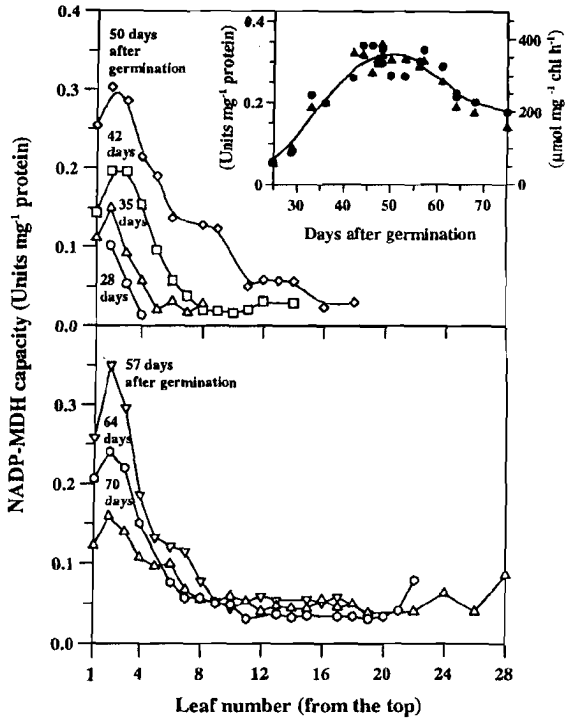

Figure 2. NADP-MDH activities in individual leaves of tobacco wild-type plants. Graphs are based on the mean values obtained from two plants for each time point. The inset in the top panel shows the calibration curve of NADP-MDH capacities in third-leaf samples. Tobacco wild-type and pseudo-wild-type plants (after regeneration from leaf discs in tissue culture) were assayed over the indicated time period. The values are either based on protein (left scale, ●) or chlorophyll (right scale, ▲) contents. chl, Chlorophyll.

and on the developmental state of the tissue. Enzyme activity in young, developing leaves was about 5- to 10-fold higher than in older, fully expanded leaves. This held true for a correlation based on protein content (Fig. 2), and also for a correlation of NADP-MDH capacity with leaf area or chlorophyll content (data not shown).

Especially in young leaves of wild-type tobacco plants NADP-MDH capacity varied substantially over the entire growth period (Fig. 2). To correlate the enzyme activities in third-leaf samples of the transformants with those of wild-type plants grown in parallel, NADP-MDH capacities were determined at various times after transfer to soil. The time-dependent differences of endogenous NADP-MDH capacities in third-leaf samples of pseudo-wild-type regenerants paralleled the result found for wild-type plants, regardless of whether the data were related to protein or to chlorophyll contents (calibration curve; Fig. 2, inset). Therefore, in all further experiments untransformed cv Xanthi wild-type plants were grown in parallel and used as controls.

Analysis of Primary Transformants (T_0 Plants)

From 33 independent transformants expressing pea *Nmdh* in sense orientation, obtained after infection with two different *A. tumefaciens* strains (L preceding the number of the transformant refers to LBA4404, $n = 11$; P refers to GV2260, $n = 22$), only four showed significant overexpression of *Nmdh* (the data for two of them are shown in Figure 3A). It was confirmed that the more than 2-fold NADP-MDH capacity in third-leaf samples of these transformants (e.g. L12) correlated with an equally enhanced signal on RNA blots (qualitative estimation, data not shown). Frequently, cosuppression of endogenous tobacco *Nmdh* was observed (Jørgensen, 1991), which indicates sufficient homology between the endogenous tobacco and the

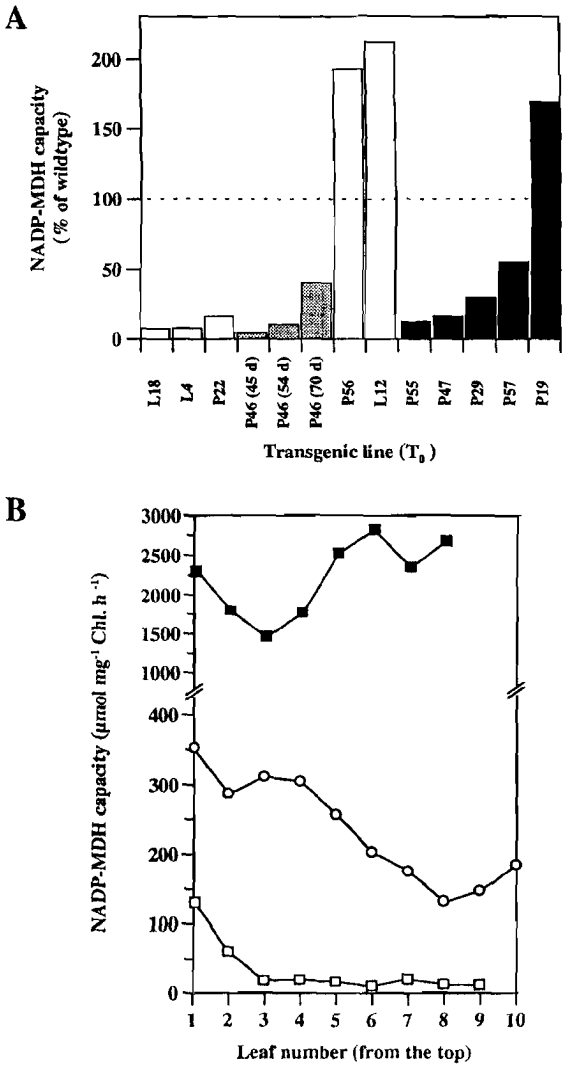

Figure 3. NADP-MDH capacities in the third leaf of selected transformants. A, Activities of the primary transformants (T_0) are shown as a percentage of those determined in third-leaf samples of tobacco wild-type plants. The calibration curve shown in Figure 2 was used as a reference (100%). A total of 36 antisense and 50 sense transformants was analyzed. Open and shaded bars, Sense plants; black bars, antisense plants. Multiple measurements were done between d 30 and 70 after transfer of plants to soil. B, NADP-MDH capacity in individual leaves of two stable L18-T_1 plants at d 43 postgermination, showing either strong overexpression (L18-T_1-B6/OE, ■) or strong cosuppression (L18-T_1-B5/UE, □) of NADP-MDH. O, Untransformed control plant (wild type). Chl, Chlorophyll.

heterologous pea gene. A recent report shows that sequences with only 71% homology can give successful cosuppression (Trevanion et al., 1997). Some of the sense transformants showed a decrease of NADP-MDH capacity to less than 20% of the wild-type level in third-leaf samples (Fig. 3A). For transformants L18, L4, and P22 this effect was constant over the entire growth period. Similarly low NADP-MDH levels were not stable in all cosuppressed transgenic sense lines. Transformant P46, for example, showed the strongest initial reduction in NADP-MDH capacity (about 5% of the wild type). However, when assaying the third leaf at d 54 and 70 after germination, levels had increased to 40% of NADP-MDH wild-type activities (Fig. 3A, gray bars).

Expression of the heterologous pea *Nmdh* cDNA in antisense orientation resulted in stable reduction of NADP-MDH capacity in transgenic tobacco plants, but antisense transformants with NADP-MDH levels that were reduced to less than 13% of the wild-type level were not obtained (Fig. 3A; Table I). After selfing most of the T_1-antisense plants showed NADP-MDH activities ranging between 50 and 100% of the wild-type level in the third leaf. The reason that one of the antisense transformants (P19) showed elevated NADP-MDH activity, which was also transmitted to the T_1 progeny (Table I), is obscure and was not analyzed further.

Quantitation of the T-DNA Integrations

Southern-blot analysis of transgenes alone is not sufficient to reveal the exact copy number of T-DNA integrations (Masle et al., 1993). To determine the number of independent T-DNA insertions in the dihaploid tobacco genome, seeds of the selfed transformants (T_1 progeny) were germinated on agar containing kanamycin. The percentage of germinating seeds was always equal to the proportion of germinated seeds without kanamycin selection. The deduced T-DNA copy numbers for selected transgenic lines are shown in Table I. For some of the transformants an estimation of one to two T-DNA integrations per genome is based on 10 to 15% kanamycin sensitivity of the T_1 progeny. Deviations from the theoretically expected value were already found in a similar study (Kilby et al., 1992) and had been ascribed to a non-Mendelian behavior of the kanamycin-resistance gene.

Characterization of T_1 Plants

For studies concerning whole-plant growth under various conditions, a high number of near-isogenic plants with stably suppressed or increased NADP-MDH levels was required. For a better comparison, T_1 individuals from different transgenic lines were categorized according to their NADP-MDH capacities into "overexpressors" (>200%), wild-type-like, and "underexpressors" (<40%). Among the selfed progeny of some transgenic sense lines (e.g. transformant L18), most T_1 individuals revealed either low (<20%) or high (>2-fold) NADP-MDH levels (Table I), which were stable in all leaves during the entire growth period (data not shown). Individuals were defined as stable when the NADP-MDH content in all available leaves was either at least 3-fold higher or less than 20% of the wild type (grown in parallel) during the entire growth period (Fig. 3B).

NADP-MDH activities in third-leaf samples of strong overexpressors were 4- to 5-fold higher compared with wild-type plants, and immunologically cross-reacting material on protein blots was increased even more (up to

Table I. *Characteristics of the various transgenic lines*

Inferred T-DNA copy numbers and NADP-MDH capacities in the third leaf of selected transformants (T_0) are compared with the distribution of NADP-MDH capacities in individual T_1 plants. WT, Tobacco wild type. T-DNA copy numbers were estimated from the percentage of kanamycin-resistant seedlings (kan^R) in the T_1 progeny of the selfed transformants (n = 50).

Line	T-DNA Copies	NADP MDH Level			
		Relative MDH level in T_0 plants	Range of MDH levels in kan^R T_1 progeny (no. of plants)		
			<40	±100	>200
			% of WT		
Sense					
L18	2	7.5	10	8	32
L4	1	8	0	44	6
P22	1–2	16	42	3	5
P46	(1)	5, 10, 40[a]	28	18	4
L12	1–2	210	0	0	50
Antisense					
P55	2	13	0	50	0
P47	2	17	3	47	0
P29	1	30	0	50	0
P57	2	55	0	50	0
P41	1	70	0	50	0
P19	1	170	0	25	25

[a] NADP-MDH capacity determined at d 45, 54, and 70 after germination.

20-fold). This estimation includes a 45-kD form in addition to the 43-kD unit length NADP-MDH band, which is also specifically recognized by the pea antiserum in overexpressors (Fig. 4C, lane OE). Subsequent experiments with isolated chloroplasts from wild-type and L18-B6-overexpressor plants revealed that at comparable levels of intactness (76 and 75%, respectively), NADP-MDH capacity and protein content in the overexpressor are elevated 5-fold compared with the wild type (data not shown). Therefore, we speculate that the 45-kD cross-reacting polypeptide most likely represents unprocessed NADP-MDH precursors in the cytosol, which are recognized by the antiserum but do not contribute to measurable activity.

Southern-blot analysis of *Hin*dIII-digested genomic DNA of individual L18-T_1 plants suggests that cosuppression effects ensue from higher T-DNA copy numbers when compared with the situation in overexpressors. Different signal intensities were observed by hybridization of the 1,125-bp internal *Hin*dIII-fragment (Fig. 4A, compare lanes UE and OE) with the radiolabeled 970-bp probe (Fig. 1). Fragments larger than 5000 bp were detected when genomic DNA was digested with *Eco*RI (one restriction site within the introduced T-DNA construct; data not shown). This indicated that multiple T-DNA integration in direct tandem repeat at one locus had not occurred.

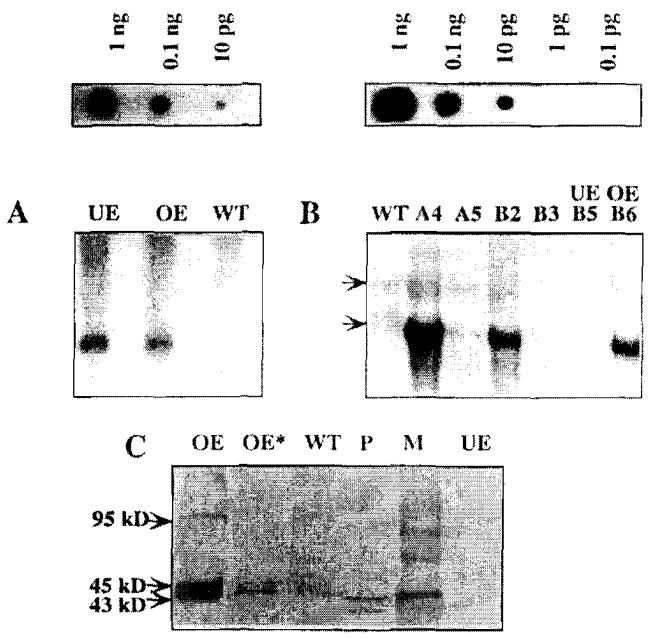

Figure 4. Analysis of *Nmdh* expression in leaf samples of L18-T_1 plants. A, For Southern blots, genomic DNA from wild type (WT), selected underexpressors (UE), or overexpressors (OE) was prepared. Ten-microgram aliquots were digested with *Hin*dIII (compare Fig. 1), separated in 0.8% agarose gels, and transferred to nylon membranes. B, RNA blots were run with 20 μg of total RNA under denaturing conditions. Southern and northern blots were hybridized with ^{32}P-labeled 970-bp *Hin*dIII fragments of pea cDNA clone *r-mdh* (Reng et al., 1993; compare Fig. 1). Signal strengths were estimated from dot-blot standard filters developed in parallel. The two arrows mark the positions of weak signals recognized by the heterologous pea probe in wild-type tobacco plants. C, Immunodetection of NADP-MDH on protein blots. Third-leaf samples were separated in a 15% SDS-polyacrylamide gel and transferred to nitrocellulose. A polyclonal rabbit antiserum raised against the purified pea enzyme was used to detect tobacco and pea NADP-MDH polypeptides. Lane M, Molecular mass standards plus 1 μg of recombinant pea NADP-MDH purified from *Escherichia coli*, essentially as described by Reng et al. (1993). Leaf extracts of pea (P), L18-T_1-B6 (OE), L18-T_1-B5 (UE), and a tobacco wild-type plant (WT) were analyzed, each equivalent to 200 μg of soluble protein. OE*, Dilution of L18-T_1-B6 extract equivalent to 20 μg of protein.

Using RNA-blot analysis of total RNA, endogenous and heterologous *Nmdh* mRNA could not be distinguished (Fig. 4B). In wild-type tobacco samples two mRNA species hybridized weakly with the heterologous cDNA probe from pea, whereas strong labeling of a single band was observed with RNA samples of individual overexpressors. High mRNA levels always correlated qualitatively with high NADP-MDH capacities (Fig. 3B) and protein contents (Fig. 4C) in individual overexpressing L18-T_1 plants, whereas *Nmdh* signals of underexpressing L18-T_1 plants on RNA and protein blots were below the detection limit when compared with wild-type controls (Fig. 4, B and C).

In heterotrophic plastids NADP-MDH activity is undetectable. Because of constitutive expression of the transgene, root extracts of L18-T_1 overexpressors showed relatively high NADP-MDH capacities (0.8–2.7 units mg^{-1} protein). In root extracts of L18-T_1 underexpressors, however, NADP-MDH activity was, as in wild-type plants, at the detection limit (0.017 ± 0.005 unit mg^{-1} protein), which indicates that in transgenic line L18 cosuppression operates at the DNA level. In contrast, relatively high NADP-MDH capacity (i.e. DTT-dependent, about 0.15 unit mg^{-1} protein) was detected in root extracts of underexpressing T_1 plants of line P46. In this case, the cosuppression effect observed in leaves seems to depend on the tissue-specific expression of the endogenous tobacco *Nmdh* gene.

Growth Analysis of T_1 and T_2 Individuals in the Greenhouse

Possible correlations of plant-growth parameters with altered NADP-MDH capacities in transgenic plants were analyzed in comparison with the wild type. Because in several lines multiple insertion events probably occurred (Table I), T_1 and T_2 individuals from eight different transgenic sense lines were used for the first set of experiments. For growth-rate analyses, plants were preselected according to their NADP-MDH capacities at d 30 before they were transferred to the greenhouse. A total of 360 individuals (including one-third of the untransformed wild-type plants and one unstable line) was analyzed in three sets. Randomly selected plants were harvested in 10- to 14-d intervals for determination of fresh and dry weights, leaf area, specific leaf weight, and NADP-MDH activity. For a better comparison, transgenic plants were classified according to their NADP-MDH capacities into overexpressors (>300% wild type), underexpressors (<20% wild type), or wild-type-like plants.

For untransformed wild-type control plants, the typical developmental change of the NADP-MDH activities, as described above (compare Fig. 2), was observed. Highest NADP-MDH capacities were scored during the period of

Table II. *Stability of NADP-MDH capacity in transgenic tobacco sense lines used for growth analysis*

NADP-MDH activities were first determined after 35 d in the greenhouse and again at harvest. The categorization is based on NADP-MDH capacities of untransformed control plants grown in parallel (100%): underexpressors (UE, <50%), overexpressors (OE, >200%), and wild-type plants (50–200%). A subset of stable transformants was used for scoring the data compiled in Figure 5.

Transgenic Line	No. of Individuals				
	Total no.	<50%	50–200%	>200%	Unstable
P8-T_1	13	0	13	0	0
P14-T_1	14	0	12	0	2
L-6-T_1	14	0	5	9	0
L12-T_1	39	0	5	30	4
L18-T_1	42	6	4	19	13
L18-T_2 (B5/UE)	49	16	0	0	33
L18-T_2 (B6/OE)	36	0	0	35	1

maximal growth (d 40–60). Analysis of the various transgenic lines that were used in these experiments revealed significant differences, not only in their NADP-MDH expression levels, but also in their stability of NADP-MDH expression. For classification, the NADP-MDH capacity of the wild-type plants at harvest was taken as 100%. Individuals in which NADP-MDH activity deviated from the initial score at d 30 were denoted as unstable and were not included in the following growth analyses (Table II).

Stable transgenic plants that were examined during the phase of maximal growth (around d 50 after germination) showed a significant correlation of their fresh and dry weights with their respective NADP-MDH capacities (Table III). Extreme underexpressors exhibited reduction in leaf area and shoot fresh or dry weights, whereas for overexpressors these parameters increased. The observation that specific fresh and dry weights (i.e. weight per leaf area) remained unaltered indicated that no change in leaf morphology had occurred. The dry weight data were used to interpolate a continuous time course of biomass accumulation (Fig. 5). The curve fit indicates that plants with a high NADP-MDH capacity developed faster and reached their final weight earlier than the wild type, whereas plants with a reduced enzyme capacity lagged behind. The differences were visible only during maximal plant growth and disappeared later in development.

Because the effect on plant growth was found for three independent transgenic lines, we consider it unlikely that the described growth phenotype is merely the result of T-DNA insertion (or insertions) at a certain locus in the tobacco genome. In short-term experiments, steady-state photosynthetic parameters, levels of other pace-making Calvin-cycle enzymes, and metabolite contents of the leaves were not significantly altered (data not shown). Apart from the differences in growth, few phenotypic deviations occurred. Some of the transformants had narrower leaves, but when assaying the T_1 progeny this did not strictly correlate with the NADP-MDH contents and can probably be attributed to tissue-culture aftereffects (Masle et al., 1993).

Growth Analysis under Climate-Controlled Conditions

To minimize effects possibly caused by the noncontrolled environmental conditions during growth in the greenhouse, T_2 plants from the most stable overexpressing (L18-T_1-B6) and underexpressing lines (L18-T_1-B5) were chosen for further growth analyses under climate-controlled conditions. After 30 d a clear correlation between NADP-MDH content and growth rate was detected. Transgenic plants with less than 20% of NADP-MDH capacity were restricted in growth, whereas overexpressors showed a faster accumulation of biomass than the corresponding wild-type plants. The effects are obvious from data scored with shoot tissue (leaves plus stem) and are

Table III. *Comparison of growth parameters*

Growth parameters were determined for wild-type tobacco and stable transgenic sense plants as given in Table II. The transgenic plants showed either extreme over- or underexpression of NADP-MDH. The data were scored during the period of maximal plant growth in the greenhouse using total overground tissue (leaves plus stem) and are the means ± SD. The average values obtained for untransformed plants (wild type) represent 100% (n = 6).

Growth Parameter	Underexpressors	Wild Type	Overexpressors
NADP-MDH capacity (μmol mg^{-1} chlorophyll h^{-1})	19 ± 10	100 ± 17	507 ± 100
Leaf area (m^2)	73 ± 7	100 ± 8	130 ± 6
Shoot fresh weight (g)	70 ± 8	100 ± 12	125 ± 16
Shoot dry weight (mg)	54 ± 7	100 ± 8	118 ± 9
Specific leaf weight (fresh) (g m^{-2})	106 ± 9	100 ± 7	95 ± 6
Specific leaf weight (dry) (mg m^{-2})	105 ± 5	100 ± 10	107 ± 10

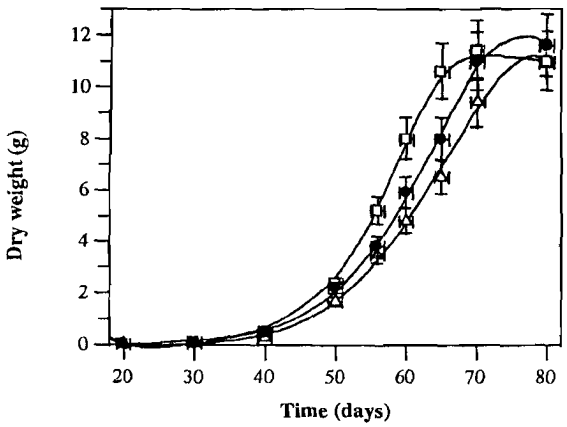

Figure 5. Graphic representation of dry weight accumulation over time. Plants were grown in the greenhouse and harvested at the indicated times. A subset (≤20% and ≥300%) of the transgenic plants used for growth analyses (Tables II and III) was compiled. The horizontal error bars indicate that the harvesting procedure took up to 3 d. The scored data were fitted by a fifth-order polynomial regression, using the software package *GRAFIT version 3.0*. □, Overexpressors; ●, untransformed wild-type plants; and △, underexpressors.

less clear with root tissue (Fig. 6), which is difficult to sample from soil-grown plants.

As already observed in the greenhouse for *Nmdh*-overexpressing plants, at the end of a prolonged growth period the enhancement in biomass production was no longer apparent. After 70 d in soil no significant differences could be detected for *Nmdh* overexpressors on a whole-plant basis compared with the wild type (Fig. 6). This was also found for selected individuals of other lines (L12 and P46). Between over- and underexpressing individuals, other striking differences became evident from the activation states of NADP-MDH (Table IV). In wild-type plants about 35% of the available enzyme is activated in vivo under the chosen growth conditions. Overexpressors reached slightly lower activation states (expressed as percentage), which means that their actual NADP-MDH activity was three times higher compared with the wild type. In contrast, underexpressors activated a large part (70–80%) of their available NADP-MDH, which, however, corresponds to only about 20% of the actual wild-type activity (Table IV). Similar observations were made when *Sorghum bicolor* NADP-MDH was overexpressed in the C_4 plant *Flaveria bidentis* (Trevanion et al., 1997).

DISCUSSION

Several recently conducted physiological studies using transgenic plants, for example, with reduced levels of regulatory Calvin-cycle enzymes (Paul et al., 1995; Price et al., 1995) or of the plastidic phosphate translocator (Riesmeier et al., 1993; Heineke et al., 1994), are based on the assumption that mRNA or protein levels, once defined for a distinct sample, remain constant in all leaves during the entire growth period. This seems to ignore the possibility of tissue-specific, age-dependent, or stress-induced endogenous control mechanisms, which could influence both the enzyme levels in wild-type plants and transgene expression in the transformants.

For the transgenic approach described here, the aim was to generate significant differences in NADP-MDH activity that remain stable during the entire life cycle of the plant. NADP-MDH activities were monitored in leaf samples of wild-type tobacco plants during the growth period. This revealed that between different leaves of individual plants, the maximal activities (i.e. NADP-MDH capacities) varied by a factor of about 10 (Fig. 2), without regard to whether the data were related to chlorophyll or protein content or to leaf area. Further variations were registered over time (see inset in Fig. 2). During maximal growth of the wild-type plants, NADP-MDH levels were about six times higher compared with the beginning or the end of the life cycle. Thus, in experiments that addressed the importance of an enzyme with respect to plant growth, the physiological and

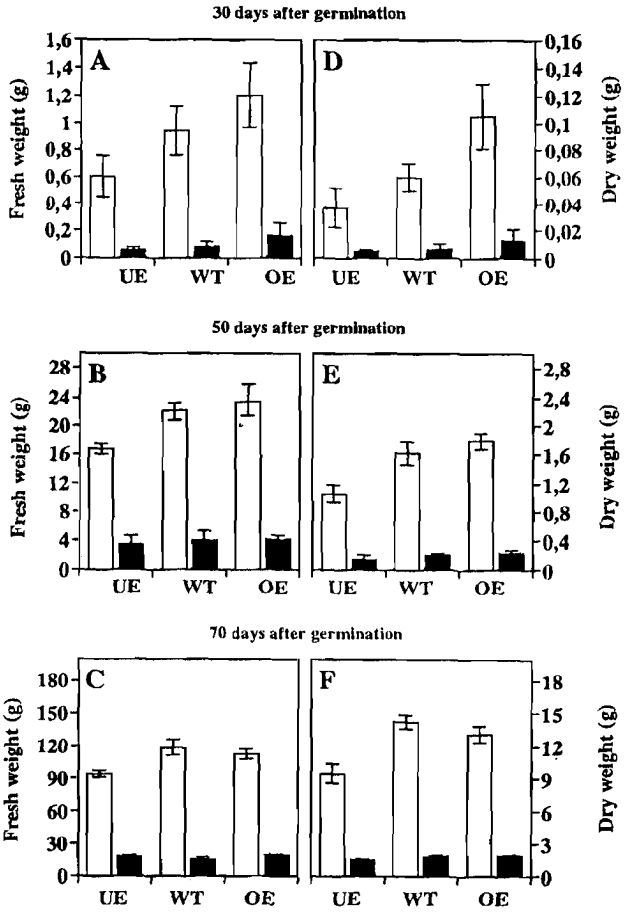

Figure 6. Growth analysis of L18-T_2 plants. Data from the T_2 progeny of selfed L18-T_1-B6 overexpressor and L18-T_1-B5 underexpressor plants are compared with those of untransformed tobacco wild type. Plants were grown at a light intensity of 250 to 350 μmol quanta m^{-2} s^{-1} (at plant height) in a growth chamber as described in "Materials and Methods." Fresh (A–C) and dry weights (D–F) of total shoot (open bars) and root tissue (filled bars) were determined at d 30 (A and D), d 50 (B and E), and d 70 (C and F) after germination. Each bar represents the mean from four individual plants; the range of deviation is indicated by a vertical line.

Table IV. *Comparison of NADP-MDH capacities and the respective activation states in leaf extracts*

Wild-type and individual stable T_2 plants of selected transgenic lines were grown in a climate chamber at 350 μmol quanta m^{-2} s^{-1}. After 55 d samples were taken 2 h after illumination using the freeze-clamp method (see "Materials and Methods"). The number of plants analyzed in the different categories varied: wild type, $n = 9$; underexpressors (<20% of wild type), $n = 4$; overexpressors (>300% of wild type), $n = 7$.

NADP-MDH	Underexpressors (L18-T_2-B5)	Wild Type	Overexpressors (L18-T_2-B6)
Capacity (μmol mg chlorophyll^{-1} h^{-1})	12 ± 5	130 ± 16	507 ± 100
Activation state (% of capacity)	72 ± 12	34 ± 8	26 ± 9
Actual activity (μmol mg chlorophyll^{-1} h^{-1})	8.7	44.0	131.0

developmental variations during the plant's life span, which for NADP-MDH occur in a range (6- to 10-fold change) that is often described as the result of successful plant transformation, must be taken into account. For the evaluation of altered enzyme levels in the different transformants, the corresponding data obtained with wild-type plants, therefore, served as a reference.

The *Nmdh* cDNA from pea was chosen for two reasons. First, overexpression is more effective with heterologous transgenes, and cosuppression effects are less frequently observed (Jørgensen, 1990). Second, it has been shown previously that silencing of endogenous genes can be similarly achieved by transformation with closely related but nonidentical sequences (e.g. Phe ammonia lyase from bean in transgenic tobacco plants [Elkind et al., 1990]; and, recently, NADP-MDH from *S. bicolor* in transgenic tobacco plants [Trevanion et a., 1997]). A number of sense transformants with strongly cosuppressed NADP-MDH activity were found, indicating sufficient homology between the endogenous and heterologous sequences. However, no good antisense effect was observed (Table I), a fact that could be explained by a weaker homology in the 5′ region that comprises the chloroplast signal sequences, since the complete pea cDNA was used for both sense and antisense constructs (Fig. 1). In most but not all cases described, extensive pairing of sense and antisense transcripts is required to efficiently block expression of the endogenous gene by triggering degradation of the double-stranded RNA molecules (Nellen and Lichtenstein, 1993).

T_1 individuals showing either extreme overexpression or extreme cosuppression effects were found among the selfed progeny of three independent transgenic lines (P22, P46, and L18). The mechanisms responsible for the high variation in *Nmdh* expression levels seem to differ between the transgenic lines (Table I), which can be explained by: (a) integration of two T-DNA copies at different (L18) or linked loci (L12); (b) copy number and/or tissue-specific effects on the introduced transgene, operating at different levels (DNA or mRNA, as indicated by different *Nmdh* expression in roots of L18 versus P46 individuals); and (c) transgene inactivation by methylation (Meyer, 1995; Matzke et al., 1996), which could account for the observation of kanamycin-resistant plants with near-wild-type levels (Table I) or developmentally unstable individuals (Table II) (Hobbs et al., 1990).

Despite the exact nature of the effects, categorization of selected individuals into groups with either stably enhanced (overexpressor, >2-fold) or reduced (underexpressor, <40%) NADP-MDH capacities, compared with the wild type (Table I), allowed for simplification of the following experiments. The possibility that only tissue-culture effects influenced *Nmdh* expression can be ruled out, because transformants with near-wild-type activities (i.e. pseudo-wild-type regenerants) showed the same leaf- and age-dependent pattern of NADP-MDH capacities as the wild-type plants. For individual transformants that showed either of the two extremes of stable *Nmdh* expression (Fig. 3B), correlation with the respective mRNA and protein contents was additionally confirmed by gel-blot analyses (Fig. 4). In strong NADP-MDH overexpressors (≥5-fold of the wild-type) a 45-kD band was reproducibly immunodetected on protein blots that could reflect precursor-polypeptide accumulation in the cytosol. In a different study efficient uptake and processing of NADP-MDH from a C_4 plant (*S. bicolor*) was observed in transgenic tobacco plants with up to 2-fold-enhanced enzyme levels (Gallardo et al., 1995).

The main interest of this work, in addition to the characterization of some genetic aspects of the transformants and of the effects on *Nmdh* expression levels, was to analyze the physiological consequences caused by altered NADP-MDH capacities in the mutant plants. The requirement for a minimal amount of this enzyme was already evident from the initial transformant screen, since a reduction to less than 5 to 7% of the wild type was not observed (Table I). Furthermore, in the selfed progeny of line L18 activities beyond this level were never observed in strongly cosuppressed individuals (Table IV). Possibly, this level defines a threshold of NADP-MDH activity needed for plant viability under the given growth conditions. Similar results were obtained upon expression of a homologous *Nmdh* antisense construct in potato. Transformants with NADP-MDH activity of less than 10% of the wild-type levels were not found (B. Müller-Röber, personal communication).

As a first approach toward a physiological analysis, the effect of altered *Nmdh* expression on plant growth was studied. The analysis focused on selected T_1 and T_2 lines (namely L6, L12, L18, P8, P14, and P46), which showed the highest numbers of stable over- or underexpressing individuals. The NADP-MDH levels in these lines ranged between 10% and 6-fold of the wild-type level. In all lines analyzed a correlation between plant growth and NADP-MDH levels was observed under both near-natural (greenhouse; Fig. 5) and climate-controlled (growth chamber; Fig.

6) conditions. The curve fit of the dry weight data shown in Figure 5 shows that the overexpressors developed (i.e. grew and aged) faster, whereas the growth of the underexpressors was retarded.

To this end, the exact nature of the interactions between NADP-MDH and plant growth remains unclear. For example, higher stromal NADP-MDH contents can lead to elevated export rates of reducing equivalents into the cytosol (Krömer, 1995). Malate can either be used for cytosolic NADH production, as required for nitrate reduction, or for mitochondrial ATP production to drive cytosolic Suc synthesis. The altered enzyme-activation states (Table IV indicate that the NADPH/NADP ratio must be higher in the chloroplast stroma of the underexpressors and considerably lower in the overexpressing plants. This is probably caused by altered rates of malate formation and export. An optimized ATP/NADPH ratio in the chloroplast stroma is one possibility to explain the positive effect of increased NADP-MDH activity, whereas a limitation of malate formation in underexpressors seems to retard plant growth. One possibility is that in *Nmdh*-underexpressing lines the activation states of other redox-modulated chloroplast enzymes are also affected. Fru-1,6-bisphosphatase is highly sensitive to less favorable stromal redox states (Holtgrefe et al., 1997).

Our search for how altered malate-valve capacities might influence the growth of tobacco plants is further complicated by the complex pattern of *Nmdh* expression observed within wild-type plants (Fig. 2). These findings are in accordance with previously published results (Merlo et al., 1993) and indicate that altered *Nmdh* expression in the mutant plants has possibly a more pronounced effect on young, expanding leaves. Here the expression of enzymes such as PEP carboxylase and nitrate reductase is increased, whereas the activities of key enzymes of the Calvin cycle are low (Vivekanandan and Edwards, 1987). In young leaves light energy is predominantly used for anabolic processes such as amino acid synthesis. Moreover, the structural differences between leaves at the various developmental stages might even affect the composition of thylakoid membranes. The chlorophyll-fluorescence characteristics of young leaves often point to effects of photoinhibition, even under low light (Guenther and Melis, 1990). This may indicate that in immature chloroplasts very little capacity is available to adapt light absorption through xanthophyll cycles and chlorophyll-fluorescence-quenching mechanisms. In this situation the increased availability of stromal acceptors might be an advantage, which would be in accordance with the finding that the expression of enzymes involved in the ascorbate-dependent detoxification of O_2 radicals is high in young tobacco leaves (Polle, 1996).

In conclusion, it is obvious that in the transgenic plants described in this study the increase in NADP-MDH capacity correlates with a temporally enhanced growth rate. To understand how this is brought about, more detailed studies are necessary. In particular, the developmental and environmental aspects of NADP-MDH requirements must be considered.

ACKNOWLEDGMENTS

The authors are grateful to Dr. W. Reng (Institut für Biophysik und Physikalische Biochemie, Universität Regensburg, Germany) for providing the pea *Nmdh*-cDNA clones, to the laboratory of Prof. M.J. Chrispeels (Department of Biology, University of California San Diego, La Jolla) for the donation of tobacco seeds, to Dr. A. Rodrigues-Franco (Facultad de Ciencias, Universidad de Cordoba, Spain) for communicating the tobacco seed-sterilization protocol, and to Dr. B. Müller-Röber (Max-Planck-Institut für Molekulare Pflanzenphysiologie, Golm, Germany) for sharing results before publication. The authors would also like to thank K. Jäger and the staff of the Botanical Garden in Osnabrück, Germany, for their help in growing the plant material.

Received April 7, 1997; accepted July 14, 1997.
Copyright Clearance Center: 0032-0889/97/115/0705/11.

LITERATURE CITED

Arnon DI (1949) Copper enzymes in isolated chloroplasts. Polyphenoloxidase in *Beta vulgaris*. Plant Physiol **24:** 1–15

Backhausen JE, Kitzmann C, Scheibe R (1994) Competition between electron acceptors in photosynthesis: regulation of the malate valve during CO_2 fixation and nitrite reduction. Photosynth Res **42:** 75–86

Bradford MM (1976) A rapid and sensitive method for the quantitation of microgram quantities of protein utilizing the principle of protein-dye binding. Anal Biochem **72:** 248–254

Champigny ML (1995) Integrations of photosynthetic carbon and nitrogen metabolism in higher plants. Photosynth Res **46:** 117–127

Davies DD (1986) The fine control of cytosolic pH. Physiol Plant **67:** 702–706

Deblaere R, Bytebier B, De Greve H, Debroeck F, Schell J, van Montagu M, Leemans J (1985) Efficient octopine Ti plasmid-derived vectors of *Agrobacterium* mediated gene transfer to plants. Nucleic Acids Res **13:** 4777–4788

Dellaporta SL, Wood J, Hicks JB (1983) A plant DNA minipreparation: version II. Plant Mol Biol Rep **1:** 19–21

Denecke J, Botterman J, Deblaere R (1990) Protein secretion in plants can occur *via* a default pathway. Plant Cell **2:** 51–59

Edwards GE, Nakamoto H, Burnell JN, Hatch MD (1985) Pyruvate, P_i dikinase and NADP-malate dehydrogenase in C_4 photosynthesis: properties and mechanism of light/dark regulation. Annu Rev Plant Physiol **36:** 255–286

Elkind Y, Edwards R, Mavandad M, Hedrick SA, Ribak O, Dixon RA, Lamb CJ (1990) Abnormal plant development and down-regulation of phenylpropanoid biosynthesis in transgenic tobacco containing a heterologous phenylalanine ammonia-lyase gene. Proc Natl Acad Sci USA **87:** 9057–9061

El-Shora H, ap Rees T (1991) Intracellular location of $NADP^+$ linked malic enzyme in C_3 plants. Planta **185:** 362–367

Gallardo F, Miginiac-Maslow M, Sangwan RS, Decottignies P, Keryer E, Dubois F, Bismuth E, Galvez S, Sangwan-Norreel B, Gadal P, and others (1995) Monocotyledonous C_4 $NADP^+$-malate dehydrogenase is efficiently synthesized, targeted to chloroplasts and processed to an active form in transgenic plants of the C_3 dicotyledon tobacco. Planta **197:** 324–332

Gerhardt R, Heldt HW (1984) Measurement of subcellular metabolite levels in leaves by fractionation of freeze-stopped material in nonaqueous media. Plant Physiol **75:** 542–547

Gietl C (1992) Malate dehydrogenase isoenzymes: cellular locations and role in the flow of metabolites between the cytoplasm and cell organelles. Biochim Biophys Acta **1100:** 217–234

Graeve K, von Schaewen A, Scheibe R (1994) Purification, characterisation, and cDNA sequence of glucose-6-phosphate dehydrogenase from potato (*Solanum tuberosum* L.). Plant J **5:** 353–361

Guenther JE, Melis A (1990) The physiological significance of photosystem II heterogeneity in chloroplasts. Photosynth Res **23:** 105–109

Heber U (1974) Metabolite exchange between chloroplasts and cytoplasm. Annu Rev Plant Physiol **25:** 393–421

Heineke D, Kruse A, Flügge UI, Frommer WB, Riesmeier JW, Willmitzer L, Heldt HW (1994) Effect of antisense repression of the chloroplast triose-phosphate translocator on photosynthetic metabolism in transgenic potato plants. Planta **193:** 174–180

Heineke D, Riens B, Grosse H, Hoferichter P, Peter U, Flügge UI, Heldt HW (1991) Redox transfer across the inner chloroplast envelope membrane. Plant Physiol **95:** 1131–1137

Höfgen R, Willmitzer L (1988) Storage of competent cells for *Agrobacterium* transformation. Nucleic Acids Res **16:** 9877

Höfte H, Faye L, Dickinson C, Herman EM, Chrispeels MJ (1991) The protein-body proteins phytohemagglutinin and tonoplast intrinsic protein are targeted to vacuoles in leaves of transgenic tobacco. Planta **184:** 431–437

Holtgrefe S, Backhausen JE, Kitzmann C, Scheibe R (1997) Regulation of steady-state photosynthesis in isolated intact chloroplasts under constant light: responses of carbon fluxes, metabolite pools and enzyme-activation states to changes of the electron pressure. Plant Cell Physiol (in press)

House CM, Anderson JW (1980) Light-dependent reduction of nitrate by pea chloroplasts in the presence of nitrate reductase and C_4 dicarboxylic acids. Phytochemistry **19:** 1925–1930

Jørgensen R (1991) Silencing of plant genes by homologous transgenes. AgBiotech News Info **4:** 265–273

Kilby NJ, Leyser HMO, Furner IJ (1992) Promoter methylation and progressive transgene inactivation in *Arabidopsis*. Plant Mol Biol **20:** 103–112

Krömer S (1995) Respiration during photosynthesis. Annu Rev Plant Physiol Plant Mol Biol **46:** 45–70

Laemmli UK (1970) Cleavage of structural proteins during the assembly of the head of bacteriophage T4. Nature **227:** 680–685

Lance C, Rustin P (1984) The central role of malate in plant metabolism. Physiol Veg **22:** 625–641

Lee RB (1980) Sources of reductant for nitrate assimilation in non-photosynthetic tissue: a review. Plant Cell Environ **3:** 65–90

Lepiniec L, Vidal J, Chollet R, Gadal P, Crétin C (1994) Phosphoenolpyruvate carboxylase: structure, regulation and evolution. Plant Sci **99:** 111–124

Logemann J, Schell J, Willmitzer L (1987) Improved method for the isolation of RNA from plant tissue. Anal Biochem **163:** 16–20

Masle J, Hudson GS, Badger MR (1993) Effects of ambient CO_2 concentration on growth and nitrogen use in tobacco (*Nicotiana tabacum*) plants transformed with an antisense gene to the small subunit of ribulose-1,5-bisphosphate carboxylase/oxygenase. Plant Physiol **103:** 1075–1088

Matzke MA, Matzke AJM, Eggleston WB (1996) Paramutation and transgene silencing: a common response to invasive DNA? Trends Plant Sci **1:** 382–388

Melzer E, O'Leary MH (1987) Anapleurotic CO_2 fixation by phosphoenolpyruvate carboxylase in C_3 plants. Plant Physiol **84:** 58–60

Merlo L, Ferretti M, Ghisi R, Passera C (1993) Developmental changes of enzymes of malate metabolism in relation to respiration, photosynthesis and nitrate assimilation in peach leaves. Physiol Plant **89:** 71–76

Meyer P (1995) Understanding and controlling transgene expression. Trends Biotechnol **13:** 332–337

Nellen W, Lichtenstein C (1993) What makes an mRNA antisense-itive? Trends Biochem Sci **18:** 419–423

Paul MJ, Knight JS, Habash D, Parry MAJ, Lawlor DW, Barnes SA, Loynes A, Gray JC (1995) Reduction in phosphoribulokinase activity by antisense RNA in transgenic tobacco: effect on CO_2 assimilation and growth in low irradiance. Plant J **7:** 535–542

Polle A (1996) Developmental changes of antioxidative systems in tobacco leaves as affected by limited sucrose export in transgenic plants expressing yeast-invertase in the apoplastic space. Planta **198:** 253–262

Price GD, Evans JR, von Caemmerer S, Yu J-W, Badger MR (1995) Specific reduction of chloroplast glyceraldehyde-3-phosphate dehydrogenase activity by antisense RNA reduces CO_2 assimilation via a reduction in ribulose bisphosphate regeneration in transgenic tobacco plants. Planta **195:** 369–378

Raghavendra AS, Padmasree K, Saradadevi K (1994) Interdependence of photosynthesis and respiration in plant cells: interactions between chloroplasts and mitochondria. Plant Sci **97:** 1–14

Reng W, Riessland R, Scheibe R, Jaenicke R (1993) Cloning, site-specific mutagenesis, expression and characterisation of full-length chloroplast NADP-malate dehydrogenase from *Pisum sativum*. Eur J Biochem **217:** 189–197

Riesmeier JW, Flügge UI, Schulz B, Heineke D, Heldt HW, Willmitzer L, Frommer WB (1993) Antisense repression of the chloroplast triose phosphate translocator affects carbon partitioning in transgenic potato plants. Proc Natl Acad Sci USA **90:** 6160–6164

Sambrook J, Fritsch EF, Maniatis PJ (1989) Molecular Cloning: A Laboratory Manual, Ed 2. Cold Spring Harbor Laboratory Press, Cold Spring Harbor, NY

Scheibe R (1987) $NADP^+$-malate dehydrogenase in C_3 plants: regulation and role of a light-activated enzyme. Physiol Plant **71:** 393–400

Scheibe R, Fickenscher K, Ashton AR (1986) Studies on the mechanism of the reductive activation of NADP-malate dehydrogenase by thioredoxin$_m$ and low-molecular-weight thiols. Biochim Biophys Acta **870:** 191–197

Scheibe R, Stitt M (1988) Comparison of NADP-malate dehydrogenase activation, Q_A reduction and O_2 evolution in spinach leaves. Plant Physiol Biochem **26:** 473–481

Skerra A (1989) Funktionelle Expression Antigen-bindender Immunglobulinfragmente in *Escherichia coli*. PhD thesis. Ludwig-Maximilians-Universität, Munich, Germany

Smirnoff N, Stewart GR (1985) Nitrate assimilation and translocation by higher plants: comparative physiology and ecological consequences. Physiol Plant **64:** 133–140

Trevanion SJ, Furbank RT, Ashton AR (1997) NADP-malate dehydrogenase in the C_4 plant *Flaveria bidentis*. Cosense suppression of activity in mesophyll and bundle-sheath cells and consequences for photosynthesis. Plant Physiol **113:** 1153–1165

Vivekanandan M, Edwards GE (1987) Leaf development and the role of NADP-malate dehydrogenase in C_3 plants. Photosynth Res **14:** 125–135

Voelker T, Sturm A, Chrispeels MJ (1987) Differences in expression between two seed lectin alleles obtained from normal and lectin-deficient beans are maintained in transgenic tobacco. EMBO J **6:** 3571–3577

von Schaewen A, Langenkämper G, Graeve K, Wenderoth I, Scheibe R (1995) Molecular characterization of the plastidic glucose-6-phosphate dehydrogenase from potato in comparison to its cytosolic counterpart. Plant Physiol **109:** 1327–1335

Winter H, Robinson DG, Heldt HW (1994) Subcellular volumes and metabolite concentrations in spinach leaves. Planta **193:** 530–535

Eur. J. Biochem. **265**, 231–239 (1999) © FEBS 1999

Isolation, characterization and cDNA cloning of nicotianamine synthase from barley

A key enzyme for iron homeostasis in plants

A. Herbik*, G. Koch, H.-P. Mock, D. Dushkov, A. Czihal, J. Thielmann, U. W. Stephan and H. Bäumlein

Institut für Pflanzengenetik und Kulturpflanzenforschung (IPK), Gatersleben, Germany

Basic cellular processes such as electron transport in photosynthesis and respiration require the precise control of iron homeostasis. To mobilize iron, plants have evolved at least two different strategies. The nonproteinogenous amino acid nicotianamine which is synthesized from three molecules of *S*-adenosyl-L-methionine, is an essential component of both pathways. This compound is missing in the tomato mutant *chloronerva*, which exhibits severe defects in the regulation of iron metabolism. We report the purification and partial characterization of the nicotianamine synthase from barley roots as well as the cloning of two corresponding gene sequences. The function of the gene sequence has been verified by overexpression in *Escherichia coli*. Further confirmation comes from reduction of the nicotianamine content and the exhibition of a *chloronerva*-like phenotype due to the expression of heterologous antisense constructs in transgenic tobacco plants. The native enzyme with an apparent M_r of $\approx$ 105 000 probably represents a trimer of *S*-adenosyl-L-methionine-binding subunits. A comparison with the recently cloned *chloronerva* gene of tomato reveals striking sequence homology, providing support for the suggestion that the destruction of the nicotianamine synthase encoding gene is the molecular basis of the tomato mutation.

Keywords: antisense constructs; *chloronerva* mutation; gene isolation; *Hordeum vulgare*; iron metabolism.

Iron is essential for fundamental cellular processes such as electron transfer in photosynthesis, respiration, nitrogen fixation as well as DNA synthesis [1]. Excessive accumulation causes severe damage to cellular components due to the formation of highly reactive hydroxyl radicals by the Fenton reaction [2]. Thus, the precise control of iron homeostasis is a basic prerequisite for cellular function. According to WHO data the health of more than three billion people worldwide is affected by iron deficient diet. Crop plants with a higher iron content, for example in the endosperm of cereals, could contribute to the improvement of this situation. In soil iron is mainly found as stable Fe(III) compounds with low solubility at neutral pH [1,3]. Therefore, plants have evolved special mechanisms of iron acquisition, classified into two strategies [4]. Strategy I plants, including dicots and nongraminaceous monocots, facilitate iron uptake mainly by increased acidification of the rhizosphere due to enhanced proton extrusion and the reduction of Fe(III) to Fe(II) by an inducible plasma membrane-bound reductase. In contrast, graminaceous monocots (strategy II plants) release phytosiderophores of the mugineic acid family into the rhizosphere. These compounds act as chelators of ferric ions and are taken up by root cells as Fe(III)-phytosiderophore complexes.

The nonproteinogenous amino acid nicotianamine (NA) is found in all multicellular plants [5] and is considered to be a key component for both strategies of iron acquisition (Fig. 1). In strategy I plants NA might function as a chelator of iron in symplastic and phloem transport [6] and in copper mobilization for xylem transport [7]. A similar role of NA is assumed for strategy II plants. Recently it was demonstrated that NA chelates both Fe(III) and Fe(II); these complexes are poor Fenton reagents, suggesting a role of NA in protecting cells from oxidative damage [8]. In addition, in strategy II plants NA was shown to be a precursor for the biosynthesis of phytosiderophores of the mugineic acid family [9]. In contrast to strategy II plants, the NA synthase (NAS) activity is not enhanced under iron deficiency in strategy I plants [10–12] suggesting that NAS activity is differently regulated in strategy I and II plants. Nevertheless, NAS is a highly important enzyme for the regulation of the iron metabolism in both strategy I and II plants.

The only plant known to lack NA is the tomato mutant *chloronerva* which is characterized by severe disturbance of iron metabolism. It exhibits intercostal chlorosis of young leaves, retarded growth of roots and shoots, excessive root branching and permanently activated strategy I reactions, such as thickened root tips, increased density of root hairs, enhanced proton extrusion and a highly active plasmalemma-bound

Correspondence to H. Bäumlein, Institut für Pflanzengenetik und Kulturpflanzenforschung (IPK), Corrensstr. 3, Gatersleben, D-06466, Germany. Fax: +49 39 482 5500, Tel.: +49 39 482 5238, E-mail: baumlein@ipk-gatersleben.de

Abbreviations: ACC, 1-aminocyclopropane-1-carboxylic acid; NA, nicotianamine; NAS, nicotianamine synthase; RACE, rapid amplification of cDNA ends; ORF, open reading frame; AdoMet, *S*-adenosyl-L-methionine; E-64, trans-eposysuccinyl-L-leucylamido(4-guanidino)-butan.

Enzymes: 1-aminocyclopropane-1-carboxylic acid synthase (EC 4.4.1.14).

**Present* address: Humboldt Universität zu Berlin, AG Angewandte Botanik, Invalidenstr. 42, D-10115 Berlin, Germany.

Dedication: this paper is dedicated to Dr Günther Scholz, Gatersleben, who initiated this field of research.

Note: the nucleotide sequence data reported in this paper have been deposited in the EMBL data bank and are accessible under the accession numbers AF136941 for NASHOR1 and AF136942 for NASHOR2.

(Received 12 May 1999, revised 9 July 1999, accepted 14 July 1999)

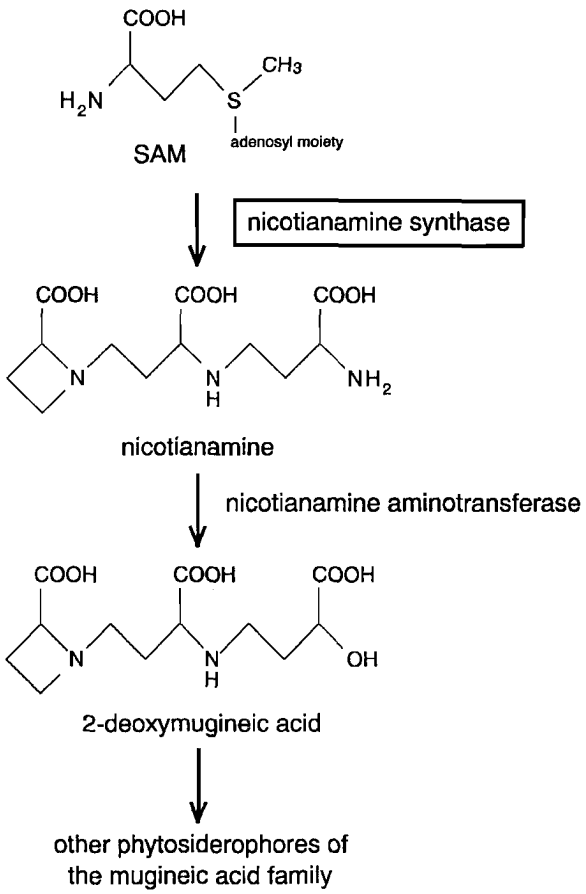

Fig. 1. The position of NA synthase and NA in the biochemical pathway leading to the phytosiderophores of the mugineic acid family.

ferrireductase. In spite of these features as an iron-deficient plant, this mutant accumulates iron in roots and shoots [13]. In addition, dramatic changes in the expression of downstream genes [11,14,15] has been observed. This pleiotropic phenotype is known as 'apparent iron deficiency syndrome'. Exogenous application of NA leads to phenotypic normalization [16,17]. Obviously, NA as well as NAS are essential components of the regulation of iron uptake mechanisms in multicellular plants.

Here we report the purification and biochemical characterization of NAS as well as the cloning of two corresponding cDNA sequences from barley. The derived amino acid sequences suggest that NAS represents a new class of enzymes. The data confirm and further extend the conclusions independently drawn by Higuchi *et al.* [18].

MATERIALS AND METHODS

Plant material

Fe-deficient seedlings of *Hordeum vulgare* L. cv. 'Bonus' were cultured under controlled conditions as described by Stephan and Procházka [19]. Wild-type plants of *Nicotiana tabaccum* L. cv. 'Petit Havanna' were used for transformation. Genomic DNA was isolated from *Arabidopsis thaliana* L. cv. 'Columbia'.

Purification of NAS

Plant material (800 g of iron deficient barley roots) was ground in liquid nitrogen and extracted in the buffer system described by Shojima *et al.* [9] supplemented with 0.2% BSA (w/v), 0.2% casein (w/v) and 10 μM trans-eposysuccinyl-L-leucylamido (4-guanidino)-butan (E-64). After centrifugation (16 000 *g*, 8 min) the supernatant was brought to 60% saturation with ammonium sulphate and centrifuged (25 000 *g*, 10 min). The resulting precipitate was dissolved in incubation buffer containing 50 mM Tris, 1 mM EDTA, 3 mM dithiothreitol, 500 μM methionine, 500 μM ATP and 10 μM E-64 (pH 8.7) and dialysed extensively against buffer A (50 mM Tris, 1 mM EDTA, 3 mM dithiothreitol, 50 μM methionine, pH 8.7). The sample was adjusted to 20% ammonium sulphate saturation and centrifuged. The supernatant was subjected to hydrophobic interaction chromatography on a Butyl-Toyopearl 650M column (Tosohaas, Stuttgart, Germany) equilibrated with 25% ammonium sulphate in buffer A. Bound proteins were eluted by decreasing the ammonium sulphate concentration. Fractions containing NAS activity were dialysed against buffer A, concentrated (Centricon; Millipore) and loaded onto an ion-exchange column (DEAE-Sephacel; Pharmacia) equilibrated with buffer A. Elution of bound proteins was achieved by gradient elution with 0.5 M NaCl in buffer A. Further purification of NAS was achieved by repetition of hydrophobic interaction chromatography on a small-scale column and ion-exchange chromatography on a Resource Q column (Pharmacia). NAS was purified on a Econo-Pac HTP column (BioRad) equilibrated with buffer A adjusted to pH 5.5. Samples were brought to pH 5.5 prior to loading by a buffer exchange on PD 10 columns (Pharmacia). Elution of NAS was performed by application of a gradient of up to 1 M potassium phosphate in buffer A (pH 8.7). All collected fractions were immediately adjusted to pH 8.7 to minimize loss of NAS activity. Finally, NAS was purified further by gel filtration on a Superdex 200 HR 30/10 column (Pharmacia). Further details of the purification procedure have been described previously [12].

NAS activity assay and determination of NA concentration

For the NAS activity assay, *S*-adenosyl-L-[carboxyl-^{14}C] methionine (Amersham) was added to the enzyme solution (final concentration 20 μM) and incubated in incubation buffer (see above) for 5 min at 30 °C. The reaction was stopped by adding MeOH to a final concentration of 50%, centrifuged (15 000 *g*, 10 min), and 1 μL of the supernatant as well as 5 μL of 1 mM nonlabelled NA was spotted onto silica gel thin layer plates (Fluka Chemie AG, Buchs, Switzerland). The plates were developed with 1-propanol/water (7 : 8). Nonlabelled NA was stained with ninhydrin and the synthesized [^{14}C]NA was quantified by a Bio-Imaging Analyser BAS 2000 [12].

For the determination of the NA concentration plant material was crushed in liquid nitrogen. The powder was mixed with water and the resulting pulp was submitted to Potter–Elvehjem homogenization after thawing. The homogenate was stirred (1 h) and deproteinized by heating to 80 °C. After centrifugation (20 min, 48 000 *g*) the supernatant was concentrated in a vacuum evaporator at 40 °C and lyophilized. The lyophylisate was dissolved in 0.2 M Na-citrate buffer pH 3.05. The NA concentration was determined after postcolumn derivatization with ninhydrin at 570 nm using an amino acid analyser (Model S 432, Sykam GmbH, Gilching, Germany) as described previously [6].

Iron determination

Plant material was dried at 105 °C and treated in 65% HNO_3 Suprapure grade (Merck) at 170 °C. The iron concentration was

measured with the atomic absorption spectrometer model SpectrAA 10 Plus (Varian Australia, Pty. Ltd, Mulgrave, Victoria, Australia) as described by Schmidke and Stephan [6].

Crosslinking of NAS and [^{14}C] *S*-adenosyl-L-methionine (AdoMet)

The crosslinking of NAS with [^{14}C]AdoMet was performed as described by Subbaramaiah and Simms [20]. Purified NAS (20 μg) was incubated with 40 μM [^{14}C]AdoMet in a total volume of 100 μL at 30 °C and illuminated with UV light (254 nm) for 10, 20 and 30 min. After exposure the proteins were separated on a denaturing gel, dried and the radioactivity was detected by the Bio-Imaging BAS 2000.

Protein electrophoresis and size determination of the native enzyme

Protein concentrations were determined using the Bradford assay. PAGE on mini gels was performed according to Laemmli [21] and the gels were stained with Coomassie blue. To estimate the mass of the active native enzyme, purified barley extract and *E. coli* extracts were used for gel filtration (Superdex HR 30/10) relative to defined size markers (Sigma).

Peptide sequencing

Internal polypeptide cleavage was performed with trypsin as described by Jenö *et al.* [22]. The peptide fragments were separated on a Hypersil BDS column (RP18) and sequenced according to a standard protocol for the HPLC-System 'Gold' (Beckman).

Rapid amplification of cDNA ends (RACE)

Based on an internal peptide sequence (QFLAPIVDP) of the putative NAS protein, the corresponding primer oligonucleotide K21271 (5′-CARTTYYTNGCNCCNATHGTNGAYCC-3′) was synthesized (Biometra) and used in combination with the anchor primer (Biometra) to amplify a 0.6-kb fragment. The Titan One Tube RT/PCR system (Boehringer) was used for amplification. Using the TOPO TA Cloning Kit (Invitrogen) the fragment was cloned into the vector pCR2.1.

Isolation and sequencing of cDNA clones

The 600 bp fragment obtained by 3′RACE was labelled using the Megaprime labelling kit (Amersham) and used as hybridization probe for the screening of a seed-specific barley cDNA library established in the λZIP Lox^{TM} vector (Gibco). The library was kindly provided by W. Weschke, IPK Gatersleben. Standard techniques for restriction enzyme digestion, cloning and library screening were used [23]. DNA sequences were determined using an ALF Sequencer (Pharmacia LKB) and the Autoread Sequencing Kit (Pharmacia). The software packages PC/GENE (Intelligenetics) and LASERGENE (DNASTAR, Inc.) were used for general sequence processing.

Expression in *E. coli*

The complete cDNA of barley NAS was reamplified using specific *Bam*HI sites containing primers and the Expand High Fidelity DNA Polymerase (Boehringer). After *Bam*HI digestion, the resulting fragment was cloned in both orientations into the *Bam*HI site of the expression vector pET12a (Novagen). The gene product was synthesized in the *E. coli* expression strain 174 (DE3).

Generation and analysis of tobacco antisense and sense plants

The NAS-like gene sequence on *Arabidopsis* chromosome 1 was amplified by PCR from genomic *Arabidopsis* DNA using the following *Bam*HI site-containing primers AR1 (N-terminal sense): 5′-CCGCCGGATCCATGGGTTGCCAAGACGAACAATTGGTGCAAAC-3′ and AR2 (C-terminal antisense): 5′-CCGCCGGATCCCGTCCTCCTTAAGACAACTGTTCC-3′ and the proof reading polymerase of the Expand High Fidelity PCR System (Boehringer Mannheim). The resulting *Bam*HI fragments were cloned in both orientations in the binary vector BinAR19 [24,25]. The leaf disc method was used for *Agrobacterium*-mediated transformation as described previously [26]. The presence of the transgene construct in independent tobacco lines was confirmed by PCR. The NA and iron contents were determined in young plants with 3–4 expanded leaves.

RESULTS

Purification and characterization of NAS from iron-deficient barley roots

Iron deficiency conditions resulted in ≈ fivefold increase of NAS activity in total barley roots (data not shown). This confirms previous results of Higuchi *et al.* [27]. Therefore, this material was used as a suitable source for enzyme isolation. Following the purification protocol described the enzyme was enriched 140-fold. The resulting single protein peak precisely coincided with the peak of enzyme activity. The pH optimum of the purified enzyme was pH 9.0, in close agreement with the data of Higuchi *et al.* [27]. Substrate saturation curves revealed maximum reaction velocity between 20 μM and 30 μM [^{14}C]AdoMet and an inhibitory effect of higher concentrations [12]. This inhibition is probably due to the instability of the AdoMet and its contamination with degradation products, such as *S*-adenosyl-homocystein, L-homocystein, 5-deoxy-methylthioadenine and the two diastereomers [28]. Due to the inhibition of NAS by its substrate degradation products, the K_m value of 6.9 μM AdoMet is an approximation.

SDS/PAGE of the purified active protein fraction consistently revealed the presence of three polypeptides with

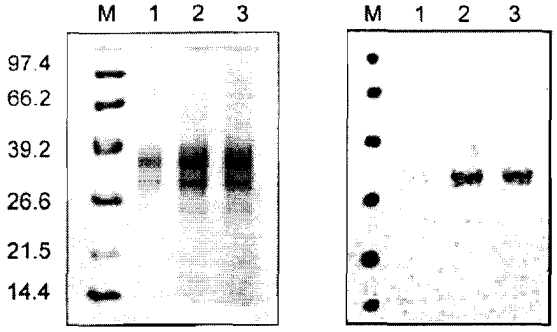

Fig. 2. (A) Electrophoretic separation of the proteins in the purified barley root extract, and (B) autoradiography after UV-cross linking with [^{14}C]-AdoMet. M, Molecular mass standard; 1–3, incubation times of 10, 20 and 30 min at 254 nm, respectively.

molecular weights of 24, 28 and 38 kDa (Fig. 2). The amount of the 24-kDa polypeptide was not sufficient for sequencing. The four internal peptides derived from the 38-kDa polypeptide showed some homology to a hypothetical gene found on the BAC clone T02004 of *A. thaliana*, which exhibits a 50% similarity to myrosinase-associated proteins. The four internal sequences derived from the 28-kDa polypeptide originally did not show obvious homology to any sequence in the database.

Both NAS and 1-aminocyclopropane-1-carboxylic acid (ACC) synthase, an important enzyme involved in ethylene biosynthesis, require AdoMet as substrate and pyridoxalphosphate as a coenzyme. When the enzyme is catalytically active, a highly reactive vinylglycine intermediate was found to be covalently linked to the active site of the ACC synthase [29]. Because of the similarity between ACC and azetidine-2-carboxyl acid, a component of NA, a photo affinity labelling experiment with [^{14}C]AdoMet was performed. The 28-kDa polypeptide was the only one which could be labelled by UV cross linking, suggesting that this polypeptide binds AdoMet as it would be expected for NAS (Fig. 2).

Tryptic digestion of the 28-kDa polypeptide and microsequencing of the resulting peptides revealed the following amino acid sequences: LEYELLAA, LEFEVLAVH, SFLYPIVDPEEI and QFLAPIVDP. The corresponding oligonucleotide primer was derived from the latter peptide sequence.

```
      *.    ...      . .*... .* ..*..* .*.** .*..**..** .*.*... .*
ARA1  MG----CQD------EQLVQTICDLYEKISKLESLKPSEDVNILFKQLVSTCIPPNPNID  50
ARA5  MA----CQN------NLVVKQIIDLYDQISKLKSLKPSKNVDTLFGQLVSTCLPTDTNID  50
HOR1  MDAQN-------KEVDALVQKITGLHAAIAKLPSLSPSPDVDALFTDLVTACVPPSP-VD  52
HOR2  MGMEGCCSNKKVMEEEALVKKITGLAAAIGELPSLSPSPEVNALFTELVTSCIPPST-VD  59
LYC1  MV----CPNS-----NPVVEKVCELYEQISRLENLSPSKDVNVLFTDLVHTCMPPNP-ID  50

MET1  MS---CYIYWD--KIKRIASRLEGMNYHFDEMDT----SGVMPLLDEIEEIAHDSTIDFE  51
      *    .           . . .  . .. .. * *.  .. . ..    .

      *...   ....* .**   ..*. *** **.*.*..*.. .    **.** .***..**.
ARA1  VTKMCDRVQEIRLNLI---KICGLAEGHLENHFSSILTSYQDN--PLHHLNIFPYYNNYL 105
ARA5  VTNMCEEVKDMRANLI---KLCGEAEGYLEQHFSTILGSLQEDQNPLDHLHIFPYYSNYL 107
HOR1  VTKLGSEAQEMREGLI---RLCSEAEGKLEAHYSDMLAAFDN---PLDHLGMFPYYSNYI 106
HOR2  VDALGPDAQEMRARLI---RLCADAEGHLEAHYSDLLAAHDN---PLDHLTLFPYFNNYI 113
LYC1  VSKLCQKIQEIRSHLI---KLCGQAEGLLESHFSKILSSYE---NPLQHLHIFPYFDNYI 104

MET1  SAKHILDDAEMNHALSLIRKFYVNLGMKLEMEKAQEVI---ESDSPWETLRSFYFYPRYL 108
      . .     ....  *.   ...  ... ** . .  .        *. .*  *... .*

      .*. ** ..*..   .   *...**.****.* .* ***. ** .. *.*.*. . **
ARA1  KLGKLEFDLLEQNLNG~FVPKSVAFIGSGPLPLTSIVLASFHLKDTIFHNFDIDPSANSL 164
ARA5  KLGKLEFDLLSQH-SS~HVPTKIAFVGSGPMPLTSIVLAKFHLPNTTFHNFDIDSHANTL 165
HOR1  NLSKLEYELLARYVPGRHRPARVAFIGSGPLPFSSYVLAARHLPDAMFDNYDLCSAANDR 166
HOR2  KLSQLEHGLLARHVPGPA-PARVAFLGSGPLPLSSLVLAARHLPDASFDNYDISGEANER 172
LYC1  KLSLLEYNILTKN-TT~NIPKKIAFIGSGPLPLTSLVLATKHLKTTCFHNYDIDVDANFM 162

MET1  ELLKNE-AALGRFRRG----ERAVFIGGGPLPLTGILLS--HVYGMRVNVVEIEPDIAEL 161
      .* ..*  .*     .   .  .*.*.**.*... .*.  *.    . . ..   ..

      ** * . * * ..** *.*.*. ..* .*. .*********..*.*.....** . *.
ARA1  ASLLVSSDPDISQRMFFHTVDIMDVTESLKSFDVVFLAALVGMNKEEKVKVIEHLQKHMA 224
ARA5  ASNLVSRDPDLSKRMIFHTTDVLNATEGLDQYDVVFLAALVGMDKESKVKAIEHLEKHMA 225
HOR1  ASKLFRADKDVGARMSFHTADVADLTGELAAYDVVFLAALVGMAAEDKTKVIAHLGAHMA 226
HOR2  ASRLVRADADAGARMAFRTADVADVTTELEGYDVVFLAALVGMAAEEKARLVEHLGRHMA 232
LYC1  ASALVAADPDMSSRMTFHTADVMDVTCALKDYDVVFLAALVGMDKEDKVKVVDHLAKYMS 222

MET1  SRKVIEGLGVDGVNVI---TGDETVIDGLE-FDVLMVAAL----AEPKRRVFRNIHRYVD 213
      .. ..  . .   .. ... .. ...  *  .**...***...  * * ..  ..  ...

       **.*..****.  .****.... ..   **..*.. **.*.*.***.*..*
ARA1  PGAVLMLRSAHGPRAFLYPIVEPCDLQ--GFEVLSIYHPTDDVINSVVISKK-------- 274
ARA5  PGAVLMLRSAHALRAFLYPIVDSSDLK--GFQLLTIYHPTDDVVNSVVIARK-------- 275
HOR1  DGAALVVRSAHGHVGFLYPIVDPQDIGRGGFEVLAVCHPDDDVVNSVIIAHKSKDVH--A 284
HOR2  PGAALVVRSAHGARGFLYPVVDPEEIRRGGFEVLTVHHPEDEVINSVIIARKAAAPPPVA 292
LYC1  PGATLMLRSAHGARAFLYPVLDPRDLR--GFEVLSVYHPTDEVINSVIIARK-------- 272

MET1  TETRIIYRTYTGMRAILYAPVSDDDIT--GFRRAGVVLPSGKVNNTSVLVFK-------- 263
      ... .  *.... ...**. ... .    **... . .* . * *.. .. *

                        .                .* .  *
ARA1  --------HPVVSIGNVGGPNSCLLKP-CNCSKTHAKMN---KNMMIEEFGAREEQLS  320
ARA5  --------LGGPTTPGVNGTRGCMFMP-CNCSKIHAIMNNRGKKNMIEEFSAIE----  320
HOR1  NERPNGVVDSTRGAVPV-VSPPCRF--G---EMVADVTHKR------EEFTNAEVAF-  329
HOR2  ADRDVPVNMPMPAQCAVAVSRPC-L--GCACELGARAHQKM------KEIAMEEMEA-  340
LYC1  --------LPVPSVPLLDGLGAYVLPSKCACAEIHA-FNPLNKMNLVEEFALEE----  317

MET1  ------------------------------CPD-------------------------  266
                      .    .    . .                ...   .
```

Fig. 3. Sequence alignment of the two different barley NA synthases (HOR1 and HOR2) with functionally unknown proteins of *A. thaliana* (ARA1 and ARA5) and the *chloronerva* gene (LYC1) of tomato. Amino acid positions are given at the right. Positions with identical and functionally similar amino acids are indicated as (*) and (.), respectively. The asterisks and points above the alignment represent the similarity among the plant sequences only. The symbols below the alignment additionally include the sequence from *M. thermoautotrophicum* (MET1).

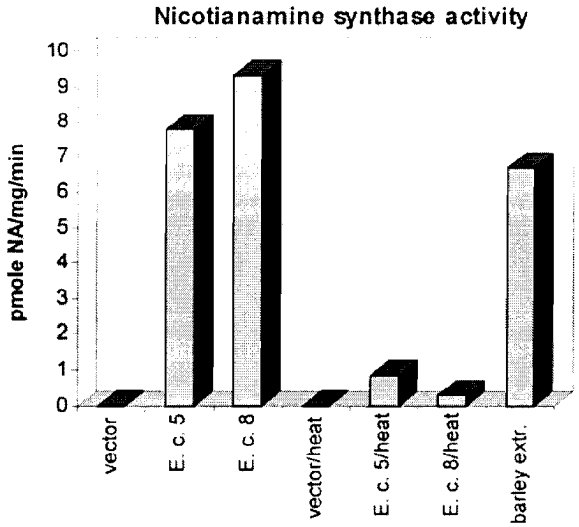

Fig. 4. Expression of the NAS specific cDNA in *E. coli*. The activity is given in pmole NA·mg^{-1}·min^{-1}. Extracts of bacteria carrying the empty expression vector as well as barley extract were used as control. *E. coli* 5 and 8 represent two independent clones (with and without heat denaturation at 100 °C for 5 min).

Cloning and sequence analysis of a putative NAS specific cDNA

To isolate the 28-kDa polypeptide encoding cDNA, the peptide derived oligonucleotide 5′-CARTTYGCNCCNATHGTN-GAYCC-3′ was used for 3′RACE. Total RNA was isolated from barley roots grown under iron deficiency conditions. A 0.6-kb DNA fragment was amplified between the gene-specific primer and the anchor primer. The nucleotide sequence of this fragment predicts an amino acid sequence which includes the N-terminal peptide FLYPIVDPE as well as the subN-terminal peptide FEVLAVH. Both peptides correspond to that derived from peptide sequencing, suggesting that the 0.6-kb sequence represents a partial cDNA fragment specific for the 28-kDa polypeptide.

The 0.6-kb fragment was used to screen a phage library of barley cDNA clones. Several clones have been isolated. The nucleotide sequences of the full-length clone NASHOR1 predicts a polypeptide of 330 amino acid residues and a molecular mass of 35 611 Da [30] and the full-length clone NASHOR2 predicts a polypeptide of 340 amino acids and a molecular mass of 36 312 Da. A third cDNA predicts an amino acid sequence identical to that of NASHOR2 but exhibits minor nucleotide changes in the 5′ and 3′ nontranslated regions. Small differences in the sequences of additional partial cDNA clones suggest the existence of a small multigene family in the barley genome. At least two loci of NAS-like gene sequences were located in the barley genome on chromosome 2H and 6H (V. Korzun, IPK Gatersleben, personal communication). In addition to the recently described NAS genes from barley [18], a database search revealed homology to several anonymous open reading frames (ORFs) found in the genomic DNA of *A. thaliana*. One homologous ORF is present on the BAC clone T12M4 (AC003114) derived from chromosome 1 and another one was found on the P1 clone MDA7 (AB011476) derived from chromosome 5 (Fig. 3). The latter sequence is highly similar but not identical to another ORF on the P1 clone MUG13 (AB005245) also derived from chromosome 5. Finally, a partial similarity could be detected with an ORF on the BAC clone M3E9 (AL022223) derived from the *Arabidopsis* chromosome 4.

Although the databases used included several total bacterial genomes as well as the genome of yeast, a NAS-like sequence was found only in the genome of *Methanobacterium thermoautotrophicum* (gene MTH675 of the complete genome, accession number AE000847).

In addition, the newly described proteins NASHOR1 and NASHOR2 exhibit 46% and 49% similarities at the amino acid sequence level, respectively, to the recently described *chloronerva* gene of tomato [31].

NAS activity in *E. coli*

The 28-kDa protein described was isolated from a NAS active fraction as one of three polypeptides. Moreover, as expected for NAS, it represents the only polypeptide in the fraction which was labelled by crosslinking with AdoMet (see above). For a

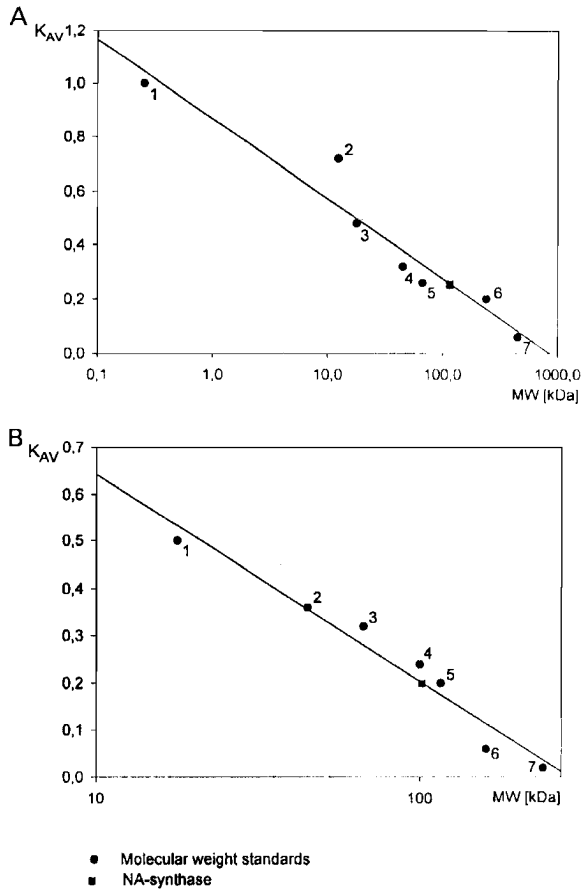

Fig. 5. Apparent molecular mass determination of the native NAS (NASHOR1) of barley. (A) Gel filtration on Superdex HR 30/10 was used on a purified preparation from barley roots. Size standards: 1, DNP-alanine (0.255 kDa); 2, cytochrome *c* (12.4 kDa); 3, myoglobin (17.8 kDa); 4, ovalbumin (45 kDa); 5, BSA (67 kDa); 6, catalase (240 kDa); 7, ferritin (450 kDa). The position of the active fraction is indicated by ■. (B) Gel filtration of purified *E. coli* extract on Superdex HR. Size standards: 1, myoglobin (17.8 kDa); 2, ovalbumin (45 kDa); 3, BSA (67 kDa); 4, hexokinase (100 kDa); 5, β-galactosidase (116 kDa); 6, γ-globulin (150 kDa); 7, catalase (240 kDa). The position of the active fraction is indicated by ■.

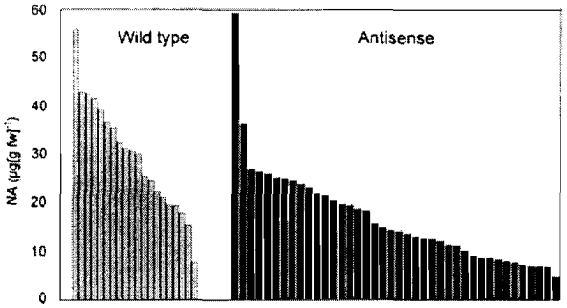

Fig. 6. NA concentrations in transgenic tobacco plants. Forty independent transgenic tobacco lines based on the NASARA1-encoding gene were compared to 20 wild-type plants. The NA concentrations are given in μg·(g fresh weight)$^{-1}$. The NA concentrations in young leaves are significantly (P = 0.001) lower in the antisense plants.

more definite proof that the protein indeed represents the NAS enzyme, the corresponding cDNA was expressed in *E. coli*. As shown in Fig. 4 NAS activity was detected in two independent clones containing the barley cDNA specific for NASHOR1 under the control of the inducible T7lac promoter of the expression vector pET12a. The vector control extracts were inactive. The enzyme activity was strongly reduced by heat treatment. A barley root extract was tested in parallel. Taken together, the data clearly demonstrate that the cloned cDNA represents a NAS of barley.

To determine the native molecular mass of the enzyme, the protein extract was subjected to gel filtration (Fig. 5). The active fraction eluted between the size marker proteins hexokinase with a molecular mass of 100 kDa and β-galactosidase with a molecular mass of 116 kDa. A corresponding experiment was performed with the active NAS purified from barley roots (Fig. 5). Here the active fraction eluted between the size marker proteins BSA (molecular mass 67 kDa) and catalase (240 kDa). In both cases the activity peak eluted at a molecular mass of ≈ 105 kDa. A comparison with the molecular mass predicted from the amino acid sequence suggests that the native enzyme probably acts as a trimer.

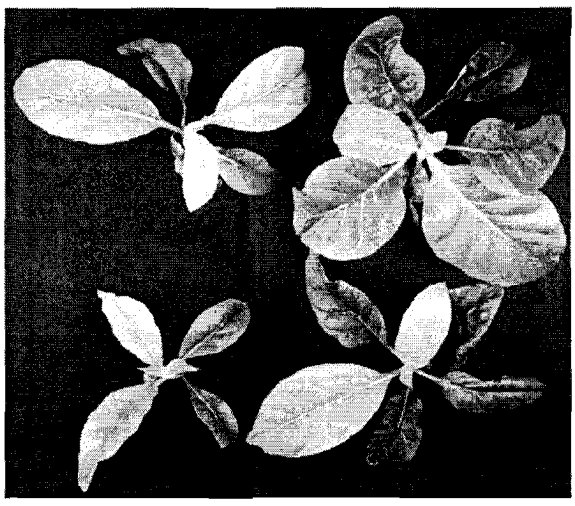

Fig. 7. Phenotype of transgenic tobacco antisense plants. The plants were transformed with an antisense construct based on the NASARA5-encoding gene. Three independent lines and a nontransformed wild-type control plant (above right) grown under the same conditions are shown.

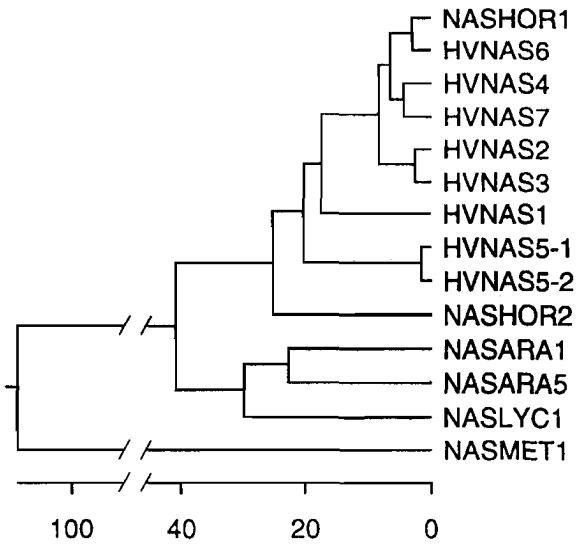

Fig. 8. Dendrogram of known NAS-like sequences. Alignment and distance analysis was performed with the MegAlign tool of the LASERGENE software package (DNASTAR). The branch lengths represent the distance between sequences. The units at the bottom line indicate the number of substitution events.

Analysis of antisense and sense constructs in transgenic tobacco

As an additional test for NAS function antisense and sense constructs of the *Arabidopsis* NASARA1 and NASARA5 encoding genes on chromosome 1 and 5 were transferred into tobacco. The dicot *Arabidopsis* sequences were used to increase the chance for an antisense effect. In total 40 independent transgenic antisense lines were generated with NASARA1. The NA concentrations in these antisense lines were compared with those in 20 nontransformed wild-type plants (Fig. 6). In spite of great variation of the NA concentration in young leaves even in the wild-type the data demonstrate a significant reduction (P = 0.001) of the NA concentration in the antisense plants. Further analyses (data not shown) demonstrated that the iron concentration in leaves of antisense plants (49.8 ± 2.1 μg·g dry weight^{-1}) was significantly higher than in sense plants (37.5 ± 5.2 μg·g dry weight^{-1}). Moreover, we have generated transgenic tobacco lines based on a NASARA5 antisense construct. At least three lines of these antisense plants exhibit a chlorotic *chloronerva*-like phenotype in young leaves (Fig. 7). Wild-type plants as well as control plants carrying the construct in sense orientation do not show the symptoms.

DISCUSSION

Iron is both an essential and a potentially toxic component of all living cells. In plants, disturbances of iron acquisition causes complex deleterious effects, as demonstrated by the tomato mutant *chloronerva*. This mutant lacks the nonproteinogenous amino acid NA. In strategy I plants such as tomato, failure of NA synthesis leads to the permanent activation of iron acquisition processes in roots including proton extrusion and increased ferric chelate reductase activity. Thus, in mutant leaves iron is accumulated to nonphysiologically high concentrations leading to the precipitation of iron in different cell compartments and organelles [32,33].

It has been suggested that NA is involved in intracellular iron binding, buffering and transport. The activity of iron-containing enzymes involved in iron stress defence is strongly increased [34] and their concentration significantly increased [11], respectively, in the NA-free but iron accumulating *chloronerva* mutant whereas the activity of the iron-metabolizing ferrochelatase of tomato chloroplasts is restricted by the presence of NA [35]. Possibly, it binds proteins potentially involved in iron sensing processes. In addition to these functions, in strategy II plants such as grasses, NA is used as substrate for the synthesis of the phytosiderophores of the mugineic acid family. These strong ferric chelators are excreted and taken up by roots after iron complexation. Recently it has been suggested that NA is involved in protecting the cell from oxidative damage [8]. The central role of NA in the regulation of iron acquisition for both strategies requires its highly controlled synthesis from three molecules of AdoMet by the enzyme NAS.

Besides the recently published NAS-encoding genes of barley [18], the cDNA derived amino acid sequence of the enzymatically active protein shows no obvious overall sequence similarity to previously described proteins, indicating that it represents a novel class of enzyme. Based on amino acid sequence distances most of the known NAS-like sequences have been arranged in a dendrogram (Fig. 8). A distantly related sequence from *M. thermoautotrophicum* (see below) is used as outgroup. The tree clearly reveals a distinct dicot and moncot cluster. It also shows the close relationship between NASHOR1 described in this study and the HVNAS6 sequence analysed by Higuchi *et al.* [18]: the sequences are highly similar but are not identical. The differences between these two genes might be due to polymorphisms between the barley varieties used. Moreover, the data demonstrate that NASHOR2 is only distantly related to the other sequences described by Higuchi *et al.* [18] and obviously represents a new NAS-like gene of barley. It remains to be analysed whether all of these genes encode active NAS enzymes and whether they are differentially expressed in plant organs and/or developmental stages.

Interestingly, only one NAS-like sequence could be detected in the database used outside of the plant kingdom. A very distantly related protein sequence could be found in the genome of the archaeon *M. thermoautotrophicum*, but not in bacterial or yeast genomes. The sequence was used as outgroup to construct the similarity gene tree shown in Fig. 8. As this archaeon is known as a symbiotic species of eukaryotes one might speculate that plant NAS-like genes originate from a horizontal gene transfer event. Whether the archaeon gene product is enzymatically active is not yet known. Remarkably, this NAS-like gene sequence of *M. thermoautotrophicum* is flanked (3.4 kb upstream) by a gene sequence (MTH673) which resembles a Mg chelatase-encoding gene. Whether this is of any functional significance remains to be determined.

The amino acid sequence of the active enzyme also lacks domains similar to other enzymes which accept AdoMet as substrate as well, like DNA-methylases, other AdoMet-dependent methyltransferases and ACC synthase [36]. This might be explained by different substrate binding and/or reaction mechanisms. Thus, methylases catalyse the transfer of the methyl group and ACC-synthase catalyses the formation of a cyclopropane ring from the methionine skeleton itself. In contrast, the NAS reaction mechanism probably involves the coupling of three methionine skeletons in total, perhaps resembling nonribosomal peptide synthesis.

The molecular mass of the active enzyme in purified barley extracts as well as after expression in *E. coli* was determined to be ≈ 105 kDa (Fig. 5). The molecular mass of the cDNA-derived amino acid sequences of NASHOR1 and NASHOR2 were calculated to be 35 611 and 36 312 Da, respectively. These values suggest that the native enzyme probably consists of three subunits. It is not yet known whether various subunits encoded by different genes can be assembled into an active holoenzyme. The trimeric structure of the active enzyme is in striking contrast to the interpretation suggested by Higuchi *et al.* [18]. These authors determined the molecular mass of NAS in a partially purified barley extract and tentatively conclude that native NAS exists as a monomer. The reason for this dicrepancy is not yet clear. We have analysed the native molecular mass of the active fraction both in highly purified barley extract as well as in extracts from recombinant *E. coli* cells to be 105 kDa. Nevertheless, we cannot completely exclude that this size is the result of aggregation. Otherwise, it is possible that both forms exhibit (perhaps different) enzyme activity. In this case it is conceivable that the trimerization vs. monomerization could be the basis of a putative mechanism of regulation of enzyme activity, but this remains to be analysed further.

It has been proposed that NA is synthesized either from three molecules of AdoMet [27] or from three molecules of azetidine-2-carboxylic acid [37,38]. Although details of the reaction mechanism are not yet known (see above), one might speculate that three subunits are necessary for the initial binding of three substrate molecules. The detected enzyme activity after expression of the subunit specific cDNA in *E. coli* further demonstrates that the proposed trimeric holoenzyme is able to catalyse both the linkage of three substrate molecules and the formation of the azetidine ring. The synthesis of sufficient amounts of active NAS in *E. coli* provides an excellent prerequisite for the analysis of the reaction mechanism and might facilitate the crystallization of the enzyme.

The pleiotropic phenotype and the lack of NA in the tomato mutant *chloronerva* suggested that either the NAS gene or its regulation is affected by the mutation. The recent identification of the *chloronerva* gene by map-based cloning [31] revealed extensive sequence similarities between the *chloronerva* gene and the NAS gene of barley (Fig. 3). This supports the conclusion that a mutation in the tomato NAS-encoding gene is the molecular basis of the *chloronerva* mutation. This conclusion is further supported by the expression of antisense constructs in transgenic tobacco plants. As shown in Fig. 6 the NA content is significantly reduced in plants transformed with an antisense construct of the NAS-like *Arabidopsis* gene sequence NASARA1. As expected from various other antisense experiments the antisense effect varies in different transgenic lines probably because of position effects. To date we have not found a transgenic tobacco line with undetectable amounts of NA as it is the case in the *chloronerva* mutant of tomato. One reason for the limited effect on NA content could be the insufficient similarity between the *Arabidopsis* and the tobacco NAS gene sequence. Currently, we are analysing the function of the antisense construct in the homologous *Arabidopsis* host background.

The significantly higher iron concentration in the antisense plants is probably the consequence of the lowered NA concentration (Fig. 6). As in the mutant *chloronerva*, the enhanced activity of the iron acquisition reactions is considered to be the reason for the increased iron uptake.

Finally, we could demonstrate the occurrence of a *chloronerva*-like phenotype in at least three different transgenic tobacco lines using antisense constructs based on NASARA5 (Fig. 7). To our knowledge this is the first demonstration of the

phenotype in a plant other than the *chloronerva* mutant of tomato. As it is also observed on older leaves of *chloronerva*, the phenotype is partially transient and disappears at later developmental stages.

In summary, the availability of NAS gene sequences both from dicots and monocots is the basis for further investigations concerning the regulation of iron homeostasis in plants and provides promising tools for the manipulation of iron acquisition processes in crop plants.

ACKNOWLEDGEMENTS

The authors thank Ch. Horstmann for peptide sequencing and S. König for DNA sequencing. The project was supported by the Deutsche Forschungsgemeinschaft (grants Ba1235/3–1 and Ba 1235/3–2). We thank J. Friedrich and E. Liemann for excellent technical assistance and U. Wobus, T. J. Buckhout and S. Gubatz for critical reading of the manuscript. We greatly appreciate the gift of the barley cDNA-library from W. Weschke, IPK Gatersleben.

REFERENCES

1. Welch, R.M. (1995) Micronutrient nutrition of plants. *Crit. Rev. Plant Sci.* **14**, 49–82.
2. Briat, J.F., Fobis-Loisy, I., Grignon, N., Lobréaux, S., Pascal, N., Savino, G., Thioron, S., Van Wirén, N. & Van Wuytswinkel, O. (1995) Cellular and molecular aspects of iron metabolism in plants. *Biol. Cell* **84**, 69–81.
3. Guerinot, M.L. & Yi, Y. (1994) Iron: nutritious, noxious, and not readily available. *Plant Physiol.* **104**, 815–820.
4. Marschner, H. & Römheld, V. (1994) Strategies of plants for acquisition of iron. *Plant Soil* **165**, 261–274.
5. Rudolph, A., Becker, R., Scholz, G., Procházka, Z., Toman, J., Macek, T. & Herout, V. (1985) The occurrence of the amino acid nicotianamine in plants and microorganisms. A reinvestigation. *Biochem. Physiol. Pflanzen* **180**, 557–563.
6. Schmidke, I. & Stephan, U.W. (1995) Transport of metal micronutrients in the phloem of castor bean (*Ricinus communis*) seedlings. *Physiol. Plant.* **95**, 147–153.
7. Pich, A., Scholz, G. & Stephan, U.W. (1994) Iron dependent changes of heavy metals, nicotianamine, and citrate in different plant organs and in the xylem exudate of two tomato genotypes. Nicotianamine as possible copper translocator. *Plant Soil* **165**, 189–196.
8. Von Wirén, N., Klair, S., Bansal, S., Briat, J.F., Khodr, H., Shioiri, T., Leigh, R.A. & Hider, R.C. (1999) Nicotianamine chelates both Fe III and Fe II. Implications for metal transport in plants. *Plant Physiol.* **119**, 1107–1114.
9. Shojima, S., Nishizawa, N.K. & Mori, S. (1989) Establishment of a cell-free system for the biosynthesis of nicotianamine. *Plant Cell Physiol.* **30**, 673–677.
10. Higuchi, K., Nishizawa, N.K., Yamaguchi, H., Römheld, V., Marschner, H. & Mori, S. (1995) Response of nicotianamine synthase activity to Fe-deficiency in tobacco plants as compared with barley. *J. Exp. Bot.* **289**, 1061–1063.
11. Herbik, A., Giritch, A., Horstmann, C., Becker, R., Balzer, H.J., Bäumlein, H. & Stephan, U.W. (1996) Iron and copper nutrition-dependent changes in protein expression in a tomato wild type and the nicotianamine-free mutant *chloronerva*. *Plant Physiol.* **111**, 533–540.
12. Herbik, A. (1997) *Proteinchemische und molekularbiologische Charakter-isierung der Tomatenmutante* chloronerva. PhD Thesis, Humboldt University, Berlin, Germany.
13. Scholz, G., Becker, R., Pich, A. & Stephan, U.W. (1988) The regulation of iron uptake and possible functions of nicotianamine in higher plants. *Biochem. Physiol. Pflanzen* **183**, 257–169.
14. Giritch, A., Herbik, A., Balzer, H.J., Ganal, M., Stephan, U.W. & Bäumlein, H. (1997) A root specific iron-regulated gene of tomato encodes a lysyl-tRNA-synthetase-like protein. *Eur. J. Biochem.* **244**, 310–317.
15. Giritch, A., Ganal, M., Stephan, U.W. & Bäumlein, H. (1998) Structure, expression and chromosomal localisation of the metallothionein-like gene family of tomato. *Plant Mol. Biol.* **37**, 701–714.
16. Scholz, G., Becker, R., Pich, A. & Stephan, U.W. (1992) Nicotianamine – a common constituent of strategies I and II of iron aquisition by plants: a review. *J. Plant Nutr.* **15**, 1647–1665.
17. Stephan, U.W. & Scholz, G. (1993) Nicotianamine: mediator of transport of iron and heavy metals in the phloem? *Physiol. Plant.* **88**, 522–529.
18. Higuchi, K., Suzuki, K., Nakanishi, H., Yamaguchi, H., Nishizawa, N.K. & Mori, S. (1999) Cloning of nicotianamine synthase genes, novel genes involved in the biosynthesis of phytosiderophores. *Plant Physiol.* **119**, 471–479.
19. Stephan, U.W. & Prochazka, Z. (1984) Physiological disorders of the nicotianamine-auxotroph tomato mutant chloronerva. I. Growth characteristics and physiological abnormalities related to iron and nicotianamine supply. *Acta Bot. Neerl.* **38**, 147–153.
20. Subbaramaiah, K. & Simms, S.A. (1992) Photolabelling of CherR methyltransferase with *S*-Adenosyl-L-methionine (AdoMet). *J. Biol. Chem.* **267**, 8636–8642.
21. Laemmli, U.K. (1970) Cleavage of structural proteins during the assembly of the head of bacteriophage T4. *Nature* **227**, 680–685.
22. Jenö, P., Mini, T., Moes, S., Hintermann, E. & Horst, M. (1995) Internal sequencing from proteins digested in polyacrylamide gels. *Anal. Biochem.* **224**, 75–82.
23. Sambrook, J., Fritsch, E.F. & Maniatis, T. (1989) *Molecular Cloning. A Laboratory Manual*, 2nd edn. Cold Spring Harbor Laboratory Press, New York, USA.
24. Bevan, M. (1984) Binary *Agrobacterium* vectors for plant transformation. *Nucleic Acids Res.* **12**, 8711–8721.
25. Höfgen, R. & Willmitzer, L. (1990) Biochemical and genetic analysis of different patatin isoforms expressed in various organs of potato (*Solanum tuberosum* L.). *Plant Sci.* **66**, 221–230.
26. Bäumlein, H., Boerjan, W., Nagy, I., Bassüner, R., Van Montagu, M., Inzé, D. & Wobus, U. (1991) A novel protein gene from *Vicia faba* is developmentally regulated in transgenic tobacco and *Arabidopsis* plants. *Mol. Gen. Genet.* **225**, 459–467.
27. Higuchi, K., Kanazawa, K., Nishizawa, N.K., Chino, M. & Mori, S. (1994) Purification and characterization of nicotianamine synthase from Fe-deficient barley roots. *Plant Soil* **165**, 173–179.
28. Satoh, S. & Yang, S. (1989) Specificity of *S*-adenosyl-L-methionine in the inactivation and labelling of 1-aminocyclopropane-1-carboxylate synthase isolated from tomato fruits. *Archiv. Biochem. Biophys.* **271**, 107–112.
29. Yip, W.K., Dong, J.G., Kenny, J.W. & Thomsom, G.A. (1990) Characterization and sequencing of the active site of 1-aminocyclopropane-1-carboxylate synthase. *Proc. Natl Acad. Sci. USA* **87**, 7930–7934.
30. Bäumlein, H., Ganal, M., Herbik, A., Ling, H.Q., Mock, H.P. & Stephan, U.W. (1998) Nicotianamin-Synthase-Gene, ihre Isolierung und ihre Verwendung. *Patent, Amtliches Aktenzeichen* 198243073.
31. Ling, H.Q., Koch, G., Bäumlein, H. & Ganal, M. (1999) Map-based cloning of *chloronerva* – a gene involved in iron uptake of higher plants encoding nicotianamine synthase. *Proc. Natl Acad. Sci. USA* **96**, 7098–7103.
32. Becker, R., Fritz, E. & Manteuffel, R. (1995) Subcellular localization and characterization of excessive iron in the nicotianamine-less tomato mutant *chloronerva*. *Plant Physiol.* **108**, 269–275.
33. Liu, D.H., Adler, K. & Stephan, U.W. (1998) Iron-containing particles accumulate in organelles and vacuoles of leaf and root cells in the nicotianamine-free tomato mutant *chloronerva*. *Protoplasma* **201**, 213–220.
34. Pich, A. & Scholz, G. (1993) The relationship between the activity of various iron-containing and iron-free enzymes and the presence of nicotianamine in tomato seedlings. *Physiol. Plant.* **88**, 172–178.
35. Stephan, U.W. (1995) The plant-endogenous Fe (II)-chelator

nicotianamine restricts the ferrochelatase activity to tomato chloroplasts. *J. Exp. Bot.* **46**, 531–537.

36. Joshi, C.P. & Chiang, V.L. (1998) Conserved sequence motifs in plant *S*-adenosyl-L-methionine-dependent methyltransferases. *Plant Mol. Biol.* **37**, 663–674.
37. Ma, J.F. & Nomoto, K. (1994) Incorporation of label from ^{13}C, ^{2}H and ^{15}N-labelled methionine molecules during the biosynthesis of 2′-deoxymugineic acid in roots of wheat. *Plant Physiol.* **105**, 607–610.
38. Ma, J.F., Shinada, T., Matsuda, T. & Nomoto, K. (1995) Biosynthesis of phytosiderophores, mugineic acids, associated with methionine cycling. *J. Biol. Chem.* **270**, 16549–16554.

The Plant Journal (1999) **17**(4), 385–395

Glyoxalase I from *Brassica juncea*: molecular cloning, regulation and its over-expression confer tolerance in transgenic tobacco under stress

Veena,[1,2] Vanga S. Reddy[1] and Sudhir K. Sopory[1,2,*]
[1]*International Centre for Genetic Engineering and Biotechnology, Aruna Asaf Ali Marg, New Delhi 110067, India, and*
[2]*School of Life Sciences, Jawaharlal Nehru University, New Delhi 110067, India*

Summary

Despite its ubiquitous presence, the role of glyoxalase I has not been well investigated in plants. In order to find out its physiological functions, we have cloned and characterized a cDNA from *Brassica juncea* encoding glyoxalase I (*Gly I*) and made transgenic tobacco plants harbouring *Gly I* in both sense and antisense orientation. The transgenic nature of the plants was confirmed by Southern blotting, and the estimated number of genes inserted ranged from one to six. The transcript and protein levels of glyoxalase I were also monitored in transgenic plants. The expression of glyoxalase I in *B. juncea* was upregulated in response to salt, water and heavy metal stresses. In response to a high concentration of salt, the transcript level averaged threefold higher in 72 h, and an increase in the protein was also seen by immunoblotting. The transgenic plants over-expressing glyoxalase I showed significant tolerance to methylglyoxal and high salt, as tested in detached leaf disc senescence assay. A comparison of plants expressing high and low levels of glyoxalase I showed that the tolerance to different salt concentrations was correlated with the degree of glyoxalase I expression. Our results suggest an important role of glyoxalase I in conferring tolerance to plants under stress conditions.

Introduction

The glyoxalase system is ubiquitous in nature and consists of two enzymes: glyoxalase I (EC 4.4.1.5) and glyoxalase II (EC 3.1.2.6), which act co-ordinately to convert 2-oxoaldehydes into 2-hydroxyacids using reduced glutathione as a cofactor (reviewed in Thornalley, 1993). The reaction catalysed by glyoxalase I (Aronsson *et al.*, 1978; Mannervik, 1980; Sellin *et al.*, 1983) and glyoxalase II (Uotila, 1989) is shown in Figure 1. Methylglyoxal is a primary physiological substrate for glyoxalase I (Kalapos, 1994; Phillips and Thornalley, 1993). It is a potent cytotoxic compound known to arrest growth and react with DNA and protein (Papoulis *et al.*, 1995), and increases sister chromatid exchanges (Faggin *et al.*, 1985; Thornalley, 1990).

Glyoxalases in animals and microbial systems have been known for more than 80 years. However, the physiological significance of this system is still unclear. The glyoxalase system has been proposed to be involved in protection against α-oxoaldehyde cytotoxicity, regulation of cell division and proliferation, microtubular assembly, vesicle mobilization, growth of tumours, and clinical complications associated with various diseases, for example diabetes mellitus (reviewed in Thornalley, 1990, 1993).

Glyoxalase I and II have been purified and characterized from a few plant species (Deswal *et al.*, 1993). An increased glyoxalase I activity was reported in rapidly dividing and non-differentiated cells/tissues compared with differentiated tissues (Deswal *et al.*, 1993; Paulus *et al.*, 1993; Ramaswamy *et al.*, 1983, 1984; Seraj *et al.*, 1992; Sethi *et al.*, 1988). Treatments that stimulate cell growth, including hormones (auxins, cytokinins, etc.) and light, also increased glyoxalase I activity (Chakravarty and Sopory, 1990, 1998). Conversely, inhibition of cell growth resulted in lower levels of glyoxalase I activity (Deswal *et al.*, 1993; Paulus *et al.*, 1993; Sethi *et al.*, 1988). Accordingly this system has been often regarded as a 'marker for cell growth and division' (Paulus *et al.*, 1993). However, a causal relationship between glyoxalase activity and rapid cell growth has not yet been established. In fact, tomato glyoxalase I was upregulated in response to salt stress, osmotic and phytohormonal stimuli (Espartero *et al.*, 1995). The ubiquitous nature and high expression of glyoxalase I in metabolically active cells/tissues, such as meristematic, newly dividing cells, or cells undergoing stress, indicate the fundamental importance of this system in plants.

Genes encoding glyoxalase I enzyme have been isolated and characterized from few microbial and mammalian species, such as *Pseudomonas putida* (Lu *et al.*, 1994; Rhee *et al.*, 1988), *Homo sapiens* (human) (Kim *et al.*, 1993; Ranganathan *et al.*, 1993; Ridderstrom and Mannervik, 1996), *Saccharomyces cerevisiae* and *Schizosaccharomyces pombe* (yeast) (Devlin *et al.*, 1995; Gentles *et al.*, 1995; Inoue and Kimura, 1996), *Escherichia coli* (Daub *et al.*, 1996) and *Salmonella typhimurium* (Clugston *et al.*, 1997). Glyoxalase II gene has also been cloned from human (Ridderstrom *et al.*, 1996) and yeast (Bito *et al.*, 1997). A

Received 5 October 1998; revised 11 December 1998; accepted 14 December 1998.
*For correspondence (fax +91 11 6162316; e-mail sopory@hotmail.com)

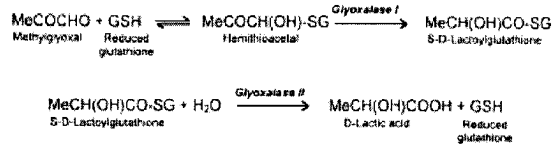

Figure 1. The reaction catalysed by glyoxalase I and glyoxalase II.

significant conservation was observed among the glyoxalase I and glyoxalase II sequences at the nucleotide as well as at the protein level. Recently the 3-dimensional structure of human glyoxalase I was determined, which should help in exploring the mechanism of glyoxalase I-catalysed reactions (Cameron *et al.*, 1997). In comparison with the studies on micro-organisms and human, the only published cDNA sequence of glyoxalase I from plants is of tomato (Espartero *et al.*, 1995) and two genes for glyoxalase II from *Arabidopsis* (Maiti *et al.*, 1997; Ridderstrom and Mannervik, 1997).

To investigate the physiological significance of the glyoxalase system in plants, we have cloned and characterized a glyoxalase I gene from *Brassica juncea*. The expression of glyoxalase I in this system was found to be upregulated in response to salt, water and heavy metal stresses. In order to decipher its functional importance, the *Gly I* gene from *Brassica* was introduced into tobacco plants in both sense and antisense orientation. The detached leaves from plants over-expressing glyoxalase I showed significant tolerance against high concentrations of salt and methylglyoxal, compared with the wild type and antisense transgenic plants. The present data suggest that glyoxalase I may have an important role during stress.

Results

Isolation of glyoxalase I cDNA clone from B. juncea

As a part of our study to understand the physiological significance of the glyoxalase system in higher plants, we isolated and characterized the gene for glyoxalase I from *B. juncea*. The glyoxalase I enzyme was purified to homogeneity as described elsewhere (Deswal and Sopory, 1991) and polyclonal antibodies were raised against the purified protein. Immunoprecipitation assays and Western blot analysis suggested a high specificity of these antibodies for glyoxalase I protein (data not shown). A mannitol-stressed cDNA expression library was prepared and immunologically screened. Eight immunopositive clones were identified, rescreened and purified until homogeneous. A sequence analysis of the longest insert (pBSGLYIVA3) suggested that it encodes a full length cDNA, which is 784 bp in length with an ORF of 558 bp, a 5′ untranslated region of 44 bp, a 3′ untranslated region of 163 bp including a consensus polyadenylation signal, and a 19-bp poly(A)+ tail (Genbank accession number Y13239). The deduced amino acid sequence revealed a protein consisting of 185 amino acid residues with a predicted mass of 20.782 kDa. The alignment of the deduced amino acid sequence from the *B. juncea Gly I* (B.j *Gly I*) with the tomato *Glx I* indicated significantly high homology (80%) between them. Figure 2 shows the alignment of B.j GLY I with human, *Pseudomonas*, yeast, *E. coli* and *Salmonella* glyoxalase I sequences. A significant homology throughout the coding region suggested the evolutionarily conserved nature of the protein. Amino acid residues that are proposed to be involved in metal and glutathione binding sites were also found to be conserved among all glyoxalase I sequences.

Over-expression of Gly I *from* B. juncea *in* E. coli

To verify that the isolated cDNA clone from *B. juncea* indeed codes for functional glyoxalase I, the complete ORF was cloned under the control of the T7 promoter in pRSETA vector (Novagen) to get a recombinant plasmid pRSETA-*Gly I*, and over-expressed in *E. coli* [BL21(DE3)]. Following induction with IPTG (0.5 mM), the over-expressed *Gly I* showed 1200-fold higher glyoxalase I activity compared with cells transformed with vector alone (550.47 units mg^{-1} protein versus 0.444 units mg^{-1} protein). SDS–PAGE analysis showed a highly expressed 24 kDa additional protein in *E. coli* transformed with pRSETA-*Gly I* (data not shown). Western blot analysis (Figure 3, inset) identified the over-expressed Gly I in the soluble extracts from only induced *E. coli* cells transformed with the recombinant plasmid. However, a faint band at the 34 kDa position in an extract from uninduced *E. coli* cells might represent the endogenous glyoxalase I of the host cells (Thornalley, 1990).

To check the sensitivity of *E. coli* cells over-expressing glyoxalase I, the transformed cells with recombinant and control plasmids were grown on medium containing increasing concentrations of methylglyoxal. As shown in Figure 3, the growth of the control cells was completely inhibited at a 6 mM concentration of methylglyoxal compared with the cells over-expressing glyoxalase I, which were found to withstand methylglyoxal up to 20 mM. All these experiments clearly established that the recombinant cDNA clone isolated in the present study codes for a functional glyoxalase I protein.

Upregulation of Gly I *under abiotic stress in* B. juncea

Total RNA from cotyledonary leaves of the *Brassica* seedlings stressed with different concentrations of sodium chloride, mannitol and zinc chloride was isolated and probed with radiolabelled *Gly I* cDNA under high stringency condition. As seen in Figure 4, a transcript of approximately 0.8 kb was detected and a dose-dependent upregulation of the glyoxalase I transcript was observed.

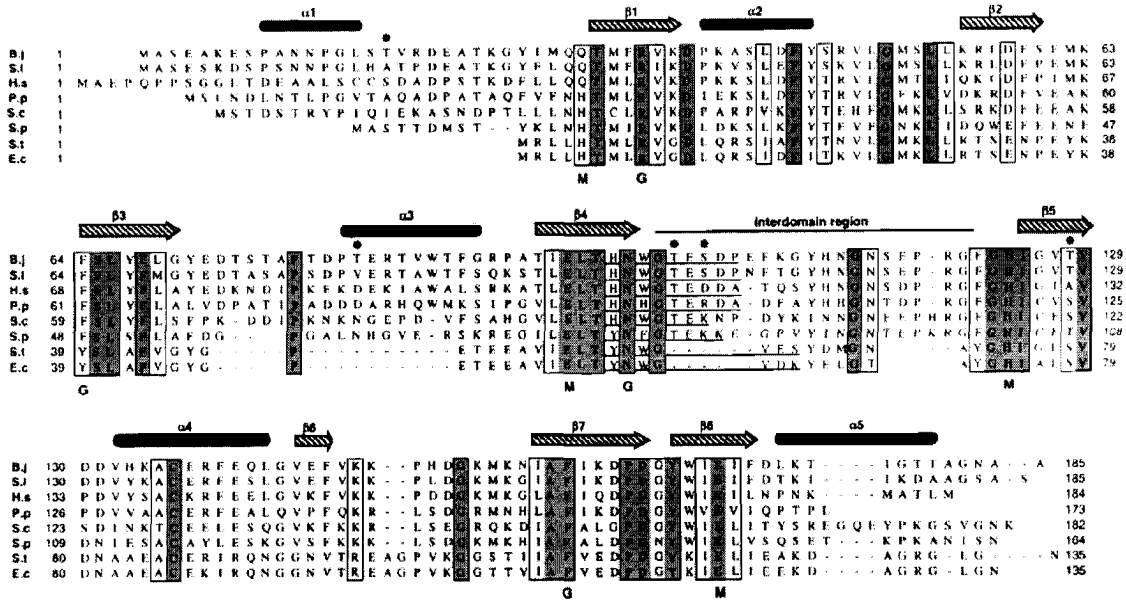

Figure 2. Multi-sequence alignment of the deduced amino acid sequence of the *Gly I* cDNA clone from *B. juncea* with previously reported glyoxalase I sequences. Sequences were aligned using the MacVector ClustalW program. Amino acid residues conserved in all sequences are boxed together. The residues that are identical to B.j GLY I sequence are shaded dark grey, those that are conserved but not identical are in a white background. The positions of the amino acid residues in the original sequences are indicated on right. Predicted domains of conserved secondary structure are indicated by bars (α helix; β sheet). The underlined sequence represents the proposed catalytic loop region. Probable residues involved in metal binding are marked by 'M', to glutathione by 'G' and putative phosphorylation sites by '*'. B.j, *B. juncea* (GenBank accession number Y13239); S.l, *Solanum lycopersicum* (Z48183); H.s, *Homo sapiens* (L07837); P.p, *Pseudomonas putida* (L33880); S.c, *Saccharomyces cerevisiae* (P50107); S.p, *Schizosaccharomyces pombe* (Q09751); S.t, *Salmonella typhimurium* (U57364); E.c, *E. coli* (U57363).

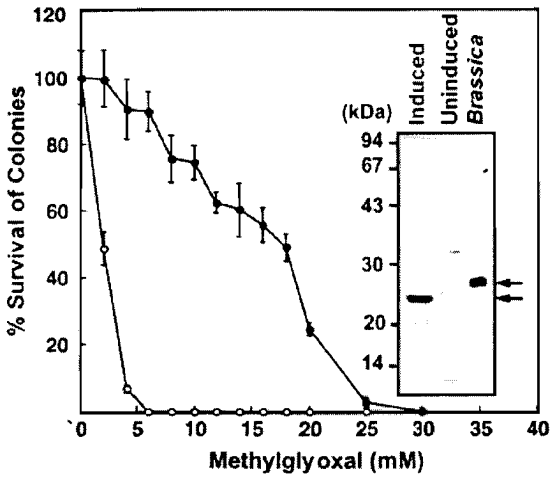

Figure 3. Methylglyoxal cytotoxicity test on *E. coli* cells over-expressing *Gly I* cDNA.
Escherichia coli cells transformed with pRSETA-*Gly I* (●) and pRSETA (○) vector were plated on LB amp medium supplemented with 1 mM of IPTG and various concentrations of methylglyoxal (0 -30 mM). The inset shows an immunoblot of protein profiles of uninduced and induced *E. coli* cells transformed with pRSETA-*Gly I* after 2 h of induction with 0.5 mM IPTG. Soluble protein extract from *B. juncea* was used as a control.

Treatment with 800 mM of sodium chloride resulted in a three to 3.5-fold increase, whereas mannitol (400 mM) and zinc chloride (200 mM) showed two- to threefold enhancement in the level of the transcript. As maximum induction of the *Gly I* transcript was observed during the salt stress, all further studies were concentrated on salt-induced expression of glyoxalase I gene. As shown in Figure 5, it follows that the steady-state levels of *Gly I* transcript increased with the duration of salt treatment in cotyledonary leaves (Figure 5a) as well as in roots (Figure 5b), and at 72 h an approximately threefold higher level was seen compared with control. Western blot analysis also showed a significant accumulation of glyoxalase I protein in a time-dependent manner (Figure 5, inset). Consequently there was also an increase in the specific activity of glyoxalase I (nearly threefold).

Over-expression of Gly I *in tobacco plants*

To establish the functional significance of the glyoxalase I in plants, *Gly I* from *B. juncea* was over-expressed as well as downregulated in tobacco plants using a transgenic approach. The *Gly I* cDNA was cloned into pBI121 (Clontech) in both sense and antisense orientations under the control of the CaMV 35S promoter. The details of the construct used in transformation of tobacco are shown

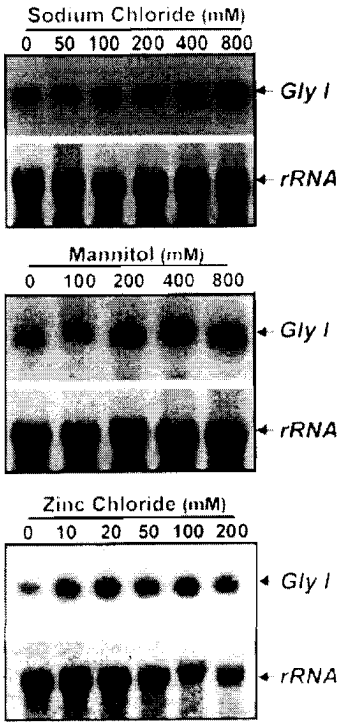

Figure 4. Induction of *Gly I* in response to abiotic stresses.
Total RNA was isolated from cotyledonary leaves of *B. juncea* seedlings that were stressed with different concentrations of sodium chloride, mannitol and zinc chloride for 72 h. The *Gly I* (approximately 0.8 kb) transcript is shown by an arrow. The same blot was reprobed with *16S rRNA* to show the loading control of RNA.

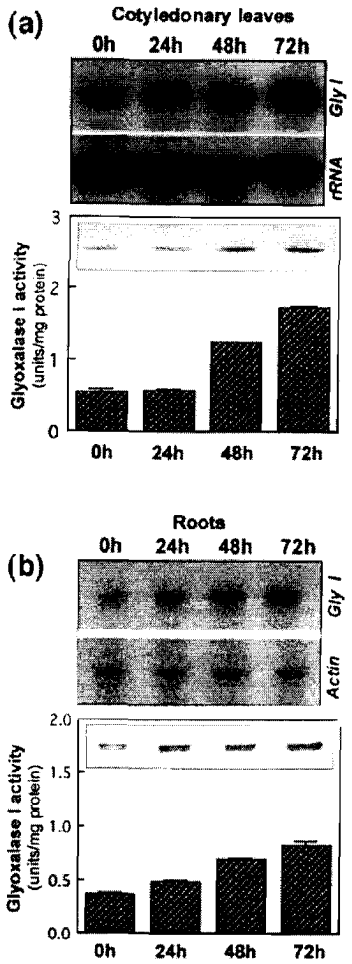

Figure 5. *Kinetics of glyoxalase I expression in response to salt stress.*
The 4-day-old *B. juncea* seedlings were either treated with or without 800 mM sodium chloride and grown for different time periods (0, 24, 48 and 72 h).
(a) Total RNA (30 μg) isolated from cotyledonary leaves and roots of the salt-treated seedlings was probed with radiolabelled *Gly I* gene. The same blot was reprobed with *16S rRNA* or *actin* to show the loading control of RNA.
(b) Glyoxalase I activity and protein levels (in inset) in the cotyledonary leaves and roots of salt-treated seedlings. For Western analysis total soluble proteins isolated from cotyledonary leaves (2 μg) and roots (5 μg) were transferred onto nitrocellulose membrane and immunostained with glyoxalase I antibodies.

in Figure 6(a). The preliminary screening of kanamycin-resistant putative transgenic plants was done using a histochemical GUS assay (Jefferson, 1987) and by analysing the expression of the reporter gene (GUS or *uidA*). A total of 150 kanamycin-resistant and *uidA*-positive plants was selected. Out of these, a few transgenic plants (seven plants derived from the transformation experiments with plasmid pBIS-1 and four plants each from experiments with plasmids pBIS-2 and pBI-A) were analysed for stable integration, copy number and expression of the transgenes. Figure 6(b) shows a Southern blot analysis using the *Gly I* gene as a probe. A common band of expected size approximately 0.8 kb was detected in all transgenic lines, because digestion of genomic DNA isolated from these plants with *Eco*RI enzyme released a *Gly I* cDNA fragment from all the constructs used in the transformation experiment. The intensity of the hybridized signal in each lane was variable, indicating the multiple insertion of the *Gly I* gene in the tobacco genome. The estimated number of the genes inserted in various plants ranged from one to six copies. In addition, restriction digestion of genomic DNA from the same set of selected transgenic plants with *Bam*HI resulted in the appearance of bands at different positions, suggesting that transgenic lines are produced from different transformation events (data not shown).

Plants transformed with sense and antisense constructs were analysed for the presence of *Gly I* and *uidA* transcripts. Figure 6(c) shows the hybridization pattern of total RNA probed with *Gly I* cDNA, which revealed the presence of ≈ 0.8 kb transcript in all the transgenic plants transformed with pBIS-1, and two transcripts of ≈ 0.8 kb and ≈ 2.7 kb in pBIS-2-transformed plants. The presence of 0.8 kb

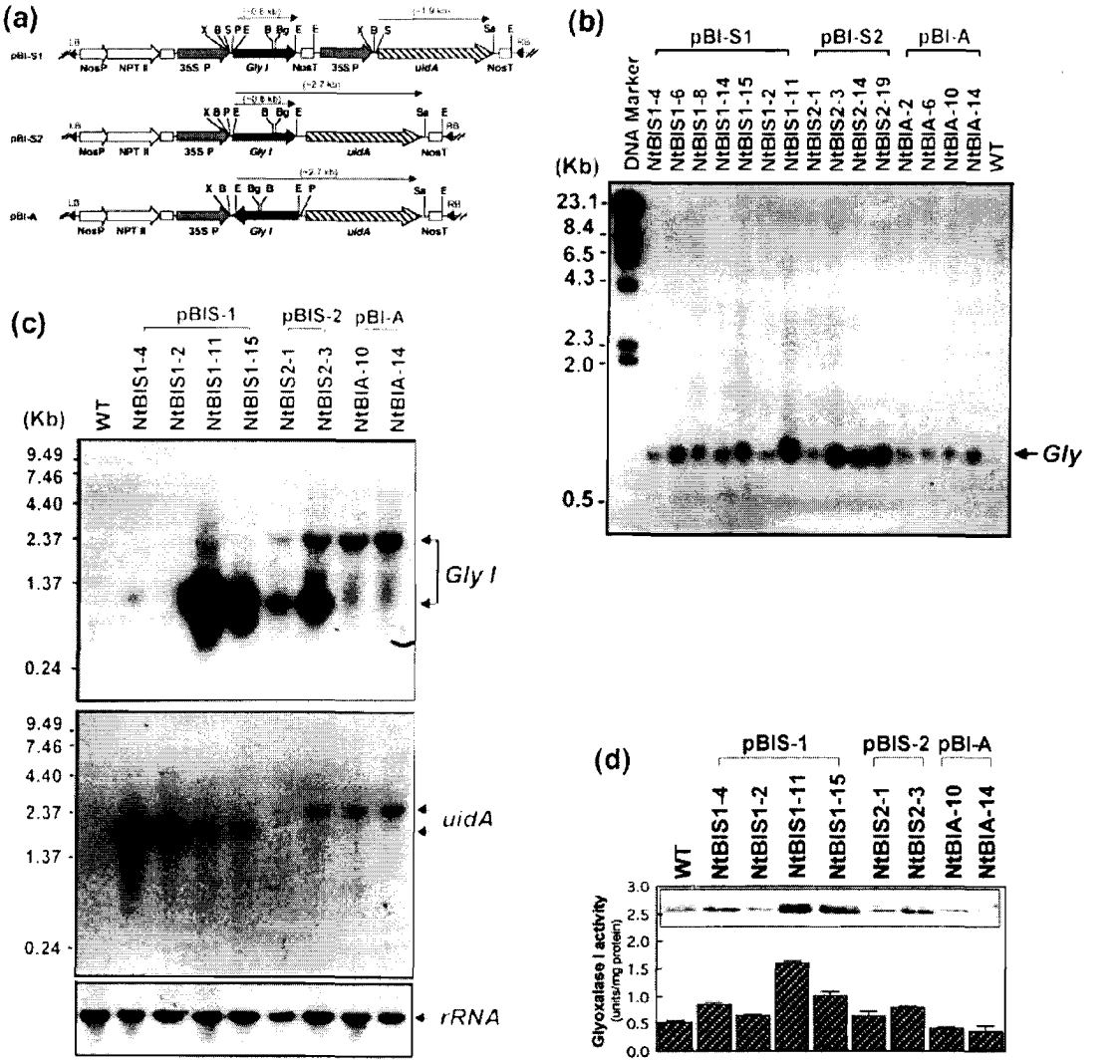

Figure 6. Transformation of tobacco using *Gly I* gene.
(a) Schematic representation of constructs used to express *Gly I* in tobacco plants.
(b) Southern blot analysis of transgenic plants. Genomic DNA (10 μg) isolated from the leaves of the kanamycin-resistant tobacco plants transformed with pBI-S1, pBI-S2 or pBI-A constructs were digested with *Eco*RI and probed with the radiolabelled *Gly I* cDNA fragment.
(c) Expression of *Gly I* and *uidA* genes in transgenic tobacco. Northern blots of total RNA (30 μg) isolated from transgenic plants were hybridized with radiolabelled *Gly I*, *uidA*, and *16S rRNA* gene probes. The same blot was hybridized after stripping the earlier probe each time. The individual *Gly I*, *uidA* transcripts, the fusion transcript between *Gly I* and *uidA*, depending upon the type of construct used in the transformation, and the *16S rRNA* transcripts are indicated by arrows.
(d) The glyoxalase activity and protein level (in inset) in wild-type and transgenic tobacco plants. The immunoblot was developed with glyoxalase I polyclonal antibodies.

transcript indicates that transcription initiation and termination of *Gly I* occurs on its own, which was expected due the presence of transcription initiation (ATG), termination (TGA) and poly(A)+ signals in the cloned cDNA fragment in the vectors (pBIS-1 and pBIS-2). In pBIS-2 the ≈ 2.7 kb hybridizing signal represents the fusion transcript between *Gly I* and *uidA*. In pBI-A-transformed plants, *Gly I* was placed in antisense orientation, therefore only a single fusion transcript of size ≈ 2.7 kb between *Gly I* and *uidA* was observed. When the same blot was probed with *uidA*, an expected transcript of ≈ 1.9 kb, corresponding to the size of *uidA*, was detected in the plants transformed with pBIS-1 vector (due to an independent transcription termination signal for the *Gly I* in these vectors), and a ≈ 2.7 kb

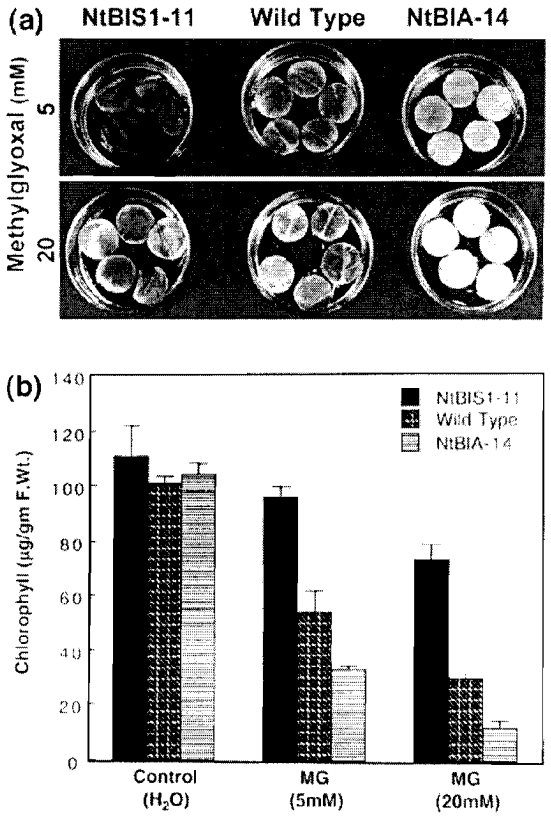

Figure 7. Retardation/promotion of methylglyoxal-promoted senescence in transgenic tobacco plants by over-expression or downregulated expression of *Gly I*.
Phenotypic differences (a) and chlorophyll content (mg g^{-1} fresh weight) (b) from methylglyoxal-treated leaf discs of transgenic plant NtBIS1–11 (transformed with *Gly I* sense construct pBI-S1), NtBIA-14 (transformed with *Gly I* antisense construct, pBI-A) and wild-type plants floated in 5 mM and 20 mM of methylglyoxal solution for 24 h under continuous white light (100 µEm^{-2} sec^{-1}) at 25 ± 2°C.

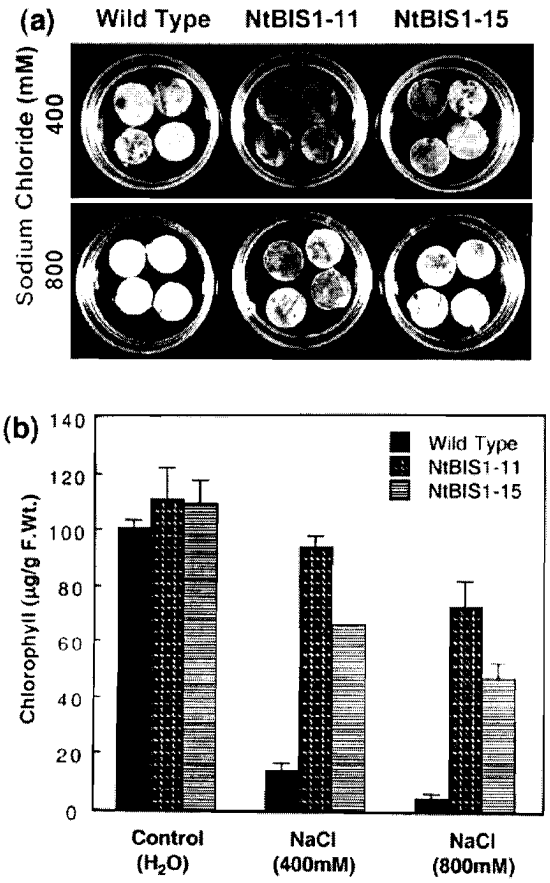

Figure 8. Retardation of salt stress-promoted senescence in transgenic tobacco plants over-expressing *Gly I* in sense.
Phenotypic differences (a) and chlorophyll content (mg g^{-1} fresh weight) (b) from sodium chloride-treated leaf discs of transgenic plants transformed with *Gly I* sense construct, pBI-S1 (NtBIS1–11 and NtBIS1–15) and wild-type plants floated in 400 mM and 800 mM sodium chloride solution for 72 h under continuous white light (100 µEm^{-2} sec^{-1}) at 25 ± 2°C.

transcript in the plants transformed with pBIS-2 and pBI-A vectors.

Western blot analysis of the transgenic tobacco plants transformed with pBI-S1 and pBI-S2 vectors showed higher levels of glyoxalase I protein (Figure 6d, inset). As seen in Figure 6(d), the *B. juncea* glyoxalase I antibodies also cross-reacted with a ≈ 27 kDa protein of wild-type tobacco. The activity of glyoxalase I in these transgenic plants was higher (up to sixfold in NtBIS-11) compared with the wild type. Plants expressing *Gly I* in antisense orientation showed a lower level of glyoxalase I protein and enzyme activity compared with the wild-type tobacco plants, indicating that inhibition in the expression of endogenous glyoxalase I is due to the presence of antisense *Gly I* mRNA. However, transgenic plants expressing glyoxalase I in sense and antisense were found to be morphologically indistinguishable from wild-type plants.

Tolerance of transgenic tobacco plants against methylglyoxal and salt

Leaf discs of transgenic tobacco plants were floated either on methylglyoxal or sodium chloride solutions for 24 h and 72 h, respectively. Figure 7(a) shows the phenotypic differences among wild-type, sense and antisense transgenic plants after 24 h of methylglyoxal treatment. Plants expressing the *Gly I* gene in antisense orientation (NtBIA-14) showed early bleaching/senescence compared with wild-type tobacco plants. However, plants over-expressing the *Gly I* gene (NtBIS1–11) showed tolerance to methylglyoxal treatment with no significant bleaching. In general leaf discs from control as well as transgenic plants were more sensitive to higher concentrations of methylglyoxal (20 mM). Measurement of the chlorophyll content in these plants after 24 h treatment further confirmed the observed phenotypic differences in the treated leaf discs (Figure 7b).

Incubation of the leaf discs, obtained from wild-type and sense transgenic plants over-expressing high (NtBIS1–11) and medium (NtBIS1–15) levels of glyoxalase I, in 400 and 800 mM of sodium chloride, showed an early bleaching of wild-type leaf discs compared with sense transgenic plants, as shown in Figure 8(a). At both (400 mM and 800 mM) salt concentrations, the decrease in the chlorophyll content in NtBIS1–11 and NtBIS1–15 was less compared with the wild-type plants (Figure 8b). These results provide evidence for a positive relationship between the expression of *Gly I* and tolerance under salt stress.

Discussion

In the present study, we have cloned and characterized glyoxalase I cDNA from *B. juncea*. We have generated transgenic tobacco plants in which glyoxalase I was either over-expressed or down-regulated to various degrees to understand its physiological significance in higher plants.

Analysis of the isolated *Gly I* cDNA clone has revealed significant homology at the nucleotide as well as at the amino acid level with other reported glyoxalase I sequences from plant, animal and microbial systems. The ORF of *Gly I* codes for 185 amino acids and shows zinc and glutathione binding domains at the positions similar to the other known glyoxalase I. The calculated molecular mass was found to be lower than the size of the functional protein expressed in *E. coli* (24 kDa) and the apparent molecular mass of the purified glyoxalase I from *B. juncea* ($\approx$ 27 kDa). Even in tomato the molecular mass of the deduced amino acid sequence of glyoxalase I was 20.7 kDa, whereas over-expressed protein in yeast was found to have a size of 24 kDa (Espartero *et al.*, 1995). In fact, the polyclonal antibodies raised against *B. juncea* glyoxalase I cross-reacted with tomato glyoxalase I with an apparent molecular mass of 27 kDa, similar to that of glyoxalase I from *B. juncea* (data not shown). These variations in the molecular mass of glyoxalase I suggest that the protein might be undergoing post-translational modifications. Analysis of the deduced *B. juncea* glyoxalase I protein sequence revealed one serine and four threonine phosphorylation sites and two N-myristoylation sites. Evidence for post-translational modification of glyoxalase I in yeast has been presented (Inoue *et al.*, 1990). At present the significance of these modifications is unclear. It seems, however, that all post-translational modification sites may not be essential for the activity of glyoxalase I, as *E. coli*-expressed protein showed very high specific activity (1200-fold) and these cells conferred tolerance against high concentrations of methylglyoxal.

Various studies on animal and microbial systems have suggested a possible role of glyoxalase system during cell division and proliferation (Thornalley, 1993). In plants too, similar correlations have been reported (Deswal *et al.*, 1993; Paulus *et al.*, 1993; Seraj *et al.*, 1992). The activity of glyoxalase I has also been shown to be affected by various exogenous factors (Chakravarty and Sopory, 1998; Deswal *et al.*, 1993; Sethi *et al.*, 1988). Recently glyoxalase I from tomato was shown to be upregulated under salt and water stress (Espartero *et al.*, 1995). In addition to salt and water stress, upregulation of glyoxalase I transcript was also observed in response to zinc (a heavy metal) in *B. juncea*. In fact salt, water and heavy metal stresses significantly increased the level of transcript, protein and specific activity of glyoxalase I. This suggests that the upregulation of glyoxalase I may be a general effect in response to abiotic stresses.

To confirm further the role of the glyoxalase system during stress, we generated transgenic tobacco plants that were over-expressing *Gly I* gene in sense and antisense orientations. The effect of stress was tested using the leaf senescence assay method (Fan *et al.*, 1997). The plants over-expressing *Gly I* in sense showed significant tolerance against high concentrations of sodium chloride compared with wild-type plants. The resistance against salt stress was clearly indicated by delayed yellowing and the presence of high chlorophyll content in the leaf discs obtained from sense transgenic plants.

The exact mechanism of how over-expression of glyoxalase I in sense transgenic plants confers tolerance, as assayed by the senescence of leaves, in response to salt stress is not known. It could be that under stress cells become metabolically active, which is mirrored by upregulation of enzymes involved in glycolysis and the TCA cycle (Umeda *et al.*, 1994). As a result of this, an increase in the flux of triose phosphate could lead to an increase in the concentration of methylglyoxal, which has been shown to decrease the rate of cell division (Scaife, 1969; Szent-Gyorgi and Egyud, 1966) and causes cell death (Kalapos *et al.*, 1991). In plants too, a high concentration of methylglyoxal and low glyoxalase I activity have been reported in Douglas fir needles (Smits and Johnson, 1981) and in differentiated tissues of higher plants (reviewed in Deswal *et al.*, 1993). Exogenous application of methylglyoxal in pea calli resulted in a decline in the rate of cell division (Ramaswamy *et al.*, 1983). A system producing more glyoxalase could therefore convert methylglyoxal into a non-toxic form, thus preventing the system from its cytotoxic and mutagenic effects during stress conditions. To test this, leaves of transgenic plants over-expressing *Gly I* when incubated in higher concentrations of methylglyoxal showed increased tolerance compared with wild-type plants. One of the plants expressing *Gly I* in antisense and showing less protein and enzyme activity showed higher sensitivity to methylglyoxal compared with wild type; however, complete bleaching was not seen. This could be due to the presence of residual *Gly I* activity in the antisense

plants, which also did not show any change in phenotype compared with the wild type.

Besides detoxification of methylglyoxal, the glyoxalase system could also play a role in providing tolerance under stress by recycling glutathione that would be 'trapped' spontaneously by methylglyoxal to form hemithioacetal (Creighton *et al.*, 1988; Thornalley, 1990), thereby maintaining the glutathione homeostasis. Methylglyoxal has been shown to decrease the level of protein thiol (Baskaran and Balasubramanian, 1990) and reduced glutathione GSH (Kalapos *et al.*, 1991; Leoncini *et al.*, 1989). It is known that reduced glutathione is essential for the effective scavenging of toxic compounds (such as H_2O_2 and organic hydrogen peroxides) and for the maintenance of other antioxidants such as ascorbates and tocopherols (Alscher, 1989). It is likely that changes in GSH:GSSG ratios could alter redox-sensitive regulatory proteins, such as thioredoxin and glutaredoxin, that could in turn control the activities of enzymes having a critical role during cell division/proliferation or stress (Brigellius, 1985; Wolin and Mohazzab, 1996). In addition, GSH is known to stimulate a variety of defence responses in plants (May *et al.*, 1998; Wingate *et al.*, 1988). Moreover, over-expression of genes involved in the regulation of glutathione homeostasis (namely glutathione reductase, glutathione S-transferase/glutathione peroxidase) in transgenic plants has been shown to result in an increased tolerance against oxidative stress (Aono *et al.*, 1993; Broadbent *et al.*, 1995; Foyer *et al.*, 1991; Noctor *et al.*, 1998; Roxas *et al.*, 1997). Unlike these studies, the advantage of transgenic plants over-expressing *Gly I* would lie in reducing the level of methylglyoxal under stress conditions and enabling regeneration of free glutathione from hemithioacetal. As no significant differences were observed in the growth and development pattern of wild-type, sense and antisense transgenic plants, over-expression of *Gly I* may have an advantage in that it could confer tolerance in response to abiotic stresses without having any adverse effect on the normal plant growth and development.

Experimental procedures

Purification of glyoxalase I and raising antibodies

Glyoxalase I enzyme from *B. juncea* was purified to homogeneity following ammonium sulphate precipitation, affinity (S-hexylglutathione sepharose 4B), and gel-filtration column chromatography as described by Deswal and Sopory (1991). The specific activity of the enzyme was determined according to the protocol described by Ramaswamy *et al.* (1983) and expressed in units mg^{-1} of protein. The polyclonal antibodies against purified glyoxalase I protein were raised by immunizing New Zealand White rabbits with intradermal injections of 250 μg of antigen (glyoxalase I) emulsified with Freund's adjuvant. The glyoxalase I IgG antibodies were purified using the ammonium sulphate precipitation method (Harlow and Lane, 1988). The specificity of antibodies against glyoxalase I was checked by immunoprecipitation assay and Western blotting.

Construction and screening of the B. juncea *cDNA expression library*

Total RNA was isolated from cotyledonary leaves of mannitol (400 mM)-stressed 7-day-old *B. juncea* seedlings (Chomczynski and Sacchi, 1987). Poly (A)+ RNA from total RNA was isolated using oligo (dT)-cellulose (Sambrook *et al.*, 1989). The cDNA synthesis was done using a Time Saver cDNA synthesis kit (Pharmacia). The cDNA was linked to *Eco*RI adapters and cloned into *Eco*RI-digested Lambda Zap II arms followed by packaging with Gigapack II gold extracts and amplification according to the manufacturer's instructions (Stratagene). The resulting phage library contained 1×10^{10} plaque forming units (p.f.u.) per ml. A total of (2×10^5) plaques was screened immunologically using a 1 : 2500 dilution of the glyoxalase I antibodies as per the standard protocols (Sambrook *et al.*, 1989). The immuno-positive plaques were purified to single species. Phagemid DNA in the form of pBluescript SK(–) was excised from the Lambda Zap II vector using an ExAssist/SOLR *in vivo* excision kit (Stratagene). The sequencing was done using Sequenase™ version 2 kit (USB). The deduced amino acid sequence from the cDNA clone (pBSGLYIVA3: Genbank accession number Y13239) was aligned with other known glyoxalase I sequences using the ClustlW alignment program (Mac vector, Version 6).

Over-expression of Gly I *from* B. juncea *in* E. coli

The coding region of the gene was amplified using PCR, with primers 5′-CGGGGTACCATGGCGTCGGAAGCGAAGG-3′ and 5′-TGCTCTAGAGCTCTCAAGCTGCGTTTCCGGCTG-3′ designed to create a *Nde*I site at 5′ end and *Xho*I site (underlined) at the 3′ end. The amplified DNA was subcloned into *E. coli* expression vector pRSETA at *NdeI*/*Xho*I sites (Novagen), resulting in the plasmid pRSETA-*Gly I* which was introduced into *E. coli* [BL21(DE3)] cells for protein over-expression. The *E. coli* cells carrying pRSETA-*Gly I* and pRSETA vectors were grown at 37°C in LB medium containing 100 μg ml^{-1} ampicillin to an OD_{600} of 0.5, and induced with 0.5 mM IPTG. Cells were harvested after 2 h and protein profiles were analysed by 12% SDS–PAGE (Laemmli, 1970). For estimation of glyoxalase I activity, *E. coli* cells were suspended in the extraction buffer, and following sonication and centrifugation at 12 000 ***g*** for 15 min at 4°C the enzyme activity was measured in the supernatant as described earlier.

The methylglyoxal cytotoxicity test was performed by plating overnight grown *E. coli* cells carrying pRSETA-*Gly I* and pRSETA vectors on an LB agar plate supplemented with 50 μg ml^{-1} ampicillin, 1 mM IPTG and various concentrations of methylglyoxal ranging from 0 to 30 mM. Plates were incubated at 37°C overnight and the total number of colonies in each plate was counted and percentage survival of the *E. coli* cells calculated.

Plasmid vectors and generation of transgenic plants

Two vectors, pBI-S1 and pBI-S2, for over-expression and one vector, pBI-A, for antisense suppression of glyoxalase I, were constructed for tobacco transformation (Figure 4a). In PBI-S1, the *Gly I* and the reporter *uidA* genes are under the control of separate CaMV 35S promoters and NOS polyadenylation signals, whereas in PBI-S2 these are under a control of single CaMV 35S promoter.

The PBI-A is like PBI-S2, but the *Gly I* is placed in an antisense orientation. The full-length *B. juncea Gly I* cDNA *Xba*I/*Eco*RV fragment from pBGLYIVA3 was placed at the *Xba*I/*Sac*I-digested pBI221 vector (Clontech) to create the pBI221-*Gly I* vector. The chimeric glyoxalase I gene cassette was excised as a *Pvu*II fragment from pBI221-*Gly I* and cloned into a pBI121 binary vector (Clontech) at the *Hin*dIII site (end filled) to create the pBI-S1 vector. The PBI-S2 and PBI-A vectors were constructed by cloning a *Eco*RV/*Sma*I fragment from (pBSGLYIVA3) plasmid containing full-length *Gly I* cDNA into the *Sma*I site of the pBI121 vector in sense and antisense orientations, respectively.

The recombinant plasmids were transferred into *Agrobacterium tumefaciens* (LBA4404). Tobacco (*Nicotiana tabacum* cv. Petit Havana) leaf discs were transformed following a leaf disc transformation procedure (Horsch *et al.*, 1985) with *Agrobacterium* containing pBI-S1, pBI-S2 or pBI-A. Putative transgenic plants were screened using a histochemical GUS assay (Jefferson, 1987). A number of primary transformants (T_0) were selected and analysed further.

Stress treatments to B. juncea *seedlings*

The roots of intact 4-day-old *B. juncea* seedlings were transferred into various concentrations of sodium chloride (0, 50, 100, 200, 400 and 800 mM), mannitol (0, 100, 200, 400 and 800 mM) and zinc chloride (0, 10, 20, 50, 100 and 200 mM) for different time intervals. Cotyledonary leaves and roots of the stressed seedlings were harvested after 0, 24, 48 and 72 h. Seedlings grown in water for the same period of time were taken as a control.

Nucleic acid extraction and analysis

Genomic DNA was isolated using the CTAB (N-cetyl-N, N, N,-trimethylammonium bromide) method (Murray and Thompson, 1980), and following digestion with appropriate restriction enzymes was blotted onto Hybond N+ nylon membranes (Amersham). Total RNA was isolated following an extraction method described by Chomczynski and Sacchi (1987). About 30 μg of total RNA samples were fractionated on a 1.2% formaldehyde agarose gel, transferred onto a nylon membrane and probed with either of the radiolabelled *Gly I*, *uidA*, *16S rRNA* and *actin* genes. Hybridization was carried at 65°C in 5 × SSC, 5 × Denhardt's, 0.1% SDS and 100 μg ml^{-1} denatured salmon sperm DNA for 16–18 h. Membranes were washed twice in 0.5 × SSC, 0.1% SDS and 0.1 × SSC, 0.1% SDS for 15 min each at 65°C. Relative signal intensities were normalized by reprobing the blots with *16S rRNA* and *actin* genes. Hybridization signals were quantified by densitometric scanning of autoradiograms using a laser densitometer (LKB Ultrascan, Sweden). The number of *Gly I* gene copies inserted into tobacco genome was determined by including a calibrated amount of pBGLYIVA3 plasmid (one, three and five copies per genome) for reconstruction in Southern blot analysis as described by Croy (1993). The intensity of the signal obtained in each lane was compared with the intensity of the signal obtained in the lanes containing digested genomic DNA from the transgenic plants.

Protein extraction, SDS–PAGE and immunoblotting

Total soluble proteins were extracted in 1 : 2 (w/v) of 100 mM sodium phosphate buffer (pH 7.0) containing 16 mM $MgSO_4$, 50% glycerol, 1 mM PMSF and 0.2% polyvinylpyrrolidone. The protein concentration was estimated spectrophotometrically by the Bradford (1976) method. About 2–5 μg of total proteins were electrophoresed on 12% SDS–PAGE, electroblotted on nitrocellulose membranes and immunodecorated with glyoxalase I antibodies (1 : 2500). Goat anti-rabbit IgG conjugated with alkaline phosphatase (Sigma) was used as a secondary antibody. The antigen–antibody complexes were visualized by the reaction of NBT/BCIP as described in Harlow and Lane (1988).

Analysis of transgenic plants for methylglyoxal and salt sensitivity

Healthy and fully expanded leaves from wild-type and transgenic plants were detached and washed briefly in deionized water. Leaf discs of 1 cm diameter were cut and floated in 5 ml of methylglyoxal (5 and 20 mM) and sodium chloride (400 and 800 mM) solutions for 24 h and 72 h, respectively. This method of leaf treatment was based on that described by Fan *et al.* (1997) with minor modifications. The treatment was carried in continuos white light (100 μEm^{-2} sec^{-1}) at 25 ± 2°C. The chlorophyll content was measured as described by Arnon (1949).

Acknowledgements

This research was supported from the internal grants of ICGEB and partly from the Department of Biotechnology, Government of India. Veena was supported by UGC, Ministry of Human Resource Development, Government of India for Junior Research Fellowship. We acknowledge fruitful discussions with Drs M. P. Kalapos and A. Kimura during the course of this study, and Professors S. C. Maheshwari and V.S. Chauhan for critical reading of the manuscript.

References

Alscher, R.G. (1989) Biosynthesis and antioxidant function of glutathione in plants. *Physiol. Plant.* **77**, 457–464.

Aono, M., Kubo, A., Saji, H., Tanaka, K. and Kondo, N. (1993) Enhanced tolerance to photooxidative stress of transgenic *Nicotiana tabacum* with high chloroplastic glutathione reductase activity. *Plant Cell Physiol.* **34**, 129–136.

Arnon, D.I. (1949) Copper enzymes in isolated chloroplasts: polyphenol oxidase in *Beta vulgaris*. *Plant Physiol.* **24**, 1–15.

Aronsson, A.-C., Marmstal, E. and Mannervik, B. (1978) Glyoxalase I, a zinc metalloenzyme of mammals and yeast. *Biochem. Biophys. Res. Commun.* **81**, 4235–4240.

Baskaran, S. and Balasubramanian, K.A. (1990) Effect of methylglyoxal on protein thiol and amino groups in isolated rat enterocytes and colonocytes and activity of various brush border enzymes. *Indian J. Biochem. Biophys.* **27**, 13–17.

Bito, A., Haider, M., Hadler, I. and Breitenbach, M. (1997) Identification and phenotypic analysis of two glyoxalase II encoding genes from *Saccharomyces cerevisiae*, *GLO2* and *GLO4*, and intracellular localization of the corresponding proteins. *J. Biol. Chem.* **272**, 21509–21519.

Bradford, M.M. (1976) A rapid and sensitive method for the quantitation of microgram quantities of protein utilizing the principle of protein-dye binding. *Anal. Biochem.* **72**, 248–254.

Brigellius, R. (1985) In *Oxidative Stress* (Sies, H., ed.). New York: Academic Press, pp. 243–272.

Broadbent, P., Creissen, G.P., Kular, B., Wellburn, A.R. and Mullineaux, P. (1995) Oxidative stress responses in transgenic

tobacco containing altered levels of glutathione reductase activity. *Plant J.* **8**, 247–255.

Cameron, A.D., Olin, B., Ridderstrom, M., Mannervik, B. and Jones, T.A. (1997) Crystal structure of human glyoxalase I – evidence for gene duplication and 3D domain swapping. *EMBO J.* **16**, 3386–3395.

Chakravarty, T.N. and Sopory, S.K. (1990) Light stimulated cell proliferation and glyoxalase-I activity in callus cultures of *Amaranthus paniculatus*. In *Progress in Plant Cellular and Molecular Biology* (Nijkamp, H.J.J., Van-der Plas, L.H.W. and Aartrijk, V.J., eds). Dordrecht: Kluwer Academic, pp. 379–384.

Chakravarty, T.N. and Sopory, S.K. (1998) Blue light stimulation of cell proliferation and glyoxalase I activity in callus cultures of *Amaranthus paniculatus*. *Plant Sci.* **132**, 63–69.

Chomczynski, P. and Sacchi, N. (1987) Single-step method of RNA isolation by acid guanidinium thiocyanate-phenol-chloroform extraction. *Anal. Biochem.* **162**, 156–159.

Clugston, S.L., Daub, E., Kinach, R., Miedema, D., Barnard, J.F.L. and Honek, J.F. (1997) Isolation and sequencing of a gene coding for glyoxalase I activity from *Salmonella typhimurium* and comparison with other glyoxalase I sequences. *Gene*, **186**, 103–111.

Creighton, D.J., Migliorini, M., Pourmotabbed, T. and Guha, M.K. (1988) Optimization of efficiency in the glyoxalase pathway. *Biochemistry*, **27**, 7376–7384.

Croy, E.J., Ikemura, T., Shirsat, A. and Croy, R.R.D. (1993) Plant nucleic acids. In *Plant Molecular Biology*, Labfax (Croy, R.R.D., ed.). Bios Scientific (Blackwell Scientific Publications), pp. 29–31.

Daub, E., Kinach, R., Miedema, D., Barnard, J.F.L., Clugston, S.L. and Honek, J.F. (1996) Escherichia coli *glyoxalase I*. Genbank Accession Number U57363.

Deswal, R. and Sopory, S.K. (1991) Purification and partial characterization of glyoxalase I from a higher plant, *B. juncea*. *FEBS Lett.* **282**, 277–280.

Deswal, R., Chakravarty, T.N. and Sopory, S.K. (1993) The glyoxalase system in higher plants: regulation in growth and differentiation. *Biochem. Soc. Trans.* **21**, 527–530.

Devlin, K., Churcher, C.M., Barrell, B.G., Rajandream, M.A. and Walsh, S.V. (1995) *Swiss Protein Bank Accession Number Q09751.*

Espartero, J., Sanchez-Aguayo, I. and Pardo, J.M. (1995) Molecular characterization of glyoxalase-I from a higher plant; upregulation by stress. *Plant Mol. Biol.* **29**, 1223–1233.

Faggin, P., Bassi, A.M., Finollo, R. and Brambilla, G. (1985) Induction of sister chromatid exchanges in Chinese hamster ovary cells by the biotic ketoaldehyde methylglyoxal. *Mut. Res.* **144**, 189–191.

Fan, L., Zheng, S. and Wang, X. (1997) Antisense suppression of phospholipase Dα retards abscisic acid- and ethylene-promoted senescence of postharvest *Arabidopsis* leaves. *Plant Cell*, **9**, 2183–2196.

Foyer, C.H., Lelandais, M., Galap, C. and Kunert, K.J. (1991) Effect of elevated cytosolic glutathione reductase activity on the cellular glutathione pool and photosynthesis in leaves under normal and stressed conditions. *Plant Physiol.* **97**, 863–872.

Gentles, S., Bowman, S., Barrell, B.G., Rajandream, M.A. and Walsh, S.V. (1995) *Swiss Protein Bank Accession Number P50107.*

Harlow, E. and Lane, D. (1988) *Antibodies: A Laboratory Manual*. New York: Cold Spring Harbor Laboratory Press.

Horsch, R.B., Fry, J.E., Hoffmann, N.L., Eichholtz, D., Rogers, S.G. and Fraley, R.T. (1985) A simple and general method for transferring genes into plants. *Science*, **227**, 1229–1231.

Inoue, Y. and Kimura, A. (1996) Identification of the structural gene for glyoxalase I from *Saccharomyces cerevisiae*. *J. Biol. Chem.* **271**, 25958–25965.

Inoue, Y., Choi, B.-Y., Murata, K. and Kimura, A. (1990) Sexual response of *Saccharomyces cerevisiae*: phosphorylation of yeast glyoxalase I by cell extract of mating factor-treated cells. *J. Biochem.* **108**, 4–6.

Jefferson, R.A. (1987) Assaying chimeric genes in plants: the GUS fusion system. *Plant Mol. Biol. Report*, **5**, 387–405.

Kalapos, M.P. (1994) Methylglyoxal toxicity in mammals. *Toxicol. Lett.* **73**, 3–24.

Kalapos, M.P., Schaff, Zs., Garzo, T., Antonie, F. and Mandl, J. (1991) Accumulation of phenols in isolated hepatocytes after pretreatment with methylglyoxal. *Toxicol. Lett.* **58**, 181–191.

Kim, N.-S., Umezawa, Y., Ohmura, S. and Kato, S. (1993) Human glyoxalase I: cDNA cloning, expression and sequence similarity to glyoxalase I from *Pseudomonas putida*. *J. Biol. Chem.* **268**, 11217–11221.

Laemmli, L.K. (1970) Cleavage of structural proteins during the assembly of the head of the bacteriophage T4. *Nature*, **227**, 680–685.

Leoncini, G., Maresca, M. and Buzi, E. (1989) Inhibition of the glycolytic pathway by methylglyoxal in human platelets. *Cell Biochem. Funct.* **7**, 65–70.

Lu, T., Crieghton, D.J., Antoine, M., Fenselau, C. and Lovett, P.S. (1994) The gene encoding glyoxalase I from *Pseudomonas putida*: cloning, over-expression, and sequence comparison with human glyoxalase I. *Gene*, **150**, 93–96.

Maiti, M.K., Krishnasamy, S., Owen, H.A. and Makaroff, C.A. (1997) Molecular characterization of glyoxalase II from *Arabidopsis thaliana*. *Plant Mol. Biol.* **35**, 471–481.

Mannervik, B. (1980) Glyoxalase I. In *Enzymatic Basis of Detoxification Volume 2* (Jakoby, W.B., ed.). New York: Academic Press, pp. 263–273.

May, M.J., Vernoux, T., Leaver, C., Van Montagu, M. and Inze, D. (1998) Glutathione homeostasis in plants: implications for environmental sensing and plant development. *J. Exp. Bot.* **49**, 649–667.

Murray, M.G. and Thompson, W.F. (1980) Rapid isolation of high-molecular-weight plant DNA. *Nucl. Acids Res.* **8**, 4321–4325.

Noctor, G., Arisi, A.-C.M., Jouanin, L., Kunert, K.J., Rennenberg, H. and Foyer, C.H. (1998) Glutathione: biosynthesis, metabolism and relationship to stress tolerance explored in transformed plants. *J. Exp. Bot.* **49**, 623–647.

Papoulis, A., Al-Abed, Y. and Bucala, R. (1995) Identification of N2-(1-carboxylethyl) guanine (CEG) as a guanine advanced glycosylation endproduct. *Biochemistry*, **34**, 648–655.

Paulus, C., Knollner, B. and Jacobson, H. (1993) Physiological and biochemical characterization of glyoxalase I, a general marker for cell proliferation, from a soybean cell suspension. *Planta*, **189**, 561–566.

Phillips, S.A. and Thornalley, P.J. (1993) The formation of methyglyoxal from triose phosphates. *Eur. J. Biochem.* **212**, 101–105.

Ramaswamy, O., Guha-Mukherjee, S. and Sopory, S.K. (1983) Presence of glyoxalase I in pea. *Biochem. Int.* **7**, 307–318.

Ramaswamy, O., Guha-Mukherjee, S. and Sopory, S.K. (1984) Correlation of glyoxalase I activity with cell proliferation in *Datura* callus culture. *Plant Cell Report*, **3**, 121–124.

Ranganathan, S., Walsh, E.S., Godwin, A.K. and Tew, K.D. (1993) Cloning and characterization of human colon glyoxalase I. *J. Biol. Chem.* **268**, 5661–5667.

Rhee, H.-I., Sato, N., Murata, K. and Kimura, A. (1988) Nucleotide sequence of the glyoxalase I gene of *Pseudomonas putida*. *Agric. Biol. Chem.* **52**, 2243–2246.

Ridderstrom, M. and Mannervik, B. (1996) Optimized heterologous expression of the human zinc enzyme glyoxalase I. *Biochem. J.* **314**, 463–467.

Ridderstrom, M. and Mannervik, B. (1997) Molecular cloning and characterization of the thiolesterase glyoxalase II from *Arabidopsis thaliana*. *Biochem. J.* **322**, 449–454.

Ridderstrom, M., Saccucci, F., Hellman, U., Bergman, T., Principato, G. and Mannervik, B. (1996) Molecular cloning, heterologous expression, and characterization of human glyoxalase II. *J. Biol. Chem.* **271**, 319–328.

Roxas, V.P., Smith, R.K., Allen, E.R. and Allen, R.D. (1997) Overexpression of glutathione S-transferase/glutathione peroxidase enhances the growth of transgenic tobacco seedlings during stress. *Nature Biotech.* **15**, 988–991.

Sambrook, J., Fritsch, E.F. and Maniatis, T. (1989) *Molecular Cloning: A Laboratory Manual*, 2nd edn. New York: Cold Spring Harbor Laboratory Press.

Scaife, J.F. (1969) Mitotic inhibition induced in human kidney cells by methylglyoxal and kethoxal. *Experientia*, **25**, 178–179.

Sellin, S., Eriksson, L.E.G., Aronsson, A.-C. and Mannervik, B. (1983) Octahedral metal coordination in the active site of glyoxalase as evidenced by properties of Co (II)-glyoxalase I. *J. Biol. Chem.* **258**, 2091–2093.

Seraj, Z.I., Sarker, A.B. and Islam, A.S. (1992) Plant regeneration in a jute species (*C. capsularis*) and its possible relationship with glyoxalase-I. *Plant Cell Report*, **12**, 29–33.

Sethi, U., Basu, A. and Guha-Mukherjee, S. (1988) Control of cell proliferation and differentiation by regulating polyamine biosynthesis in cultures of *Brassica* and its correlation with glyoxalase I activity. *Plant Sci.* **56**, 167–175.

Smits, M.M. and Johnson, M.A. (1981) Methylglyoxal: enzyme distribution relative to its presence in Douglas-fir needles and absence in Douglas-fir needle callus. *Arch. Biochem. Biophys.* **208**, 431–439.

Szent-Gyorgi, A. and Egyud, L.G. (1966) On the regulation of cell division. *Proc. Natl Acad. Sci. USA*, **56**, 203–207.

Thornalley, P.J. (1990) The glyoxalase system: new developments towards functional characterization of metabolic pathways fundamental to biological life. *Biochem. J.* **269**, 1–11.

Thornalley, P.J. (1993) The glyoxalase system in health and disease. *Mol. Aspects Med.* **14**, 287–371.

Umeda, M., Hara, C., Matsubayashi, Y., Li, H.-H., Liu, Q., Tadokoro, F., Aotsuka, S. and Uchimiya, H. (1994) Expressed sequence tags from cultured cells of rice (*Oryza sativa* L.) under stressed conditions: analysis of transcripts of genes engaged in ATP-generating pathways. *Plant Mol. Biol.* **25**, 469–478.

Uotila, L. (1989) Glutathione thiol esterases. In *Glutathione: Chemical, Biochemical and Medical Aspects, Coenzymes and Cofactors Volume III, Part A*, (Dolphin, D., Poulson, R. and Avramovic, O., eds). New York: Wiley-Interscience, pp. 767–804.

Wingate, V.P.M., Lawton, M.A. and Lamb, C.J. (1988) Glutathione causes a massive and selective induction of plant defence genes. *Plant Physiol.* **87**, 206–210.

Wolin, M.S. and Mohazzab, H.K.M. (1996) In *Oxidative Stress and the Molecular Biology of Antioxidant Defenses* (Scandalios, J.G., ed.). New York: Cold Spring Harbor Laboratory Press, pp. 21–48.

GenBank accession number Y13239 (*B. juncea Gly I* cDNA).